EFFECT OF LOCAL PRESSURE TRANSIENTS ON THE DEFORMATIONS AND STRESSES IN CYLINDRICAL DUCTS

VOLUME I - THEORY AND DESIGN CHARTS

Joseph Padlog and Herbert Reismann

REPORT NO. 2286-950002

JUNE 26, 1966

(PREPARED UNDER CONTRACT NO. NAS8-11215)

GEORGE C MARSHALL SPACE FLIGHT CENTER
NATIONAL AERONAUTICS AND SPACE ADMINISTRATION
HUNTSVILLE, ALABAMA 35812

BELL AEROSYSTEMS - A textron COMPANY

FOREWORD

This report was prepared by Bell Aerosystems Company under NASA Contract NAS8-11215 and covers work performed during the period 1 May 1965 to 31 May 1966. The contract was administered under the direction of Mr. Jerrell M. Thomas, Contracting Officers Representative, and Mr. George Tovar, Alternate, Contracting Officers Representative, at NASA, George C. Marshall Space Flight Center.

The authors wish to acknowledge the assistance and contributions of the following personnel: W. A. Luberacki, D. M. Dupree, R. G. Dworak, Y. M. Echenoz, R. A. Van Slooten and J. F. Bolton.

Most of the numerical results presented in this report were obtained with the computer facilities at the George C. Marshall Space Flight Center Huntsville, Alabama in close cooperation with J. Thomas and G. Tovar.

ABSTRACT

Axially symmetric dynamic response solutions for infinite and finite length cylinders subjected to pressure transients which arise in propulsion systems are presented in Volume I. Pressure transient types considered in detail are of the spike, step, ramp and sinusoidal forms. Solutions for simple-simple and fixed-fixed boundary conditions are given and used as the basis for design charts which yield maximum stresses. A discussion of advanced problems is included.

Volume II is a User's Manual for a General Purpose Digital Computer Program capable of predicting the dynamic response of cylinders subjected to ramp and sinusoidal pressure transients. The dynamic response for many traverses of a pressure transient from one end of the cylinder to the other can be computed by the program for the case where one end of the cylinder is closed (by a valve) and the other end attached to a relatively large container.

CONTENTS

CONTENTS (CONT)

ILLUSTRATIONS

TABLES

SYMBOLS

c = Viscous damping coefficient

$c_{CR} = \sqrt{\frac{\rho E}{g}} \frac{h}{R}$, critical damping coefficient for n = 1

$D = \frac{E h^3}{12 (1-\nu^2)}$

e = half wave length of sinusoidal pressure transient

E = Young's modulus

F_n = nondimensional function of time

h = cylinder wall thickness

k = wave number

k_n = eigenvalue

$K_n = k_n \ell$

ℓ = length of cylinder

$m = \frac{\rho h}{g}$

M_x = axial bending moment per unit of circumferential length

$M_o = \frac{pRh}{\sqrt{12 (1-\nu^2)}}$

$M_{o_P} = \frac{P h^{1/2} R^{1/2}}{4\sqrt{12 (1-\nu^2)}}$

M_ϕ = hoop bending moment per unit axial length

$\bar{M}_x$ = nondimensional axial bending moment per unit of circumferential length

n = subscript, indicates mode number

N = number of terms taken in series solution

N_ϕ = hoop membrane force per unit length

N_x = axial membrane force per unit length

p = maximum intensity of radial pressure load

P = ring line load per unit of circumferential length

$\bar{q}$ = normal force intensity

q = intensity of radial pressure load

Q_x = shear force per unit length

Q = Fourier load transform

R = mean cylinder radius

t = time

t_c = valve closure time

$t_o = \frac{\ell}{v}$

T_n = function of time

u = axial displacement component

v = speed of transient pressure

v_G = group velocity

w = radial displacement component of cylinder

$W_n(\bar{\xi})$ = eigenfunction

$W(\alpha)$ = Fourier deflection transform

$w_o = \frac{p R^2}{E h}$

$w_{o_P} = \frac{P\sqrt[4]{12\,(1-\nu^2)}}{E}\left(\frac{R}{h}\right)^{3/2}$

$\bar{w}$ = nondimensional radial displacement of cylinder

x = axial coordinate of cylinder

$\alpha = c\,\frac{R}{h}\sqrt{\frac{q}{\rho E}}$, nondimensional damping parameter

$\bar{\alpha} = \alpha\sqrt{\frac{\beta}{2\lambda}}$

$\beta = \frac{\ell^2}{Rh}\sqrt{12\,(1-\nu^2)}$, length parameter

$\gamma = \sqrt[4]{\frac{Eh}{R^2 D}}$

Γ = frequency

$\epsilon = \frac{e}{\ell}$

ϵ_x = axial strain

ϵ_ϕ = circumferential strain

λ = $\frac{\rho v^2}{2Eg} \frac{R}{h} \sqrt{12(1-\nu^2)}$, speed parameter

ν = Poisson's ratio

$\bar{\xi}$ = γ (x-vt), dimensionless moving coordinate, infinite shell

ρ = weight density

ϕ = phase velocity

ξ = $\frac{x}{\ell}$, dimensionless axial coordinate, finite shell

σ_x = stress in axial direction

σ_θ = stress in circumferential direction

τ = $\frac{t}{t_o}$, nondimensional time

$\tau_c = \frac{t_c}{t_o}$ = nondimensional valve closure time

ω = natural frequency

$\bar{\omega}$ = damped natural frequency

Ω = nondimensional natural frequency

$\bar{\Omega}$ = nondimensional damped natural frequency

Additional symbols are defined in the text where they occur.

I. INTRODUCTION

During the various phases of operation of the propulsion systems of space vehicles, severe pressure transients are experienced by the component cylindrical ducts. This report presents the results of a study of the dynamic response of circular cylinders subjected to pressure transient forms commonly encountered in propulsion systems with the prime objective of providing analytical procedures and design charts capable of dealing with the stringent minimum weight requirements of aerospace vehicles. In general, a method is developed for the solution of the basic equation for circular cylinders subjected to axial symmetric pressures of any type. However, the method was used in this study to obtain dynamic solutions to the more common pressure transient types and the pertinent stresses required for minimum weight design purposes summarized into design charts.

Results of a literature survey are reported in Appendix A. In general, the survey revealed that although the basic equations for the problem at hand are well defined, pertinent dynamic solutions and their application to predicting the correct local stress fields in cylinders subjected to transient pressures were limited.

Transient pressures appear in the form of pressure or rarefraction waves which propagate along ducts at approximately the speed of sound in the contained fluid. These pressure waves have various forms which depend on the nature of the disturbance responsible for them and are discussed in Section II. All dynamic elastic solutions obtained are based on the assumption that the form and velocity of propagation of the pressure transients are known.

The basic equations used in the analysis are derived in Section III. Two solutions are then obtained for the infinite shell, one for the spike load and the other for the step pressure form. In addition, a method for deriving the dynamic response with damping of a finite length duct subjected to axial symmetric pressures is developed. For illustrative purposes, several problems are solved in detail in this Section. The work

is limited to two boundary conditions, i.e. cylinders with both ends simply supported and cylinders with both ends fixed. Although it is shown that the method can be readily used to obtain solutions for all possible combinations of admissable boundary conditions, the two selected boundary conditions are deemed sufficient for practical reasons.

For purposes of presentation of the results of this study in a concise manner convenient for use by the analyst, nondimensional variables and design parameters are introduced in the latter part of Section III. These variables and parameters are introduced into the governing equations and dynamic solutions obtained for the finite length shell are summarized in nondimensional form.

A presentation of typical dynamic response results obtained from the solutions is given in Section IV. In addition, the significance of damping, shear deformation, rotatory inertia, and infinite duct solutions are discussed.

Design charts which yield maximum stresses as a function of the design parameters are presented together with an illustrative example in Section V.

A discussion of the nature of advanced problems which may arise or be significant in ducting problems is presented in Section VI. Finally, conclusions and recommendations are summarized in Section VII.

II. TRANSIENT LOAD CONDITIONS

Transient pressures in propulsion systems are created by various means such as opening or closing valves, pump surges, and the flutter of check valves. Such situations are especially severe during rocket engine start or shutdown. In this section, pressure transient conditions of interest are identified, idealized and represented mathematically for analytical purposes. A complete description of the ramp and sinusoidal pressure forms is given.

The most severe transient pressure loading cases to be anticipated are those associated with the rate of valve closure. When a valve is closed, the kinetic energy of the fluid is converted into pressure. A pressure wave then travels along the duct with velocity v. The velocity of propagation of the pressure transient is equal to the speed of sound of the fluid if the walls of the duct are inelastic. However, for elastic ducts, the speed of propagation of the pressure transient may be significantly less than the speed of sound in the fluid (see Reference 2-1).

The peak magnitude of the pressure wave, denoted as p, is indpendent of the rate of valve closure and is only dependent on the initial fluid velocity, mass density of the fluid, and the velocity v, of propagation of the pressure pulse (see Reference 2-1). However, the shape of the pressure transient will depend on the rate of valve closure and for a constant rate of valve closure, the form of the pressure transient, referred to as a ramp, will appear as shown in Figure II-1.

Valve closure time is defined by the symbol t_c. Thus for instantaneous valve closure time, $t_c = 0$, the pressure transient will appear immediately after valve closure as shown in Figure II-2a. The sequence of transient pressures which are induced in a duct when a valve is closed at one end and the other end is attached to a tank is shown in Figure II-2. The end of the duct connected to the tank can be considered as an open end which reflects a pressure front as a rarefaction. Hence the transient pressure during the time interval $t_o < t < 2\,t_o$ will be as shown in Figure II-2b. The time $t_o = \ell/v$, i.e., t_o is equal to the time it takes the transient pressure front to traverse the length of the duct.

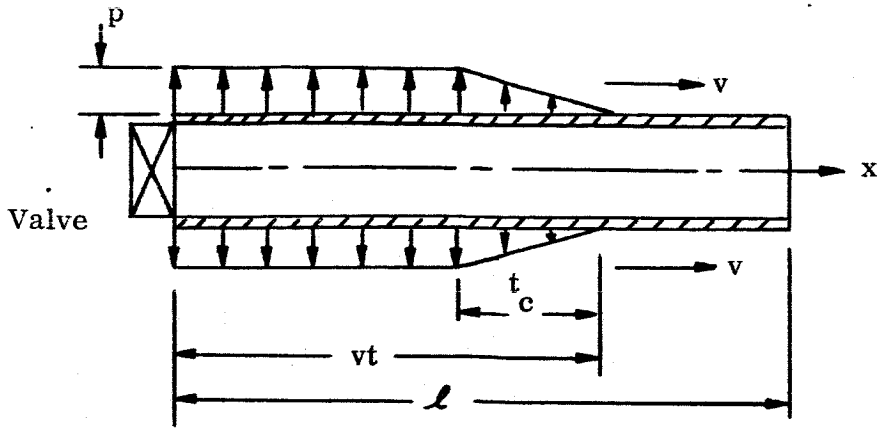

Figure II-1. Ramp Pressure Wave Shape

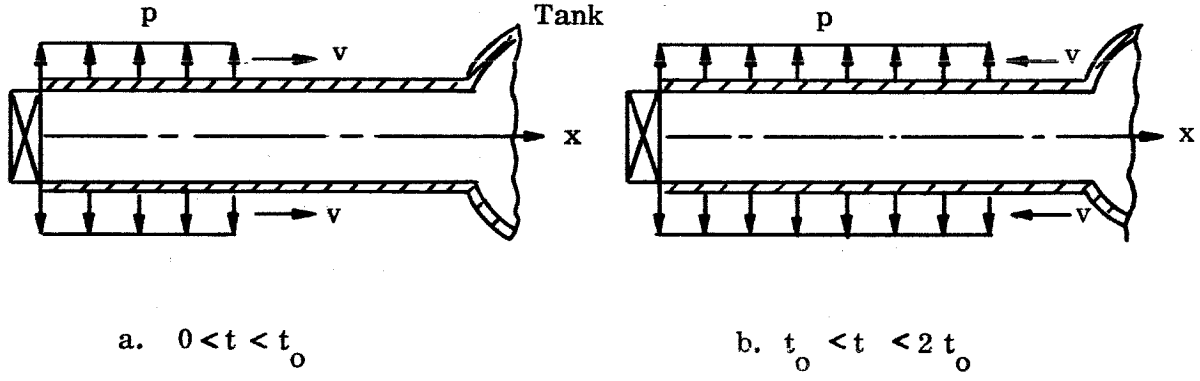

a. $0 < t < t_o$

b. $t_o < t < 2t_o$

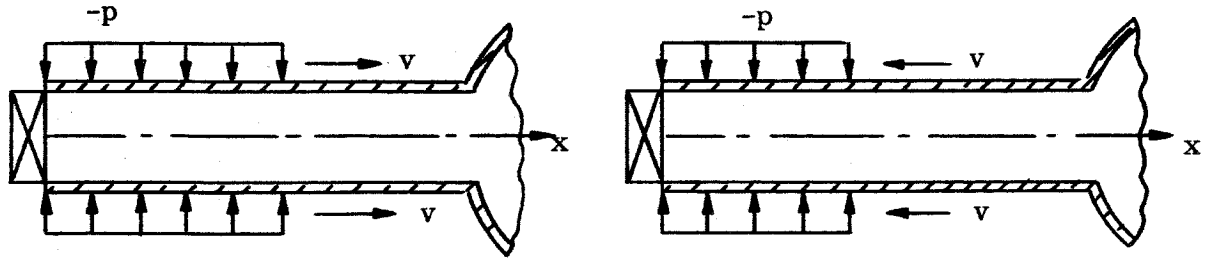

c. $2t_o < t < 3t_o$

d. $3t_o < t < 4t_o$

Figure II-2. Step Pressure Wave Shape

Since a closed duct end will reflect a pressure front into a pressure and a rarefaction into a rarefaction, succeeding traverses of the transient pressure will appear as shown in Figures II-2c and II-2d.

All four distinct transient pressure traverses shown in Figure II-2 will be continually repeated in sequence if there is no friction. The presence of friction will tend to decrease the magnitude of the pressure pulse as it traverses the cylinder. In addition, depending on the characteristics of the reflecting media at the ends of the cylinder, there may be a pressure drop with each reflection. In the present study the magnitude of the pressure transient was assumed to remain constant. However, the dynamic solution techniques presented in the next section are not restricted to this assumption.

The description of the ramp pressure transient history which reduces to the step case is now described in detail. It is assumed that the valve closure time, t_c, is less than the time, t_o, required for the pressure transient to traverse the cyclinder, i.e., $t_c < t_o$.

For $0 \leq t \leq t_c$

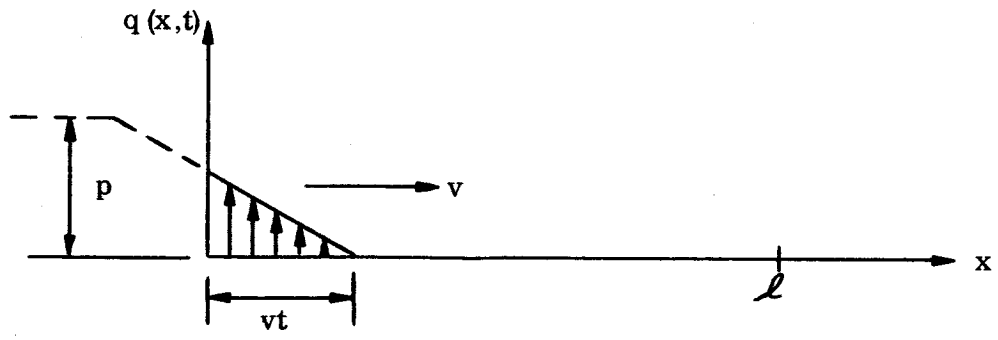

$$q(x,t) = \frac{-p}{vt_c}(x - vt) \qquad o \leq x \leq vt \qquad (2\text{-}1)$$

$$q(x,t) = 0 \qquad vt \leq x \leq \ell$$

For $t_c < t < t_o$

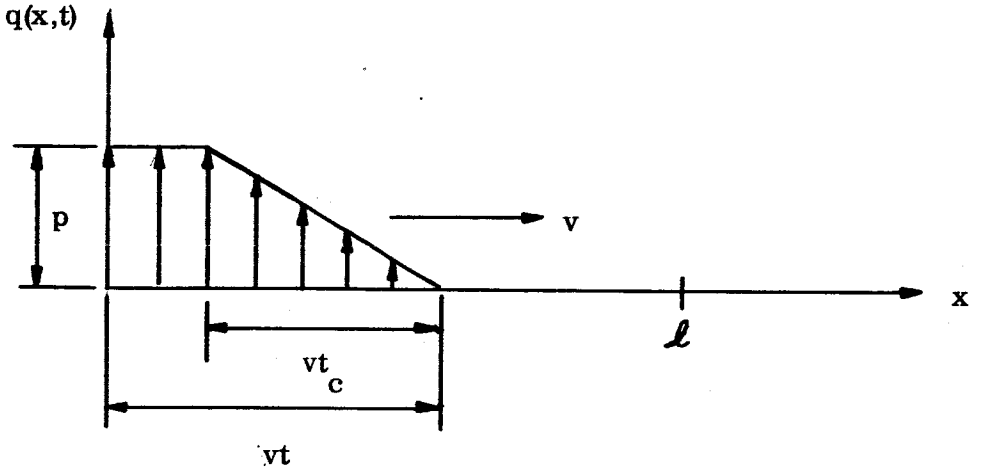

$$
\begin{aligned}
q(x,t) &= p && 0 \le x \le vt - vt_c \\
q(x,t) &= \frac{-p}{vt_c}(x - vt) && vt - vt_c \le x \le vt \\
q(x,t) &= 0 && vt \le x \le \ell
\end{aligned}
\qquad (2\text{-}2)
$$

Succeeding expressions for the transient pressure history are conveniently represented as the superposition of right and left traveling waves. Thus at $t_o = \ell/v$, the situation is as shown in the following sketch.

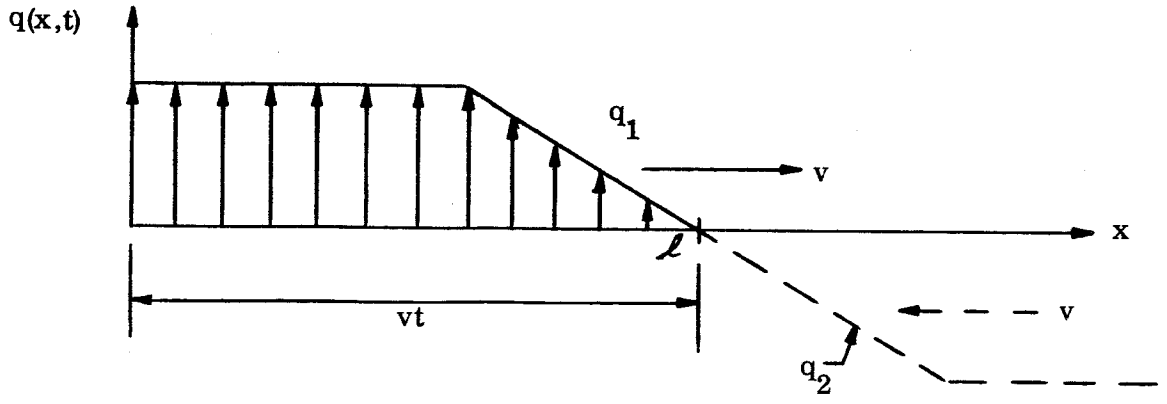

For the time period $t_o \leq t \leq t_o + t_c$

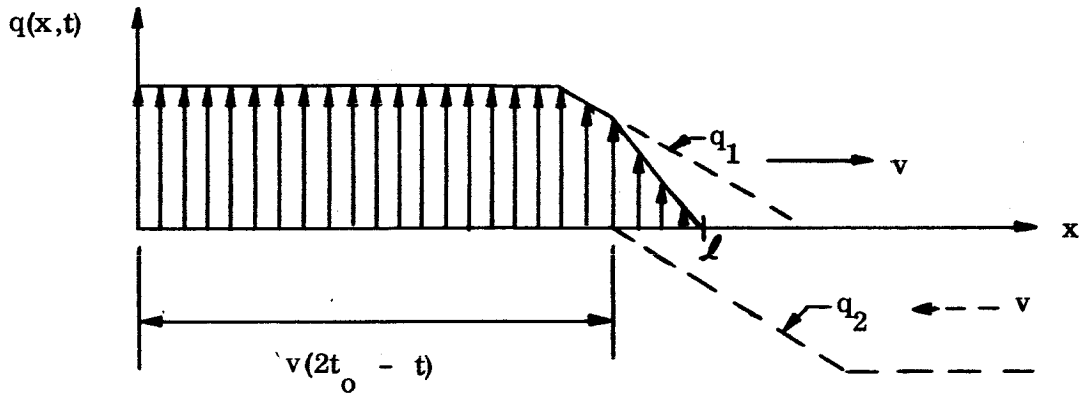

$$q(x,t) = q_1(x,t) + q_2(x,t) \qquad 0 \leq x \leq \ell \qquad (2\text{-}3)$$

Where the right traveling load is given by

$$q_1(x,t) = p \qquad 0 \leq x \leq vt - vt_c$$

$$q_1(x,t) = \frac{-p}{vt_c}(x - vt) \qquad vt - vt_c \leq x \leq \ell \qquad (2\text{-}4)$$

and the left traveling load is given by

$$q_2(x,t) = 0 \qquad 0 \leq x \leq 2\ell - vt$$

$$q_2(x,t) = \frac{-p}{vt_c}(x + vt - 2\ell) \qquad 2\ell - vt \leq x \leq \ell \qquad (2\text{-}5)$$

Similarly for $t_o + t_c \leq t \leq 2\,t_o$

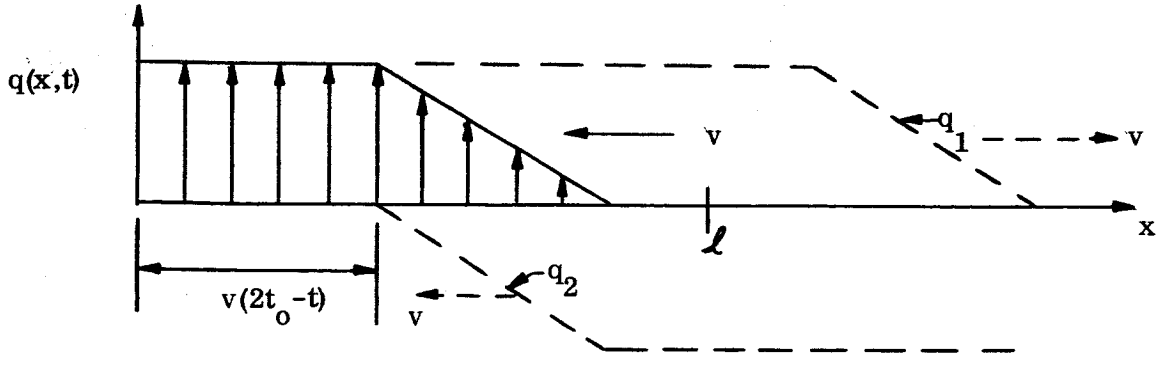

Right traveling load

$$q_1(x,t) = p \qquad 0 \le x \le \ell$$

Left traveling load

$$q_2(x,t) = 0 \qquad 0 \le x \le 2\ell - vt$$

$$q_2(x,t) = \frac{-p}{vt_c}(x + vt - 2\ell) \qquad 2\ell - vt \le x \le 2\ell - vt + vt_c \qquad (2\text{-}6)$$

$$q_2(x,t) = -p \qquad 2\ell - vt + vt_c \le x \le \ell$$

For

$$2t_o \le t \le 2t_o + t_c$$

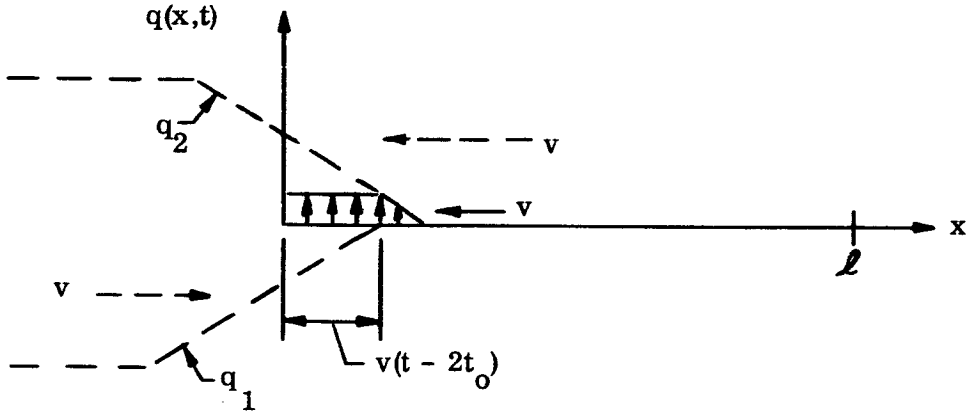

Right traveling load

$$q_1(x,t) = \frac{p}{vt_c}(x - vt + 2\ell) \qquad 0 \le x \le vt - 2\ell$$

$$q_1(x,t) = 0 \qquad vt - 2\ell \le x \le \ell \qquad (2\text{-}7)$$

Left traveling load

$$q_2(x,t) = \frac{-p}{vt_c}(x + vt - 2\ell - vt_c) \qquad 0 \le x \le 2\ell - vt + vt_c$$

$$q_2(x,t) = 0 \qquad vt - 2\ell + vt_c \le x \le \ell \qquad (2\text{-}8)$$

For

$$2\,t_o + t_c \le t \le 3\,t_o$$

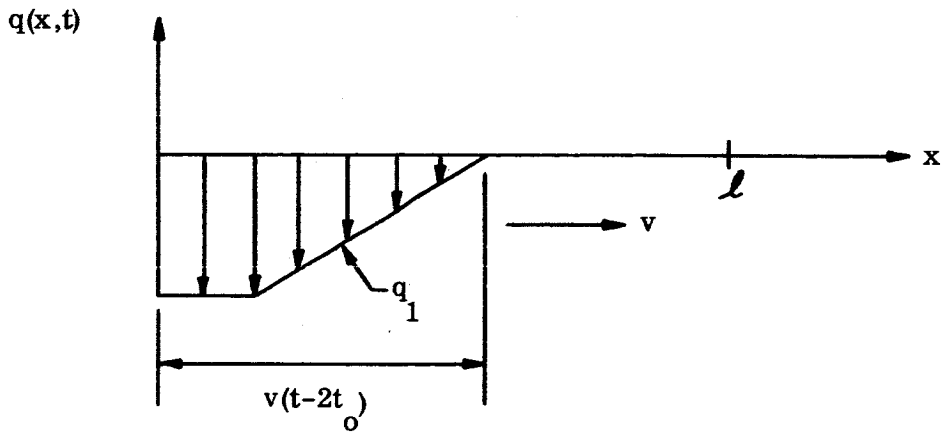

Right traveling load

$$q_1(x,t) = -p \qquad 0 \le x \le vt - 2\ell - vt_c$$

$$q_1(x,t) = \frac{p}{vt_c}(x - vt + 2\ell) \qquad vt - 2\ell - vt_c \le x \le vt - 2\ell \qquad (2\text{-}9)$$

$$q_1(x,t) = 0 \qquad vt - 2\ell \le x \le \ell$$

For

$$3\,t_o \le t \le 3\,t_o + t_c$$

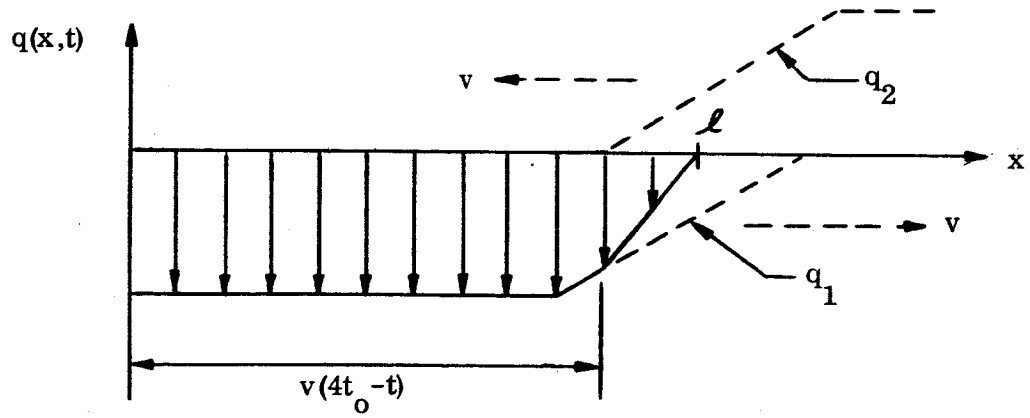

Right traveling load

$$q_1(x,t) = -p \qquad 0 \le x \le vt - 2\ell - vt_c$$

$$q_1(x,t) = \frac{p}{vt_c}(x - vt + 2\ell) \qquad vt - 2\ell - vt_c \le x \le \ell \qquad (2\text{-}10)$$

Left traveling load

$$q_2(x,t) = 0 \qquad 0 \le x \le 4\ell - vt$$

$$q_2(x,t) = \frac{p}{vt_c}(x + vt - 4\ell) \qquad 4\ell - vt \le x \le \ell \qquad (2\text{-}11)$$

For

$$3t_o + t_c \le t \le 4t_o$$

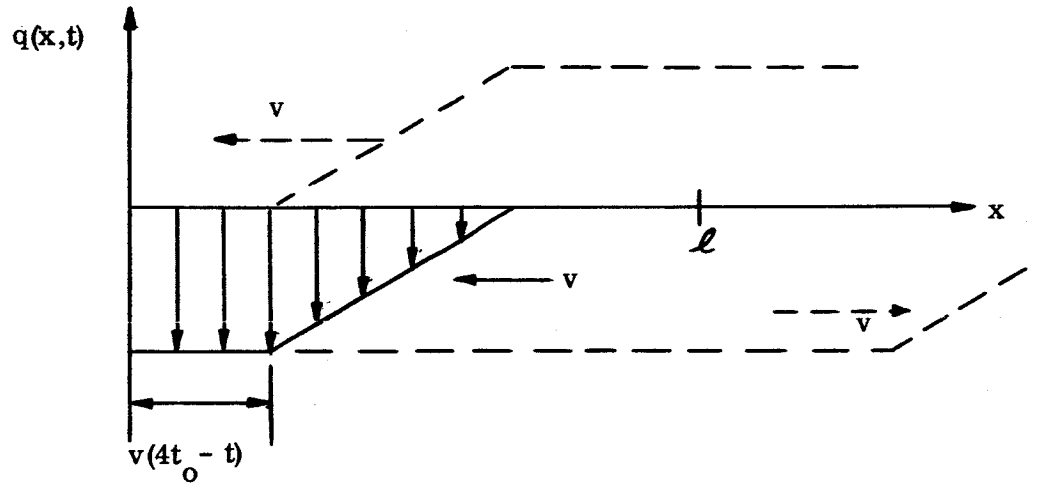

Left traveling load

$$q(x,t) = -p \qquad 0 \le x \le 4\ell - vt$$

$$q(x,t) = \frac{p}{vt_c}(x + vt - 4\ell - vt_c) \qquad 4\ell - vt \le x \le 4\ell - vt + vt_c \qquad (2\text{-}12)$$

$$q(x,t) = 0 \qquad 4\ell - vt + vt_c \le x \le \ell$$

The sequence of pressure transients delineated above corresponds to four complete traverses of the pressure front during the time $4t_o$. This process is continued into the next time interval by superposition of the pressure transient expressions for the first time interval, $0 \le t \le t_c$, with the pressure expressions for the last time interval $4t_o \le t \le 4t_o + t_c$ which is defined as follows:

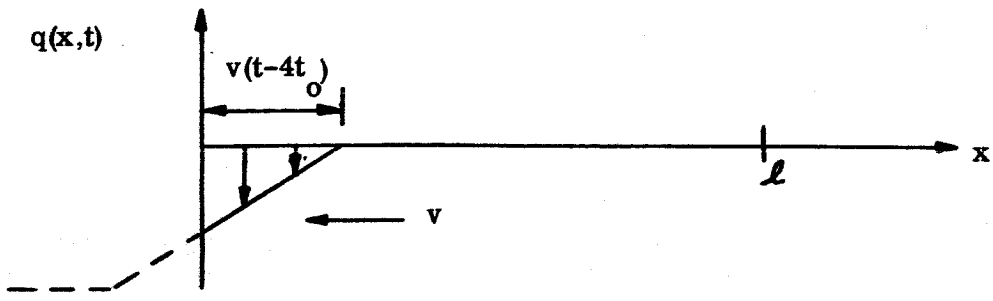

Left traveling load

$$q(x,t) = \frac{p}{vt_c}(x + vt - 4\ell - vt_c) \qquad 0 \le x \le 4\ell - vt + vt_c$$

$$q(x,t) = 0 \qquad 4\ell - vt + vt_c \le x \le \ell \qquad (2\text{-}13)$$

For valve opening, the form of the pressure transients are essentially the same as the first two traverses described above except that the pressures will be of opposite sign. The sequence of events which occur after these two traverses will depend on the characteristics of the ducting and hardware on the down stream side of the valve.

Impulsive type transient pressures which are caused by pump surges, instability of combustion processes, etc., can be represented by a traveling sinusoidal pressure form. Here, again, it will be assumed that the sinusoidal pulse emanates at the left end of the duct, which thereafter is considered closed, and reflected at the other end which is connected to a relatively large vessel. Thus, as was the case for the ramp pressure form, the right end of the cylinder is assumed open and the left end closed.

The mathematical representation of two traverses of the pressure transient are required to represent the complete characteristics of this transient pressure condition. The sequence of pressure formulas for this case is summarized below. The half wave-length of the assumed sinusoid is denoted by e and it is assumed that $e < \ell$.

At the start of the pressure cycle we have for $0 \leq t \leq \frac{e}{v}$

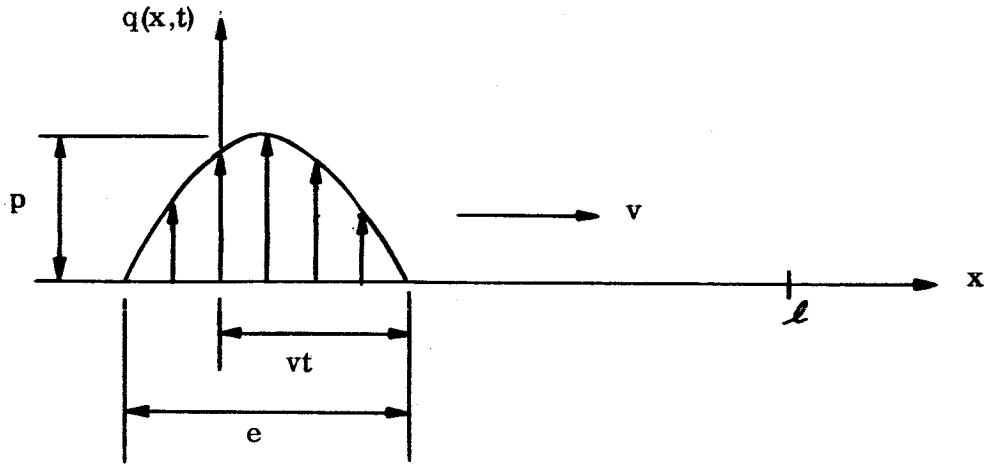

$$q(x,t) = -p \sin \pi \frac{(x - vt)}{e} \qquad 0 \leq x \leq vt$$

$$q(x,t) = 0 \qquad vt \leq x \leq \ell \qquad (2\text{-}14)$$

For

$$\frac{e}{v} \leq t \leq t_o$$

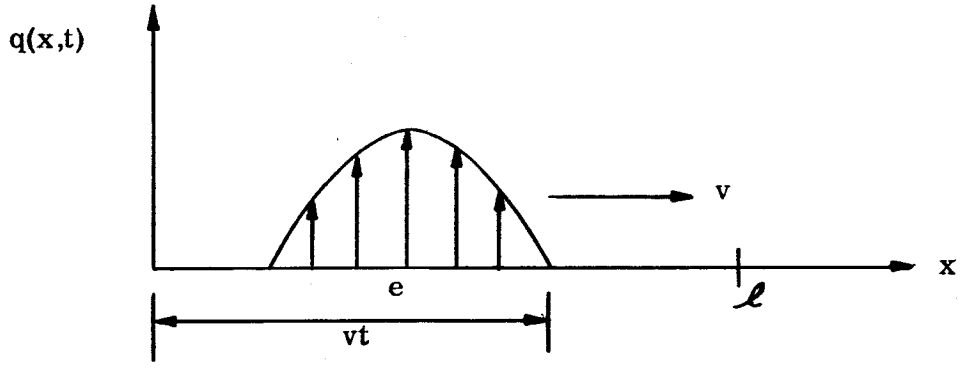

$$q(x,t) = 0 \qquad 0 \leq x \leq vt - e$$

$$q(x,t) = -p \sin \pi \frac{(x - vt)}{e} \qquad vt - e \leq x \leq vt \qquad (2\text{-}15)$$

$$q(x,t) = 0 \qquad vt \leq x \leq \ell$$

The following transient pressure form is represented by the superposition of right and left traveling sinusoid loads. Thus for the interval of time

$$t_o \leq t \leq t_o + \frac{e}{v}$$

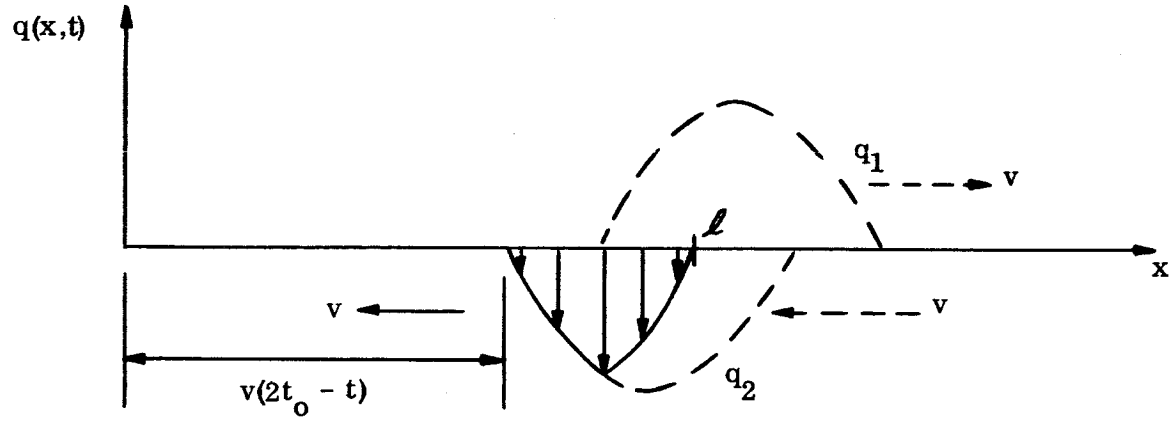

Right traveling load

$$q_1(x,t) = 0 \qquad 0 \leq x \leq vt - e$$

$$q_1(x,t) = -p \sin \pi \frac{(x-vt)}{e} \qquad vt - e \leq x \leq \ell \qquad (2\text{-}16)$$

Left traveling load

$$q_2(x,t) = 0 \qquad 0 \leq x \leq 2\ell - vt$$

$$q_2(x,t) = -p \sin \pi \frac{(x + vt - 2\ell)}{e} \qquad 2\ell - vt \leq x \leq \ell \qquad (2\text{-}17)$$

For

$$t_o + \frac{e}{v} \leq t \leq 2\, t_o$$

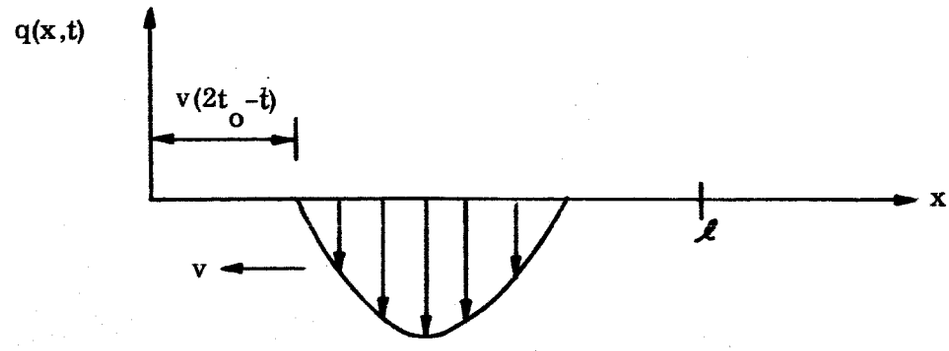

$$
\begin{aligned}
q(x,t) &= 0 && 0 \le x \le 2\ell - vt \\
q(x,t) &= -p \sin\pi\left(\frac{x + vt - 2\ell}{e}\right) && 2\ell - vt \le x \le 2\ell - vt + e \\
q(x,t) &= 0 && 2\ell - vt + e \le x \le \ell
\end{aligned}
\qquad (2\text{-}18)
$$

Finally, the expressions for the interval $2\,t_o \le t \le 2\,t_o + \frac{e}{v}$ as shown in the sketch below is given by the superposition of

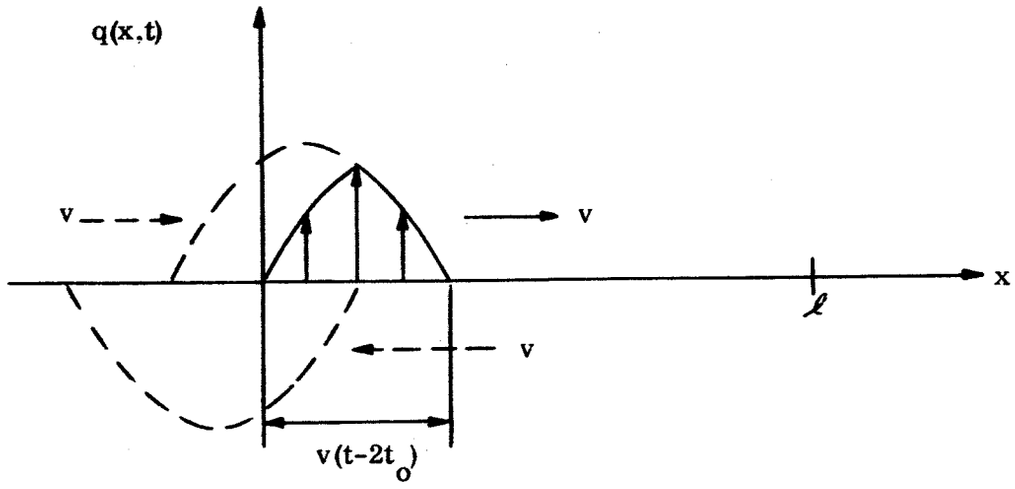

The right traveling load defined for the interval $0 \le t \le \frac{e}{v}$ and the left traveling load defined by

$$
\begin{aligned}
q(x,t) &= -p \sin\pi\,\frac{(x + vt - 2\ell)}{e} && 0 \le x \le 2\ell - vt + e \\
q(x,t) &= 0 && 2\ell - vt + e \le x \le \ell
\end{aligned}
\qquad (2\text{-}19)
$$

As was the case for the ramp, the defined pressures are used in sequence as time progresses.

In the limit as $e \rightarrow 0$, and the area under the pressure distribution curve $\rightarrow P$ the sinusoidal pressure will approach the spike pressure transient case which is illustrated in Figure III-9.

A. REFERENCES

2-1. E. Ring, "Rocket Propellant and Pressurization Systems," Chapter 7, Prentice-Hall, Inc., Englewood Cliffs, N.J., 1964, pp. 44-60.

2-2. J. Parmakian, "Waterhammer Analysis, "Prentice-Hall, Inc., New York, 1955.

2-3. G.R. Rich, "Hydraulic Transients," 2nd. Ed., Dover Publications, Inc., New York, 1963.

III. THEORETICAL DEVELOPMENT

A. BASIC EQUATIONS

For purposes of the present investigation, the basic structural model is the thin-walled cylindrical shell of circular cross-section. It will be assumed that the shell is made of an elastic, homogeneous, isotropic material, that it is loaded in an axi-symmetric manner, and that its deformation is due to stretching and flexure, shear deformations being neglected for the present. Moreover, it is assumed that the shell wall thickness is small compared to the shell radius, i.e., $h \ll R$.

In accordance with these stipulations, a free-body diagram of the shell element is shown in Figure III-1. Summing forces in the w direction and then taking the limit as $\Delta x \rightarrow 0$, $\Delta \theta \rightarrow 0$ we obtain

$$\frac{\partial Q_x}{\partial x} - \frac{N_\phi}{R} + \bar{q} = 0 \tag{3-1}$$

Taking moments about an axis which is perpendicular with respect to the X-Z plane and taking the same limit, we obtain

$$Q_x + \frac{\partial M_x}{\partial x} = 0 \tag{3-2}$$

Equations (3-1) and (3-2) are the equilibrium equations of the shell. The appropriate strain-displacement relations are

$$\epsilon_x = \frac{\partial u}{\partial x}, \quad \epsilon_\phi = \frac{w}{R} \tag{3-3}$$

and the stress-strain relations (Hooke's law) are

$$N_x = \frac{Eh}{1-\nu^2}(\epsilon_x + \nu\epsilon_\phi)$$

$$N_\phi = \frac{Eh}{1-\nu^2}(\epsilon_\phi + \nu\epsilon_x) \tag{3-4}$$

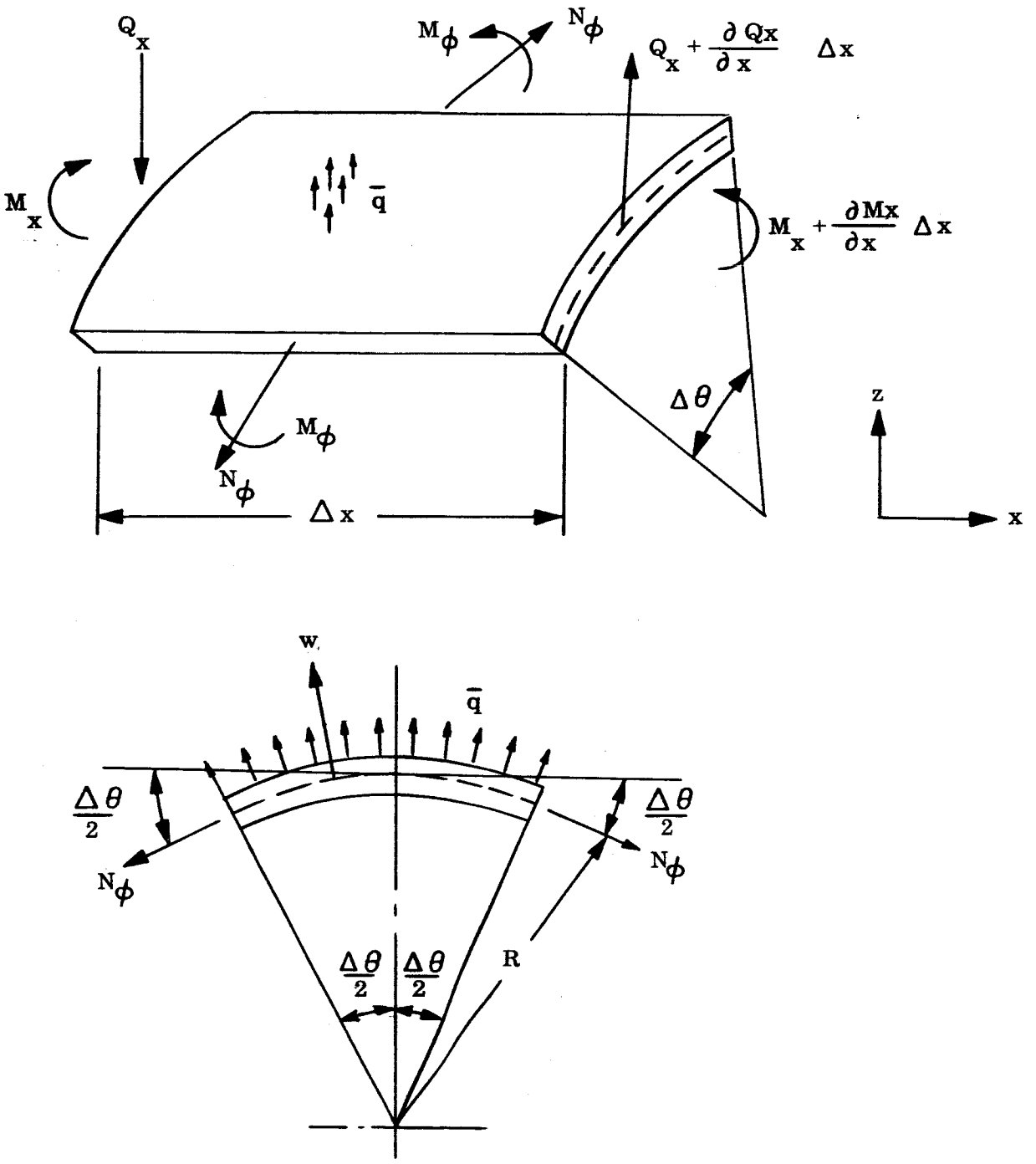

Figure III-1.. Shell Element

It will be assumed (see reference 3-i) that $N_x = 0$. Upon substitution of equation's (3-3) into equation's (3-4) we have

$$N_x = \frac{Eh}{1-\nu^2}\left(\frac{\partial u}{\partial x} + \nu \frac{w}{R}\right) = 0$$

$$N_\phi = \frac{Eh}{1-\nu^2}\left(\frac{w}{R} + \nu \frac{\partial u}{\partial x}\right) = 0 \qquad (3\text{-}5)$$

Thus

$$\frac{\partial u}{\partial x} = -\frac{w}{R}\nu \qquad (3\text{-}6)$$

and

$$N_\phi = \frac{Eh}{R} w \qquad (3\text{-}7)$$

From classical thin-plate theory, we have (Reference 3-2)

$$M_\phi = \nu M_x \qquad (3\text{-}8)$$

$$M_x = D \frac{\partial^2 w}{\partial x^2} \qquad (3\text{-}9)$$

where $D = Eh^3/12(1-\nu^2)$. Combining equations (3-1), (3-2), (3-7) and (3-9) we obtain

$$D \frac{\partial^4 w}{\partial x^4} + \frac{Eh}{R^2} w = \bar{q} \qquad (3\text{-}10)$$

The normal force intensity $\bar{q}$ is now decomposed into three distinct parts:

inertia force = $-m \dfrac{\partial^2 w}{\partial t^2}$

damping force = $-2c \dfrac{\partial w}{\partial t}$

surface traction = $q(x, t)$

Therefore

$$\bar{q} = q - 2c\frac{\partial w}{\partial t} - m\frac{\partial^2 w}{\partial t^2} \tag{3-11}$$

and equation (3-10) becomes

$$D\frac{\partial^4 w}{\partial x^4} + \frac{Eh}{R^2} w + 2c\frac{\partial w}{\partial t} + m\frac{\partial^2 w}{\partial t^2} = q(x, t) \tag{3-12}$$

Equation (3-12) is regarded as the basic equation for the present investigation.

B. SHELL OF INFINITE LENGTH

1. Spike Pressure Wave

A solution of equation (3-12) will now be developed for a shell of unbounded length under neglect of damping (c = 0). The shell is assumed to be subjected to a spike loading of magnitude P (ring-line load, see Figure III-2) which translates with uniform speed v in the direction of the shell axis x.

As a prerequisite for a unique solution, we require certain basic physical shell properties with respect to wave propagation along the x-axis. Under neglect of damping and assuming zero surface tractions, equation (3-12) assumes the form

$$D\frac{\partial^4 w}{\partial x^4} + \frac{Eh}{R^2} w + m\frac{\partial^2 w}{\partial t^2} = 0 \tag{3-13}$$

If we assume the existence of waves of the type

$$w = e^{i(kx - \Gamma t)} \tag{3-14}$$

where k is the wave number and Γ is the frequency, and substitute equation (3-14) into equation (3-13), we obtain the following dispersion relation (relation between frequency and wave number):

$$\Gamma = \sqrt{\frac{D}{m} k^4 + \frac{Eh}{m R^2}} \tag{3-15}$$

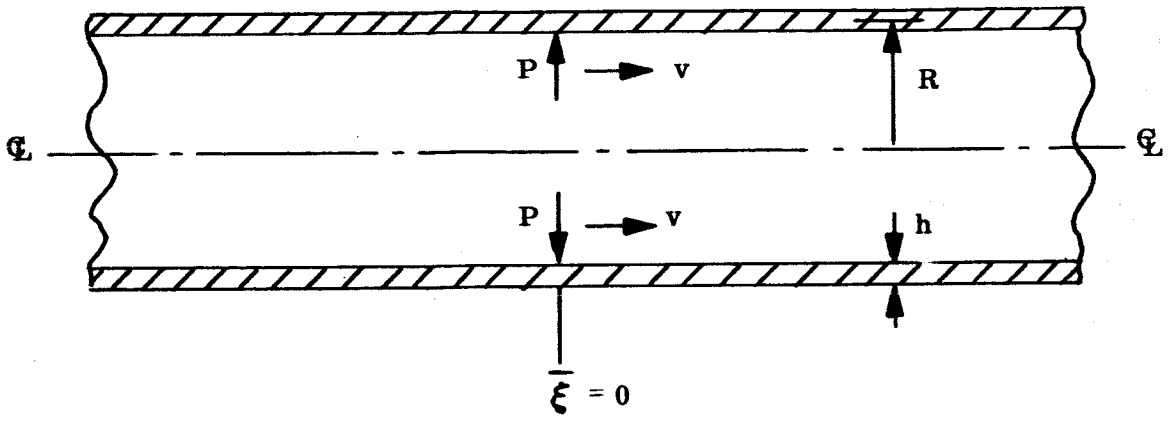

Figure III-2. Infinite Duct ~ Moving Spike

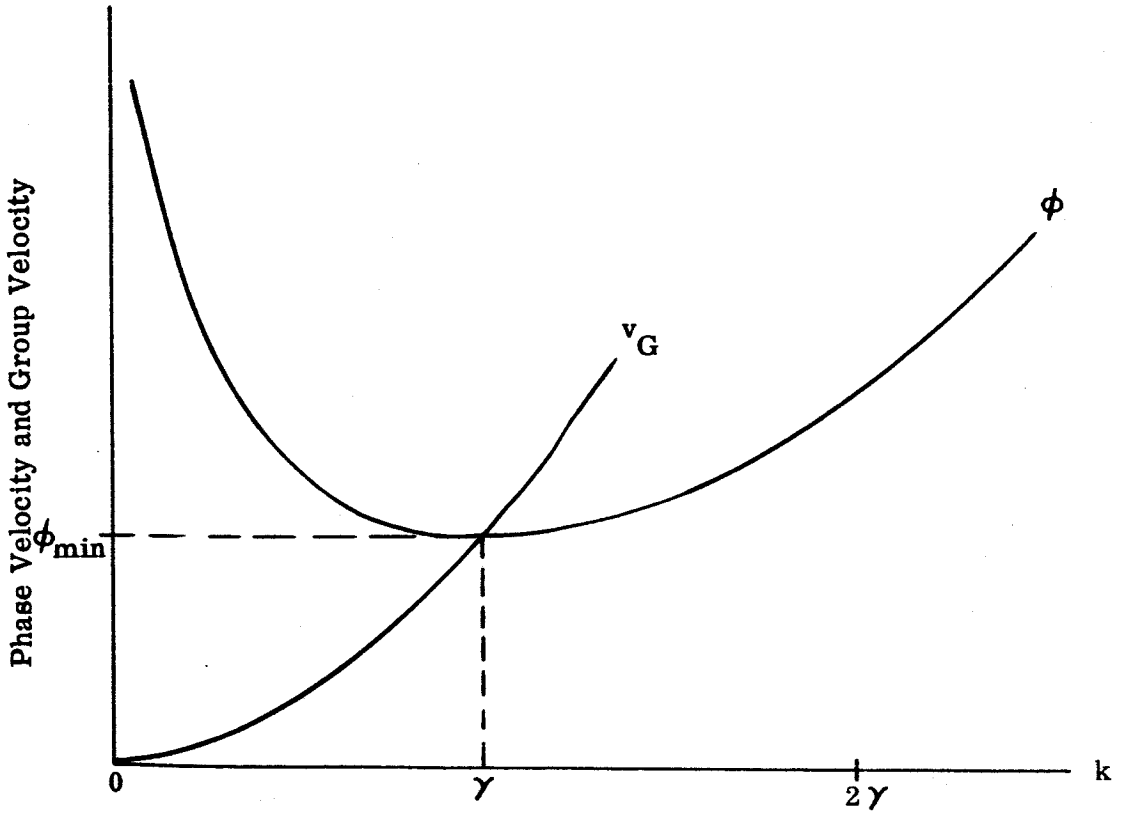

Figure III-3. Phase and Group Velocity versus Wave Number

The phase velocity ϕ is given by (see Reference 3-3)

$$\phi = \frac{\Gamma}{k} = \sqrt{\frac{D}{m} k^2 + \frac{Eh}{mR^2 k^2}} \tag{3-16}$$

and the group velocity is

$$v_G = \frac{d\Gamma}{dk} = \frac{\frac{2D}{m} k^3}{\sqrt{\frac{D}{m} k^4 + \frac{Eh}{mR^2}}} \tag{3-17}$$

A typical plot of phase and group velocity, using equations (3-16) and (3-17), is shown in Figure III-3. The following general statement can be proved by elementary means with the help of equations (3-16) and (3-17): The minimum phase velocity occurs at the point where the phase velocity and group velocity are equal. At that point, the wave number has the value $k = \gamma = \sqrt[4]{\frac{Eh}{R^2 D}}$. We shall use this result in the subsequent development.

It will be convenient to nondimensionalize the coordinate x and to describe the response of the shell in a moving coordinate system. Thus we let

$$\bar{\xi} = (x - v t)\gamma \tag{3-18}$$

where $\gamma = \sqrt[4]{\frac{Eh}{DR^2}}$

If we change variables in equation (3-12) in accordance with equation (3-18) and neglect damping, we obtain

$$\frac{d^4 w}{d\bar{\xi}^4} + 2\lambda \frac{d^2 w}{d\bar{\xi}^2} + w = \frac{R^2}{Eh} q(\bar{\xi}) \tag{3-19}$$

where

$$2\lambda = \frac{\sqrt{12(1-\nu^2)}\, mRv^2}{Eh^2} \tag{3-20}$$

The change of variable, equation (3-18), may be given the following physical interpretation: An observer fixed with respect to the x-coordinate will see the (spike) load advance in the direction of the positive x-axis, and to him the deflection of the shell will appear to be a function of x and t. However, an observer fixed with respect to the $\bar{\xi}$ -axis will move with the advancing load and to him the deflection surface will appear stationary, i.e., independent of t and a function of $\bar{\xi}$ alone. We note that by neglecting damped transients due to the starting of the motion, we have made the implicit assumption that the load has been moving for a sufficiently long period. Thus, we shall concentrate on the steady-state dynamical process as characterized by equation (3-19).

A formal solution of equation (3-19) will be obtained by the Fourier Transform Approach. We define the following (complex) Fourier transform pairs:

$$w(\bar{\xi}) = \frac{1}{\sqrt{2\pi}} \int_{-\infty}^{\infty} W(\alpha)\, e^{-i\bar{\xi}\alpha}\, d\alpha \qquad (3\text{-}21a)$$

$$W(\alpha) = \frac{1}{\sqrt{2\pi}} \int_{-\infty}^{\infty} w(\bar{\xi})\, e^{i\alpha\bar{\xi}}\, d\bar{\xi} \qquad (3\text{-}21b)$$

$$q(\bar{\xi}) = \frac{1}{\sqrt{2\pi}} \int_{-\infty}^{\infty} Q(\alpha)\, e^{-i\bar{\xi}\alpha}\, d\alpha \qquad (3\text{-}22a)$$

$$Q(\alpha) = \frac{1}{\sqrt{2\pi}} \int_{-\infty}^{\infty} q(\bar{\xi})\, e^{i\alpha\bar{\xi}}\, d\bar{\xi} \qquad (3\text{-}22b)$$

We now Fourier transform equation (3-19) with respect to $\bar{\xi}$, i.e., we multiply each term of equation (3-19) by $e^{i\alpha\bar{\xi}}\, d\bar{\xi}$ and integrate between the limits $-\infty < \bar{\xi} < \infty$ If it is assumed that $w(\bar{\xi}) \to 0$, $w'(\bar{\xi}) \to 0$, $w''(\bar{\xi}) \to 0$, $w'''(\bar{\xi}) \to 0$ as $\bar{\xi} \to \pm\infty$ then we obtain

$$W(\alpha) = \frac{R^2}{Eh} \quad \frac{Q(\alpha)}{(\alpha^4 - 2\lambda\alpha^2 + 1)} \qquad (3\text{-}23)$$

Upon substitution of equation (3-23) into equation (3-21a), we obtain the formal solution of equation (3-19):

$$w(\bar{\xi}) = \frac{R^2}{\sqrt{2\pi}} \quad \frac{1}{Eh} \quad \int_{-\infty}^{\infty} \frac{Q(\alpha)\, d\alpha}{(\alpha^4 - 2\lambda\ \alpha^2 + 1)} \tag{3-24}$$

To obtain the Fourier transform representation of the spike load, we shall consider the limiting case of a uniformly distributed load. With reference to Figure III-4, we have

$$\begin{aligned} q(\bar{\xi}) &= 0, \qquad \bar{\xi} > |\beta| \\ q(\bar{\xi}) &= p, \qquad \bar{\xi} < |\beta| \end{aligned} \tag{3-25}$$

Thus, using equation (3-22b), we have

$$Q(\alpha) = \frac{1}{\sqrt{2\pi}} \int_{-\infty}^{\infty} p\, e^{\ i\alpha\bar{\xi}}\ d\bar{\xi} = \frac{\gamma}{\sqrt{2\pi}} \frac{2\beta p}{\gamma} \quad \frac{\sin \alpha\beta}{\alpha\beta}$$

If we now take the limit of $Q(\alpha)$ as $\beta \rightarrow 0$ and $\frac{2\beta p}{\gamma} \rightarrow P$ we obtain the Fourier transform representation of the traveling spike load:

$$Q(\alpha) = \frac{\gamma}{\sqrt{2\pi}} \quad P \tag{3-26}$$

The improper integral in equation (3-24) will now be evaluated, when $Q(\alpha)$ is given by equation (3-26), by the method of the calculus of residues. There will be two distinct cases which must be considered: The poles of the integrand in equation (3-24) are (a) complex and (b) real. In case (a) equation (3-24) assumes the form

$$w(\bar{\xi}) = \frac{\gamma R^2 P}{2\pi Eh} \quad \int_{-\infty}^{\infty} \frac{e^{\ -i\bar{\xi}\alpha}\ d\alpha}{(\alpha\ -a-ib)\ (\alpha\ +a+ib)\ (\alpha\ -a+ib)\ (\alpha\ +a-ib)} \tag{3-27}$$

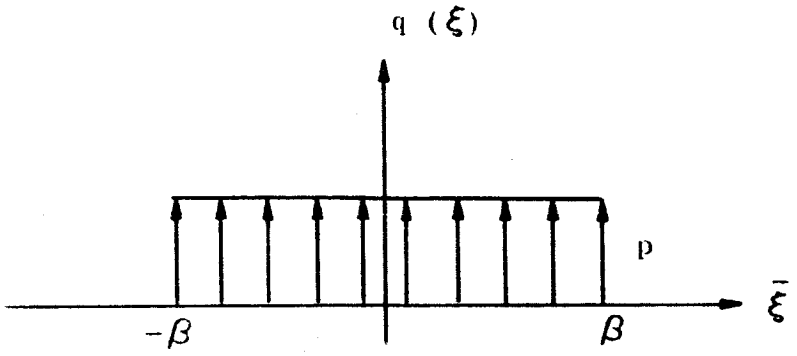

Figure III-4. Load Distribution

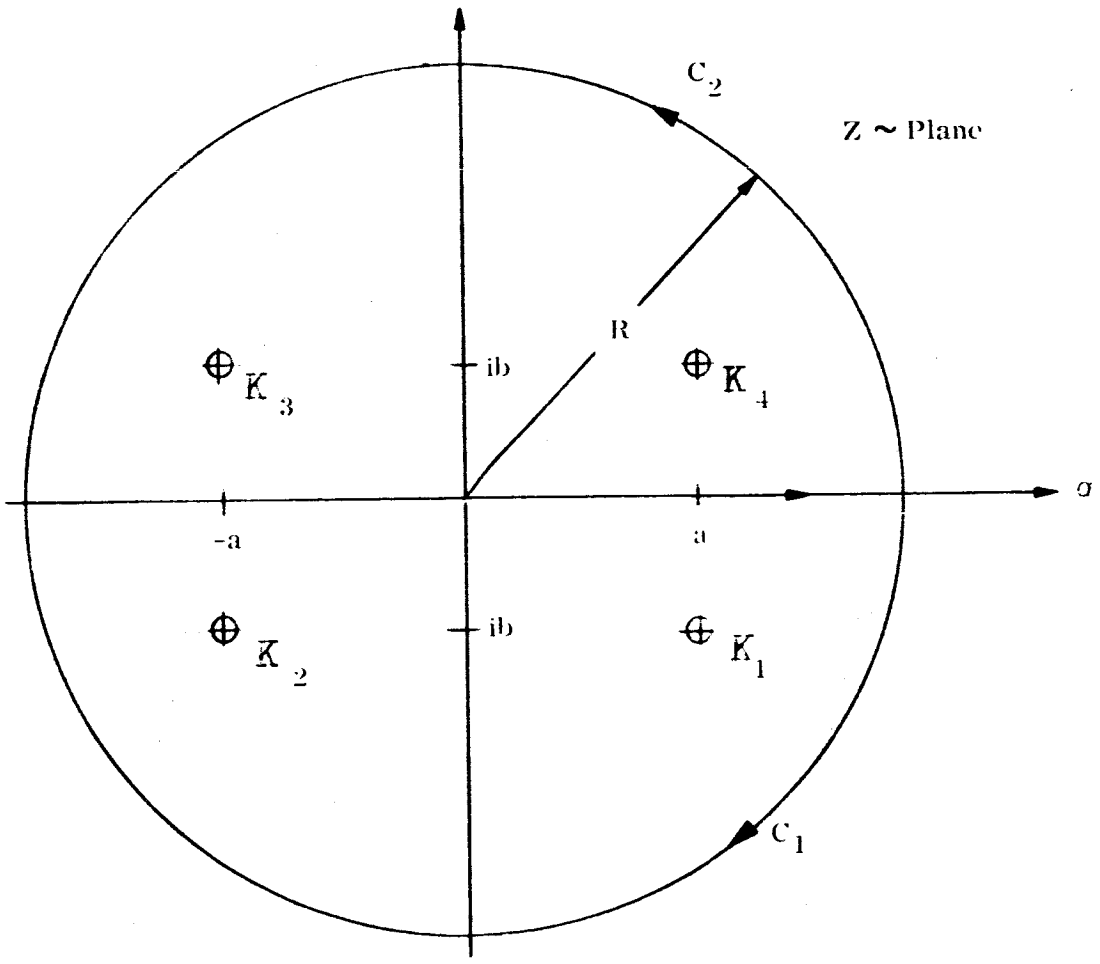

Figure III-5. Contour of Integration, $\lambda < 1$, (Spike Load)

where

$$a = \sqrt{\frac{1+\lambda}{2}} \qquad b = \sqrt{\frac{1-\lambda}{2}} \tag{3-28}$$

and $\lambda <$ 1. It will be convenient to consider the following contour integral in the complex z plane:

$$I = \oint \frac{e^{-i\bar{\xi} z}\, dz}{(z-a-ib)\,(z+a+ib)\,(z-a+ib)\,(z+a-ib)} \tag{3-29}$$

The contour over which this integral is to be evaluated consists of (see Figure III-5) the upper or lower semi-circle of radius R and the segment of the real axis $R > |a|$. It is easy to show that the line integral, equation (3-29), vanishes for $\bar{\xi} < 0$ when taken over the upper semi-circle C_2 as $R \to \infty$. Similarly, it vanishes for $\bar{\xi} > 0$ when taken over the lower semi-circle C_1 as $R \to \infty$. Thus by virtue of the residue theorem we have for $\bar{\xi} \geq 0$

$$w(\bar{\xi}) = \frac{\gamma R^2 P}{2\pi Eh} \cdot 2\pi i\,(K_1 + K_2), \quad \bar{\xi} \geq 0 \tag{3-30a}$$

$$w(\bar{\xi}) = \frac{\gamma R^2 P}{2\pi Eh} \cdot 2\pi i\,(K_3 + K_4), \quad \bar{\xi} \leq 0 \tag{3-30b}$$

where

$$K_1 = \frac{e^{-i\bar{\xi}\,(a-ib)}}{(-2ib)\,(2a)\,(2)\,(a-ib)} \tag{3-31a}$$

$$K_2 = \frac{e^{-i\bar{\xi}\,(-a-ib)}}{(2)\,(-a-ib)\,(-2a)\,(-2ib)} \tag{3-31b}$$

$$K_3 = \frac{e^{-i\bar{\xi}\,(-a+ib)}}{(-2a)\,(2ib)\,(2)\,(-a+ib)} \tag{3-31c}$$

$$K_4 = \frac{e^{-i\bar{\xi}\,(a+ib)}}{(2)\,(a+ib)\,(2ib)\,(2a)} \tag{3-31d}$$

Upon combination of equations (3-30) and (3-31) and a certain amount of simplification we obtain the solution of equation (3-19) valid for $\lambda < 1$:

$$w(\bar{\xi}) = \frac{R^2 \gamma P}{Eh} \frac{e^{-b\bar{\xi}}}{(4ab)} (a \cos a\bar{\xi} + b \sin a\bar{\xi}), \quad \bar{\xi} \geq 0 \qquad (3\text{-}32a)$$

$$w(\bar{\xi}) = \frac{R^2 \gamma P}{Eh} \frac{e^{b\bar{\xi}}}{(4ab)} (a \cos a\bar{\xi} - b \sin a\bar{\xi}), \quad \bar{\xi} \leq 0 \qquad (3\text{-}32b)$$

where a and b are defined in equation (3-28).

In case (b) where $\lambda > 1$ we must proceed in a different manner. In this case the poles of the integrand of equation (3-24) lie on the real axis, and it is appropriate to write equation (3-24) as

$$w(\bar{\xi}) = \frac{R^2 \gamma P}{2\pi Eh} \int_{-\infty}^{\infty} \frac{e^{i\bar{\xi}\alpha} \, d\alpha}{(\alpha + A)(\alpha - A)(\alpha + B)(\alpha - B)} \qquad (3\text{-}33)$$

where

$$A = a + b, \qquad B = a - b$$
$$a = \sqrt{\frac{\lambda + 1}{2}}, \qquad b = \sqrt{\frac{\lambda - 1}{2}} \qquad (3\text{-}34)$$

and $\lambda > 1$. The improper integral in equation (3-33) will be evaluated by residue calculus, and the method is analagous to the case $\lambda < 1$ except for the path of integration in the vicinity of the poles (see Figure III-6), where the path is indented. The association of the poles with the upper or lower half plane depends on physical (energy) considerations. With reference to Figure III-3, we note that corresponding to a given phase velocity greater than ϕ_{min}, there are two wave numbers k_1, k_2, one of them, $k_1 < \gamma$, the other $\gamma < k_2$. For k_2, the group velocity is always greater than the phase velocity, and therefore this represents waves moving ahead of the spike at $\bar{\xi} = 0$. For the

smaller wave number k_1, the group velocity is always smaller than the phase velocity, and therefore k_1 corresponds to waves behind the spike. Since energy must travel away from the moving spike disturbance, it becomes clear from the foregoing that the poles at $\alpha = \pm A$ are associated with the case $\bar{\xi} > 0$, while the poles at $\alpha = \pm B$ are associated with the case $\bar{\xi} < 0$. This explains the manner of indentation of the contour in Figure III-6. Thus, invoking the residue theorem we have

$$w(\bar{\xi}) = -\frac{\gamma R^2 P}{2\pi Eh} \cdot 2\pi i (K_1 + K_2), \quad \bar{\xi} > 0 \tag{3-35a}$$

$$w(\bar{\xi}) = \frac{\gamma R^2 P}{2\pi Eh} \cdot 2\pi i (K_3 + K_4), \quad \xi < 0 \tag{3-35b}$$

where K_1, K_2 K_3 and K_4 are the values of the residue of the integrand function of equation (3-33) at $\alpha = A, -A, B, -B$, respectively. These values are given by

$$K_1 = \frac{e^{+i\bar{\xi}A}}{(2A)(A+B)(A-B)} \tag{3-36a}$$

$$K_2 = \frac{e^{-i\bar{\xi}A}}{(-2A)(-A+B)(-A-B)} \tag{3-36b}$$

$$K_3 = \frac{e^{+i\bar{\xi}B}}{(B+A)(B-A)(2B)} \tag{3-36c}$$

$$K_4 = \frac{e^{-i\bar{\xi}B}}{(A-B)(A+B)(2B)} \tag{3-36d}$$

If we now combine equation's (3-35) and (3-36) and simplify, we obtain the solution for $\lambda > 1$:

$$\begin{aligned} w(\bar{\xi}) &= -\frac{\gamma R^2 P}{Eh} \frac{1}{A(A^2 - B^2)} \sin A\bar{\xi}, \quad \bar{\xi} > 0 \\ w(\bar{\xi}) &= \frac{\gamma R^2 P}{Eh} \frac{1}{B(B^2 - A^2)} \sin B\bar{\xi}, \quad \bar{\xi} < 0 \end{aligned} \tag{3-37}$$

where A and B are defined in equation (3-34).

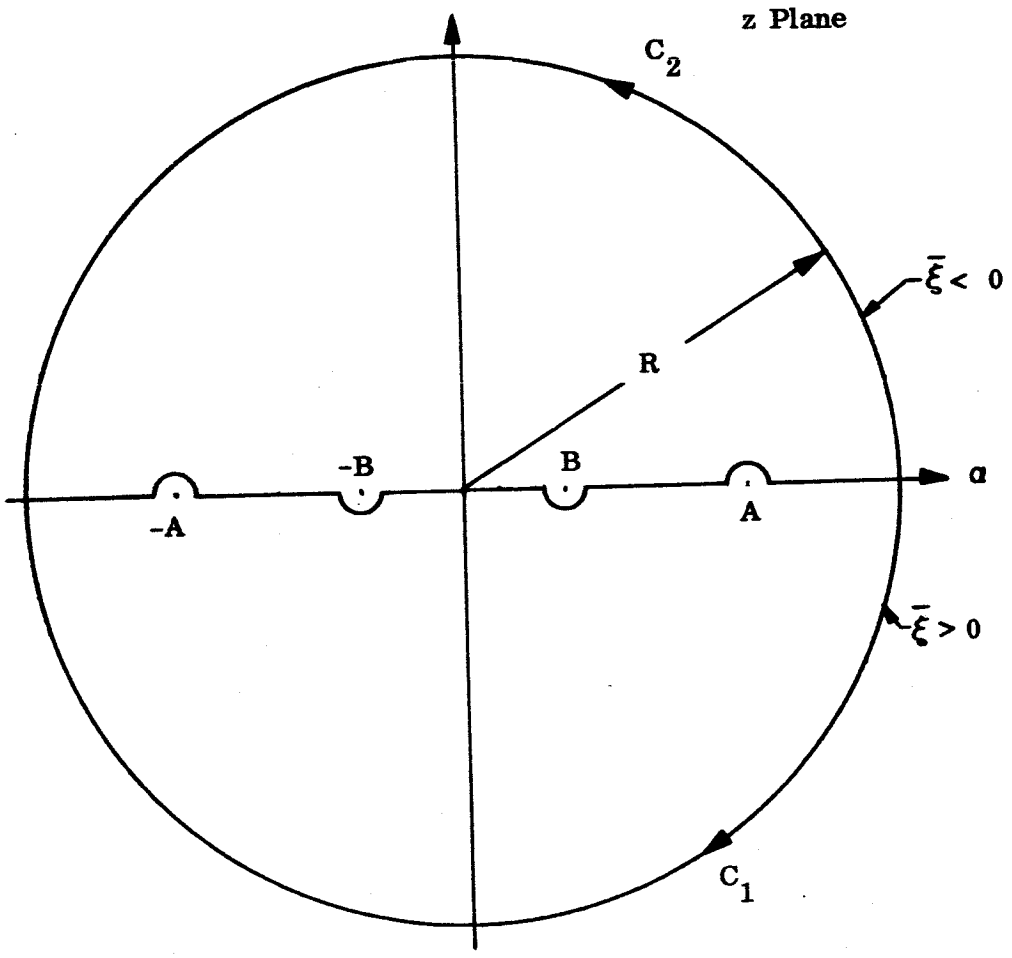

Figure III-6.. Contour of Integration, $\lambda > 1$, (Spike Load)

2. Step Pressure Wave Shape

We now consider a shell of unbounded length subjected to a uniformly distributed radial pressure load of intensity p advancing in the positive x-direction as shown in Figure III-7. The load is characterized by

$$q = p = \text{constant}, \quad \bar{\xi} < 0$$
$$q = 0, \quad \bar{\xi} > 0 \tag{3-38}$$

With reference to Equation (3-19) we have

$$\frac{d^4 w^{(1)}}{d\bar{\xi}^4} + 2\lambda \frac{d^2 w^{(1)}}{d\bar{\xi}^2} + w^{(1)} = 0 \tag{3-39}$$

$$\frac{d^4 w^{(2)}}{d\bar{\xi}^4} + 2\lambda \frac{d^2 w^{(2)}}{d\bar{\xi}^2} + w^{(2)} = \frac{pR^2}{Eh}$$

where the superscripts (1) and (2) refer to the region $\bar{\xi} > 0$ and $\bar{\xi} < 0$, respectively. Solution of Equation (3-39) must be bounded for $\bar{\xi} \to \pm\infty$, and at $\bar{\xi} = 0$ we require that the deflection, slope, moment, and shear be continuous, i.e.,

$$w^{(1)}(0) = w^{(2)}(0)$$

$$\left(\frac{dw^{(1)}}{d\bar{\xi}}\right)_{\bar{\xi}=0} = \left(\frac{dw^{(2)}}{d\bar{\xi}}\right)_{\bar{\xi}=0}$$

$$\left(\frac{d^2 w^{(1)}}{d\bar{\xi}^2}\right)_{\bar{\xi}=0} = \left(\frac{d^2 w^{(2)}}{d\bar{\xi}^2}\right)_{\bar{\xi}=0} \tag{3-40}$$

$$\left(\frac{d^3 w^{(1)}}{d\bar{\xi}^3}\right)_{\bar{\xi}=0} = \left(\frac{d^3 w^{(2)}}{d\bar{\xi}^3}\right)_{\bar{\xi}=0}$$

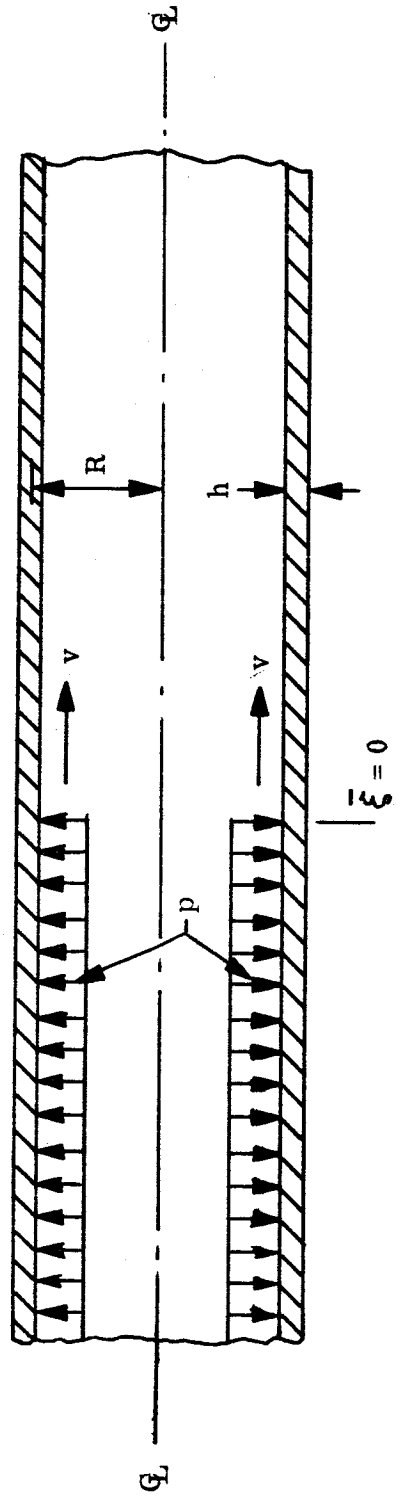

Figure III-7. Infinite Duct ~ Step Pressure Wave Shape

The characteristic equation obtained by assuming $w^{(i)} = e^{\alpha \bar{\xi}}$, i = 1, 2; α = constant, and substituting in the homogeneous Equation (3-39) is: $\alpha^4 + 2\lambda\alpha^2 + 1 = 0$ (3-41)

and its roots are

$$\sqrt{2}\ \alpha = \pm\left(\sqrt{-\lambda - 1} \pm \sqrt{1 - \lambda}\right) \tag{3-42}$$

Evidently the roots of Equation (3-41) are complex for $0 < \lambda < 1$ and pure imaginary for $1 < \lambda$. Solutions of Equation (3-39) subject to the conditions prescribed by Equation (3-40) and bounded at $\bar{\xi} \to \pm\infty$ are found in the usual manner when the roots of the characteristic equation are complex ($0 < \lambda < 1$):

$$\frac{w^{(1)}}{w_o} = \frac{e^{-a\bar{\xi}}}{2}\left(\cos b\,\bar{\xi} + \frac{a^2 - b^2}{2ab}\sin b\,\bar{\xi}\right),\ \bar{\xi} \geq 0$$

$$\frac{w^{(2)}}{w_o} = \frac{e^{a\bar{\xi}}}{2}\left(-\cos b\,\bar{\xi} + \frac{a^2 - b^2}{2ab}\sin b\,\bar{\xi}\right) + 1,\ \bar{\xi} \leq 0 \tag{3-43}$$

where

$$\sqrt{2}\ a = \sqrt{1 - \lambda}\ ; \quad \sqrt{2}\ b = \sqrt{1 + \lambda}$$

$$w_o = \frac{p R^2}{Eh}$$

In the case of pure imaginary roots ($1 < \lambda$), the solutions of Equation (3-39) are

$$w^{(1)} = C_1^{(1)} \cos a\,\bar{\xi} + C_2^{(1)} \sin a\,\bar{\xi} + C_3^{(1)} \cos b\,\bar{\xi} + C_4^{(1)} \sin b\,\bar{\xi}$$

$$w^{(2)} = C_1^{(2)} \cos b\,\bar{\xi} + C_2^{(2)} \sin b\,\bar{\xi} + C_3^{(2)} \cos a\,\bar{\xi} + C_4^{(2)} \sin a\,\bar{\xi} \tag{3-44}$$

where

$$\sqrt{2}\ a = \sqrt{1 + \lambda} + \sqrt{-1 + \lambda}$$

$$\sqrt{2}\ b = \sqrt{1 + \lambda} - \sqrt{-1 + \lambda}$$

and there are only four equations (3-40) to determine the eight constants of integration $C_i^{(j)}$, i = 1, 2, 3, 4,; j = 1, 2. At this point we may use the concept of group velocity to determine the appropriate steady state motion. The group velocity

is the velocity of energy transport, and the physically appropriate solution requires a flow of energy away from the load front. With reference to Figure III-3, we note that corresponding to a given phase velocity greater than ϕ_{min}, there are two wave numbers, k_1 and k_2, one of them $k_1 < \gamma$, the other $\gamma < k_2$. For k_2, the group velocity is always greater than the phase velocity, and therefore this represents waves moving ahead of the load front at $\bar{\xi} = 0$. For the smaller wave number k_1, the group velocity is always smaller than the phase velocity, and therefore k_1 corresponds to waves behind the load front. Since $a > b$, this argument enables us to set

$$C_3^{(1)} = C_4^{(1)} = C_3^{(2)} = C_4^{(2)} = 0$$

in Equation (3-44). The remaining constants in Equation (3-44) are now determined by applying continuity conditions expressed by Equation (3-40), and the results are ($1 < \lambda$):

$$\frac{w^{(1)}}{w_o} = -\frac{b^2 \cos a\bar{\xi}}{a^2 - b^2}; \quad \bar{\xi} \geq 0$$

$$\frac{w^{(2)}}{w_o} = -\frac{a^2 \cos b\bar{\xi}}{a^2 - b^2} + 1; \quad \bar{\xi} \leq 0 \qquad (3\text{-}45)$$

where

$$\sqrt{2}\, a = \sqrt{1+\lambda} + \sqrt{-1+\lambda}$$

$$\sqrt{2}\, b = \sqrt{1+\lambda} - \sqrt{-1+\lambda}$$

$$w_o = \frac{pR^2}{Eh}$$

C. SHELL OF FINITE LENGTH

1. General Development for Arbitrary Homogeneous Boundary Conditions

a. Free Vibrations

We assume a solution of the form

$$w = W(x) \cdot T(t) \tag{3-46}$$

of the homogeneous Equation (3-12) (i.e., $q = 0$). Upon substitution of Equation (3-46) into Equation (3-12), division by $W \cdot T$, and some re-arrangement, we obtain a separation of variables

$$-\frac{m}{D}\frac{\ddot{T}}{T} - \frac{2c}{D}\frac{\dot{T}}{T} = \frac{W^{IV}}{W} + \frac{Eh}{DR^2} = \frac{m\omega^2}{D} \tag{3-47}$$

where ω^2 is an undetermined constant.

Consequently

$$\ddot{T} + \frac{2c}{m}\dot{T} + \omega^2 T = 0 \tag{3-48}$$

and

$$W^{IV} - k^4 W = 0 \tag{3-49}$$

where

$$k^4 = \frac{m}{D}\omega^2 - \frac{Eh}{DR^2} \tag{3-50}$$

The admissible, homogeneous boundary conditions corresponding to Equation (3-49) may be stated as follows:

One member of each of the products

(wQ), $(w'M)$

vanishes at $x = 0, \ell$.

It can be shown (see Reference 3-4) that for a given set of homogeneous (admissable) boundary conditions there exists a denumerable infinity of mode shapes W_n,

$n = 1, 2, 3, \ldots$ which satisfy Equation (3-49). Moreover, corresponding to each mode shape W_n there is a natural frequency ω_n, and vice versa. These mode shapes satisfy the orthogonality relation

$$\int_0^{\ell} W_m(x) \cdot W_n(x)\, dx = 0 \tag{3-51}$$

provided $m \neq n$. For instance, when the ends of the shell are simply supported we have

$$W_n = W_n'' = 0, \text{ at } x = 0 \text{ and } x = \ell \tag{3-52}$$

In this case the solution of Equation (3-49) which satisfies the boundary conditions, Equation (3-52), is

$$W_n(x) = \sin \frac{n\pi x}{\ell}, \quad n = 1, 2, 3, \ldots \tag{3-53}$$

and the associated frequencies are

$$\omega_n^2 = \frac{1}{m}\left(\frac{Eh}{R^2} + \frac{n^4 \pi^4}{\ell^4} D\right) \tag{3-54}$$

When the ends of the shell are clamped we require

$$W_n = W_n' = 0 \quad \text{at} \quad x = 0 \quad \text{and} \quad x = \ell \tag{3-55}$$

In this case the mode shapes are given by

$$W_n(x) = \cosh k_n x - \cos k_n x - \alpha_n (\sinh k_n x - \sin k_n x) \tag{3-56}$$

where

$$\alpha_n = \frac{\cos k_n \ell - \cosh k_n \ell}{\sin k_n \ell - \sinh k_n \ell}$$

and $k_n \ell$ are the roots of the equation

$$\cos k_n \ell \cdot \cosh k_n \ell = 1$$

Frequencies associated with the mode shapes of Equation (3-56) are given by

$$\omega_n^2 = \frac{D}{m}\left(k_n^4 + \frac{Eh}{DR^2}\right) \qquad (3\text{-}57)$$

where $n = 1, 2, 3, \ldots$

b. Forced Vibration

We now consider the complete Equation (3-12) and assume a solution of the form

$$w(x, t) = \sum_{n = 1, 2 \ldots}^{\infty} T_n(t) \cdot W_n(x) \qquad (3\text{-}58)$$

Upon substitution of Equation (3-58) into Equation (3-12), and subsequent utilization of Equation (3-47) we obtain

$$\sum_{n = 1, 2, \ldots}^{\infty} \left(\ddot{T}_n + \frac{2c}{m}\dot{T}_n + \omega_n^2 T_n\right) W_n = \frac{1}{m} q(x, t) \qquad (3\text{-}59)$$

Both sides of Equation (3-59) are now multiplied by $W_m(x)$, and are then integrated over the length of the duct. Upon application of the orthogonality relation, Equation (3-51), we obtain

$$\ddot{T}_n + \frac{2c}{m}\dot{T}_n + \omega_n^2 T_n = \frac{4}{m\ell K_n}\int_o^{\ell} q(x, t) \cdot W_n(x)\, dx \qquad (3\text{-}60)$$

where

$$K_n = \frac{4}{\ell}\int_o^{\ell} W_n^2(x)\, dx \qquad (3\text{-}61)$$

The initial conditions for the duct are now translated into the initial conditions on T_n. At $t = 0$ we have (see Equation (3-58)

$$w(x, o) = w_o(x) = \sum_{n = 1, 2, \ldots}^{\infty} T_n(o) \cdot W_n(x) \qquad (3\text{-}62)$$

$$\dot{w}\ (x,\ o) = \dot{w}_o\ (x) = \sum_{n\ =\ 1,\ 2,\ \ldots}^{\infty} \dot{T}_n\ (o) \cdot W_n\ (x) \qquad (3\text{-}63)$$

Multiply Equation (3-62) by $W_m\ (x)$ and integrate the result over the length of the shell. Upon application of Equation (3-51) we obtain

$$T_n\ (o) = \frac{4}{\ell K_n} \int_o^{\ell} w_o\ (x)\ W_n\ (x)\ dx \qquad (3\text{-}64)$$

A similar procedure, when applied to Equation (3-63) results in

$$\dot{T}_n\ (o) = \frac{4}{\ell K_n} \int_o^{\ell} \dot{w}_o\ (x)\ \ W_n\ (x)\ dx \qquad (3\text{-}65)$$

It may be concluded that for given mode shapes $W_n\ (x)$, load $q\ (x, t)$, and initial conditions $w_o\ (x)$ and $\dot{w}_o\ (x)$, we may calculate the shell response by solving Equation (3-60) subject to initial conditions Equation (3-64) and (3-65). Specific application of the above theory follow.

2. Sample Specific Solutions

a. Dimensional Form

(1) Simple Support

(a) Spike

We now consider the specific case of a spike (ring load) traveling with speed v through the duct. The duct is simply supported at x = o and x = ℓ. Thus the eigenfunctions are given by Equation (3-53), and the associated frequencies of free vibration are given by Equation (3-54). It is now required to expand the spike load in an infinite series of the eigenfunctions. This will be accomplished by the expansion of a distributed load of length 2ϵ (as shown in Figure III-8), and then taking the limit as $\epsilon \to 0$. With reference to Figure III-8 we have

$$\begin{aligned} q\ (x,\ t) &= 0, && o < x < vt - \epsilon \\ q\ (x,\ t) &= p, && vt - \epsilon < x < vt + \epsilon \\ q\ (x,\ t) &= o, && vt + \epsilon < x < \ell \end{aligned} \qquad (3\text{-}66)$$

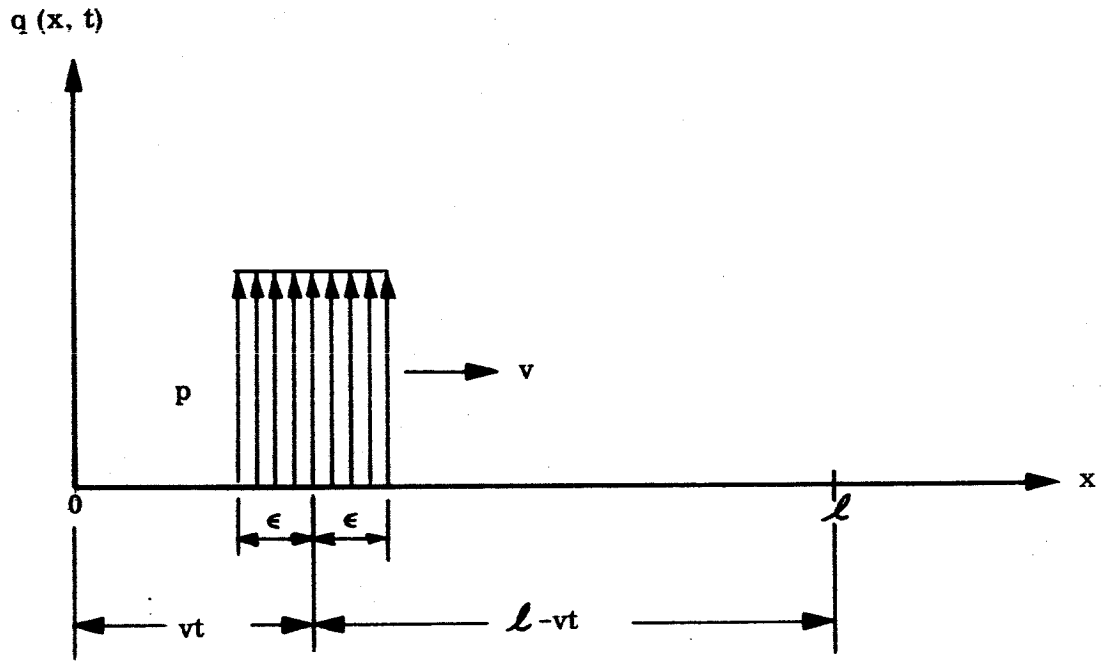

Figure III-8. Spike Load as the Limit of a Distributed Load

Consequently

$$\int_0^{\ell} q(x,t) \cdot W_n(x)\,dx = \int_{vt-\epsilon}^{vt+\epsilon} p \sin \frac{n\pi x}{\ell}\,dx$$

$$= \frac{2p\ell}{n\pi} \sin \frac{n\pi vt}{\ell} \sin \frac{n\pi \epsilon}{\ell}$$

If we now take the limit of this expression as $\epsilon \to 0$ and $2\epsilon p = P$ we obtain

$$\int_0^{\ell} q(x,t) \cdot W_n(x)\,dx = P \sin \frac{n\pi vt}{\ell} \qquad (3\text{-}67)$$

For the return cycle we have

$$q(x,t) = 0, \qquad 0 < x < 2\ell - vt - \epsilon$$
$$q(x,t) = -p, \qquad 2\ell - vt - \epsilon < x < 2\ell - vt + \epsilon$$
$$q(x,t) = 0, \qquad 2\ell - vt + \epsilon < x < \ell$$

and we have

$$\int q(x,t) \cdot W_n(x)\,dx = -\int_{2\ell-vt-\epsilon}^{2\ell-vt+\epsilon} p \sin \frac{n\pi x}{\ell}\,dx$$

$$= \frac{2pl}{n\pi} \sin \frac{n\pi vt}{\ell} \sin \frac{n\pi \epsilon}{\ell}$$

as before. We may continue this process and show that for the three cycles shown in Figure III-9 the expression, Equation (3-67) holds with appropriate time intervals as indicated in Figure III-9. We also note that for the simply supported duct (see Equations (3-61) and (3-53)

$$K_n = \frac{4}{\ell} \int_0^{\ell} W_n^2\,dx = \frac{4}{\ell} \int_0^{\ell} \left(\sin \frac{n\pi x}{\ell} \right)^2 dx = 2 \qquad (3\text{-}68)$$

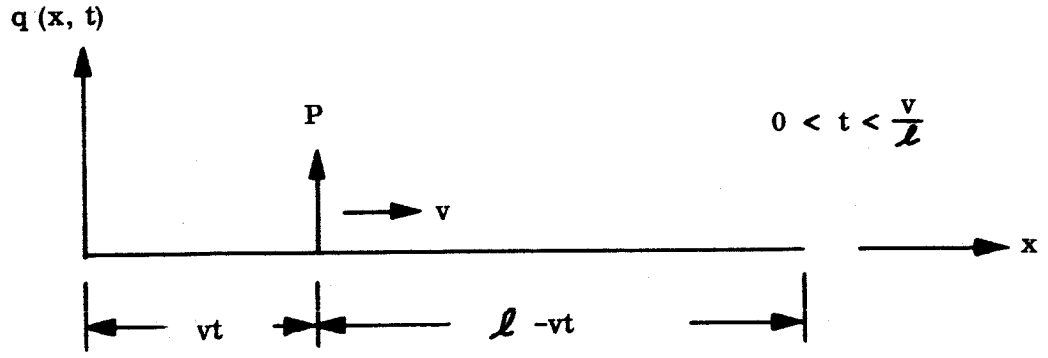

Figure III-9a

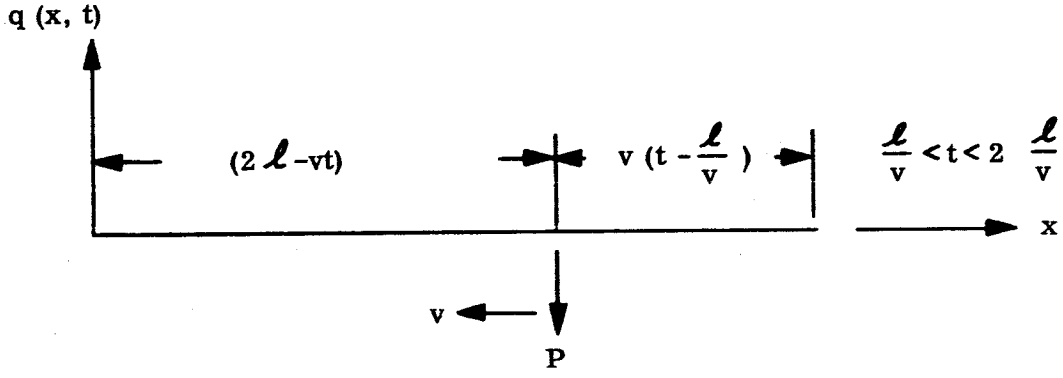

Figure III-9b

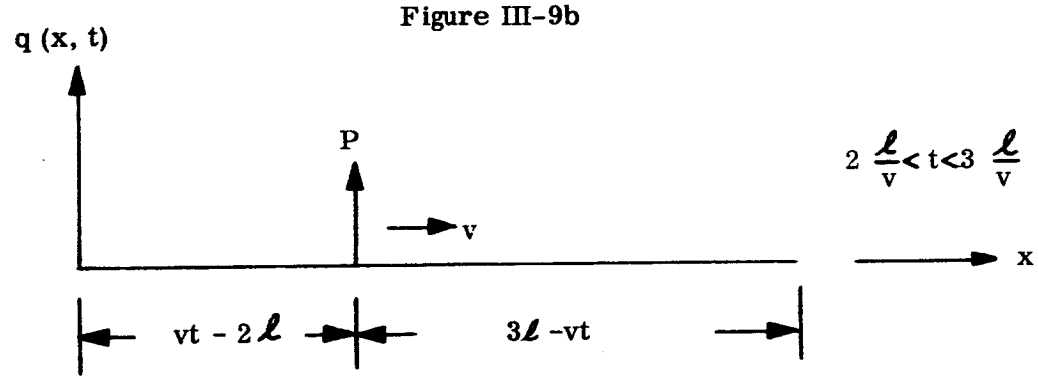

Figure III-9c

Figure III-9. Moving Spike Load

Combining Equations (3-67), (3-68), and (3-60) we obtain

$$\ddot{T}_n + \frac{2c}{m}\dot{T}_n + \omega_n^2 T_n = \frac{2}{m\ell} P \sin \frac{n\pi vt}{\ell} \qquad (3\text{-}69)$$

It is now assumed that the duct is undisturbed with respect to displacement and velocity at t = 0. Thus, from Equations (3-64) and (3-65) we have the initial conditions

$$T_n(o) = \dot{T}_n(o) = 0 \qquad (3\text{-}70)$$

With the assumption that damping is below its critical value, i.e., $\omega_n^2 > (c/m)^2$, the solution of Equation (3-69) subject to the initial conditions, Equation (3-70) is given by

$$T_n(t) = \frac{\frac{2P}{m\ell\ \omega_n^2}}{\left[\left(1 - \frac{a^2}{\omega_n^2}\right)^2 + \left(\frac{2ca}{m\ \omega_n^2}\right)^2\right]} \left\{ a e^{-\frac{c}{m}t}\left(\frac{2c}{m\ \omega_n^2}\right)\cos \bar{\omega}_n t \right.$$

$$+ \frac{1}{\bar{\omega}_n}\left[\frac{2c^2}{m^2\ \omega_n^2} - \left(1 - \frac{a^2}{\omega_n^2}\right)\right]\sin \bar{\omega}_n t + \left(1 - \frac{a^2}{\omega_n^2}\right)\sin a t$$

$$\left. - \frac{2ca}{m\ \omega_n^2}\cos a t \right\} \qquad (3\text{-}71)$$

where

$$a = \frac{n\pi v}{t}$$

$$\bar{\omega}_n^2 = \omega_n^2\left[1 - \left(\frac{c}{m\omega_n}\right)^2\right]$$

$$\omega_n^2 = \frac{D}{m\ell^4}\left[\frac{Eh\ell^4}{DR^2} + n^4\pi^4\right]$$

$$D = \frac{Eh^3}{12(1-\nu^2)}$$

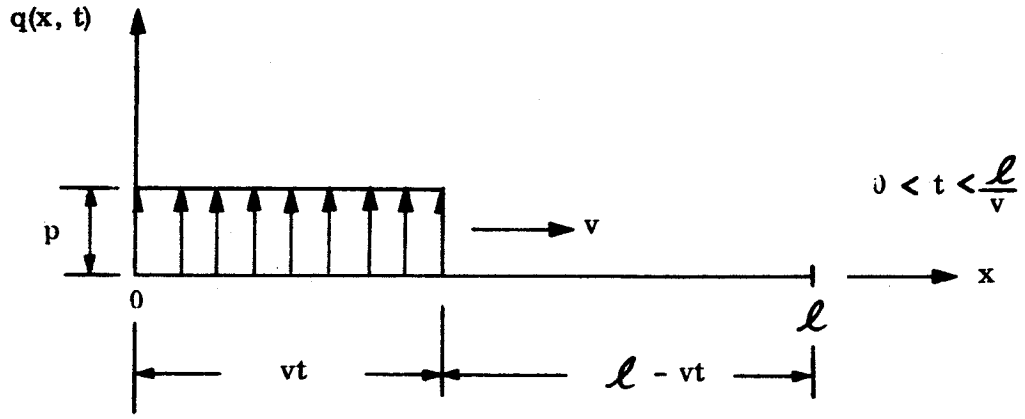

Figure III-10a

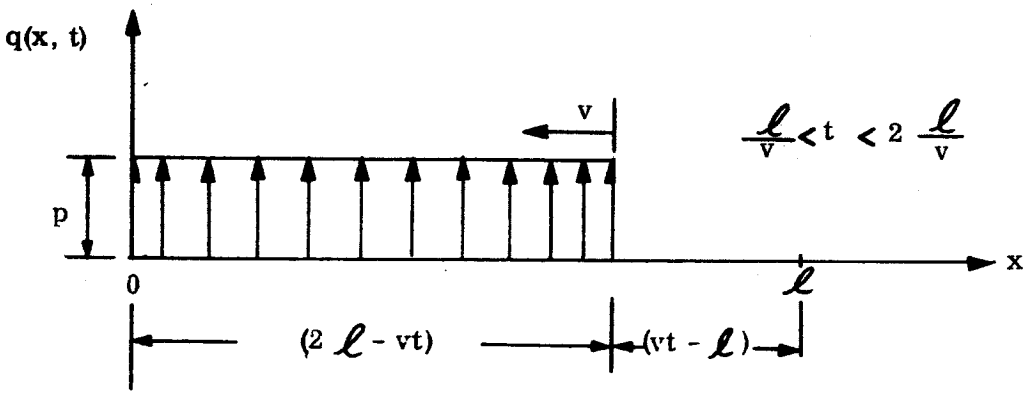

Figure III-10b

Figure III-10. Moving Step Load

Thus the complete solution for the simply supported shell, applicable to the loading cases indicated in Figure III-9, and appropriately restricted to the time intervals indicated in the figure, is given by

$$w = \sum_{n=1}^{\infty} T_n(t) \sin \frac{n\pi x}{\ell} \tag{3-72}$$

where $T_n(t)$ is defined in Equation (3-71).

(b) Step

We now calculate the response of a simply supported cylindrical duct to a uniformly distributed pressure load in the form of a step moving in the direction of the duct axis. We shall neglect damping in the subsequent calculations, i.e., $c = 0$. In this case we have (see Figure III-10a)

$$\begin{aligned} q(x, t) &= p, \qquad 0 < x < vt \\ q(x, t) &= o, \qquad vt < x < \ell \end{aligned} \tag{3-73}$$

Consequently, for $0 < t < \frac{\ell}{v}$ we have

$$\int_o^{\ell} q(x, t) \cdot W(x)\, dx = \int_o^{vt} p \sin \frac{n\pi x}{\ell}\, dx$$

$$= \frac{p\ell}{n\pi}\left(1 - \cos \frac{n\pi vt}{\ell}\right) \tag{3-74}$$

For the unloading phase $\frac{\ell}{v} < t < 2\frac{\ell}{v}$ as shown in Figure III-10, we have

$$\begin{aligned} q(x, t) &= p, \qquad 0 < x < 2\ell - vt \\ q(x, t) &= o, \qquad 2\ell - vt < x < \ell \end{aligned} \tag{3-75}$$

and

$$\int_o^{\ell} q(x, t) \cdot W(x)\, dx = \int_o^{2\ell - vt} p \sin \frac{n\pi x}{\ell}\, dx = \frac{p\ell}{n\pi}\left(1 - \cos \frac{n\pi vt}{\ell}\right) \tag{3-76}$$

Substitution of Equations (3-68) and (3-74) into Equation (3-60) (with c = 0) results in

$$\ddot{T}_n + \omega_n^2 T_n = \frac{2p}{mn\pi}\left(1 - \cos\frac{n\pi vt}{\ell}\right) \tag{3-77}$$

The initial conditions are expressed by Equation (3-70). The solution of Equation (3-77) subject to initial conditions, Equation (3-70), is $\left(\omega_n \neq \frac{n\pi v}{\ell}\right)$

$$T_n(t) = \frac{2pn\pi v^2}{m\ell^2}\,\frac{\cos\omega_n t}{\omega_n^2\left(\omega_n^2 - \frac{n^2\pi^2 v^2}{\ell^2}\right)} + \frac{2p}{mn\pi}\left[\frac{1}{\omega_n^2} - \frac{\cos\frac{n\pi vt}{\ell}}{\left(\omega_n^2 - \frac{n^2\pi^2 v^2}{\ell^2}\right)}\right] \tag{3-78}$$

where

$$\omega_n^2 = \frac{D}{m\ell^4}\left[\frac{Eh\ell^4}{DR^2} + n^4\pi^4\right]$$

Thus, the response of the simply supported duct to the moving pressure load shown in Figure III-10 is given by Equation (3-72), where $T_n(t)$ is expressed by Equation (3-78), and t is suitably restricted as indicated in Figure III-10.

(2) Clamped-Clamped

(a) Spike

In calculating the response of a clamped duct to a propagating disturbance in the form of a spike we apply the limiting procedure, as before, to a uniformly distributed load over the length 2ϵ. Thus the load distribution is given by Equation (3-66), but the eigenfunctions are characterized by Equation (3-56).

Consequently

$$\int_0^{\ell} q(x,t) \cdot W_n(x)\,dx = p\int_{vt-\epsilon}^{vt+\epsilon}\left[\cosh k_n x - \cos k_n x - \alpha_n\left(\sinh k_n x - \sin k_n x\right)\right] dx$$

$$= \frac{2p}{k_n}\left(\sinh k_n\epsilon \cosh k_n vt - \sin k_n\epsilon \cos k_n vt\right.$$

$$\left. - \alpha_n \sinh k_n vt \sinh k_n\epsilon + \alpha_n \sin k_n vt \sin k_n\epsilon\right) \qquad (3\text{-}79)$$

We now take the limit of Equation (3-79) as $\epsilon \to 0$ and $2p\epsilon \to P$

$$\int_0^{\ell} q(x,t)\, W_n(x)\,dx = P\left(\cosh k_n vt - \cos k_n vt\right.$$

$$\left. - \alpha_n \sinh k_n vt + \alpha_n \sin k_n vt\right) \qquad (3\text{-}80)$$

We also note that in the case of a clamped duct (see Reference 3-4)

$$\int_0^{\ell} W_n^2(x)\,dx = \frac{\ell}{4} K_n$$

where

$$K_n = \left[\frac{d^2 W_n}{d(k_n x)^2}\right]^2_{x=\ell} \qquad (3\text{-}81)$$

Upon substitution of Equation (3-56) into Equation (3-81) we obtain

$$K_n = \left[\cosh k_n\ell + \cos k_n\ell - \alpha_n\left(\sinh k_n\ell + \sin k_n\ell\right)\right]^2 = 4 \qquad (3\text{-}82)$$

Combining Equations (3-60), (3-80), and (3-82) we obtain

$$\ddot{T}_n + \omega_n^2 T_n = \frac{P}{m\ell}\left(\cosh k_n vt - \cos k_n vt - \alpha_n \sinh k_n vt + \alpha_n \sin k_n vt\right) \qquad (3\text{-}83)$$

The solution of Equation (3-83) for the non-resonant case

$$\omega_n^2 = \frac{D}{m\ell^4}\left(\frac{Eh\ell^4}{DR^2} + k_n^4 \ell^4\right) \neq k_n^2 v^2$$

and for initial conditions, Equation (3-70), is

$$T_n(t) = A_n \cos \omega_n t + B_n \sin \omega_n t$$

$$+ \frac{P}{m\ell}\left(\frac{\cosh k_n vt - \alpha_n \sinh k_n vt}{\omega_n^2 + k_n^2 v^2} + \frac{\alpha \sin k_n vt - \cos k_n vt}{\omega_n^2 - k_n^2 v^2}\right) \qquad (3\text{-}84)$$

where

$$A_n = \frac{2P}{m\ell} \cdot \frac{k_n^2 v^2}{\left(\omega_n^4 - k_n^4 v^4\right)}$$

$$B_n = -\frac{2\alpha_n P k_n^3 v^3}{m\ell\omega_n} \cdot \frac{1}{\omega_n^4 - k_n^4 v^4}$$

and the complete solution valid for $0 < t < \frac{\ell}{V}$ corresponding to the moving spike in a clamped shell is given by Equation (3-72), where $T_n(t)$ is represented by Equation (3-84).

(b) Step

The loading is shown in Figure III-10a and is expressed by Equation (3-73). It is applied to a clamped duct. Thus, for $0 < t < \frac{\ell}{V}$,

$$\int_0^{\ell} q(x, t)\ W_n(x)\, dx = \int_0^{vt} p\left(\cosh k_n x - \cos k_n x - \alpha_n \sinh k_n x + \alpha_n \sin k_n x\right) dx = \frac{p}{k_n}\left(\sinh k_n vt - \sin k_n vt - \alpha_n \cosh k_n vt - \alpha_n \cos k_n vt + 2\alpha_n\right) \qquad (3\text{-}85)$$

Combining Equations (3-60),(3-85) and (3-82), we obtain (without damping c = 0)

$$\ddot{T}_n + \omega_n^2 T_n = \frac{p}{m\ell k_n}\left(\sinh k_n vt - \sin k_n vt - \alpha_n \cosh k_n vt - \alpha_n \cos k_n vt + 2\alpha_n\right) \tag{3-86}$$

The solution of Equation (3-86) subject to initial conditions, Equation (3-70), is given by ($\omega_n^2 \neq k_n^2 v^2$):

$$T_n(t) = A_n \cos \omega_n t + B_n \sin \omega_n t + \frac{p}{m\ell k_n}\left(\frac{\sinh k_n vt - \alpha_n \cosh k_n vt}{\omega_n^2 + k_n^2 v^2} - \frac{\sin k_n vt + \alpha_n \cos k_n vt}{\omega_n^2 - k_n^2 v^2} + \frac{2\alpha_n}{\omega_n^2}\right) \tag{3-87}$$

where

$$A_n = \frac{2p\alpha_n}{m\ell k_n}\left(\frac{\omega_n^2}{\omega_n^4 - k_n^4 v^4} + \frac{1}{\omega_n^2}\right)$$

$$B_n = \frac{2pv^3 k_n^2}{m\ell\omega_n}\left(\frac{1}{\omega_n^4 - k_n^4 v^4}\right)$$

Thus the complete solution valid for $0 < t < \frac{\ell}{v}$ corresponding to the moving spike in a clamped shell is given by Equation (3-72), where $T_n(t)$ is characterized by Equation (3-87).

b. Dimensionless Form

The preceding sample solution for shells of finite length were derived in dimensional form and clearly illustrate the solution technique. However, design charts presented in this report are nondimensional and consequently for convenience in their preparation solutions were derived directly in nondimensional form using the nondimensional form of Equation (3-60) which is given by Equation (3-109). Thus T_n is essentially replaced by its nondimensional counterpart F_n. The procedures used to determine directly the nondimensional solutions, which are summarized in Section II-E are outlined below for the ramp and sinusoidal pressure transients. Reference in the following is made to equations in Section II-D and II-E and therefore it is suggested that they be read first.

(1) Simple Supports

(a) Ramp

Substitution of $A_n(\tau)$ as given by Equation (3-114) into Equation (3-109) yields the differential equations for the time dependent function $F_n(\tau)$ for the ramp. Thus for the first two time intervals $0 \leq \tau \leq \tau_c$ and $\tau_c \leq \tau \leq 1$ (refer to Figure III-12a) we obtain respectively for $0 \leq \tau \leq \tau_c$; $(F_n = F_{n_1})$

$$\frac{d^2F_n}{d\tau^2} + 2\bar{\alpha}\frac{dF_n}{d\tau} + \Omega_n^2 F_n = \frac{\beta}{\lambda K_n}\left[\frac{\tau}{\tau_c} - \frac{1}{K_n \tau_c}\sin K_n\tau\right] \tag{3-88}$$

for $\tau_c \leq \tau \leq 1$; $(F_n = F_{n_2})$

$$\frac{d^2F_n}{d\tau^2} + 2\bar{\alpha}\frac{dF_n}{d\tau} + \Omega_n^2 F_n = \frac{\beta}{\lambda K_n}\left[1 - \frac{1}{K_n \tau_c}\left(\sin K_n\tau - \sin K_n(\tau - \tau_c)\right)\right] \tag{3-89}$$

The general form at the solution of these second order differential equations is given by Equation 3-120. The constants of integration A_{1_n} and B_{1_n} in the solution

for the first time interval $0 \leq \tau \leq \tau_c$ are obtained from the following initial conditions (refer Equation 3-70).

$$F_{n_1}(o) = 0 \tag{3-90}$$

$$\frac{d F_{n_1}(o)}{d\tau} = 0$$

The constants of integration A_{2_n} and B_{2_n} in the solution for the second time interval $\tau_c \leq \tau \leq 1$ are determined from the conditions at time $\tau = \tau_c$. These conditions are

$$F_{n_1}(\tau_c) = F_{n_2}(\tau_c)$$

$$\frac{dF_{n_1}}{d\tau}(\tau_c) = \frac{d F_{n_2}}{d\tau}(\tau_c) \tag{3-91}$$

Finally, the solutions to Equations (3-88) and (3-89), subjected to initial conditions of Equations (3-90) and (3-91) are given by Equations (3-120) and (3-124).

(b) Sinusoid

The governing differential equations for the time dependent function $F_n(\tau)$ for the sinusoid are obtained from Equations (3-109) and (3-115). Thus for the time intervals $0 \leq \tau \leq \epsilon$ and $\epsilon \leq \tau \leq 1$ (refer Figure III-12b) we have respectively

$0 \leq \tau \leq \epsilon$; $(F_n = F_{n_1})$

$$\frac{d^2F_n}{d\tau^2} + 2\bar{\alpha}\frac{dF_n}{d\tau} + \Omega_n^2 F_n = \frac{\beta}{\lambda K_n}\left[\frac{n\epsilon}{1-\epsilon^2 n^2}\left(\sin K_n\tau - n\epsilon \sin\frac{\pi\tau}{\epsilon}\right)\right] \tag{3-92}$$

$$\epsilon \leq \tau \leq 1; \quad (F_n = F_{n_2})$$

$$\frac{d^2 F_n}{d\tau^2} + 2\bar{a}\frac{dF_n}{d\tau} + \Omega_n^2 F_n = \frac{\beta}{\lambda K_n}\left[\frac{n\epsilon}{1-\epsilon^2 n^2}\left(\sin K_n \tau + \sin K_n (\tau - \epsilon)\right)\right] \tag{3-93}$$

The initial conditions for Equation (3-92) are (refer to Equation 3-70)

$$F_{n_1}(o) = 0$$

$$\frac{dF_{n_1}(o)}{d\tau} = 0 \tag{3-94}$$

The constants of integration for Equations (3-92) and (3-93) are obtained for conditions which must be satisfied at $\tau = \epsilon$. These conditions are

$$F_{n_1}(\epsilon) = F_{n_2}(\epsilon)$$

$$\frac{dF_{n_1}(\epsilon)}{d\tau} = \frac{dF_{n_2}(\epsilon)}{d\tau} \tag{3-95}$$

The solutions to Equations (3-92) and (3-93) which satisfy Equations (3-94) and (3-95) are given by Equations (3-120) and (3-125).

(2) Clamped - Clamped

(a) Ramp

Equations (3-109) and (3-117) yield the differential equations for the time dependent function $F_n(\tau)$ for the ramp and clamped-clamped boundary condition. The

differential equations for the intervals $0 \leq \tau \leq \tau_c$ and $\tau_c \leq \tau \leq 1$ are given by

$0 \leq \tau \leq \tau_c$; $(F_n = F_{n_1})$

$$\frac{d^2F_n}{d\tau^2} + 2\bar{\alpha}\frac{dF_n}{d\tau} + \Omega_n^2 F_n = \frac{\beta}{2\lambda K_n^2 \tau_c}\left[\left(\cosh K_n\tau + \cos K_n\tau - 2\right) - \bar{\alpha}_n\left(\sinh K_n\tau + \sin K_n\tau\right) + 2K_n\alpha_n\tau\right] \tag{3-96}$$

$\tau_c \leq \tau \leq 1$; $(F_n = F_{n_2})$

$$\frac{d^2F_n}{d\tau^2} + 2\bar{\alpha}\frac{dF_n}{d\tau} + \Omega_n^2 F_n = \frac{\beta}{2\lambda K_n^2 \tau_c}\left[\left(\cosh K_n\tau - \cosh K_n(\tau - \tau_c)\right) + \left(\cos K_n\tau - \cos K_n(\tau - \tau_c)\right) - \alpha_n\left(\sinh K_n\tau - \sinh K_n(\tau - \tau_c)\right) - \alpha_n\left(\sin K_n\tau - \sin K_n(\tau - \tau_c)\right) + 2K_n\alpha_n\tau_c\right] \tag{3-97}$$

The solutions to Equations (3-96) and (3-97) are obtained with initial conditions given by Equations (3-90) and (3-91) and are given by Equations (3-120) and (3-128).

(b) Sinusoid

For this case the differential equations for $F_n(\tau)$ are obtained from Equations (3-109) and (3-118). Thus for the time periods $0 \leq \tau \leq \epsilon$ and $\epsilon \leq \tau \leq 1$ (refer to Figure III-12) we have

for $0 \leq \tau \leq \epsilon$; $(F_n = F_{n_1})$

$$\frac{d^2F_n}{d\tau^2} + 2\bar{\alpha}\frac{dF_n}{d\tau} + \Omega_n^2 F_n = \frac{\beta\epsilon}{2\lambda\pi}\left[\cos\frac{\pi\tau}{\epsilon} - \cosh\frac{\pi\tau}{\epsilon} + \frac{\tau\pi}{\epsilon}\sin\frac{\pi\tau}{\epsilon} - \alpha_n\left(2\sin\frac{\pi\tau}{\epsilon} - \sinh\frac{\pi\tau}{\epsilon} - \frac{\pi\tau}{\epsilon}\cos\frac{\pi\tau}{\epsilon}\right)\right] \tag{3-98}$$

for $\epsilon \leq \tau \leq 1$; $(F_n = F_{n_2})$

$$\frac{d^2F_n}{d\tau^2} + 2\bar{\alpha}\frac{dF_n}{d\tau} + \Omega_n^2 F_n = \frac{\beta\epsilon}{2\lambda\pi}\left[\cosh\frac{\pi\tau}{\epsilon} + \cosh\frac{\pi(\tau-\epsilon)}{\epsilon} - \frac{\pi\tau}{\epsilon}\sin\frac{\pi\tau}{\epsilon} + \frac{\pi(\tau-\epsilon)}{\epsilon}\sin\frac{\pi(\tau-\epsilon)}{\epsilon} - \alpha_n\left(\sinh\frac{\pi\tau}{\epsilon} + \sinh\frac{\pi(\tau-\epsilon)}{\epsilon} + \frac{\pi\tau}{\epsilon}\cos\frac{\pi\tau}{\epsilon} + \frac{\pi(\tau-\epsilon)}{\epsilon}\cos\frac{\pi(\tau-\epsilon)}{\epsilon}\right)\right] \tag{3-99}$$

The solutions to these differential equations are obtained with initial conditions of Equations (3-94) and (3-95) and are given by Equations (3-120) and (3-129).

D. NONDIMENSIONALIZATION AND DESIGN PARAMETERS

From a designer's point of view, it is desirable to reduce the number of design charts to a minimum. This is accomplished by the introduction of design parameters which combine as many of the problem variables as possible. From a nondimensionalization of the elastic response solutions obtained for the infinite and finite length cylinder, three independent design parameters were indicated. These are designated as the speed parameter, λ , length parameter, β , and damping parameter, α .

The speed parameter, λ , was introduced quite naturally earlier in the determination of the dynamic solution for the infinite shell (see Equation 3-20) and is defined as follows:

$$\lambda = \frac{\rho v^2}{2Eg} \frac{R}{h}\sqrt{12(1-\nu^2)} \qquad (3\text{-}100)$$

where v is the speed of the pressure transient front and ρ is the weight density of the cylinder material. It is significant to note that λ is equal to the ratio of the squares of the speed of the traveling pressure transient and the critical speed for an infinitely long cylinder.

For convenience for the determination of λ , Figure III-11 was prepared and gives λ directly as a function of the velocity of the pressure transient and the expression $\frac{\rho\sqrt{1-\nu^2}}{E}$. It appears that for many materials we have $\frac{\rho\sqrt{1-\nu^2}}{E} = 0.95 \times 10^{-8}$. Examination of Figure III-11 indicates that the practical range of values for λ is $0 < \lambda < 6$. However, values of $\lambda \geq 10$ are possible. In general, small values of λ will govern in the relatively thick walled piping systems of the smaller propulsion systems whereas large values of λ prevail for the relatively large thin walled ducts used in big booster propulsion systems.

The two remaining independent design parameters are the length parameter defined as

$$\beta = \frac{\ell^2}{Rh}\sqrt{12(1-\nu^2)} \qquad (3\text{-}101)$$

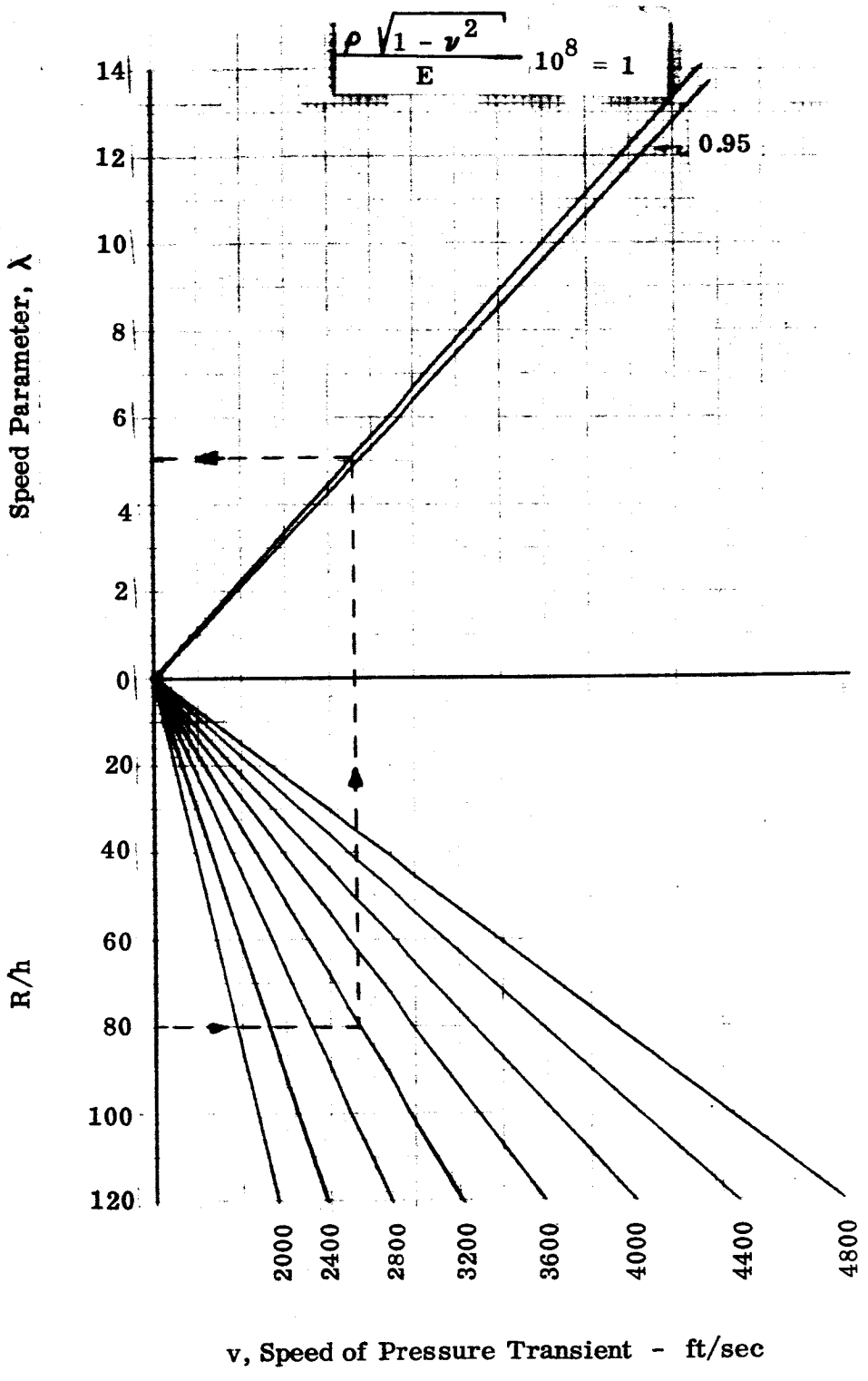

Figure III-11. Graphical Determination of Speed Parameter

and the damping parameter defined as

$$\alpha = \frac{cR}{h}\sqrt{\frac{g}{\rho E}} \qquad (3\text{-}102)$$

where c is the viscous damping coefficient.

From an examination of the various cylinder geometries of interest in propulsion systems, it was found that the length parameter can vary over a relatively large range primarily due to the ℓ^2 term. However, it appears that for most practical circumstances β will vary in the range

$$10^2 \leq \beta \leq 10^6$$

However, it must be noted again that values of $\beta < 10^2$ and $\beta > 10^6$ are possible.

The damping parameter defined by Equation (3-102) is actually the ratio of the viscous damping coefficient and the critical damping coefficient for the first harmonic, i.e., n = 1. The critical damping coefficient is thus given by

$$c_{cr} = \frac{h}{R}\sqrt{\frac{\rho E}{g}} \qquad (3\text{-}103)$$

Hence for the solutions presented in this report, the damping parameter will be limited to the range of values

$$0 \leq \alpha \leq 1.0$$

The actual value of α that should be used in a design situation is not known, and its determination is beyond the scope of the present report. However, as will be shown later, it could be a significant factor in the determination of the true dynamic response of ducts with contained fluid. This aspect of the problem is discussed further in Section VI with regard to the interaction of fluid and duct motions (coupled motion).

The dynamic solutions were nondimensionalized in such a manner as to yield non-dimensional radial deflections $\bar{w}$ and axial bending moment $\bar{M}_x$. These parameters are defined by

$$\bar{w} = \frac{w}{w_o}; \quad \bar{M}_x = \frac{M_x}{M_o} \qquad (3\text{-}104)$$

where

$$w_o = \frac{pR^2}{Eh} \; ; \quad M_o = \frac{p\,Rh}{\sqrt{12\,(1-\nu^2}} \tag{3-105}$$

The spike load is essentially a limiting case of the sinusoidal pressure load but it must be given in terms the radial line load P instead of the pressure p. As a consequence of this fact, the expressions for w_o and M_o for the spike are given by

$$w_{o_P} = \frac{P^4\sqrt{12\,(1-\nu^2}}{E}\left(\frac{R}{h}\right)^{3/2}$$

$$M_{o_P} = \frac{Ph^{1/2}R^{1/2}}{4\sqrt{12\,(1-\nu^2)}} \tag{3-106}$$

The hoop and circumferential bending moment stress resultants are given in terms of $\bar{w}$ and $\bar{M}_x$ by (see Equations 3-7 and 3-8).

$$N_\phi = \frac{Eh\,w_o}{R}\,\bar{w}$$

$$M_\phi = \nu\, M_o\, \bar{M}_x \tag{3-107}$$

By the suitable combination of the stresses σ_x and σ_ϕ obtained from the stress resultants M_x, M_ϕ and N_ϕ, the state of biaxial stresses at any point in the duct can be determined. (see Section V-C, Illustrative Application of Design Charts.)

Nondimensional variables introduced with regard to the representation of the ramp and sinusoidal pressure transients are shown in Figure III-12. Other nondimensional variables are introduced as they appear.

E. SUMMARY AND SOLUTION OF FINAL GOVERNING EQUATIONS

1. Final Governing Equations

Introductions of the nondimensional design parameters and variables discussed in Section III-D into the expressions presented in Section III-C for the dynamic solution of a cylinder of finite length results in the following nondimensional forms for the deflection and bending moment expressions

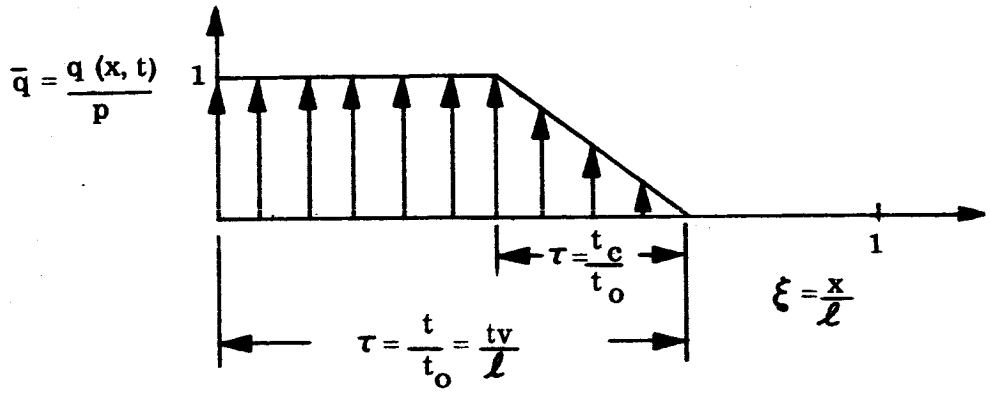

(a) Ramp

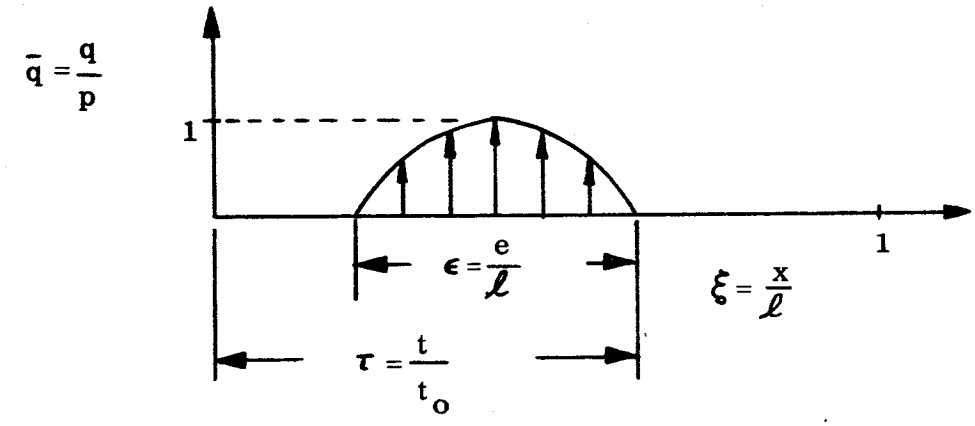

(b) Sinusoid

Figure III-12. Nondimensional Representation of Pressure Wave Shapes

$$\bar{w} = \sum_{n=1}^{\infty} F_n(\tau)\, W_n(\xi)$$

$$\bar{M}_x = \frac{1}{\beta} \sum_{n=1}^{\infty} F_n(\tau)\, \frac{\partial^2 W_n(\xi)}{\partial \xi^2} \qquad (3\text{-}108)$$

The function $F_n(\tau)$ is obtained as the solution of the following differential equation which is the nondimensional form of Equation (3-60)

$$\frac{d^2 F_n}{d\tau^2} + 2\bar{\alpha} \frac{dF_n}{d\tau} + \Omega_n^2 F_n = A_n(\tau) \qquad (3\text{-}109)$$

where

$$\bar{\alpha} = \alpha \sqrt{\frac{\beta}{2\lambda}} \qquad (3\text{-}110)$$

$$\Omega_n^2 = \frac{1}{2\lambda\beta} (\beta^2 + K_n^4)$$

Note that Ω_n is the nondimensional natural frequency. The nondimensional function $A_n(\tau)$ corresponds to the expression on the right hand side of Equation 3-60 and is given by

$$A_n(\tau) = \frac{2\beta}{\lambda \mathbb{K}_n} \int_0^1 \bar{q}(\xi,\tau)\, W_n(\xi)\, d\xi \qquad (3\text{-}111)$$

where $\bar{q} = q/p$, the nondimensional pressure.

The functions $W_n(\xi)$, $\mathbb{K}_n$ and K_n vary with the prescribed boundary conditions and they are summarized, for the cases treated in this study, as follows. For simple-simple support conditions

$$\left.\begin{aligned} W_n(\xi) &= \sin K_n \xi \\ \frac{\partial^2 W_n}{\partial \xi^2} &= -K_n^2 \sin K_n \xi \\ \mathbb{K}_n &= 2 \\ K_n &= n\pi \end{aligned}\right\} \qquad (3\text{-}112)$$

and for fixed-fixed support conditions

$$\left.\begin{aligned} W_n(\xi) &= \cosh K_n \xi - \cos K_n \xi - \alpha_n (\sinh K_n \xi - \sin K_n \xi) \\ \alpha_n &= \frac{\cos K_n - \cosh K_n}{\sin K_n - \sinh K_n} \\ K_n &= 4 \\ 1 &= \cos K_n \cosh K_n \end{aligned}\right\} \quad (3\text{-}113)$$

Note that K_n are the roots of the last expression of Equations 3-113

Substitution of the expressions for the various transient pressure cases defined in Chapter II into Equation 3-111 and integrating results in the function $A_n(\tau)$, the nonhomogenious part of the differential equation, Equation 3-109. The functions obtained for the ramp and sinusoid transient pressures are summarized below for the two boundary conditions under investigation.

(1) Simple-Simple Supports

(a) Ramp Pressure Form, $\tau_c \leq 1$

$$0 \leq \tau \leq \tau_c \qquad A_n(\tau) = \frac{\beta}{\lambda K_n}\left[\frac{\tau}{\tau_c} - \frac{1}{K_n \tau_c} \sin K_n \tau\right]$$

$$\tau_c \leq \tau \leq 1 \qquad A_n(\tau) = \frac{\beta}{\lambda K_n}\left[1 - \frac{1}{K_n \tau_c}\left(\sin K_n \tau - \sin K_n (\tau - \tau_c)\right)\right]$$

$$1 \leq \tau \leq 1 + \tau_c \qquad A_n(\tau) = \frac{\beta}{\lambda K_n}\left[1 + \frac{1}{K_n \tau_c}\left(\sin K_n (\tau - \tau_c) + \sin K_n (2 - \tau)\right)\right]$$

$$1 + \tau_c \leq \tau \leq 2 \qquad A_n(\tau) = \frac{\beta}{\lambda K_n}\left[1 - \frac{1}{K_n \tau_c}\left(\sin K_n (2 - \tau + \tau_c) - \sin K_n (2 - \tau)\right)\right]$$

$$2 \leq \tau \leq 2 + \tau_c \qquad A_n(\tau) = \frac{-\beta}{\lambda K_n}\left[\frac{2\tau - 4 - \tau_c}{\tau_c} - \frac{1}{K_n \tau_c}\left(\sin K_n (\tau - 2) - \sin K_n (\tau - 2 - \tau_c)\right)\right]$$

$$2+\tau_c \le \tau \le 3 \qquad A_n(\tau) = \frac{-\beta}{\lambda K_n}\left[1 - \frac{1}{K_n \tau_c}\left(\sin K_n(\tau-2) - \sin K_n(\tau-2-\tau_c)\right)\right]$$

$$3 \le \tau \le 3+\tau_c \qquad A_n(\tau) = \frac{-\beta}{\lambda K_n}\left[1 + \frac{1}{K_n \tau_c}\left(\sin K_n(\tau-2-\tau_c) - \sin K_n(4-\tau)\right)\right]$$

$$3+\tau_c \le \tau \le 4 \qquad A_n(\tau) = \frac{-\beta}{\lambda K_n}\left[1 + \frac{1}{K_n \tau_c}\left(\sin K_n(\tau-4-\tau_c) + \sin K_n(4-\tau)\right)\right]$$

$$4 \le \tau \le 4+\tau_c \qquad A_n(\tau) = \frac{\beta}{\lambda K_n}\left[\frac{\tau-4-\tau_c}{\tau_c} + \frac{1}{K_n \tau_c}\left(\sin K_n(\tau-4-\tau_c)\right)\right]$$

$$+ A_n(\tau)\Big| \quad 0 \le \tau \le \tau_c \qquad (3\text{-}114)$$

(b) **Sinusoidal Pressure Form $\epsilon \le 1$**

For this transient pressure form the expressions obtained for $A_n(\tau)$ become unbounded when $n = \frac{1}{\epsilon}$. Because of this circumstance, the function $A_n(\tau)$ was evaluated for two cases, i.e., when $n \neq \frac{1}{\epsilon}$ and when $n = \frac{1}{\epsilon}$. For $n \neq \frac{1}{\epsilon}$

$$0 \le \tau \le \epsilon \qquad A_n(\tau) = \frac{\beta}{\lambda K_n}\left[\frac{n\epsilon}{1-\epsilon^2 n^2}\left(\sin K_n \tau - n\epsilon \sin \frac{\pi \tau}{\epsilon}\right)\right]$$

$$\epsilon \le \tau \le 1 \qquad A_n(\tau) = \frac{\beta}{\lambda K_n}\left[\frac{n\epsilon}{1-\epsilon^2 n^2}\left(\sin K_n \tau + \sin K_n(\tau-\epsilon)\right)\right]$$

$$1 \le \tau \le 1+\epsilon \qquad A_n(\tau) = \frac{\beta}{\lambda K_n}\left[\frac{n\epsilon}{1-\epsilon^2 n^2}\left(\sin K_n(\tau-\epsilon) - \sin K_n(2-\tau)\right)\right]$$

$$1+\epsilon \le \tau \le 2 \qquad A_n(\tau) = \frac{-\beta}{\lambda K_n}\left[\frac{n\epsilon}{1-\epsilon^2 n^2}\left(\sin K_n(2-\tau+\epsilon) + \sin K_n(2-\tau)\right)\right]$$

$$2 \le \tau \le 2+\epsilon \qquad A_n(\tau) = \frac{\beta}{\lambda K_n}\left[\frac{n\epsilon}{1-\epsilon^2 n^2}\left(-\sin K_n(2-\tau+\epsilon) + \sin K_n(\tau-2)\right)\right]$$

$$2+\epsilon \le \tau \le 3 \qquad A_n(\tau) = \frac{\beta}{\lambda K_n}\left[\frac{n\epsilon}{1-\epsilon^2 n^2}\left(\sin K_n(\tau-2) + \sin K_n(\tau-2-\epsilon)\right)\right]$$

$$3 \le \tau \le 3+\epsilon \qquad A_n(\tau) = \frac{\beta}{\lambda K_n}\left[\frac{n\epsilon}{1-\epsilon^2 n^2}\left(\sin K_n(\tau - 2 - \epsilon) - \sin K_n(4-\tau)\right)\right]$$

$$3+\epsilon \le \tau \le 4 \qquad A_n(\tau) = \frac{-\beta}{\lambda K_n}\left[\frac{n\epsilon}{1-\epsilon^2 n^2}\left(\sin K_n(4-\tau) + \sin K_n(4-\tau+\epsilon)\right)\right]$$

$$4 \le \tau \le 4+\epsilon \qquad A_n(\tau) = \frac{-\beta}{\lambda K_n}\left[\frac{n\epsilon}{1-\epsilon^2 n^2}\left(\sin K_n(4-\tau+\epsilon)\right)\right] + A_n(\tau)\Big|_{0 \le \tau \le \epsilon}$$

And for $n = \frac{1}{\epsilon}$ (3-115)

$$0 \le \tau \le \epsilon \qquad A_n(\tau) = \frac{-\beta}{2\lambda}\left[\tau \cos \pi \frac{\tau}{\epsilon} - \frac{\epsilon}{\pi} \sin \pi \frac{\tau}{\epsilon}\right]$$

$$\epsilon \le \tau \le 1 \qquad A_n(\tau) = \frac{-\beta}{2\lambda}\left[\tau \cos \pi \frac{\tau}{\epsilon} + (\tau - \epsilon) \cos \pi \frac{(\tau-\epsilon)}{\epsilon}\right]$$

$$1 \le \tau \le 1+\epsilon \qquad A_n(\tau) = \frac{-\beta}{2\lambda}\left[(\tau-\epsilon)\cos \pi \frac{(\tau-\epsilon)}{\epsilon} - (2-\tau)\cos \pi (2-\tau)\right] .$$

$$1+\epsilon \le \tau \le 2 \qquad A_n(\tau) = \frac{\beta}{2\lambda}\left[(2-\tau+\epsilon)\cos \pi \frac{(2-\tau+\epsilon)}{\epsilon} + (2-\tau)\cos \pi \frac{(2-\tau)}{\epsilon}\right]$$

$$2 \le \tau \le 2+\epsilon \qquad A_n(\tau) = \frac{\beta}{2\lambda}\left[(2-\tau+\epsilon)\cos \pi \frac{(2-\tau+\epsilon)}{\epsilon} - (\tau-2)\cos \pi \frac{(\tau-2)}{\epsilon}\right]$$

$$2+\epsilon \le \tau \le 3 \qquad A_n(\tau) = \frac{-\beta}{2\lambda}\left[(\tau-2)\cos \pi \frac{(\tau-2)}{\epsilon} + (\tau-2-\epsilon)\cos \pi \frac{(\tau-2-\epsilon)}{\epsilon}\right]$$

$$3 \le \tau \le 3+\epsilon \qquad A_n(\tau) = \frac{-\beta}{2\lambda}\left[(\tau-2-\epsilon)\cos \pi \frac{(\tau-2-\epsilon)}{\epsilon} - (4-\tau)\cos \pi \frac{(2-\tau)}{\epsilon}\right]$$

$$3+\epsilon \le \tau \le 4 \qquad A_n(\tau) = \frac{\beta}{2\lambda}\left[(4-\tau)\cos \pi \frac{(4-\tau)}{\epsilon} + (4-\tau+\epsilon)\cos \pi \frac{(4-\tau+\epsilon)}{\epsilon}\right]$$

$$4 \le \tau \le 4+\epsilon \qquad A_n(\tau) = \frac{\beta}{2\lambda}\left[(4-\tau+\epsilon)\cos \pi \frac{(4-\tau+\epsilon)}{\epsilon}\right] + A_n\Big|_{0 \le \tau \le \epsilon}$$

(3-116)

(2) Clamped - Clamped Supports

(a) Ramp Pressure Form $\tau_c \leq 1$

$$0 \leq \tau \leq \tau_c \qquad A_n(\tau) = \frac{\beta}{2\lambda K_n^2 \tau_c}\left[\left(\cosh K_n\tau + \cos K_n\tau - 2\right) - \alpha_n\left(\sinh K_n\tau + \sin K_n\tau\right) + 2K_n\alpha_n\tau\right]$$

$$\tau_c \leq \tau \leq 1 \qquad A_n(\tau) = \frac{\beta}{2\lambda K_n^2 \tau_c}\left[\left(\cosh K_n\tau - \cosh K_n(\tau - \tau_c)\right) + \left(\cos K_n\tau - \cos K_n(\tau - \tau_c)\right) - \alpha_n\left(\sinh K_n\tau - \sinh K_n(\tau - \tau_c)\right) - \alpha_n\left(\sin K_n\tau - \sin K_n(\tau - \tau_c)\right) + 2K_n\alpha_n\tau_c\right]$$

$$1 \leq \tau \leq 1 + \tau_c \qquad A_n(\tau) = \frac{\beta}{2\lambda K_n^2 \tau_c}\left[\left(2\cosh K_n - \cosh K_n(\tau - \tau_c) - \cosh K_n(2 - \tau)\right) + \left(2\cos K_n - \cos K_n(\tau - \tau_c) - \cos K_n(2 - \tau)\right) - \alpha_n\left(2\sinh K_n - \sinh K_n(\tau - \tau_c) - \sinh K_n(2 - \tau)\right) - \alpha_n\left(2\sin K_n - \sin K_n(\tau - \tau_c) - \sin K_n(2 - \tau)\right) + 2K_n\alpha_n\tau_c\right]$$

$$1 + \tau_c \leq \tau \leq 2 \qquad A_n(\tau) = \frac{\beta}{2\lambda K_n^2 \tau_c}\left[\left(\cosh K_n(2 - \tau + \tau_c) - \cosh K_n(2 - \tau)\right) + \left(\cos K_n(2 - \tau + \tau_c) - \cos K_n(2 - \tau)\right) - \alpha_n\left(\sinh K_n(2 - \tau + \tau_c) - \sinh K_n(2 - \tau)\right) - \alpha_n\left(\sin K_n(2 - \tau + \tau_c) - \sin K_n(2 - \tau)\right) + 2K_n\tau_c\alpha_n\right]$$

$$2 \le \tau \le 2 + \tau_c \qquad A_n(\tau) = \frac{\beta}{2\lambda K_n^2 \tau_c} \Big[\Big(\cosh K_n (2 - \tau + \tau_c) - \cosh K_n (\tau - 2) \Big)$$

$$+ \Big(\cos K_n (2 - \tau + \tau_c) - \cos K_n (\tau - 2) \Big)$$

$$- \alpha_n \Big(\sinh K_n (2 - \tau + \tau_c) - \sinh K_n (\tau - 2) \Big)$$

$$- \alpha_n \Big(\sin K_n (2 - \tau + \tau_c) - \sin K_n (\tau - 2) \Big)$$

$$- 2 K_n \alpha_n (2\tau - 4 + \tau_c) \Big]$$

$$2 + \tau_c \le \tau \le 3 \qquad A_n(\tau) = \frac{\beta}{2\lambda K_n^2 \tau_c} \Big[\Big(\cosh K_n (\tau - 2) - \cosh K_n (\tau - 2 - \tau_c) \Big)$$

$$+ \Big(\cos K_n (\tau - 2) - \cos K_n (\tau - 2 - \tau_c) \Big)$$

$$- \alpha_n \Big(\sinh K_n (\tau - 2) - \sinh K_n (\tau - 2 - \tau_c) \Big)$$

$$- \alpha_n \Big(\sin K_n (\tau - 2) - \sin K_n (\tau - 2 - \tau_c) \Big)$$

$$+ 2 K_n \alpha_n \tau_c \Big]$$

$$3 \le \tau \le 3 + \tau_c \qquad A_n(\tau) = \frac{\beta}{2\lambda K_n^2 \tau_c} \Big[\Big(\cosh K_n (\tau - 2 - \tau_c) + \cosh K_n (4 - \tau) - 2 \cosh K_n \Big)$$

$$+ \Big(\cos K_n (\tau - 2 - \tau_c) + \cos K_n (4 - \tau) - 2 \cos K_n \Big)$$

$$- \alpha_n \Big(\sinh K_n (\tau - 2 - \tau_c) + \sinh K_n (4 - \tau) - 2 \sinh K_n \Big)$$

$$- \alpha_n \Big(\sin K_n (\tau - 2 - \tau_c) + \sin K_n (4 - \tau) - 2 \sin K_n \Big)$$

$$- 2 K_n \alpha_n \tau_c \Big]$$

$$3 + \tau_c \le \tau \le 4 \qquad A_n(\tau) = \frac{-\beta}{2\lambda K_n^2 \tau_c} \Big[\Big(\cosh K_n (4 - \tau + \tau_c) - \cosh K_n (4 - \tau) \Big)$$

$$+ \Big(\cos K_n (4 - \tau + \tau_c) - \cos (4 - \tau) \Big)$$

$$- \alpha_n \Big(\sinh K_n (4 - \tau + \tau_c) - \sinh K_n (4 - \tau) \Big)$$

$$- \alpha_n \left(\sin K_n (4 - \tau + \tau_c) - \sin K_n (4 - \tau) \right)$$

$$+ 2 K_n \alpha_n \tau_c \Big]$$

$4 \le \tau \le 4 + \tau_c$

$$A_n(\tau) = \frac{-\beta}{2\lambda K_n^2 \tau_c} \Big[\Big(\cosh K_n (4 - \tau + \tau_c) + \cos K_n (4 - \tau + \tau_c) - 2 \Big)$$

$$- \alpha_n \left(\sinh K_n (4 - \tau + \tau_c) + \sin K_n (4 - \tau + \tau_c) \right)$$

$$+ 2 K_n \alpha_n \tau_c \Big] + A_n(\tau) \Big|_{0 \le \tau \le \tau_c} \qquad (3\text{-}117)$$

(b) **Sinusoidal Pressure Form $\epsilon \le 1$**

As was the situation for the case of simple-simple supports, there are two sets of functions required for $A_n(\tau)$, i.e., for $K_n = \frac{\pi}{\epsilon}$ and $K_n \neq \frac{\pi}{\epsilon}$. For $K_n = \frac{\pi}{\epsilon}$ we have

$0 \le \tau \le \epsilon$

$$A_n(\tau) = \frac{-\beta\epsilon}{2\lambda\pi} \Big[\cos \frac{\pi\tau}{\epsilon} - \cosh \frac{\pi\tau}{\epsilon} + \frac{\tau\pi}{\epsilon} \sin \frac{\pi\tau}{\epsilon}$$

$$- \alpha_n \left(2 \sin \frac{\pi\tau}{\epsilon} - \sinh \frac{\pi\tau}{\epsilon} - \frac{\pi\tau}{\epsilon} \cos \frac{\pi\tau}{\epsilon} \right) \Big]$$

$\epsilon \le \tau \le 1$

$$A_n(\tau) = \frac{\beta\epsilon}{2\lambda\pi} \Big[\cosh \frac{\pi\tau}{\epsilon} + \cosh \frac{\pi(\tau - \epsilon)}{\epsilon} - \frac{\pi\tau}{\epsilon} \sin \frac{\pi\tau}{\epsilon}$$

$$+ \frac{\pi(\tau - \epsilon)}{\epsilon} \sin \frac{\pi(\tau - \epsilon)}{\epsilon}$$

$$- \alpha_n \left(\sinh \frac{\pi\tau}{\epsilon} + \sinh \frac{\pi(\tau - \epsilon)}{\epsilon} + \frac{\pi\tau}{\epsilon} \cos \frac{\pi\tau}{\epsilon} \right.$$

$$\left. + \frac{\pi(\tau - \epsilon)}{\epsilon} \cos \frac{\pi(\tau - \epsilon)}{\epsilon} \right) \Big]$$

$1 \le \tau \le 1 + \epsilon$

$$A_n(\tau) = \frac{\beta\epsilon}{2\lambda\pi} \Big[2 \cos \frac{\pi(\tau - 1)}{\epsilon} \cosh \frac{\pi}{\epsilon} + \cosh \frac{\pi(\tau - \epsilon)}{\epsilon}$$

$$- \cosh \frac{\pi(2 - \tau)}{\epsilon} - \frac{2\pi}{\epsilon} \cos \frac{\pi(\tau - 1)}{\epsilon} \sin \frac{\pi}{\epsilon} - \frac{\pi(\tau - \epsilon)}{\epsilon}$$

$$\sin \frac{\pi(\tau - \epsilon)}{\epsilon}$$

$$+\frac{\pi(2-\tau)}{\epsilon}\sin\frac{\pi(2-\tau)}{\epsilon}-\alpha_n\left(2\cos\frac{\pi(\tau-1)}{\epsilon}\sinh\frac{\pi}{\epsilon}\right.$$

$$+\sinh\frac{\pi(\tau-\epsilon)}{\epsilon}-\sinh\frac{\pi(2-\tau)}{\epsilon}+\frac{2\pi}{\epsilon}\cos\frac{\pi(\tau-1)}{\epsilon}\cos\frac{\pi}{\epsilon}$$

$$\left.\left.+\frac{\pi(\tau-\epsilon)}{\epsilon}\cos\frac{\pi(\tau-\epsilon)}{\epsilon}-\frac{\pi(2-\tau)}{\epsilon}\cos\frac{\pi(2-\tau)}{\epsilon}\right)\right]$$

$1+\epsilon\leq\tau\leq 2$

$$A_n(\tau)=\frac{-\beta\epsilon}{2\lambda\pi}\left[\cosh\frac{\pi(2-\tau+\epsilon)}{\epsilon}+\cosh\frac{\pi(2-\tau)}{\epsilon}\right.$$

$$-\frac{\pi(2-\tau+\epsilon)}{\epsilon}\sin\frac{\pi(2-\tau+\epsilon)}{\epsilon}-\frac{\pi(2-\tau)}{\epsilon}\sin\frac{\pi(2-\tau)}{\epsilon}$$

$$-\alpha_n\left(\sinh\frac{\pi(2-\tau+\epsilon)}{\epsilon}+\sinh\frac{\pi(2-\tau)}{\epsilon}\right.$$

$$+\frac{\pi(2-\tau+\epsilon)}{\epsilon}\cos\frac{\pi(2-\tau+\epsilon)}{\epsilon}+\frac{\pi(2-\tau)}{\epsilon}$$

$$\left.\left.\cos\frac{\pi(2-\tau)}{\epsilon}\right)\right]$$

$2\leq\tau\leq 2+\epsilon$

$$A_n(\tau)=\frac{-\beta\epsilon}{2\lambda\pi}\left[2\cos\frac{\pi(\tau-2)}{\epsilon}+\cosh\frac{\pi(2-\tau+\epsilon)}{\epsilon}-\cosh\frac{\pi(2-\tau)}{\epsilon}\right.$$

$$-\frac{\pi(2-\tau+\epsilon)}{\epsilon}\sin\frac{\pi(2-\tau+\epsilon)}{\epsilon}+\frac{\pi(\tau-2)}{\epsilon}\sin\frac{\pi(\tau-2)}{\epsilon}$$

$$-\alpha_n\left(\sinh\frac{\pi(2-\tau+\epsilon)}{\epsilon}-\sinh\frac{\pi(\tau-2)}{\epsilon}\right.$$

$$\left.\left.+\frac{\pi(2-\tau+\epsilon)}{\epsilon}\cos\frac{\pi(2-\tau+\epsilon)}{\epsilon}-\frac{\pi(\tau-2)}{\epsilon}\cos\frac{\pi(\tau-2)}{\epsilon}\right)\right]$$

$2+\epsilon\leq\tau\leq 3$

$$A_n(\tau)=\frac{\beta\epsilon}{2\lambda\pi}\left[\cosh\frac{\pi(\tau-2)}{\epsilon}+\cosh\frac{\pi(\tau-2-\epsilon)}{\epsilon}\right.$$

$$-\frac{\pi(\tau-2)}{\epsilon}\sin\frac{\pi(\tau-2)}{\epsilon}-\frac{\pi(\tau-2-\epsilon)}{\epsilon}\sin\frac{\pi(\tau-2-\epsilon)}{\epsilon}$$

$$-\alpha_n\left(\sinh\frac{\pi(\tau-2)}{\epsilon}+\sinh\frac{\pi(\tau-2-\epsilon)}{\epsilon}\right.$$

$$\left.\left.+\frac{\pi(\tau-2)}{\epsilon}\cos\frac{\pi(\tau-2)}{\epsilon}+\frac{\pi(\tau-2-\epsilon)}{\epsilon}\cos\frac{\pi(\tau-2-\epsilon)}{\epsilon}\right)\right]$$

$3 \le \tau \le 3+\epsilon$

$$A_n(\tau) = \frac{\beta\epsilon}{2\lambda\pi}\left[2\cos\frac{\pi(\tau-3)}{\epsilon}\cosh\frac{\pi}{\epsilon} + \cosh\frac{\pi(\tau-2-\epsilon)}{\epsilon}\right.$$

$$-\cosh\frac{\pi(4-\tau)}{\epsilon} - \frac{2\pi}{\epsilon}\cos\frac{\pi(\tau-3)}{\epsilon}\sin\frac{\pi}{\epsilon}$$

$$-\frac{\pi(\tau-2-\epsilon)}{\epsilon}\sin\frac{\pi(\tau-2-\epsilon)}{\epsilon} + \frac{\pi(4-\tau)}{\epsilon}\sin\frac{\pi(4-\tau)}{\epsilon}$$

$$-\alpha_n\left(2\cos\frac{\pi(\tau-3)}{\epsilon}\sinh\frac{\pi}{\epsilon} + \sinh\frac{\pi(\tau-2-\epsilon)}{\epsilon}\right.$$

$$-\sinh\frac{\pi(4-\tau)}{\epsilon} + \frac{2\pi}{\epsilon}\cos\frac{\pi(\tau-3)}{\epsilon}\cos\frac{\pi}{\epsilon}$$

$$\left.\left.+\frac{\pi(\tau-2-\epsilon)}{\pi}\cos\frac{\pi(\tau-2-\epsilon)}{\epsilon} - \frac{\pi(4-\tau)}{\epsilon}\cos\frac{\pi(4-\tau)}{\epsilon}\right)\right]$$

$3+\epsilon \le \tau \le 4$

$$A_n(\tau) = \frac{-\beta\epsilon}{2\lambda\pi}\left[\cosh\frac{\pi(4-\tau+\epsilon)}{\epsilon} + \cosh\frac{\pi(4-\tau)}{\epsilon}\right.$$

$$-\frac{\pi(4-\tau+\epsilon)}{\epsilon}\sin\frac{\pi(4-\tau+\epsilon)}{\epsilon} - \frac{\pi(4-\tau)}{\epsilon}\sin\frac{\pi(4-\tau)}{\epsilon}$$

$$-\alpha_n\left(\sinh\frac{\pi(4-\tau+\epsilon)}{\epsilon} + \sinh\frac{\pi(4-\tau)}{\epsilon}\right.$$

$$\left.\left.+\frac{\pi(4-\tau+\epsilon)}{\epsilon}\cos\frac{\pi(4-\tau+\epsilon)}{\epsilon} + \frac{\pi(4-\tau)}{\epsilon}\cos\frac{\pi(4-\tau)}{\epsilon}\right)\right]$$

$4 \le \tau \le 4+\epsilon$

$$A_n(\tau) = \frac{-\beta\epsilon}{2\lambda\pi}\left[\cos\frac{\pi(4-\tau)}{\epsilon} + \cosh\frac{\pi(4-\tau+\epsilon)}{\epsilon} - \frac{\pi(4-\tau+\epsilon)}{\epsilon}\right.$$

$$\sin\frac{\pi(4-\tau+\epsilon)}{\epsilon}$$

$$-\alpha_n\left(2\sin\frac{\pi(4-\tau)}{\epsilon} + \sinh\frac{\pi(4-\tau+\epsilon)}{\epsilon}\right.$$

$$\left.\left.+\frac{\pi(4-\tau+\epsilon)}{\epsilon}\cos\frac{\pi(4-\tau+\epsilon)}{\epsilon}\right)\right] + A_n(\tau)\Big|_{0 \le \tau \le \epsilon}$$

(3-118)

And for $K_n \neq \frac{\pi}{\epsilon}$

$0 \le \tau \le \epsilon$

$$A_n(\tau) = \frac{-\beta}{\lambda}\left[\frac{\pi\epsilon}{\pi^2 + K_n^2\epsilon^2}\left((\cos\frac{\pi\tau}{\epsilon} - \cosh K_n\tau\right)\right.$$

$$-\alpha_n\left(\frac{K_n\epsilon}{\pi}\sin\frac{\pi\tau}{\epsilon} - \sinh K_n\tau\right)\Big) - \frac{\pi\epsilon}{\pi^2 - K_n^2\epsilon^2}\Big((\cos\frac{\pi\tau}{\epsilon}$$

$$\left. - \cos K_n\tau) - \alpha_n\left(\frac{K_n\epsilon}{\pi}\sin\frac{\pi\tau}{\epsilon} - \sin K_n\tau\right)\right)\Big)\Big]$$

$\epsilon \le \tau \le 1$

$$A_n(\tau) = \frac{\beta}{\lambda}\left[\frac{\pi\epsilon}{\pi^2 + K_n^2\epsilon^2}\left(\left(\cosh K_n\tau + \cosh K_n(\tau - \epsilon)\right)\right.\right.$$

$$-\alpha_n\left(\sinh K_n\tau + \sinh K_n(\tau - \epsilon)\right)\Big)$$

$$-\frac{\pi\epsilon}{\pi^2 - K_n^2\epsilon^2}\left(\left(\cos K_n\tau + \cos K_n(\tau - \epsilon)\right)\right.$$

$$\left.\left. -\alpha_n\left(\sin K_n\tau + \sin K_n(\tau - \epsilon)\right)\right)\right]$$

$1 \le \tau \le 1 + \epsilon$

$$A_n(\tau) = \frac{\beta}{\lambda}\left[\frac{\pi\epsilon}{\pi^2 + K_n^2\epsilon^2}\left(\left(2\cos\frac{\pi(\tau - 1)}{\epsilon}\cosh K_n\right.\right.\right.$$

$$\left. + \cosh K_n(\tau - \epsilon) - \cosh K_n(2 - \tau)\right)$$

$$-\alpha_n\left(2\cos\frac{\pi(\tau - 1)}{\epsilon}\sinh K_n + \sinh K_n(\tau - \epsilon)\right.$$

$$\left.\Big) - \frac{\pi\epsilon}{\pi^2 - K_n^2\epsilon^2}\Big(\Big(2\cos\frac{\pi(\tau - 1)}{\epsilon}\cos K_n\right.$$

$$\left. + \cos K_n(\tau - \epsilon) - \cos K_n(2 - \tau)\right) - \alpha_n\left(2\cos\frac{\pi(\tau - 1)}{\epsilon}\sin K_n\right.$$

$$\left.\left. + \sin K_n(\tau - \epsilon) - \sin K_n(2 - \tau)\right)\Big)\right]$$

$$1+\epsilon \le \tau \le 2 \qquad A_n(\tau) = \frac{-\beta}{\lambda}\left[\frac{\pi\epsilon}{\pi^2 + K_n^2\,\epsilon^2}\left(\cosh K_n(2-\tau+\epsilon) + \cosh K_n(2-\tau)\right.\right.$$

$$\left. - \alpha_n\left(\sinh K_n(2-\tau+\epsilon) + \sinh K_n(2-\tau)\right)\right)$$

$$- \frac{\pi\epsilon}{\pi^2 - K_n^2\,\epsilon^2}\left(\cos K_n(2-\tau+\epsilon) + \cos K_n(2-\tau)\right.$$

$$\left.\left. - \alpha_n\left(\sin K_n(2-\tau+\epsilon) + \sin K_n(2-\tau)\right)\right)\right]$$

$$2 \le \tau \le 2+\epsilon \qquad A_n(\tau) = \frac{-\beta}{\lambda}\left[\frac{\pi\epsilon}{\pi^2 + K_n^2\,\epsilon^2}\left(2\cos\frac{\pi(\tau-2)}{\epsilon} + \cosh K_n(2-\tau+\epsilon)\right.\right.$$

$$\left. - \cosh K_n(\tau-2) - \alpha_n\left(\sinh K_n(2-\tau+\epsilon) - \sinh K_n(\tau-2)\right)\right)$$

$$- \frac{\pi\epsilon}{\pi^2 - K_n^2\,\epsilon^2}\left(2\cos\frac{\pi(\tau-2)}{\epsilon} + \cos K_n(2-\tau+\epsilon)\right.$$

$$\left.\left. - \cos K_n(\tau-2) - \alpha_n\left(\sin K_n(2-\tau+\epsilon) - \sin K_n(\tau-2)\right)\right)\right]$$

$$2+\epsilon \le \tau \le 3 \qquad A_n(\tau) = \frac{\beta}{\lambda}\left[\frac{\pi\epsilon}{\pi^2 + K_n^2\,\epsilon^2}\left(\cosh K_n(\tau-2) + \cosh K_n(\tau-2-\epsilon)\right.\right.$$

$$\left. - \alpha_n\left(\sinh K_n(\tau-2) + \sinh K_n(\tau-2-\epsilon)\right)\right)$$

$$- \frac{\pi\epsilon}{\pi^2 - K_n^2\,\epsilon^2}\left(\cos K_n(\tau-2) + \cos K_n(\tau-2-\epsilon)\right.$$

$$\left.\left. - \alpha_n\left(\sin K_n(\tau-2) + \sin K_n(\tau-2-\epsilon)\right)\right)\right]$$

$$3 \le \tau \le 3+\epsilon \qquad A_n(\tau) = \frac{\beta}{\lambda}\left[\frac{\pi\epsilon}{\pi^2 + K_n^2\,\epsilon^2}\left(2\cos\frac{\pi(\tau-3)}{\epsilon}\cosh K_n\right.\right.$$

$$+ \cosh K_n(\tau - 2 - \epsilon) - \cosh K_n(4-\tau)$$

$$- \alpha_n\left(2\cos\frac{\pi(\tau-3)}{\epsilon}\sinh K_n + \sinh K_n(\tau-2-\epsilon)\right.$$

$$\left.\left. - \sinh K_n(4-\tau)\right)\right) - \frac{\pi\epsilon}{\pi^2 - K_n^2\,\epsilon^2}\left(2\cos\frac{\pi(\tau-3)}{\epsilon}\cos K_n\right.$$

$$+ \cos K_n(\tau-2-\epsilon) - \cos K_n(4-\tau) - \alpha_n\left(2\cos\frac{\pi(\tau-3)}{\epsilon}\right.$$

$$\left.\left.\sin K_n + \sin K_n(\tau-2-\epsilon) - \sin K_n(4-\tau)\right)\right)\Bigg]$$

$$3+\epsilon \le \tau \le 4 \qquad A_n(\tau) = \frac{-\beta}{\lambda}\left[\frac{\pi\epsilon}{\pi^2 + K_n^2\,\epsilon^2}\left(\cosh K_n(4-\tau+\epsilon) + \cosh K_n(4-\tau)\right.\right.$$

$$\left. - \alpha_n\left(\sinh K_n(4-\tau+\epsilon) + \sinh K_n(4-\tau)\right)\right)$$

$$- \frac{\pi\epsilon}{\pi^2 - K_n^2\,\epsilon^2}\left(\cos K_n(4-\tau+\epsilon) + \cos K_n(4-\tau)\right.$$

$$\left. - \alpha_n\left(\sin K_n(4-\tau+\epsilon) + \sin K_n(4-\tau)\right)\right)\Bigg]$$

$$4 \le \tau \le 4+\epsilon \qquad A_n(\tau) = \frac{-\beta}{\lambda}\left[\frac{\pi\epsilon}{\pi^2 + K_n^2\,\epsilon^2}\left(\cos\frac{\pi(4-\tau)}{\epsilon} + \cosh K_n(4-\tau+\epsilon)\right.\right.$$

$$-\alpha_n\left(\frac{K_n\epsilon}{\pi}\sin\frac{\pi(4-\tau)}{\epsilon} + \sinh K_n(4-\tau+\epsilon)\right)\Bigg)$$

$$- \frac{\pi\epsilon}{\pi^2 - K_n^2\,\epsilon^2}\left(\cos\frac{\pi(4-\tau)}{\epsilon} + \cos K_n(4-\tau+\epsilon)\right.$$

$$\left. - \alpha_n\left(\frac{K_n\epsilon}{\pi}\sin\frac{\pi(4-\tau)}{\epsilon} + \sin K_n(4-\tau+\epsilon)\right)\right)\Bigg]$$

$$+A_n(\tau)\Big|_{0 \le \tau \le \epsilon} \qquad (3\text{-}119)$$

The above expressions for $A_n(\tau)$ are written for the number of traverses required to completely represent the history of transient pressures. It should be noted that the last term in the last expression is a repeat of the first expression for the first time interval. Thus, the expressions for $A_n(\tau)$ are employed cyclically as time progresses.

2. Adaptation to Automatic Computation

As explained in Section II, the transient pressure forms under consideration continually traverse the cylinder from one end to the other. Algebraic expressions which yield the deflections and stresses at any time in the sequence of transient pressure traverses can be derived by the procedure employed for the sample solutions of Section III-C. However, depending on the type of transient pressure, the size and complexity of the algebraic expressions for the response solution increases with each traverse and soon becomes unwieldy. After examination of the various techniques that could be employed to overcome this problem, it was thought appropriate to adopt a conventional numerical method of solution which could be readily programmed for use on the digital computer. All the analytics pertinent to such a method of solution were presented in the previous section.

The solution of Equation 3-109 can be efficiently obtained by the predictor corrector technique of numerical integration which is explained in Reference 3-5.

This technique was used as the basis for a general purpose computer program which was programmed to give results for the ramp and sinusoidal transient pressure forms. As explained above, in the limit, these cases reduce respectively to the step and spike pressure types. The general purpose program is presented, together with illustrative problems as a users manual in Volume II of this report.

3. Summary of Solutions

As stated previously, obtaining expressions for the response of cylinders subjected to many traverses of the pressure transient is prohibitive and consequently it is best to obtain design data by numerical integration of the separated differential equation, Equation 3-109. However, under certain circumstances only the first traverse

of the pressure transient is required. In addition, such solutions which are less costly to run on digital equipment, could be used to check the numerically obtained solution and to generate design data, in spite of its limitation.

Design data presented in this document are valid for only the first traverse of the pressure transient under consideration. Expressions used to compute the data are summarized in this section. However, where it is convenient, the dynamic solutions were extended beyond the first traverse.

Since the solution is given by Equation 3-108, only expressions for the time dependent function $F_n(\tau)$ need be documented. In general, the expression for $F_n(\tau)$ for all cases treated will be of the form

$$F_n(\tau) = \bar{a}_n \left[e^{-\bar{\alpha}\tau} \left(A_{in} \cos \bar{\Omega}_n \tau + B_{in} \sin \bar{\Omega}_n \tau \right) + F_{p_{in}}(\tau) \right] \quad (3\text{-}120)$$

where $\bar{a}_n$, A_{in}, B_{in} and $F_{p_{in}}(\tau)$ depend on the form of the pressure transient under consideration and are summarized below. The subscript "i" is introduced to identify the time interval where necessary. The damped nondimensional natural frequency $\bar{\Omega}_n$ is given by

$$\bar{\Omega}_n^2 = \Omega_n^2 - \bar{\alpha}^2 \quad (3\text{-}121)$$

(a) Spike Pressure, Simple-Simple Edge Conditions $0 \leq \tau$

$$\left.\begin{aligned} F_{p_n}(\tau) &= C_n \sin n\pi\tau + D_n \cos n\pi\tau \\ \bar{a}_n &= \frac{\beta^{1/2}}{\lambda \left[(\Omega_n^2 - n^2\pi^2)^2 + (2n\pi\bar{\alpha})^2 \right]} \\ A_n &= 2n\pi\bar{\alpha} \\ B_n &= \frac{n\pi}{\bar{\Omega}_n} \left[2\bar{\alpha}^2 - (\Omega_n^2 - n^2\pi^2) \right] \\ C_n &= \Omega_n^2 - n^2\pi^2 \\ D_n &= -2n\pi\bar{\alpha} \end{aligned}\right\} \quad (3\text{-}122)$$

(b) Step Pressure, Simple-Simple Edge Conditions

$$F_{p_{in}}(\tau) = C_{in} + D_{in}\cos n\pi\tau + E_{in}\sin n\pi\tau \; ; \; \bar{a}_n = \frac{\beta}{n\pi\lambda} \qquad (3\text{-}123)$$

$0 \le \tau \le 2$, i = 1

$$A_{1n} = -(C_{1n} + D_{1n}); \; B_{1n} = \frac{1}{\bar{\Omega}_n}(\bar{a}A_{1n} - n\pi E_{1n}); \; C_{1n} = \frac{1}{\Omega_n^2}$$

$$D_{1n} = \frac{-(\Omega_n^2 - n^2\pi^2)}{(\Omega_n^2 - n^2\pi^2)^2 + (2\bar{a}n\pi)^2}; \; E_{1n} = \frac{-2\bar{a}n\pi}{(\Omega_n^2 - n^2\pi^2)^2 + (2\bar{a}n\pi)^2}$$

$2 \le \tau \le 4$, i = 2

$$A_{2n} = \frac{a_{2n}G_{1n} - G_{2n}\sin 2\bar{\Omega}_n}{a_{2n}\cos 2\bar{\Omega}_n - a_{1n}\sin 2\bar{\Omega}_n}; \; B_{2n} = \frac{G_{2n}\cos 2\bar{\Omega}_n - a_{1n}G_{1n}}{a_{2n}\cos 2\bar{\Omega}_n - a_{1n}\sin 2\bar{\Omega}_n}$$

$$a_{1n} = -\bar{a}\cos 2\bar{\Omega}_n - \bar{\Omega}_n \sin 2\bar{\Omega}_n; \; a_{2n} = -\bar{a}\sin 2\bar{\Omega}_n + \bar{\Omega}_n \cos 2\bar{\Omega}_n$$

$$G_{1n} = 2(C_{1n} + D_{1n})e^{2\bar{a}} + A_{1n}\cos 2\bar{\Omega}_n + B_{1n}\sin 2\bar{\Omega}_n$$

$$G_{2n} = 2n\pi E_{1n}e^{2\bar{a}} + A_{1n}a_{1n} + B_{1n}a_{2n}$$

$$C_{2n} = -C_{1n}; \; D_{2n} = -D_{1n}; \; E_{2n} = -E_{1n}$$

(c) Ramp Pressure, Simple-Simple Edge Conditions

$$F_{p_{in}}(\tau) = C_{in} + D_{in}\tau + E_{in}\cos n\pi\tau + G_{in}\sin n\pi\tau \; ; \; \bar{a}_n = \frac{\beta}{n\pi\lambda} \qquad (3\text{-}124)$$

$0 \le \tau \le \tau_c$, i = 1

$$A_{1n} = -C_{1n} - E_{1n}; \; B_{1n} = \frac{1}{\bar{\Omega}_n}(\bar{a}A_{1n} - D_{1n} - n\pi G_{1n})$$

$$C_{1n} = -\frac{2\bar{a}}{\tau_c \Omega_n^4}; \; D_{1n} = \frac{1}{\tau_c \Omega_n^2}$$

$$E_{1n} = \frac{2\bar{a}/\tau_c}{(\Omega_n^2 - n^2\pi^2)^2 + (n\pi 2\bar{a})^2}; \; G_{1n} = \frac{-\frac{1}{n\pi\tau_c}(\Omega_n^2 - n^2\pi^2)}{(\Omega_n^2 - n^2\pi^2)^2 + (n\pi 2\bar{a})^2}$$

$\tau_c \le \tau \le 1$, i = 2

$$A_{2n} = \frac{C_1 a_2 - C_2 \sin \bar{\Omega}_n \tau_c}{a_2 \cos \bar{\Omega}_n \tau_c - a_1 \sin \bar{\Omega}_n \tau_c} ; \quad B_{2n} = \frac{C_2 \cos \bar{\Omega}_n \tau_c - C_1 a_1}{a_2 \cos \bar{\Omega}_n \tau_c - a_1 \sin \bar{\Omega}_n \tau_c}$$

$$C_{2n} = \frac{1}{\Omega_n^2} ; \quad D_{2n} = 0$$

$$E_{2n} = \frac{-(\Omega_n^2 - n^2 \pi^2) \frac{1}{n\pi \tau_c} \sin n\pi \tau_c + \frac{2\bar{\alpha}}{\tau_c}(1 - \cos n\pi \tau_c)}{(\Omega_n^2 - n^2 \pi^2)^2 + (2\bar{\alpha} n \pi)^2}$$

$$G_{2n} = \frac{\frac{1}{n\pi\tau_c}(\Omega_n^2 - n^2 \pi^2)(1 - \cos n\pi \tau_c) - \frac{2\bar{\alpha}}{\tau_c} \sin n\pi \tau_c}{(\Omega_n^2 - n^2 \pi^2)^2 + (2\bar{\alpha} n\pi)^2}$$

$$a_1 = -\bar{\alpha} \cos \bar{\Omega}_n \tau_c - \bar{\Omega}_n \sin \bar{\Omega}_n \tau_c ; \quad a_2 = -\bar{\alpha} \sin \bar{\Omega}_n \tau_c + \bar{\Omega}_n \cos \bar{\Omega}_n \tau_c$$

$$b_1 = C_{1n} + D_{1n} \tau_c + E_{1n} \cos n\pi \tau_c + G_{1n} \sin n\pi \tau_c$$

$$b_2 = C_{2n} + D_{2n} \tau_c + E_{2n} \cos n\pi \tau_c + G_{2n} \sin n\pi \tau_c$$

$$b_3 = D_{1n} - E_{1n} n\pi \sin n\pi \tau_c + n\pi G_{1n} \cos n\pi \tau_c$$

$$b_4 = n\pi E_{2n} \sin n\pi \tau_c - n\pi G_{2n} \cos n\pi \tau_c$$

$$C_1 = e^{\bar{\alpha}\tau_c}(-b_2 + b_1) + A_{1n} \cos \bar{\Omega}_n \tau_c + B_{1n} \sin \bar{\Omega}_n \tau_c$$

$$C_2 = e^{\bar{\alpha}\tau_c}(b_3 + b_4) + a_1 A_{1n} + a_2 B_{1n}$$

(d) **Sinusoidal Pressure, Simple-Simple Edge Conditions**

$$F_{p_{in}}(\tau) = C_{in} \sin n\pi\tau + D_{in} \cos n\pi\tau + E_{in} \sin \frac{\pi\tau}{\epsilon} + G_{in} \cos \frac{\pi\tau}{\epsilon}$$

$$a_n = \frac{\beta}{\lambda\pi}\left(\frac{\epsilon}{1 - \epsilon^2 n^2}\right) \qquad (3\text{-}125)$$

$0 \le \tau \le \epsilon$, $i = 1$

$$A_{1n} = -D_{1n} - G_{1n}, \quad B_{1n} = \frac{1}{\bar{\Omega}_n}\left(\bar{\alpha} A_{1n} - n\pi C_{1n} - \frac{\pi}{\epsilon} E_{1n}\right)$$

$$C_{1n} = \frac{(\Omega_n^2 - n^2\pi^2)}{(\Omega_n^2 - n^2\pi^2)^2 + 2\bar{\alpha} n\pi)^2}, \quad D_{1n} = \frac{-2\bar{\alpha} n\pi}{(\Omega_n^2 - n^2\pi^2)^2 + (2\bar{\alpha} n\pi)^2}$$

$$E_{1n} = \frac{-n\epsilon\left(\Omega_n^2 - \frac{\pi^2}{\epsilon^2}\right)}{\left(\Omega_n^2 - \frac{\pi^2}{\epsilon^2}\right)^2 + \left(2\bar{\alpha}\frac{\pi}{\epsilon}\right)^2}, \quad G_{1n} = \frac{2\bar{\alpha} n\pi}{\left(\Omega_n^2 - \frac{\pi^2}{\epsilon^2}\right)^2 + \left(2\bar{\alpha}\frac{\pi}{\epsilon}\right)^2}$$

$\epsilon \le \tau \le 1$, $i = 2$

$$A_{2n} = \frac{a_2 C_1 - C_2 \sin\bar{\Omega}_n\epsilon}{a_2 \cos\bar{\Omega}_n\epsilon - a_1 \sin\bar{\Omega}_n\epsilon}$$

$$B_{2n} = \frac{C_2 \cos\bar{\Omega}_n\epsilon - a_1 C_1}{a_2 \cos\bar{\Omega}_n\epsilon - a_1 \sin\bar{\Omega}_n\epsilon}$$

$$C_{2n} = \frac{+(\Omega_n^2 - n^2\pi^2)(1 + \cos n\pi\epsilon) - n\pi 2\bar{\alpha} \sin n\pi\epsilon}{(\Omega_n^2 - n^2\pi^2)^2 + (n\pi 2\bar{\alpha})^2}$$

$$D_{2n} = \frac{-(\Omega_n^2 - n^2\pi^2)\sin n\pi\epsilon - (1 + \cos n\pi\epsilon) 2\bar{\alpha} n\pi}{(\Omega_n^2 - n^2\pi^2)^2 + (n\pi 2\bar{\alpha})^2}$$

$$a_1 = -\bar{\alpha}\cos\bar{\Omega}_n\epsilon - \bar{\Omega}_n \sin\bar{\Omega}_n\epsilon \; ; \quad a_2 = -\bar{\alpha}\sin\bar{\Omega}_n\epsilon + \bar{\Omega}_n\cos\bar{\Omega}_n\epsilon$$

$$b_1 = C_{1n}\sin n\pi\epsilon + D_{1n}\cos n\pi\epsilon - G_{1n}; \quad b_2 = C_{2n}\sin n\pi\epsilon + D_{2n}\cos n\pi\epsilon$$

$$b_3 = n\pi C_{1n}\cos n\pi\epsilon - n\pi D_{1n}\sin n\pi\epsilon - \frac{\pi}{\epsilon} E_{1n}; \quad b_4 = n\pi C_{2n}\cos n\pi\epsilon - D_{2n} n\pi \sin n\pi\epsilon$$

$$C_1 = e^{\bar{\alpha}\epsilon}(b_1 - b_2) + A_{1n}\cos\bar{\Omega}_n\epsilon + B_{1n}\sin\bar{\Omega}_n\epsilon$$

$$C_2 = e^{\bar{\alpha}\epsilon}(b_3 - b_4) + a_1 A_{1n} + a_2 B_{1n})$$

(e) Spike Pressure, Fixed-Fixed Edge Conditions

$$\bar{a}_n = \frac{\beta^{1/2}}{2\lambda} \tag{3-126}$$

$0 \le \tau \le 1$, $i = 1$

$$F_{p_{1n}} = C_{1n} \cosh K_n \tau + D_{1n} \cos K_n \tau + E_{1n} \sinh K_n \tau + G_{1n} \sin K_n \tau$$

$$A_{1n} = -(C_{1n} + D_{1n}), \qquad B_{1n} = \frac{1}{\bar{\Omega}_n}\left[\bar{\alpha} A_{1n} - (E_{1n} K_n + G_{1n} K_n)\right]$$

$$C_{1n} = \frac{(\Omega_n^2 + K_n^2) + 2\bar{\alpha} K_n \alpha_n}{(\Omega_n^2 + K_n^2)^2 - (2\bar{\alpha} K_n)^2}, \quad D_{1n} = \frac{-(\Omega_n^2 - K_n^2) - 2\bar{\alpha} K_n \alpha_n}{(\Omega_n^2 - K_n^2)^2 + (2\bar{\alpha} K_n)^2}$$

$$E_{1n} = \frac{-\alpha_n (\Omega_n^2 + K_n^2) - 2\bar{\alpha} K_n}{(\Omega_n^2 + K_n^2)^2 - (2\bar{\alpha} K_n)^2}, \quad G_{1n} = \frac{\alpha_n (\Omega_n^2 - K_n^2) - 2\bar{\alpha} K_n}{(\Omega_n^2 - K_n^2)^2 + (2\bar{\alpha} K_n)^2}$$

$1 \le \tau \le 2$, $i = 2$

$$F_{p_{2n}} = C_{2n} \cosh K_n (2 - \tau) + D_{2n} \cos K_n (2 - \tau) + E_{2n} \sinh K_n (2 - \tau)$$

$$+ G_{2n} \sin K_n (2 - \tau)$$

$$A_{2n} = \frac{C_1 a_2 - C_2 \sin \bar{\Omega}_n}{a_2 \cos \bar{\Omega}_n - a_1 \sin \bar{\Omega}_n}, \quad B_{2n} = \frac{C_2 \cos \bar{\Omega}_n - C_1 a_1}{a_2 \cos \bar{\Omega}_n - a_1 \cos \bar{\Omega}_n}$$

$$C_{2n} = \frac{(\Omega_n^2 + K_n^2) - 2\bar{\alpha} K_n \alpha_n}{(\Omega_n^2 + K_n^2)^2 - (2\bar{\alpha} K_n)^2}, \quad D_{2n} = \frac{-(\Omega_n^2 + K_n^2) + 2\bar{\alpha} K_n \alpha_n}{(\Omega_n^2 - K_n^2)^2 + (2\bar{\alpha} K_n)^2}$$

$$E_{2n} = \frac{-\alpha_n (\Omega_n^2 + K_n^2) + 2\bar{\alpha} K_n}{(\Omega_n^2 + K_n^2)^2 - (2\bar{\alpha} K_n)^2}, \quad G_{2n} = \frac{\alpha_n (\Omega_n^2 - K_n^2) + 2\bar{\alpha} K_n}{(\Omega_n^2 - K_n^2)^2 + (2\bar{\alpha} K_n)^2}$$

$$a_1 = -\bar{\alpha} \cos \bar{\Omega}_n - \bar{\Omega}_n \sin \bar{\Omega}_n, \quad a_{2n} = -\bar{\alpha} \sin \bar{\Omega}_n + \bar{\Omega}_n \cos \bar{\Omega}_n$$

$$b_1 = E_{1n} \sinh K_n + G_{1n} \sin K_n + C_{1n} \cosh K_n + D_{1n} \cos K_n$$

$$b_2 = E_{2n} \sinh K_n + G_{2n} \sin K_n + C_{2n} \cosh K_n + D_{2n} \cos K_n$$

$$b_3 = K_n (E_{1n} \cosh K_n + G_{1n} \cos K_n + C_{1n} \sinh K_n - D_{1n} \sin K_n)$$

$$b_4 = K_n (E_{2n} \cosh K_n + G_{2n} \cos K_n + C_{2n} \sinh K_n - D_{2n} \sin K_n)$$

$$C_1 = A_{1n} \cos\bar{\Omega}_n + B_{1n} \sin\bar{\Omega}_n + (-b_2 + b_1)\, e^{\bar{\alpha}}$$

$$C_2 = e^{\bar{\alpha}} (b_4 + b_3) + a_1 A_{1n} + a_2 B_{1n})$$

(f) Step Pressure, Fixed-Fixed Edge Supports

$$\bar{a}_n = \frac{\beta}{\lambda K_n}$$

$0 \le \tau \le 1$, $i = 1$

$$F_{p_{1n}} = C_{1n} \sinh K_n \tau + D_{1n} \sin K_n \tau + E_{1n} \cosh K_n \tau + G_{1n} \cos K_n \tau + H_{1n} \qquad (3\text{-}127)$$

$$A_{1n} = -(E_{1n} + G_{1n} + H_{1n}), \qquad B_{1n} = \frac{1}{\bar{\Omega}_n} (\bar{\alpha} A_{1n} - C_{1n} K_n - D_{1n} K_n)$$

$$C_{1n} = \frac{(\Omega_n^2 + K_n^2) + (\alpha_n 2\, \bar{\alpha} K_n)}{(\Omega_n^2 + K_n^2)^2 - (2\bar{\alpha} K_n)^2}, \qquad D_{1n} = \frac{-(\Omega_n^2 - K_n^2) - \alpha_n 2\, \bar{\alpha} K_n}{(\Omega_n^2 - K_n^2)^2 + (2\bar{\alpha} K_n)^2}$$

$$E_{1n} = \frac{-\alpha_n (\Omega_n^2 + K_n^2) - 2\bar{\alpha} K_n}{(\Omega_n^2 + K_n^2)^2 - (2\bar{\alpha} K_n)^2}, \quad G_{1n} = \frac{-\alpha_n (\Omega_n^2 - K_n^2) + 2\bar{\alpha} K_n}{(\Omega_n^2 - K_n^2)^2 + (2\bar{\alpha} K_n)^2}, \quad H_{1n} = \frac{2\alpha_n}{\Omega_n^2}$$

$1 \le \tau \le 2$, $i = 2$

$$F_{p_{2n}} = C_{2n} \sinh K_n (2 - \tau) + D_{2n} \sin K_n (2 - \tau) + E_{2n} \cosh K_n (2 - \tau) + G_{2n} \cos K_n (2 - \tau) + H_{2n}$$

$$A_{2n} = \frac{C_1 a_2 - C_2 \sin \bar{\Omega}_n}{a_2 \cos \bar{\Omega}_n - a_1 \sin \bar{\Omega}_n}, \quad B_{2n} = \frac{C_2 \cos \bar{\Omega}_n - C_1 a_1}{a_2 \cos \bar{\Omega}_n - a_1 \sin \bar{\Omega}_n}$$

$$C_{2n} = \frac{(\Omega_n^2 + K_n^2) - \alpha_n 2 \bar{\alpha} K_n}{(\Omega_n^2 + K_n^2)^2 - (2 \bar{\alpha} K_n)^2}, \quad D_{2n} = \frac{-(\Omega_n^2 - K_n^2) + \alpha_n 2 \bar{\alpha} K_n}{(\Omega_n^2 - K_n^2)^2 + (2 \bar{\alpha} K)^2}$$

$$E_{2n} = \frac{-\alpha_n (\Omega_n^2 + K_n^2) + 2 \bar{\alpha} K_n}{(\Omega_n^2 + K_n^2)^2 - (2 \bar{\alpha} K_n)^2}, \quad G_{2n} = \frac{-\alpha_n (\Omega_n^2 - K_n^2) - 2 \bar{\alpha} K_n}{(\Omega_n^2 - K_n^2)^2 + (2 \bar{\alpha} K_n)^2}, \quad H_{2n} = H_{1n}$$

$$a_1 = -\bar{\alpha} \cos \bar{\Omega}_n - \bar{\Omega}_n \sin \bar{\Omega}_n, \quad a_2 = -\bar{\alpha} \sin \bar{\Omega}_n + \bar{\Omega}_n \cos \bar{\Omega}_n$$

$$b_1 = C_{1n} \sinh K_n + D_{1n} \sin K_n + E_{1n} \cosh K_n + G_{1n} \cos K_n + H_{1n}$$

$$b_2 = C_{2n} \sinh K_n + D_{2n} \sin K_n + E_{2n} \cosh K_n + G_{2n} \cos K_n + H_{2n}$$

$$b_3 = K_n (C_{1n} \cosh K_n + D_{1n} \cos K_n + E_{1n} \sinh K_n - G_{1n} \sin K_n)$$

$$b_4 = K_n (C_{2n} \cosh K_n + D_{2n} \cos K_n + E_{2n} \sinh K_n - G_{2n} \sin K_n)$$

$$C_1 = A_{1n} \cos \bar{\Omega}_n + B_{1n} \sin \bar{\Omega}_n + e^{\bar{\alpha}} (b_1 - b_2)$$

$$C_2 = e^{\bar{\alpha}} (b_4 + b_3) + a_1 A_{1n} + a_2 B_{1n}$$

(g) Ramp Pressure, Fixed-Fixed Edge Supports

$$F_{p_{in}} = C_{in} + D_{in} \tau + E_{in} \cosh K_n \tau + G_{in} \sinh K_n \tau + H_{in} \cosh K_n \tau + I_{in} \sin K_n \tau$$

$$\bar{a}_n = \frac{\beta}{\lambda K_n^2 \tau_c} \qquad (3\text{-}128)$$

$0 \leq \tau \leq \tau_c$, i = 1

$$A_{1n} = -(C_{1n} + E_{1n} + H_{1n}) \qquad B_{1n} = \frac{1}{\bar{\Omega}_n} (\bar{\alpha} A_{1n} - D_{1n} - K_n G_{1n} - K_n I_{1n})$$

$$C_{1n} = \frac{-1}{\Omega_n^2} (2 + 2 \bar{\alpha} D_{1n}) \qquad D_{1n} = \frac{2 K_n \alpha_n}{\Omega_n^2}$$

$$E_{1n} = \frac{(\Omega_n^2 + K_n^2) + \alpha_n 2\bar{\alpha} K_n}{(\Omega_n^2 + K_n^2)^2 - (2\bar{\alpha} K_n)^2} \qquad G_{1n} = \frac{-\alpha_n (\Omega_n^2 + K_n^2) - 2\bar{\alpha} K_n}{(\Omega_n^2 + K_n^2)^2 - (2\bar{\alpha} K_n)^2}$$

$$H_{1n} = \frac{(\Omega_n^2 - K_n^2) + 2\bar{\alpha}\alpha_n K_n}{(\Omega_n^2 - K_n^2)^2 + (2\bar{\alpha} K_n)^2} \qquad I_{1n} = \frac{-\alpha_n (\Omega_n^2 - K_n^2) + 2\bar{\alpha} K_n}{(\Omega_n^2 - K_n^2)^2 + (2\bar{\alpha} K_n)^2}$$

$\tau_c \leq \tau \leq 1$, $i = 2$

$$A_{2n} = \frac{C_1 a_2 - C_2 \sin\bar{\Omega}_n \tau_c}{a_2 \cos\bar{\Omega}_n \tau_c - a_1 \sin\bar{\Omega}_n \tau_c} \qquad B_{2n} = \frac{C_2 \cos\bar{\Omega}_n \tau_c - C_1 a_1}{a_2 \cos\bar{\Omega}_n \tau_c - a_1 \sin\bar{\Omega}_n \tau_c}$$

$$C_{2n} = \frac{1}{\Omega_n^2} 2 K_n \alpha_n \tau_c \qquad D_{2n} = 0$$

$$E_{2n} = \frac{d_1 (\Omega_n^2 + K_n^2) - d_2 2\bar{\alpha} K_n}{(\Omega_n^2 + K_n^2)^2 - (2\bar{\alpha} K_n)^2} \qquad G_{2n} = \frac{d_2 (\Omega_n^2 + K_n^2) - d_1 2\bar{\alpha} K_n}{(\bar{\Omega}_n^2 + K_n^2)^2 - (2\bar{\alpha} K_n)^2}$$

$$H_{2n} = \frac{d_3 (\Omega_n^2 - K_n^2) - d_4 2\bar{\alpha} K_n}{(\Omega_n^2 - K_n^2)^2 + (2\bar{\alpha} K_n)^2} \qquad I_{2n} = \frac{d_4 (\Omega_n^2 - K_n^2) + d_3 2\bar{\alpha} K_n}{(\Omega_n^2 - K_n^2)^2 + (2\bar{\alpha} K_n)^2}$$

$$a_1 = (-\bar{\alpha}\cos\bar{\Omega}_n \tau_c - \bar{\Omega}_n \sin\bar{\Omega}_n \tau_c) \quad , \quad a_2 = (-\bar{\alpha}\sin\bar{\Omega}_n \tau_c + \bar{\Omega}_n \cos\bar{\Omega}_n \tau_c)$$

$$b_1 = C_{1n} + D_{1n}\tau_c + E_{1n}\cosh K_n \tau_c + G_{1n}\sinh K_n \tau_c + H_{1n}\cos K_n \tau_c + I_{1n}\sin K_n \tau_c$$

$$b_2 = C_{2n} + E_{2n}\cosh K_n \tau_c + G_{2n}\sinh K_n \tau_c + H_{2n}\cos K_n \tau_c + I_{2n}\sin K_n \tau_c$$

$$b_3 = D_{1n} + K_n (E_{1n}\sinh K_n \tau_c + G_{1n}\cosh K_n \tau_c - H_{1n}\sin K_n \tau_c + I_{1n}\cos K_n \tau_c)$$

$$b_4 = K_n (E_{2n}\sinh K_n \tau_c + G_{2n}\cosh K_n \tau_c - H_{2n}\sin K_n \tau_c + I_{2n}\cos K_n \tau_c)$$

$$C_1 = (b_1 - b_2) e^{\bar{\alpha}\tau_c} + A_{1n}\cos\bar{\Omega}_n \tau_c + B_{1n}\sin\bar{\Omega}_n \tau_c$$

$$C_2 = (b_3 - b_4)\, e^{\bar{\alpha}\tau_c} + a_1 A_{1n} + a_2 B_{1n}$$

$$d_1 = 1 - \cosh K_n \tau_c - \alpha_n \sinh K_n \tau_c, \qquad d_2 = -\alpha_n + \alpha_n \cosh K_n \tau_c + \sinh K_n \tau_c$$

$$d_3 = 1 - \cos K_n \tau_c - \alpha_n \sin K_n \tau_c \qquad d_4 = -\alpha_n + \alpha_n \cos K_n \tau_c - \sin K_n \tau_c$$

(h) Sinusoidal Pressure, Fixed-Fixed Edge Supports

$$F_{p_{in}} = C_{in} \cos \frac{\pi\tau}{\epsilon} + D_{in} \sin \frac{\pi\tau}{\epsilon} + E_{in} \cos K_n \tau + G_{in} \sin K_n \tau + H_{in} \cosh K_n \tau + I_{in} \sinh K_n \tau \qquad (3\text{-}129)$$

$$\bar{a}_n = \frac{\beta \pi \epsilon}{\lambda(\pi^2 + K_n^2 \epsilon^2)}$$

$0 \le \tau \le \epsilon$, $i = 1$

$$A_{1n} = -(C_{1n} + E_{1n} + H_{1n}) \qquad B_{1n} = \frac{1}{\bar{\Omega}_n}\left(\bar{\alpha} A_{1n} - \frac{\pi}{\epsilon} D_{1n} - K_n G_{1n} - I_{1n} K_n\right)$$

$$C_{1n} = \frac{(\bar{b}_n - 1)\left(\Omega_n^2 - \frac{\pi^2}{\epsilon^2} + 2\bar{\alpha}\alpha_n K_n\right)}{\left(\Omega_n^2 - \frac{\pi^2}{\epsilon^2}\right)^2 + \left(2\bar{\alpha}\frac{\pi}{\epsilon}\right)^2} \qquad D_{1n} = \frac{(\bar{b}_n - 1)\left[-\left(\Omega_n^2 - \frac{\pi^2}{\epsilon^2}\right)\alpha_n \frac{K_n \epsilon}{\pi} + 2\bar{\alpha}\frac{\pi}{\epsilon}\right]}{\left(\Omega_n^2 - \frac{\pi^2}{\epsilon^2}\right)^2 + \left(2\bar{\alpha}\frac{\pi}{\epsilon}\right)^2}$$

$$E_{1n} = \frac{-\bar{b}_n\left[\left(\Omega_n^2 - K_n^2\right) + 2\bar{\alpha} K_n \alpha_n\right]}{\left(\Omega_n^2 - K_n^2\right)^2 + \left(2\bar{\alpha} K_n\right)^2} \qquad G_{1n} = \frac{\bar{b}_n\left[\alpha_n\left(\Omega_n^2 - K_n^2\right) - 2\bar{\alpha} K_n\right]}{\left(\Omega_n^2 - K_n^2\right)^2 + \left(2\bar{\alpha} K_n\right)^2}$$

$$H_{1n} = \frac{\left(\Omega_n^2 + K_n^2\right) + 2\bar{\alpha} K_n \alpha_n}{\left(\Omega_n^2 + K_n^2\right)^2 - \left(2\bar{\alpha} K_n\right)^2} \qquad I_{1n} = \frac{-\alpha_n\left(\Omega_n^2 + K_n^2\right) - 2\bar{\alpha} K_n}{\left(\Omega_n^2 + K_n^2\right)^2 - \left(2\bar{\alpha} K_n\right)^2}$$

$$\bar{b}_n = \frac{\pi^2 + K_n^2 \epsilon^2}{\pi^2 - K_n^2 \epsilon^2}$$

$\epsilon \leq \tau \leq 1$, i = 2

$$A_{2n} = \frac{a_2 C_1 - C_2 \sin\bar{\Omega}_n \epsilon}{a_2 \cos\bar{\Omega}_n \epsilon - a_1 \sin\bar{\Omega}_n \epsilon} \qquad B_{2n} = \frac{C_2 \cos\bar{\Omega}_n \epsilon - C_1 a_1}{a_2 \cos\bar{\Omega}_n \epsilon - a_1 \sin\bar{\Omega}_n \epsilon}, \quad C_{2n} = D_{2n} = 0$$

$$E_{2n} = \frac{d_3 (\Omega_n^2 - K_n^2) - d_4 2\bar{\alpha} K_n}{(\Omega_n^2 - K_n^2)^2 + (2\bar{\alpha} K_n)^2} \qquad G_{2n} = \frac{d_4 (\Omega_n^2 - K_n^2) + d_3 2\bar{\alpha} K_n}{(\Omega_n^2 - K_n^2)^2 + (2\bar{\alpha} K_n)^2}$$

$$H_{2n} = \frac{d_1 (\Omega_n^2 + K_n^2) - d_2 2\bar{\alpha} K_n}{(\Omega_n^2 + K_n^2)^2 - (2\bar{\alpha} K_n)^2} \qquad I_{2n} = \frac{d_2 (\Omega_n^2 + K_n^2) - d_1 2\bar{\alpha} K_n}{(\Omega_n^2 + K_n^2)^2 - (2\bar{\alpha} K_n)^2}$$

$$a_1 = -\bar{\alpha} \cos\bar{\Omega}_n \epsilon - \bar{\Omega}_n \sin\bar{\Omega}_n \epsilon \qquad a_2 = -\bar{\alpha} \sin\bar{\Omega}_n \epsilon + \bar{\Omega}_n \cos\bar{\Omega}_n \epsilon$$

$$C_1 = (b_1 - b_2) e^{\bar{\alpha}\epsilon} + A_{1n} \cos\bar{\Omega}_n \epsilon + B_{1n} \sin\bar{\Omega}_n \epsilon$$

$$C_2 = (b_3 - b_4) e^{\bar{\alpha}\epsilon} + a_1 A_{1n} + a_2 B_{1n}$$

$$b_1 = -C_{1n} + E_{1n} \cos K_n \epsilon + G_{1n} \sin K_n \epsilon + H_{1n} \cosh K_n \epsilon + I_{1n} \sinh K_n \epsilon$$

$$b_2 = E_{2n} \cos K_n \epsilon + G_{2n} \sin K_n \epsilon + H_{2n} \cosh K_n \epsilon + I_{2n} \sinh K_n \epsilon$$

$$b_3 = -\frac{\pi}{\epsilon} D_{1n} + K_n (-E_{1n} \sin K_n \epsilon + G_{1n} \cos K_n \epsilon + H_{1n} \sinh K_n \epsilon + I_{1n} \cosh K_n \epsilon)$$

$$b_4 = K_n (-E_{2n} \sin K_n \epsilon + G_{2n} \cos K_n \epsilon + H_{2n} \sinh K_n \epsilon + I_{2n} \cosh K_n \epsilon)$$

$$d_1 = 1 + \cosh K_n \epsilon + \alpha_n \sinh K_n \epsilon, \quad d_2 = \sinh K_n \epsilon - \alpha_n - \alpha_n \cosh K_n \epsilon$$

$$d_3 = -\bar{b}_n (1 + \cos K_n \epsilon + \alpha_n \sin K_n \epsilon), \quad d_4 = -\bar{b}_n (\sin K_n \epsilon - \alpha_n - \alpha_n \cos K_n \epsilon)$$

F. REFERENCES

3-1 H. Reismann and J. Padlog, "Forced, Axi-Symmetric Motions of Cylindrical Shells," Bell Aerosystems Report No. 2286-950003, November 1965.

3-2 S. Timoshenko and S. Woinowski-Krieger "Theory of Plates and Shells", McGraw-Hill Book Co., New York, 1959.

3-3 H. Reismann, "Response of a Pre-Stressed Cylindrical Shell to Moving Pressure Load," Developments in Mechanics (Proc. of the Eighth Midwestern Mechanics Conference), Pergamon Press, Oxford, 1965, pp. 349-363.

3-4 S. Timoshenko and D.H. Young, "Vibration Problems in Engineering," Third Edition, D. Von Nostrand Co., Inc., New York, 1956.

3-5 W.E. Milne, "Numerical Solution of Differential Equations", John Wiley and Sons, New York, 1953.

IV. SUMMARY OF RESULTS

A. TYPICAL DYNAMICAL RESPONSE SOLUTIONS

The elastic dynamic response solutions presented in this report will yield the complete history of deflection profiles and stress fields as a function of the design parameters discussed in Section III-D. Each set of design parameters represents a specific time dependent design situation and consequently, as this study has clearly indicated, must be investigated in detail if a thorough understanding and analysis of the dynamic response of the shell is to be obtained. Such an exhaustive investigation, although feasible for a particular design situation, is not feasible for the range of values of the design parameters discussed in Section III-D. Hence, it is the intent of this section to present only sufficient detail which reveals the significant characteristics of the response of cylinders to transient pressures. This information is then used as the basis for the method adopted for the development of design charts.

1. Infinite Length Shell

Typical deflection profiles and bending moment distributions are presented for the shell of infinite length subjected to a traveling pressure spike in Figures IV-1 through IV-4. Damping was neglected ($\alpha = 0$). Two distinct deflection profiles are obtained depending on whether the speed parameter, λ, is greater or less than one. When $\lambda < 1$ the traveling deflection profile appears as a damped sinusoid that is symmetrical with respect to $\xi = 0$ as shown in Figure IV-1. The maximum deflection occurs at $\xi = 0$ and increases with an increase in λ.

When $\lambda > 1$, the deflection profile is sinusoidal as shown in Figure IV-2. Deflections and wave lengths behind the traveling spike are larger than those in front of the spike. In addition, as a result of the oscillatory character of the deflection curve about $\bar{w} = 0$, maximum negative and positive deflections of equal magnitude are experienced. The maximum deflections decrease with an increase in λ. As λ approaches one from either direction a critical condition is approached which is characterized by unbounded deflections.

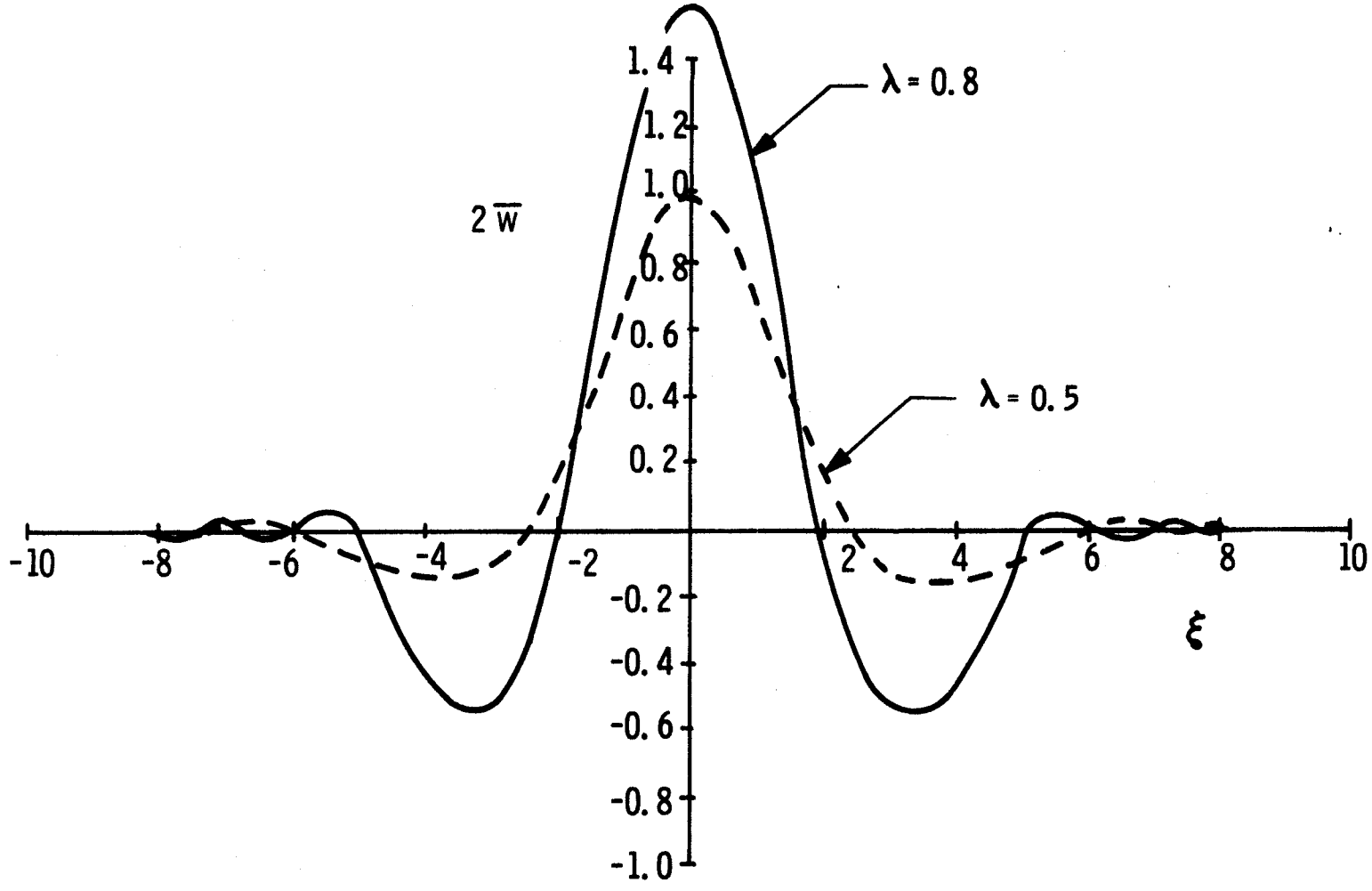

Figure IV-1. Infinite Length Shell, Spike Pressure, Deflection vs ξ , $\lambda < 1$ (Subcritical), $\alpha = 0$

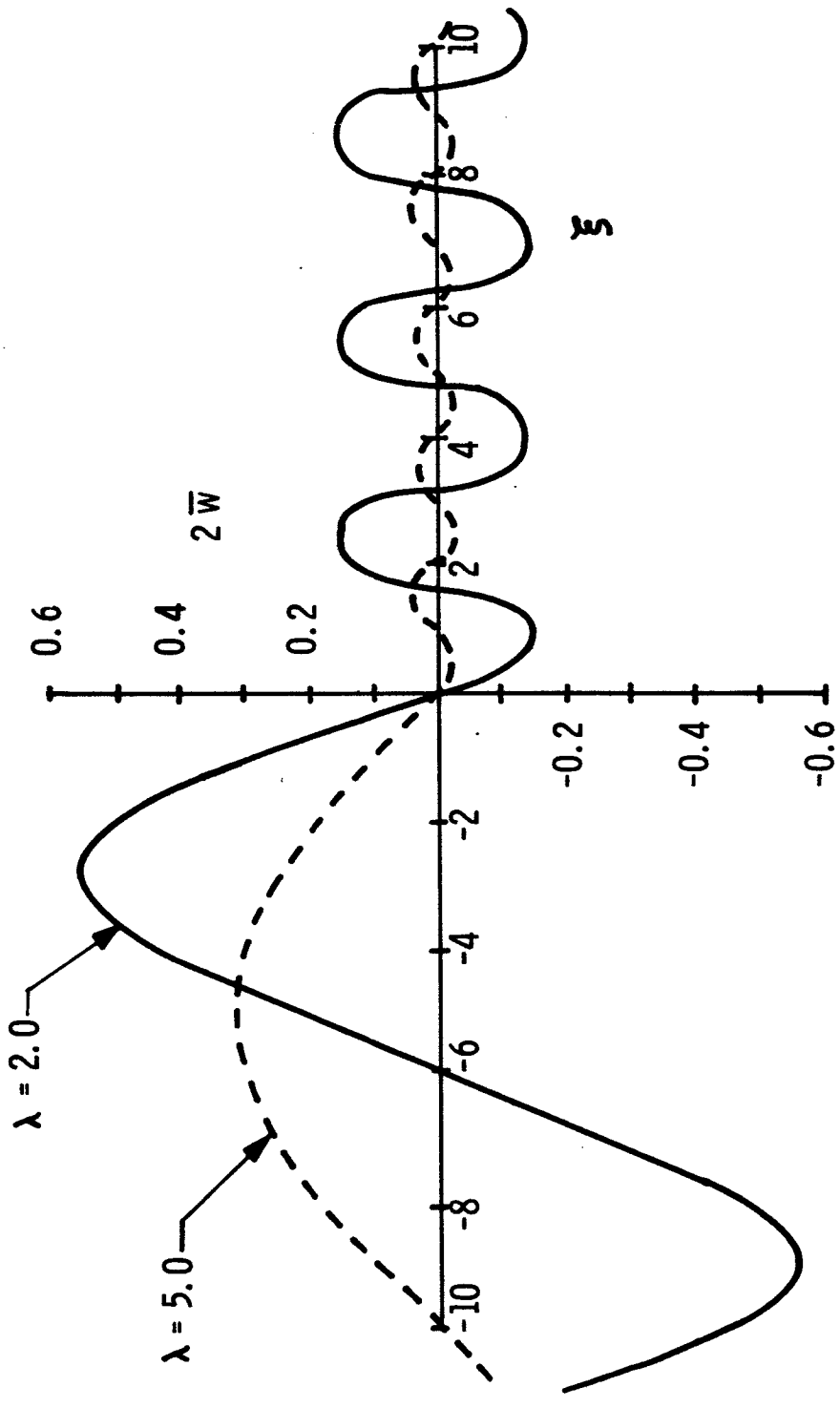

Figure IV-2. Infinite Length Shell, Spike Pressure, Deflection vs ξ, $\lambda > 1$ (Supercritical), $\alpha = 0$

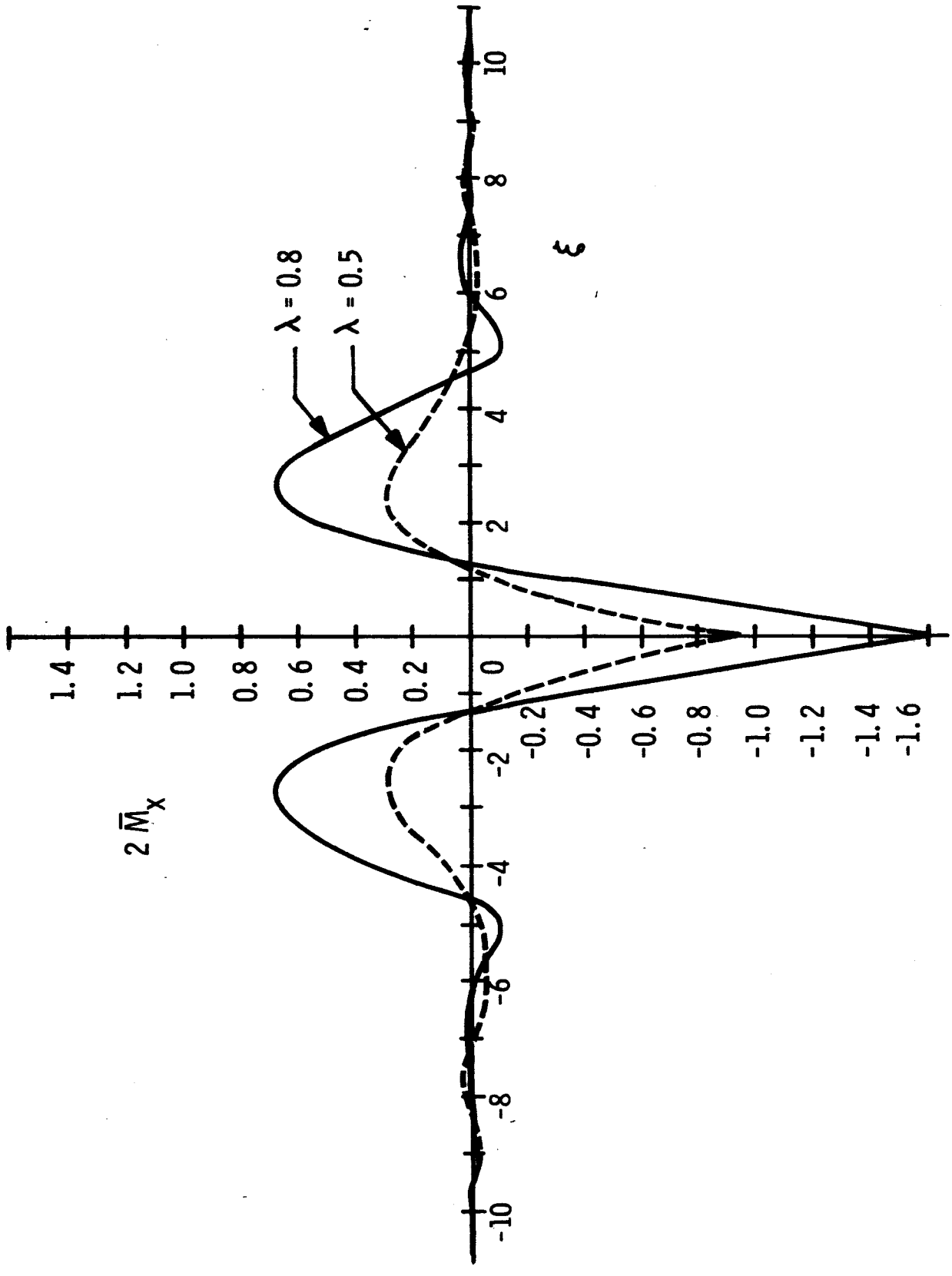

Figure IV-3. Infinite Length Shell, Spike Pressure, Bending Moment vs. ξ, $\lambda < 1$ (Subcritical), $\alpha = 0$

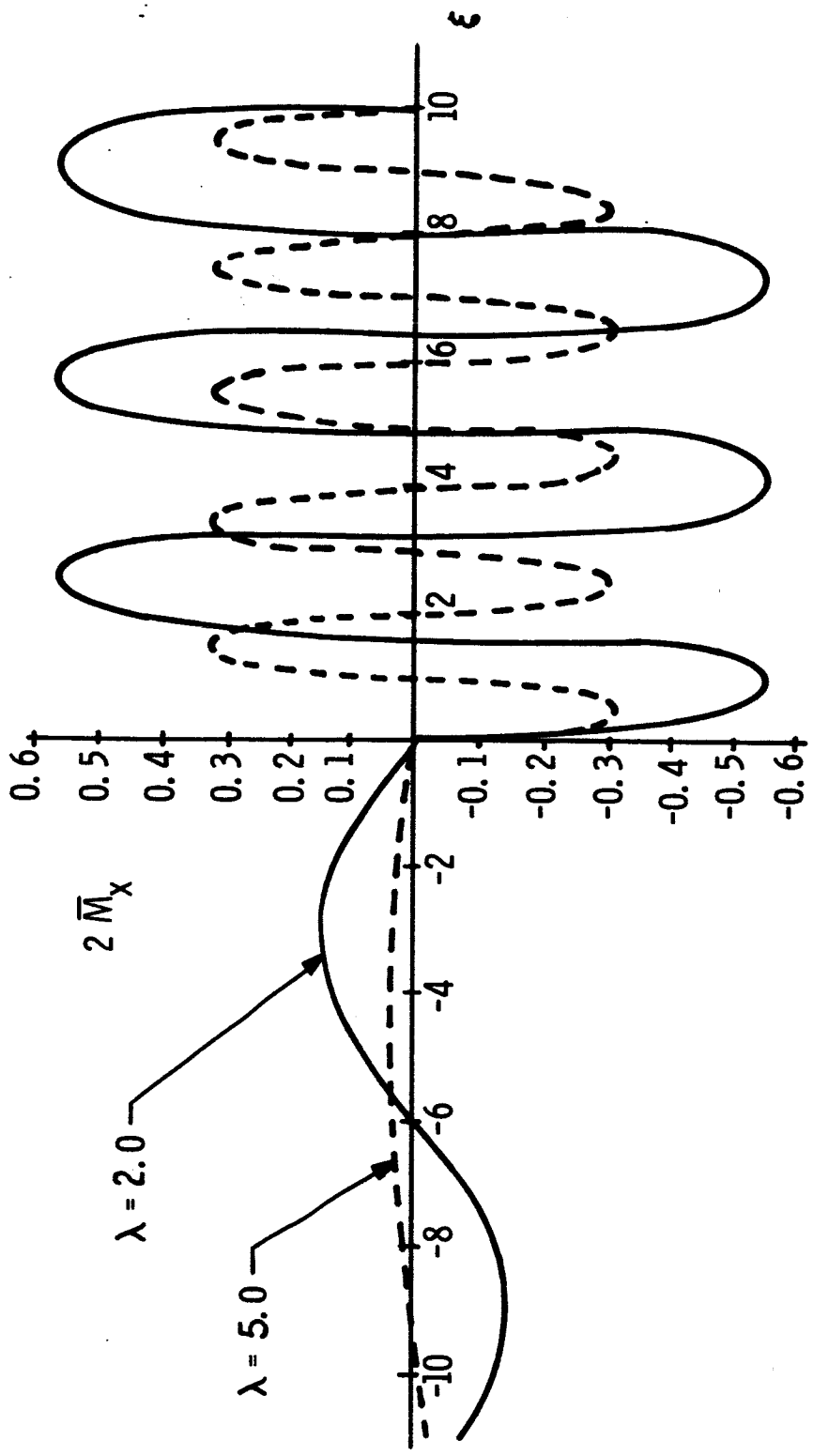

Figure IV-4. Infinite Length Shell, Spike Pressure, Bending Moment vs ξ, $\lambda > 1$ (Supercritical), $\alpha = 0$

For $\lambda < 1$, the maximum bending moment is located at $\xi = 0$ and increases with an increase in λ as shown in Figure IV-3. The maximum bending moment for $\lambda > 1$ occurs in front of the pressure spike and decreases with an increase in λ as shown in Figure IV-4.

Plots of the maximum deflection, $\bar{w}_{max}$, and the maximum bending moment, $\bar{M}_{x_{max}}$ as a function of the speed parameter, λ, are shown in Figures IV-5 and IV-6. The curves in these figures will yield the maximum hoop and bending stresses (see Equation 3-106, 3-107). For $\lambda < 1$, the maximum hoop and bending stresses act at the same point, $\xi = 0$, and therefore this data is sufficient for design purposes. However, for $\lambda > 1$, the maximum deflection does not occur at the same location as the maximum bending stress. Since for design purposes, a complete knowledge of the state of stress at a point is desirable, the deflections and bending moments present at the respective maximum bending moment and deflection locations were determined and presented in Figures IV-7 and IV-8.

Typical deflection profiles for the step pressure case are shown in Figure IV-9 (see Reference 3.3). It should be noted that the deflection profile is in the shape of waves which oscillate about $\bar{w} = 0$ for $\xi > 1$ and oscillate about $\bar{w} = 1$ for $\xi < 1$. For $\lambda < 1$ a point possessing both the maximum deflection and bending stress occurs behind the pressure wave front. For $\lambda > 1$, the maximum deflection occurs behind the pressure wave front whereas maximum bending moments occur at and in front of the pressure wave front.

Maximum deflections and bending stresses for the step pressure are given in Figures IV-10 and IV-11. It is significant to note that for $\lambda > 1$, the maximum deflection never decreases below $\bar{w}_{max} = 2$.

Solutions obtained for the infinite shell correspond to the steady-state solution and their applicability to practical shells of finite length must be ascertained. The practical significance of solutions for the infinitely long shell is discussed in Section IV-B.

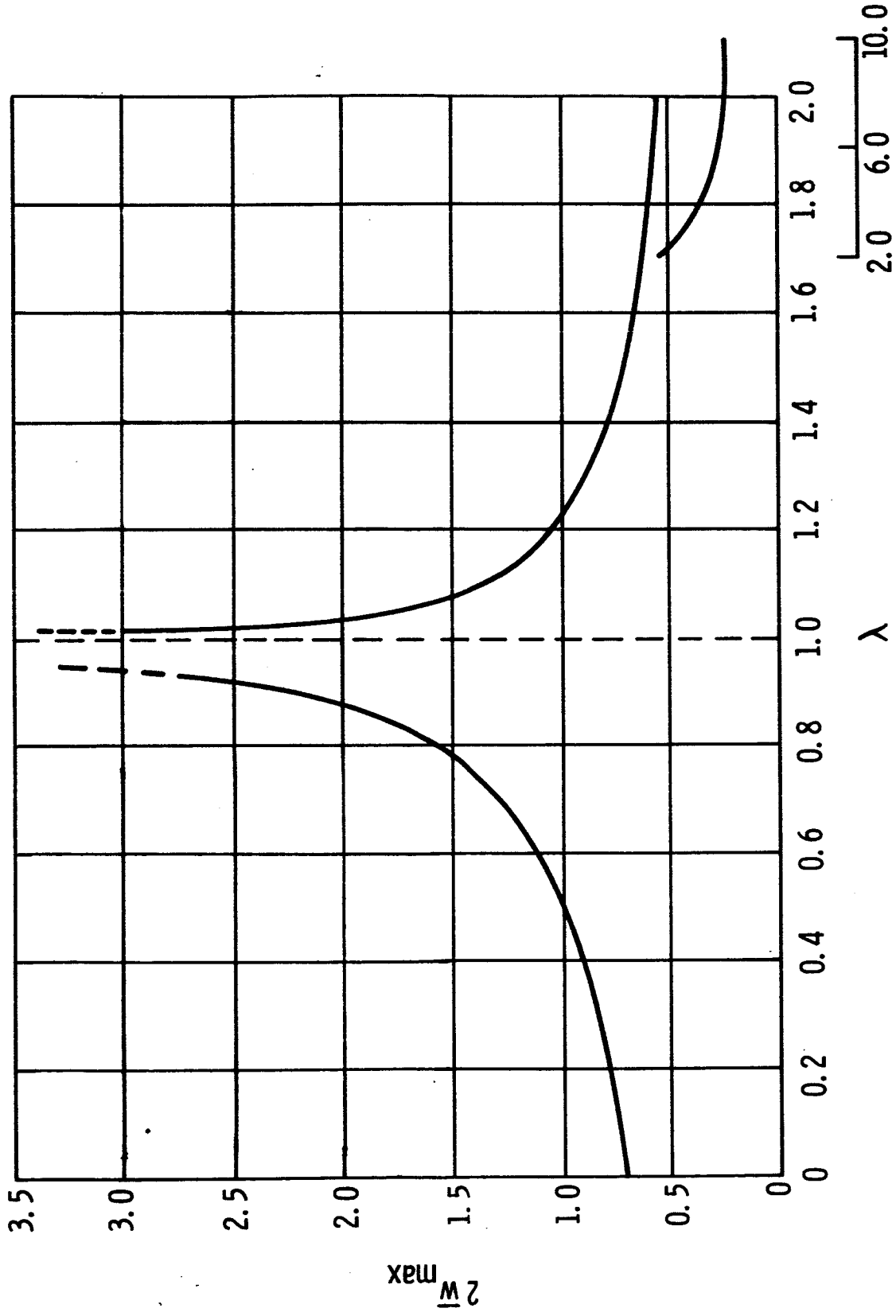

Figure IV-5. Infinite Length Shell, Spike Pressure, Maximum Deflection vs λ, $\alpha_1 = 0$

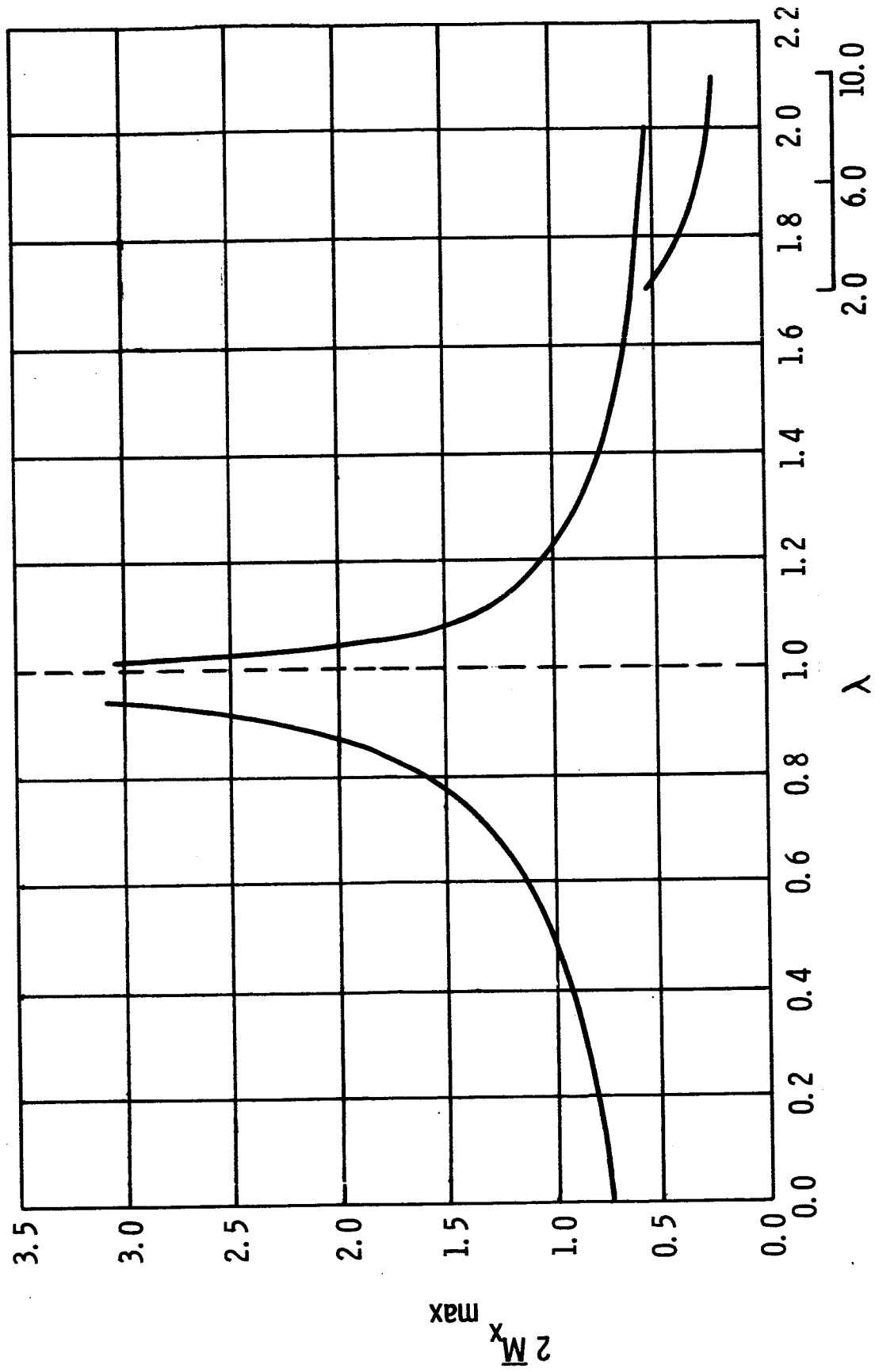

Figure IV-6. Infinite Length Shell, Spike Pressure, Maximum Bending Moment vs λ, α, = 0

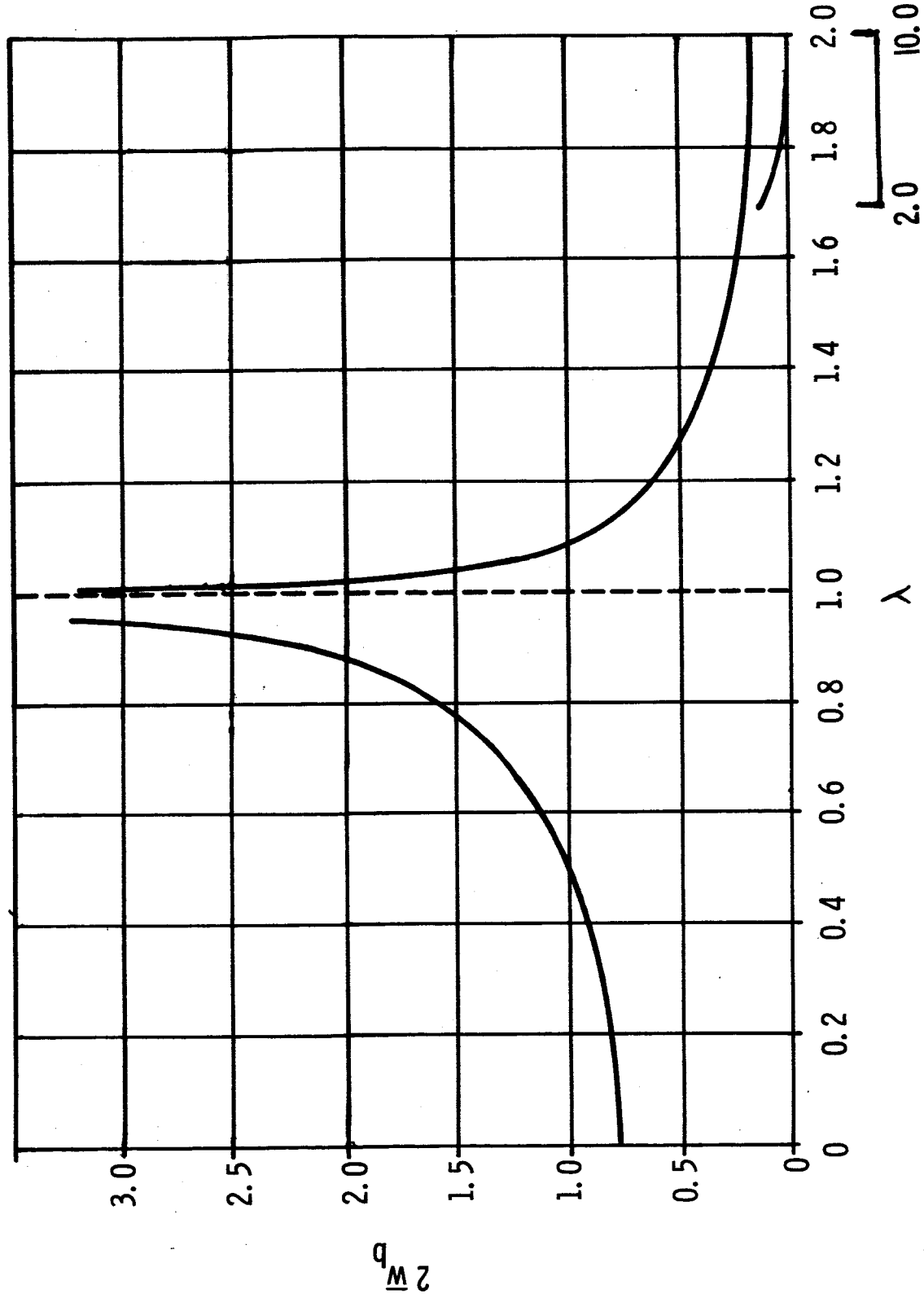

Figure IV-7. Infinite Length Shell, Spike Pressure, Deflection at Maximum Bending Stress Location vs $\lambda, \alpha_1 = 0$

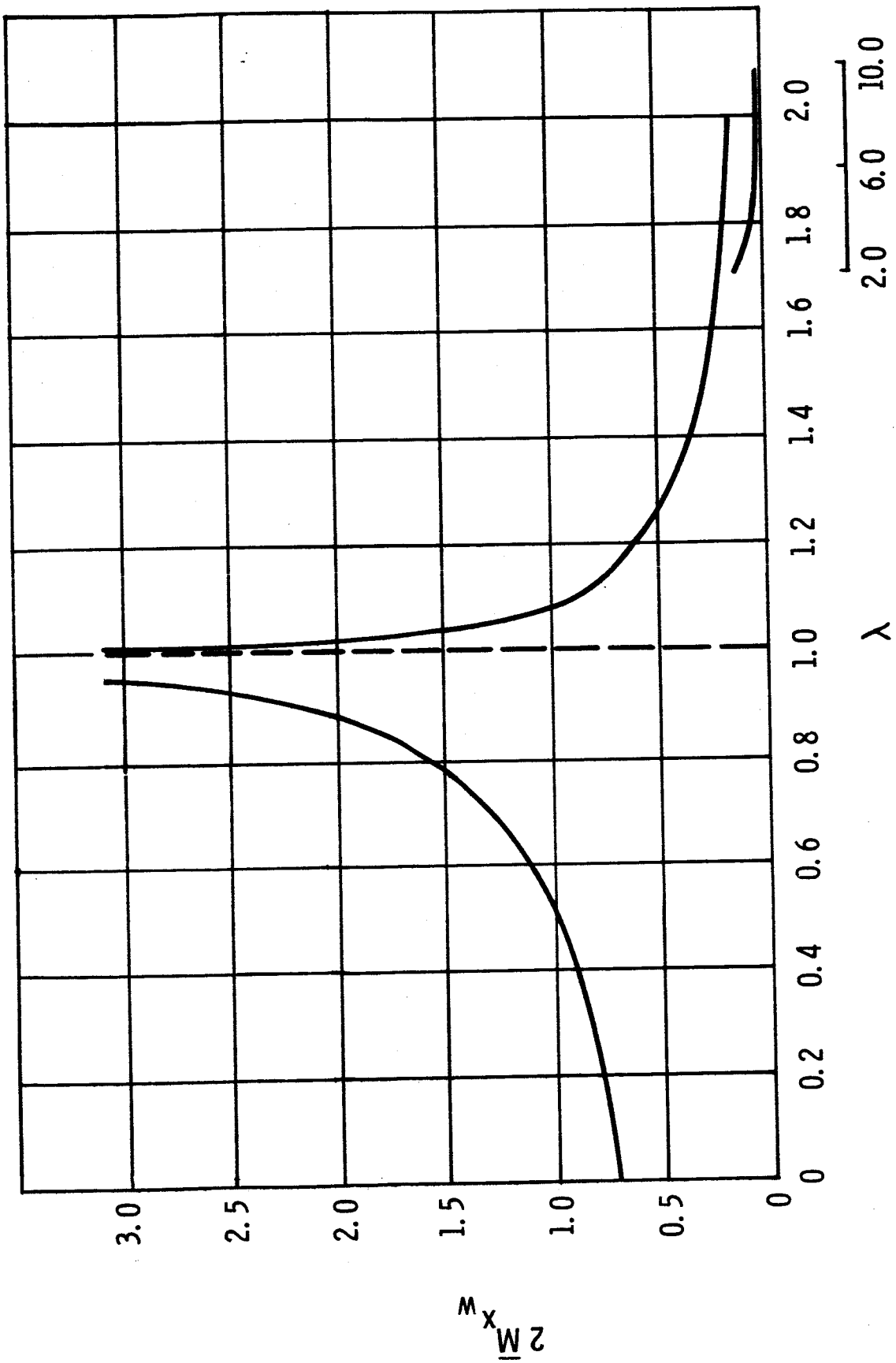

Figure IV-8. Infinite Length Shell, Spike Pressure, Bending Moment at Maximum Deflection Location vs λ , $\alpha = 0$

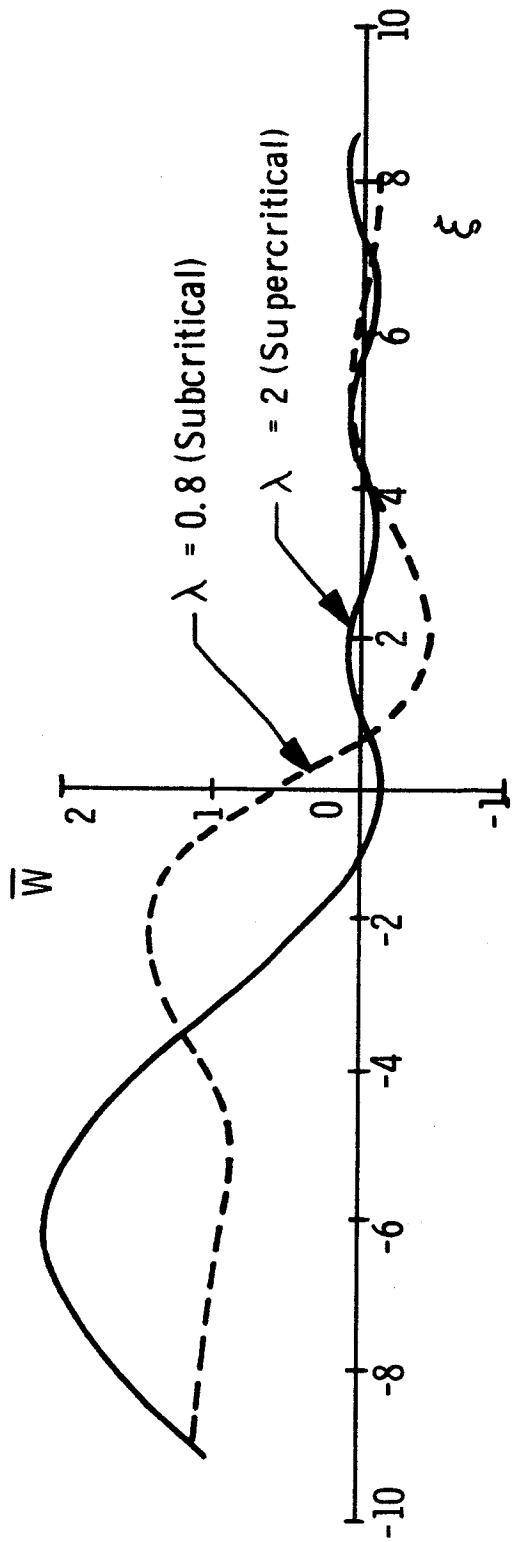

Figure IV-9. Infinite Length Shell, Step Pressure, Deflection vs ξ, $\alpha = 0$

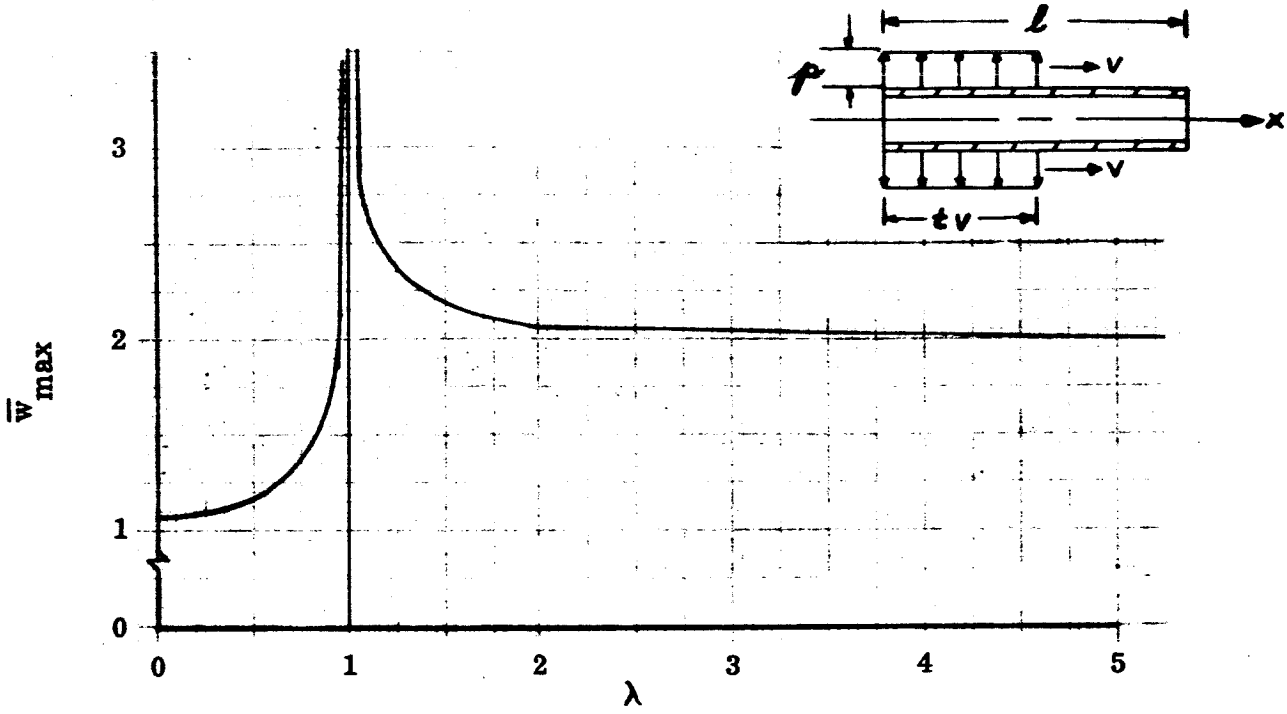

Figure IV-10. Infinite Length Shell, Step Pressure, Maximum Deflection vs λ, $\alpha = 0$

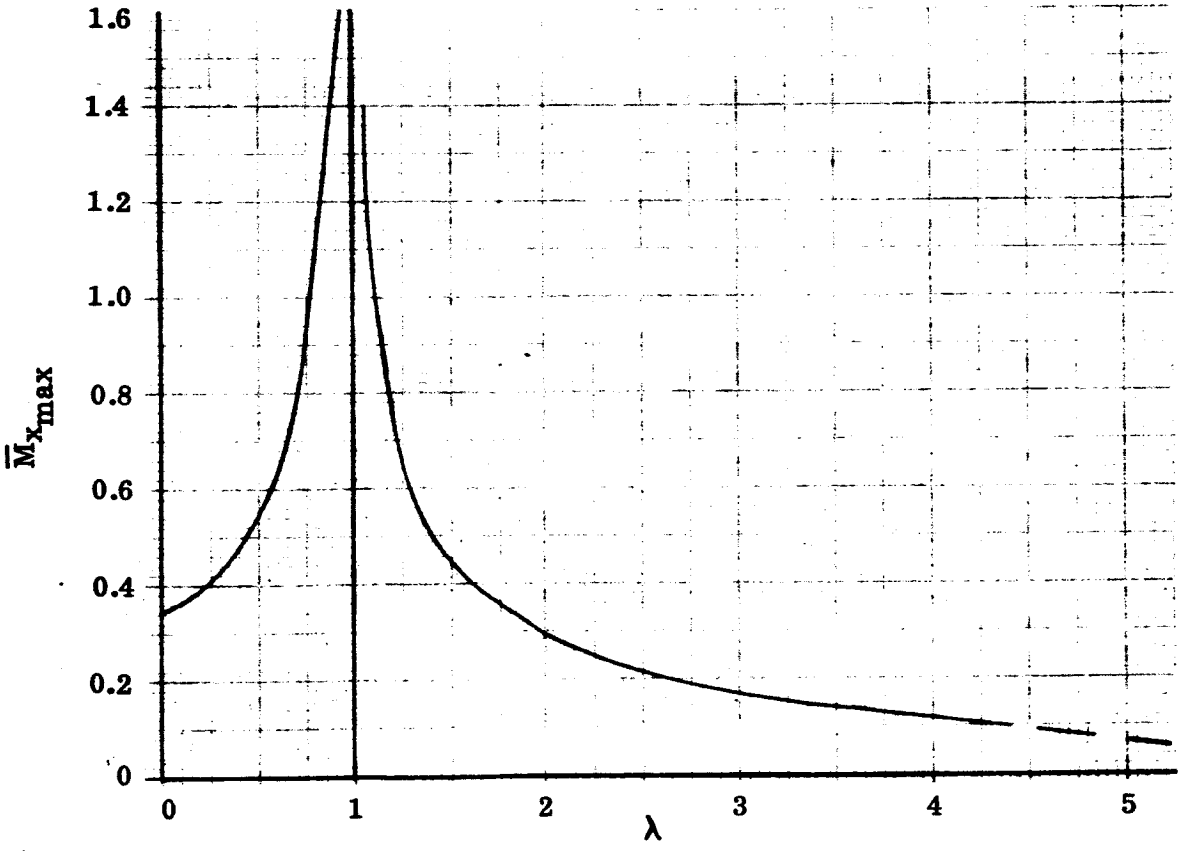

Figure IV-11. Infinite Length Shell, Step Pressure, Maximum Bending Moment vs λ, $\alpha = 0$

2. Finite Length Duct

a. Convergence of Solution

Since the elastic dynamic response solutions for the finite length cylinders are in the form of an infinite series, it is necessary to determine the number of terms, N, required for convergence of the series solution for each combination of the parameters λ and β.

Determination of the number of terms in the series solution required to yield adequate accuracy was accomplished with the aid of curves such as shown in Figures IV-12 through IV-16. These curves, which reveal the convergence characteristics of the series solutions, give the variations of the radial deflection, $\bar{w}$, and bending moment, $\bar{M}_x$, as a function of the total number of terms, N, considered in the series solution. The specific curves shown were drawn for the spike transient pressure case which was studied in some detail because it is believed to represent the most severe situation from a convergence standpoint.

Figures IV-12 through IV-15 were drawn for $\lambda = 2$, values of β from 10^2 to 10^5, time $\tau = 0.5$, $\alpha = 0$, and location $\xi = 0.5$. The curves in Figure IV-16 were obtained for $\beta = 10^5$, $\lambda = 4$, $\tau = 0.5$, $\alpha = 0$, and $\xi = 0.5$. It is evident from a study of these results that the number of terms, N, required to attain convergence increases with increase in β or λ. In addition, all of these curves exhibit two peaks which occur before the series converges. Hence, a knowledge of the location of these peaks will give a lower bound to the number of terms which must be taken in the series solution and is discussed below.

The location of the peaks in the convergence curves discussed above is related to the resonance characteristics of the shell. At resonance, we have the condition (see Equation (3-71))

$$k_n^2 v - \omega_n = 0 \qquad (4\text{-}1)$$

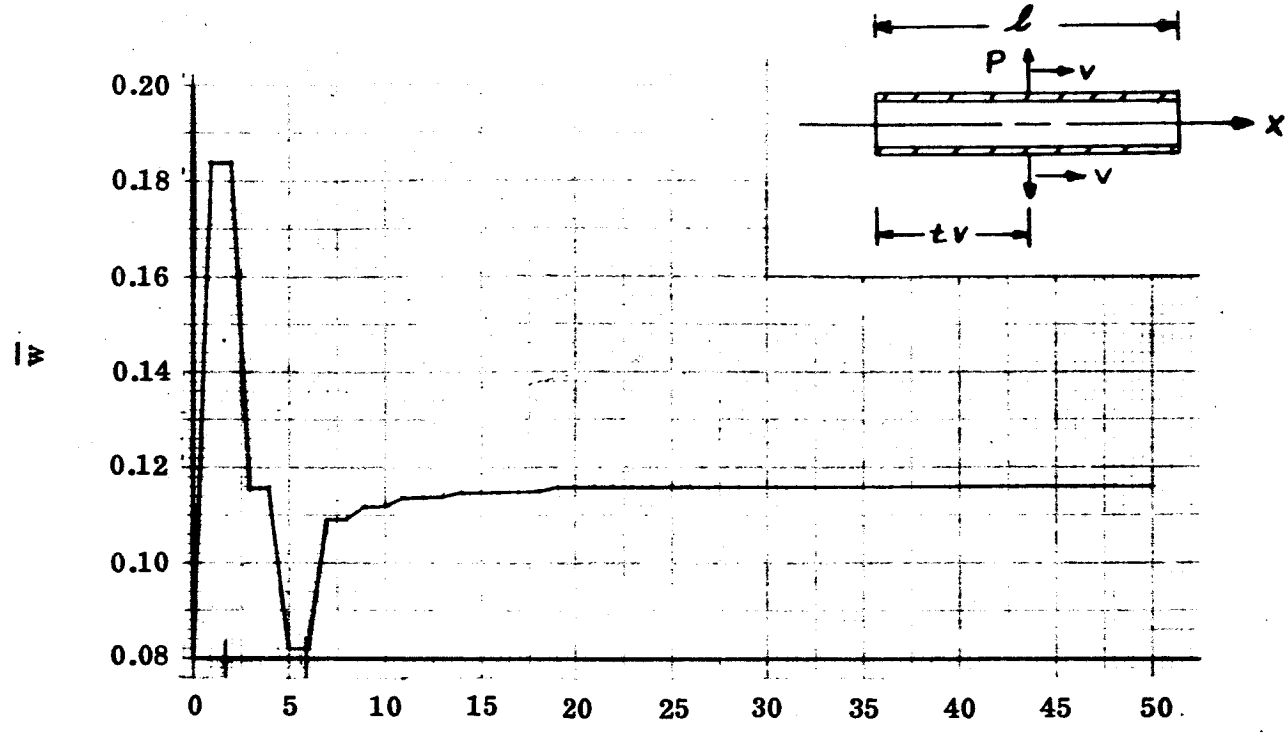

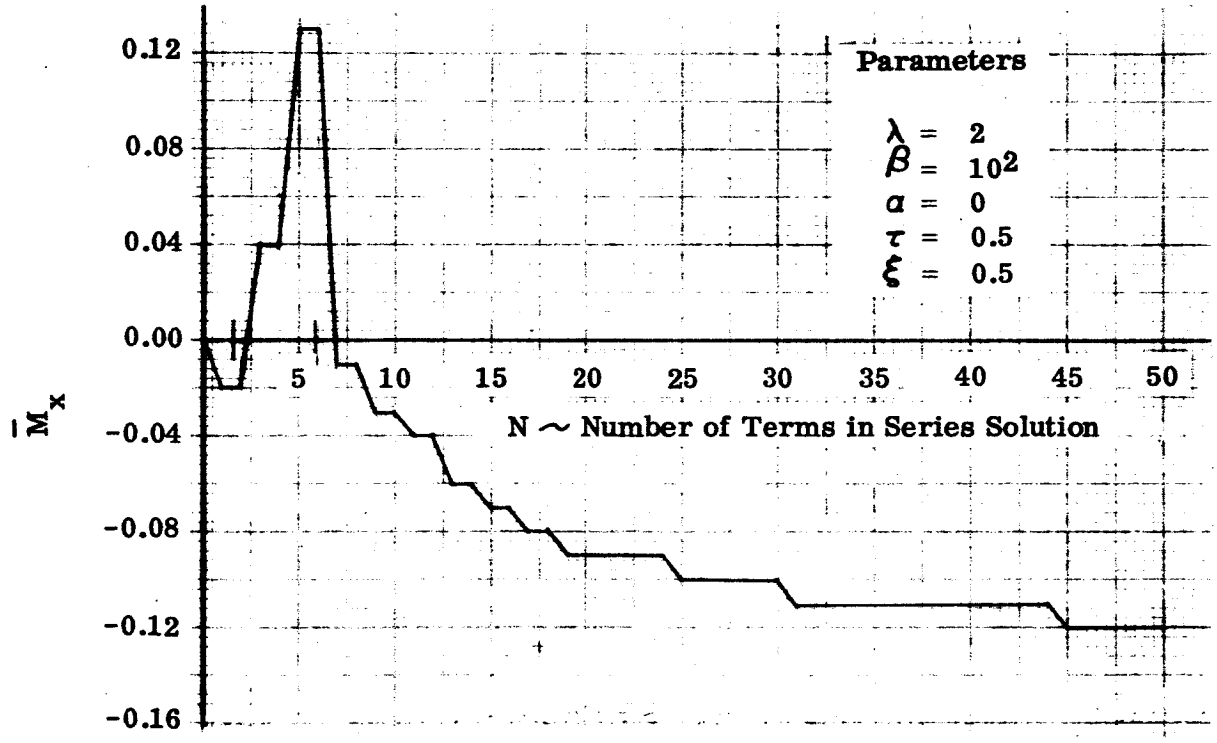

Figure IV-12. Variation of Deflection and Bending Moment with the Number of Terms in Series Solution, Spike Pressure, Simple Supports

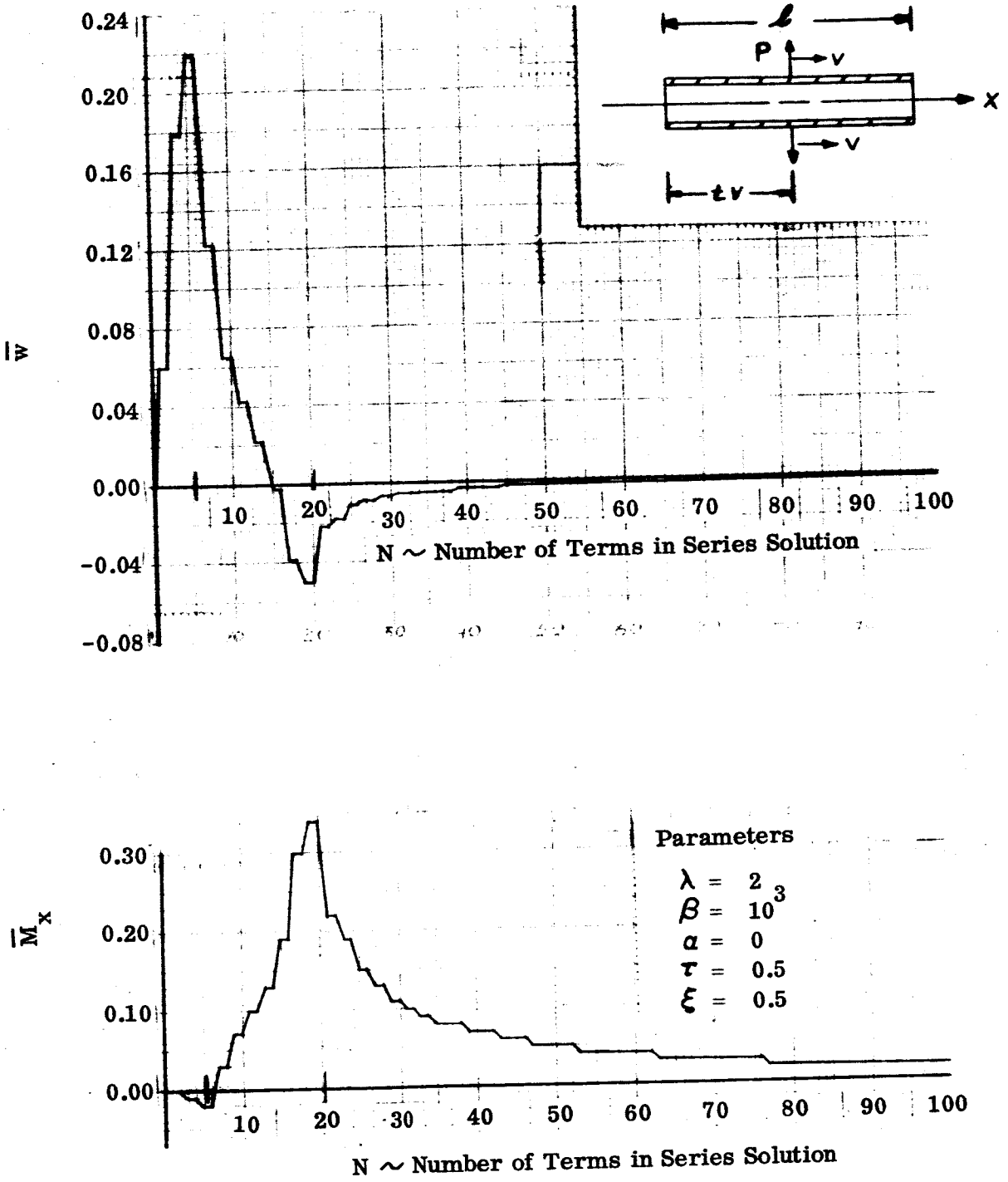

Figure IV-13. Variation of Deflection and Bending Moment with the Number of Terms in Series Solution, Spike Pressure, Simple Supports

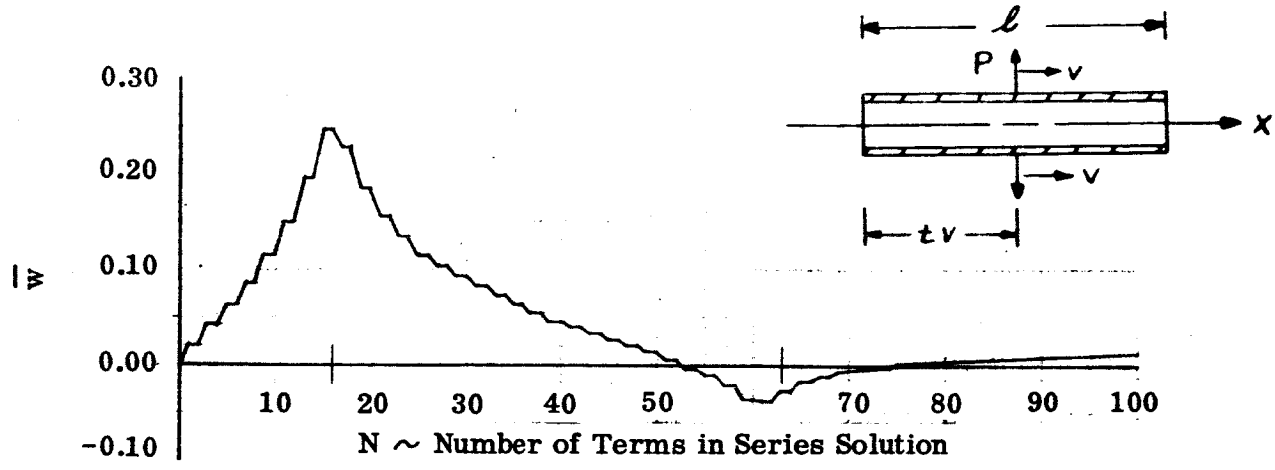

a) Deflection

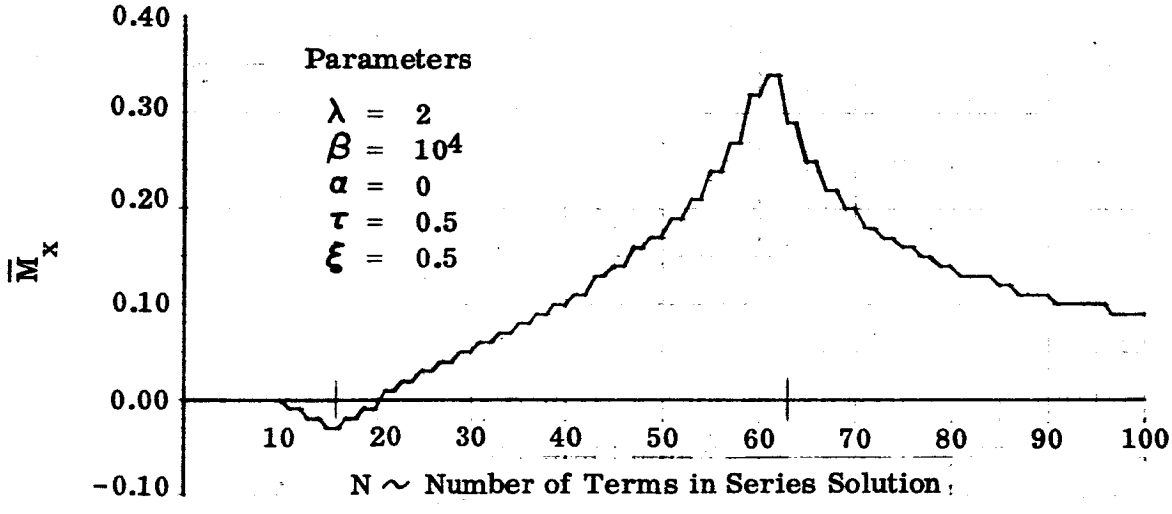

b) Bending Moment

Figure IV-14. Variation of Deflection and Bending Moment with the Number of Terms in Series Solution, Spike Pressure, Simple Supports

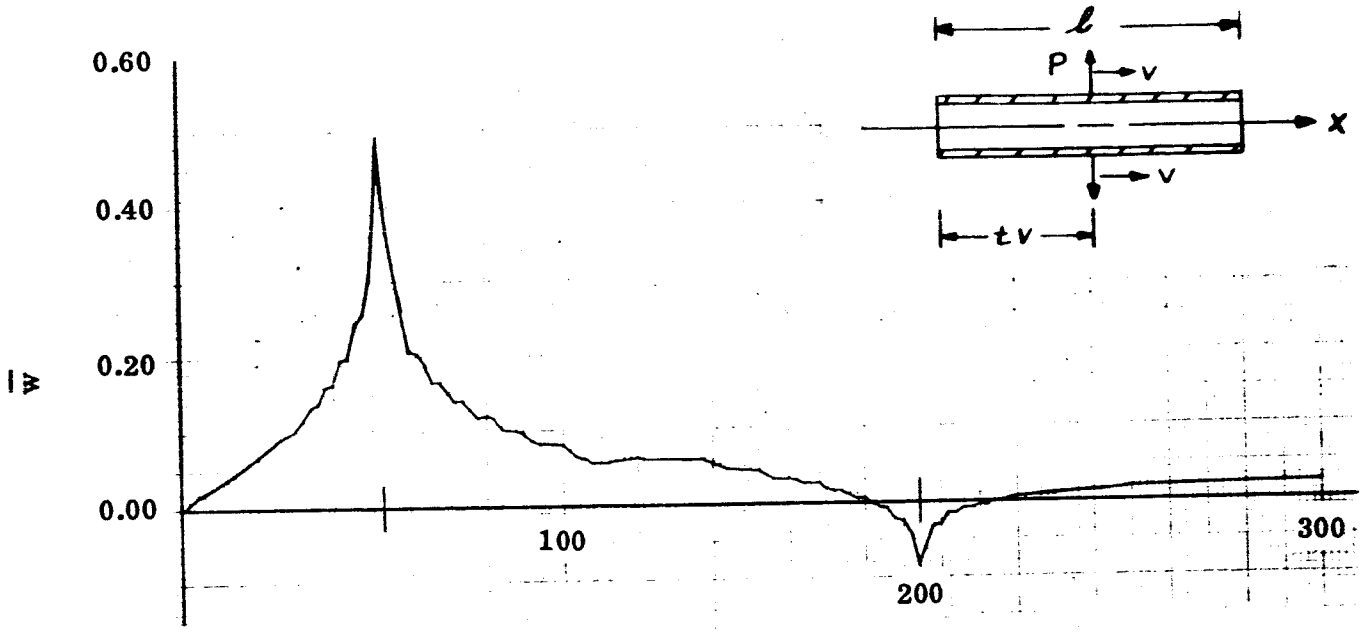

a) Deflection

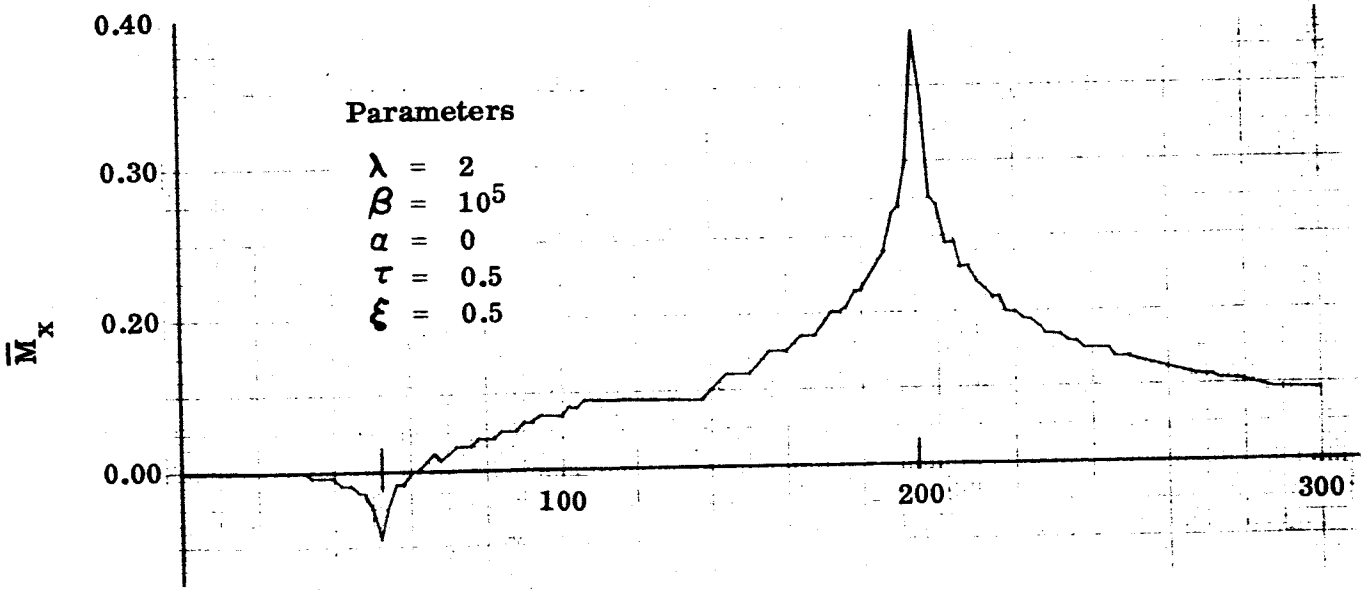

b) Bending Moment

Figure IV-15. Variation of Deflection and Bending Moment with the Number of Terms in Series Solution, Spike Pressure, Simple Supports

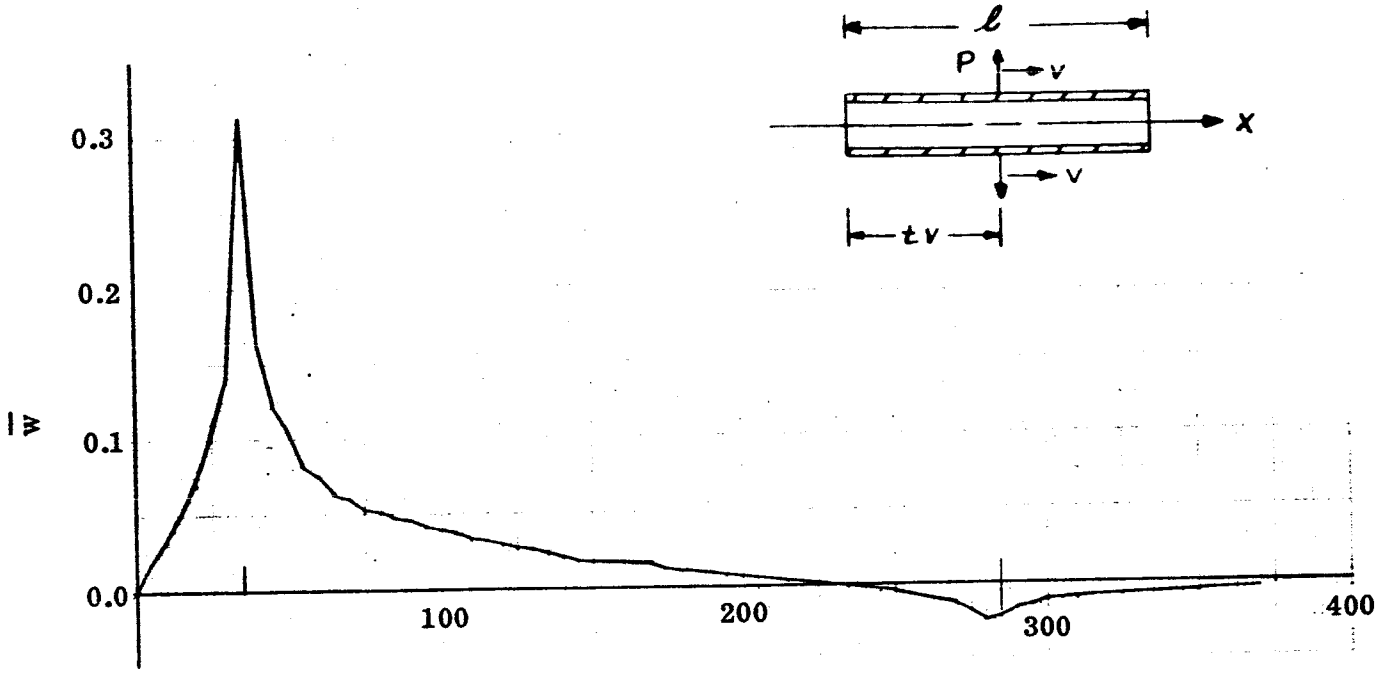

N ~ Number of Terms in Series Solution

a) Deflection

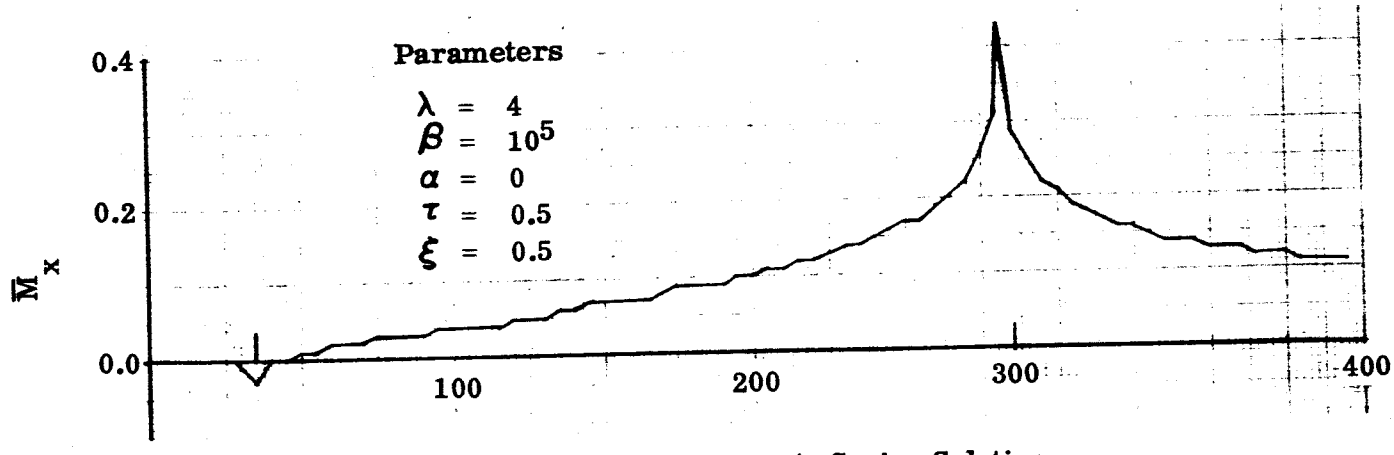

N ~ Number of Terms in Series Solution

b) Bending Moment

Figure IV-16. Variation of Deflection and Bending Moment with the Number of Terms in Series Solution, Spike Pressure, Simple Supports

Using Equation 3-57 to eliminate the natural frequency ω_n, results in

$$k_n^2 v^2 = \frac{D}{m\ell^4}\left(\frac{Eh\ell^4}{DR^2} + k_n^4 \ell^4\right) \tag{4-2}$$

Introduction of the nondimensional parameters yields

$$\frac{\beta^2}{K_n} + 1 = \frac{2\lambda\beta}{K_n^2} \tag{4-3}$$

Since as n increases, K_n for the clamped support condition approaches $n\pi$ which is equal to K_n for the simple support condition, the above expression can be in general written as

$$2\lambda = \frac{\beta}{n^2\pi^2} + \frac{n^2\pi^2}{\beta} \tag{4-4}$$

The relationship between $\frac{\beta}{n^2\pi^2}$ and λ as given by this expression is shown in Figure IV-17. Note that a resonance condition for $\lambda < 1$ does not exist but a resonance condition exists for each value of n which is independent of the form of the pressure transient. Thus, for a given mode, n, a combination of β and λ values can be determined which will excite that mode. If on the other hand a combination of β and λ values are given, it is unlikely that resonance will occur since n is an integer. However, for a given combination of β and λ values, two values of n can be obtained from Figure IV-17 or Equation 4-4 which are not, in general, integers. It appears that the values of n so determined locate the vicinity of the peak values in the convergence plots and the total number of terms, N, taken in the series solution must exceed these computed values of n.

As an aid in determining the value of n which represents a lower bound for N, Figure IV-18 was prepared. This figure was computed from Equation 4-4 and gives the larger critical harmonic number, n_{cr} as a function of β and λ. The critical harmonic number is defined as the mode number which gives resonance for a given combination of β and λ. The tick marks on the horizontal axis in Figures IV-12 through IV-16 indicate the nearest critical harmonic number for the specified combinations of β and λ.

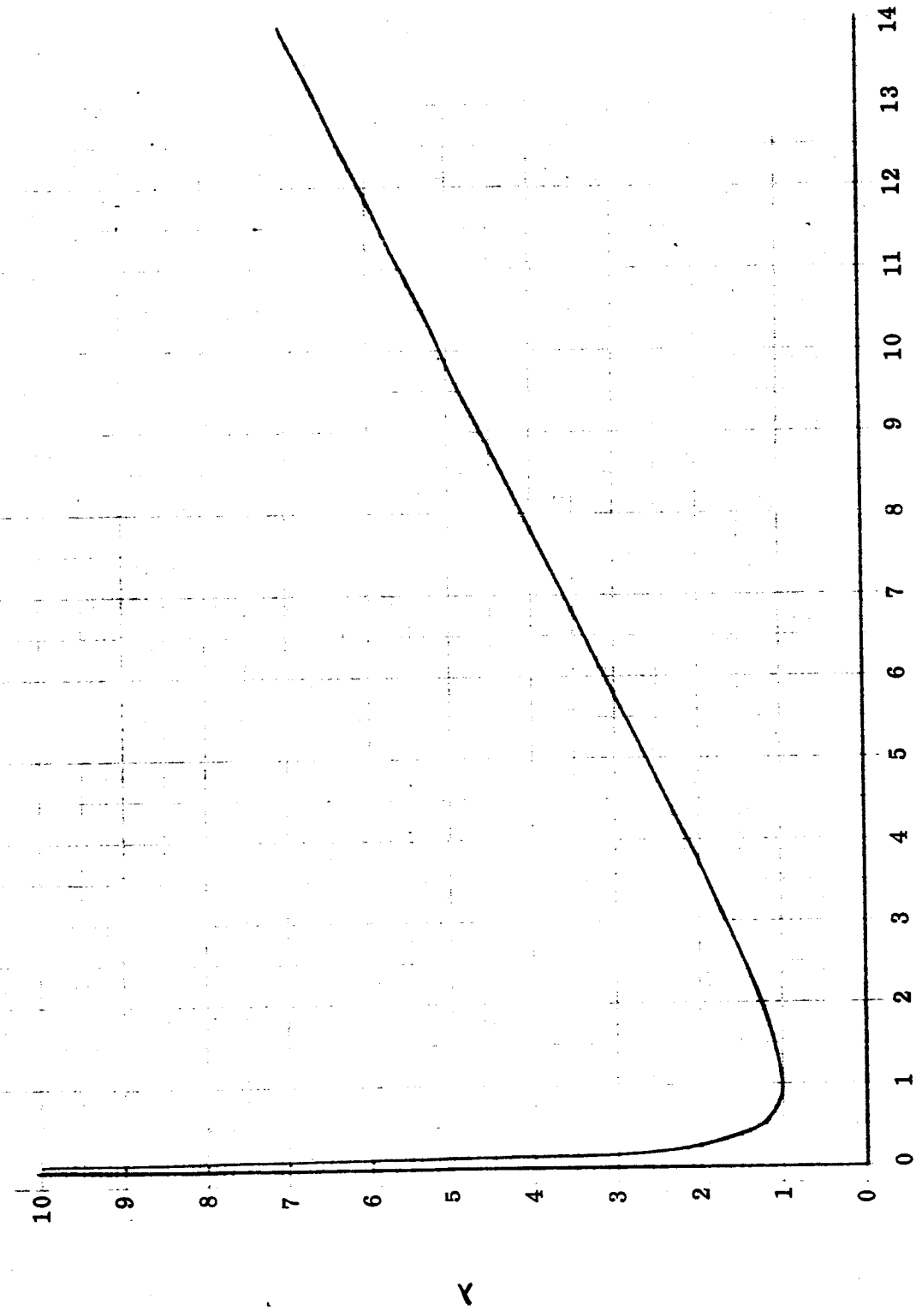

Figure IV-17. Relationship Between λ, β, and n for Resonance

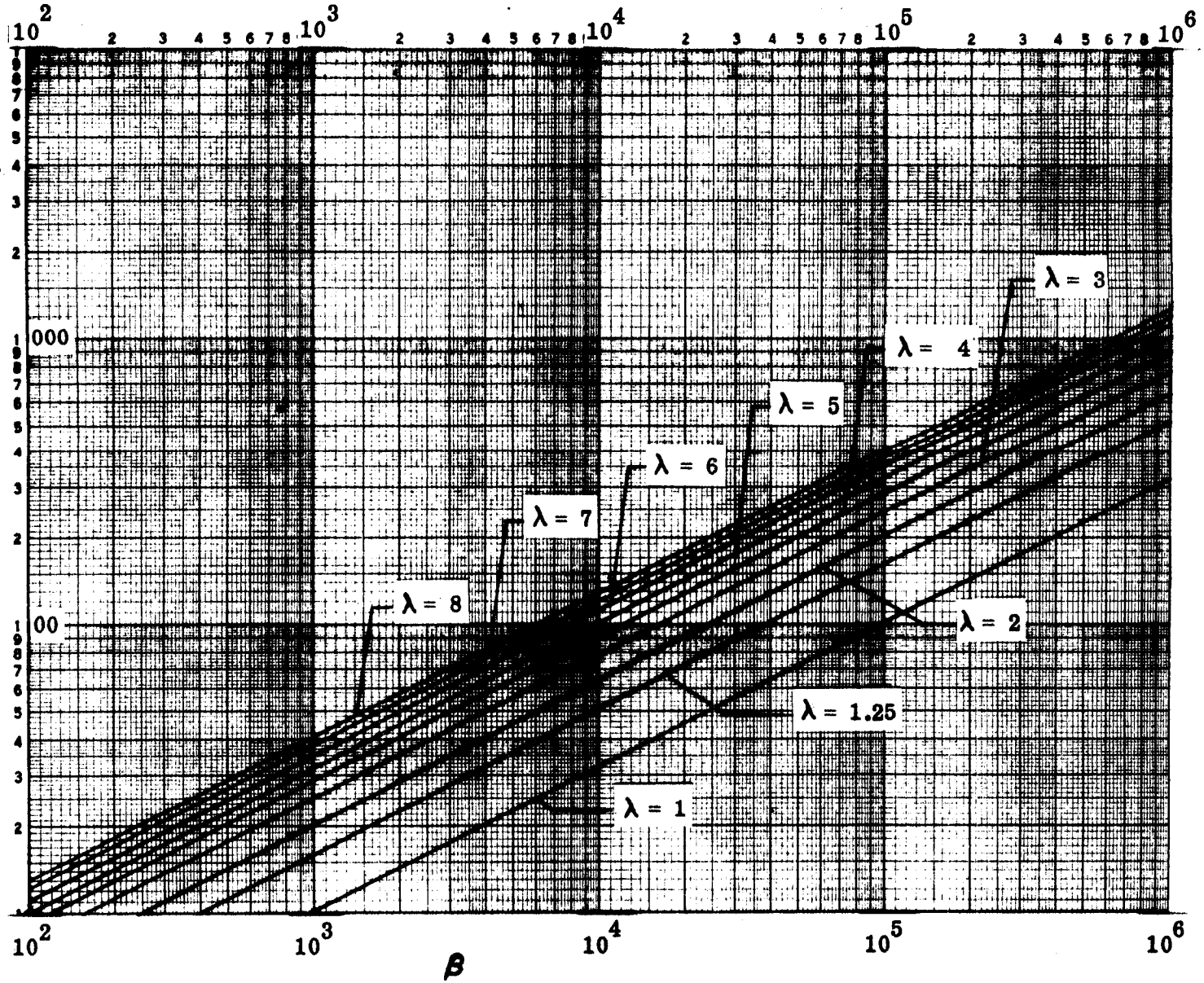

Figure IV-18. Critical Harmonic Number

For $\lambda < 1$ the series solution obtained for the spike pressure and simple supports converges in a manner as shown in Figure IV-19. The variation of deflection and bending moment with N for various values of β are indicated in this figure. The speed parameter was taken to be very small, i.e., $\lambda = 0.001$, so that the results could be compared with the exact solution given in Reference 4-1 for an infinite shell subjected to a static ring load. These results indicate that the series solution is correct for small values of λ. Evidently a relatively large number of terms must be taken in the series solution to obtain accurate values for the bending moment.

Results of this study of convergence of the series solution indicates that (as a consequence of the uniformity of the convergence characteristics above a known value of N), development of a convergence criterion for use in a computer program is possible. (see Vol. II). However, for completeness, the convergence characteristics of the remaining solutions should be studies further.

b. Deflection Profiles and Stress Distributions

There is no simple, analytical procedure by which the maximum deflection or bending moment can be determined from the series solutions presented in this report. Consequently, such a determination must be obtained by an examination of computed time dependent deflection profiles and stress distributions. Typical data of this type are presented here.

Typical deflection profiles are presented for the step pressure with $\lambda = 2$ and $\beta = 10^4$ at various times in Figure IV-20. Dynamic response results as illustrated in these figures indicate that with the exception of regions near the simply supported cylinder edges, practically all points of the duct experience comparable stress levels during the course of travel of the step pressure. It is of importance to note that the deflection profiles for $\tau = 0.2$ and 0.5 are similar to that given, for the infinite length shell subjected to a step pressure, in Figure IV-9.

The variation with time of the deflection and bending moment at $\xi = 0.5$ for the above case is shown in Figure IV-21. Data of this type are used to obtain design charts discussed in the next section.

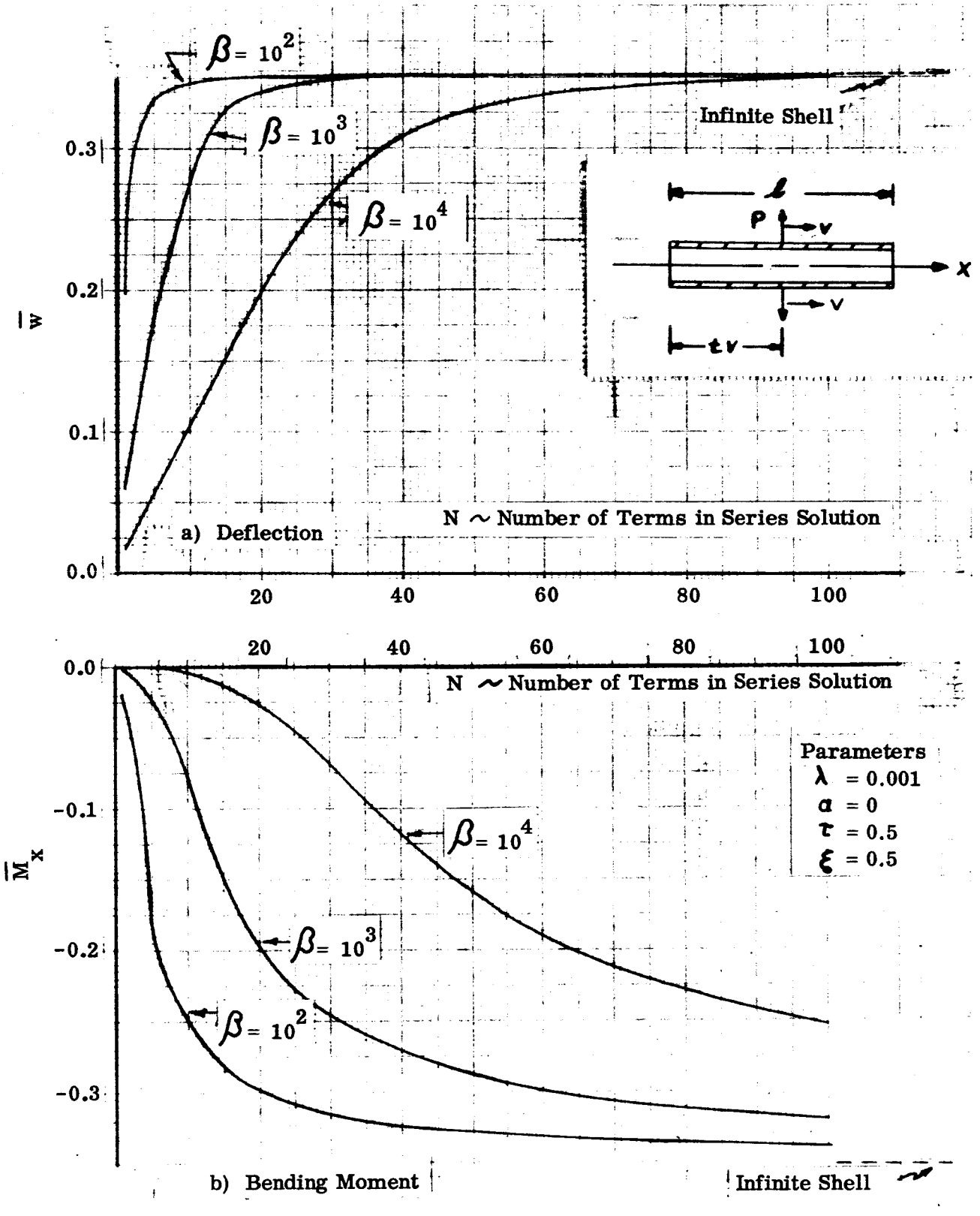

Figure IV-19. Variation of Deflection and Bending Moment With the Number of Terms in Series Solution, Spike Pressure, Simple Supports

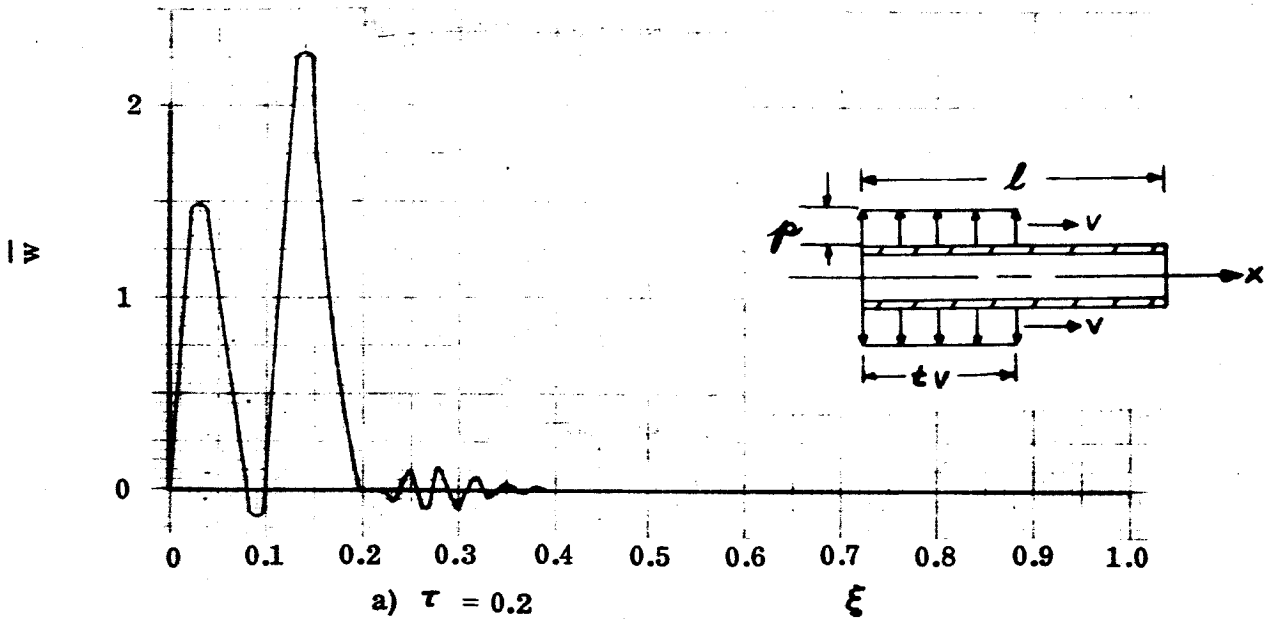

a) $\tau = 0.2$

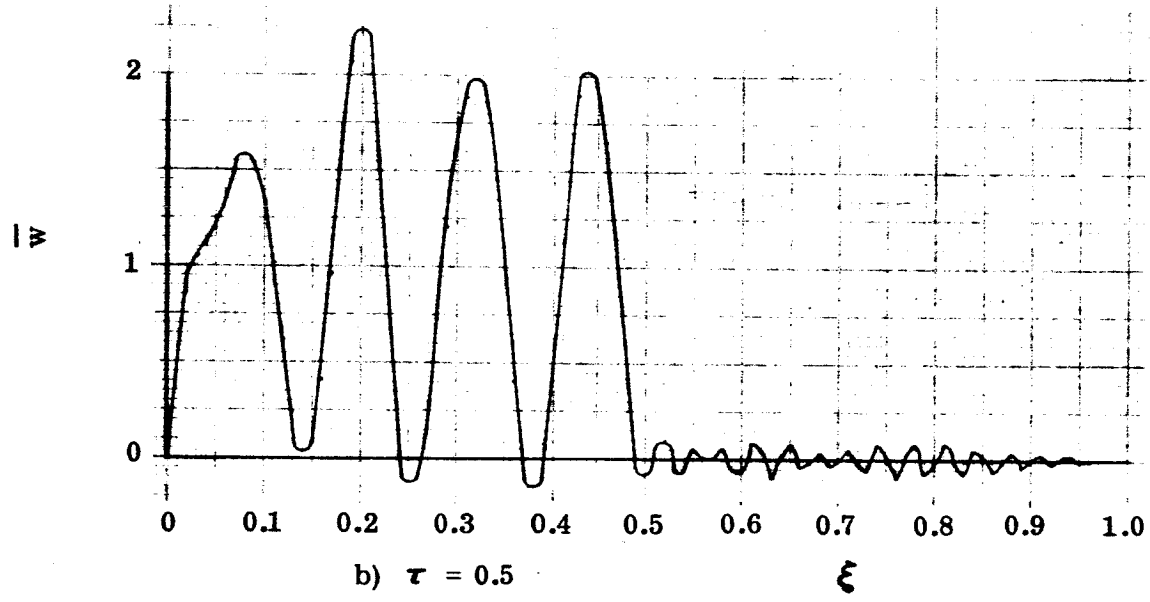

b) $\tau = 0.5$

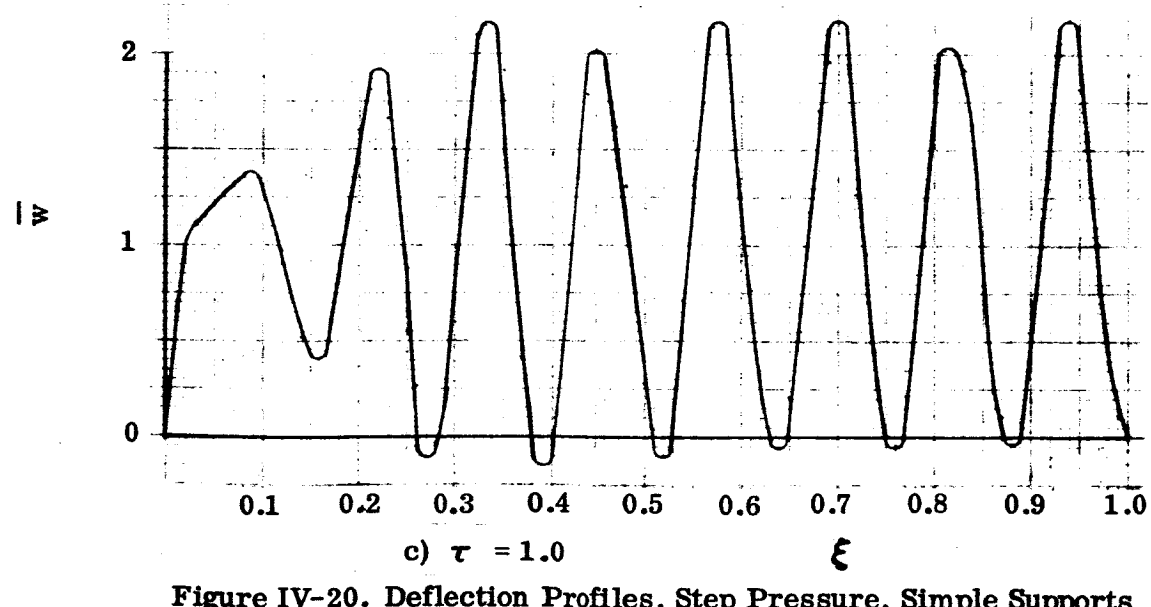

c) $\tau = 1.0$

Figure IV-20. Deflection Profiles, Step Pressure, Simple Supports
$\lambda = 2$, $\beta = 10^4$, $\alpha = 0$, N = 100

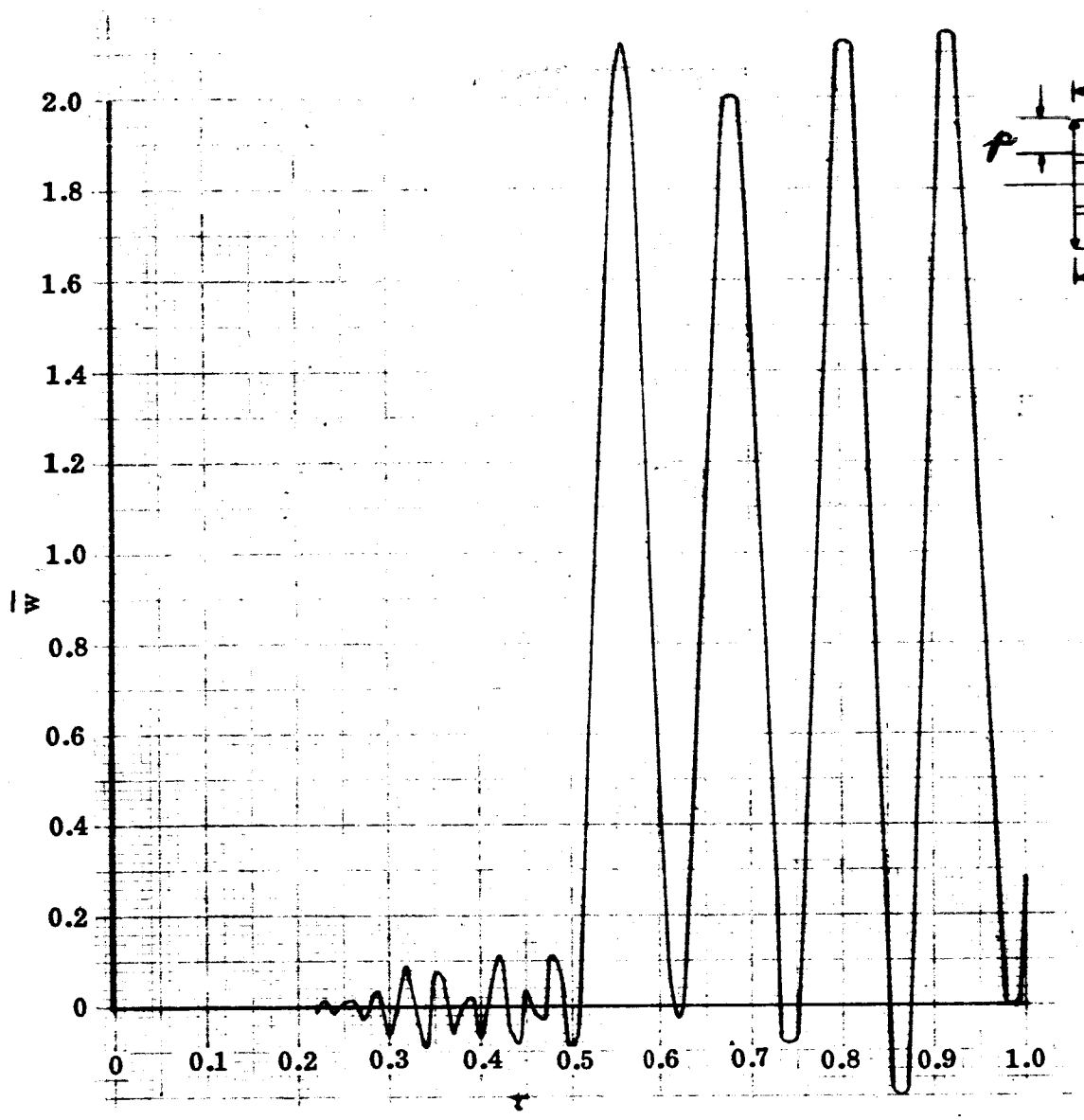

a) Deflection

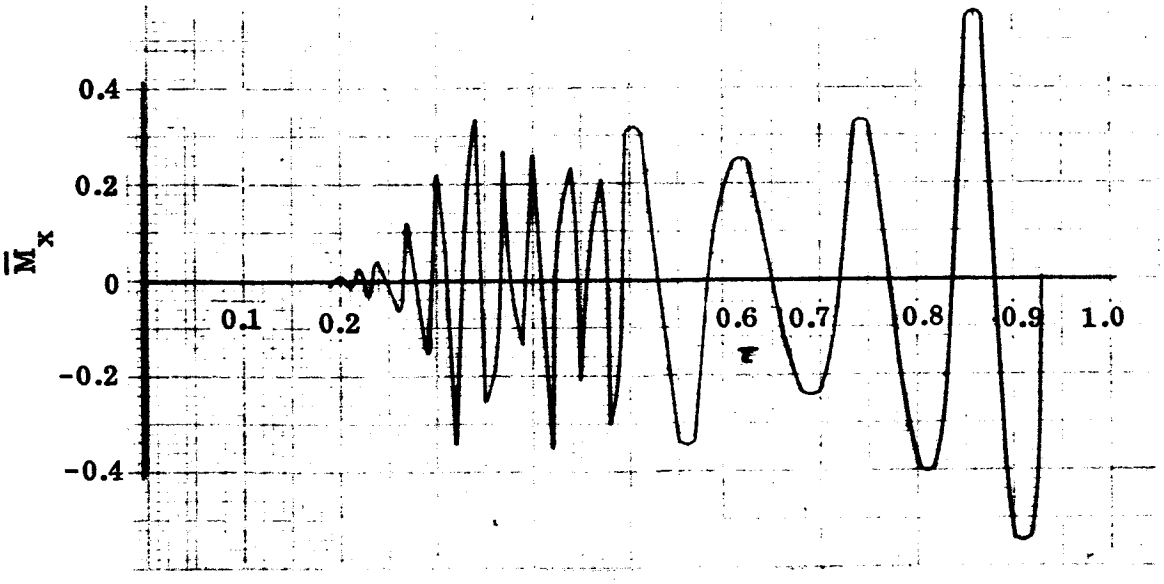

b) Bending Moment

Figure IV-21. Typical Deflection and Bending Moment Variation with Time at $\xi = 0.5$, Step Pressure, Simple Supports, $\lambda = 2$, $\beta = 10^4$, $\alpha = 0$

A typical deflection profile for the ramp transient pressure at time $\tau = 0.5$ is shown in Figure IV-22, and typical deflection and bending moment variations with time at location $\xi = 0.5$ are shown in Figure IV-23. These dynamic response results for the cylinder when subjected to a traveling ramp pressure are for a non-dimensional valve closure time at $\tau_c = 0.2$ and design parameter value of $\lambda = 2, \beta = 10^4$, $\alpha = 0$. The design parameters selected for the ramp pressure are the same used to illustrate cylinder dynamic response to a step pressure presented in Figures IV-20 and IV-21. A comparison of the above typical results obtained for the step and ramp transient pressures reveals that a significant reduction in stress level occurs with the introduction of a valve closure time. It should be noted that practically all points of the duct will experience similar time dependent stress variations and consequently are subject to failure by fatigue.

The history of deflection profiles obtained for the simply supported shell of finite length subjected to a pressure spike is shown in Figures IV-24 through IV-26. Results are shown for $\beta = 10$ and various values of λ from 0.5 to 5. Two traverses of the duct are considered. These figures clearly indicate the effects of shell edge supports on dynamic response of a relatively short duct.

Additional typical dynamic response curves are presented in Volume II of this report.

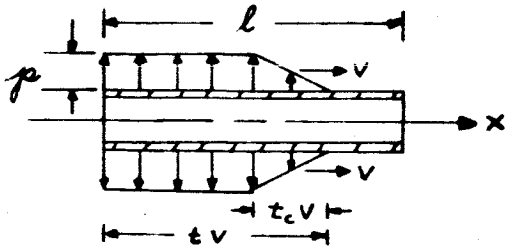

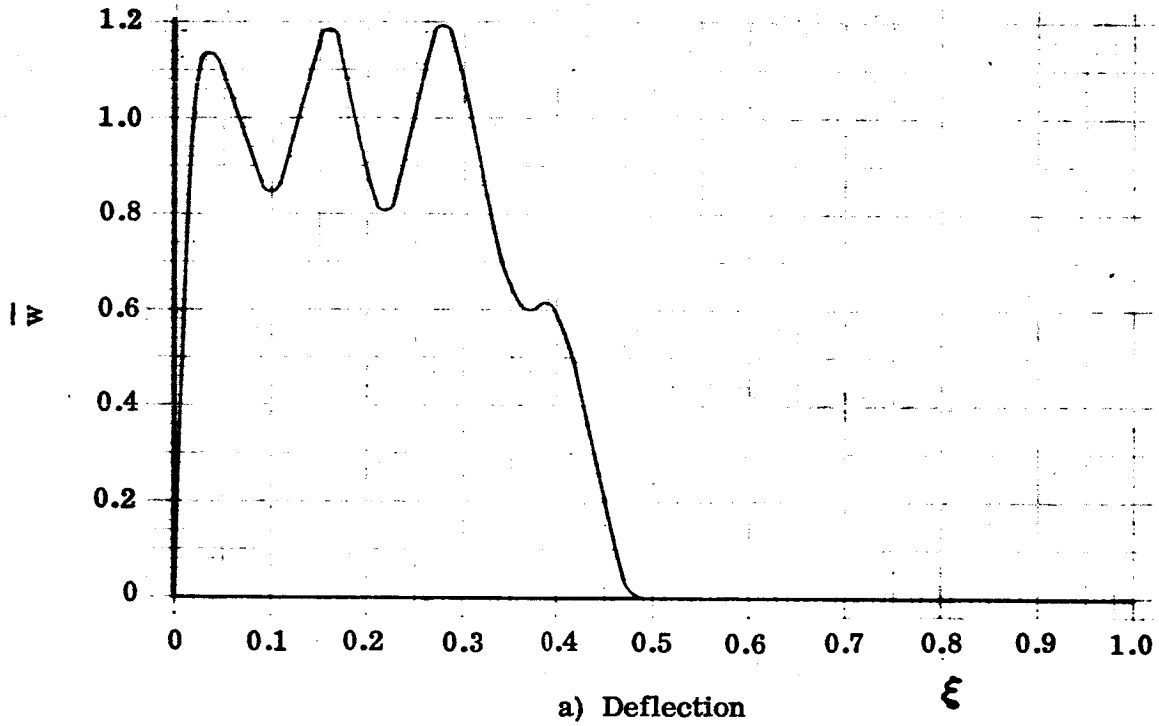

a) Deflection

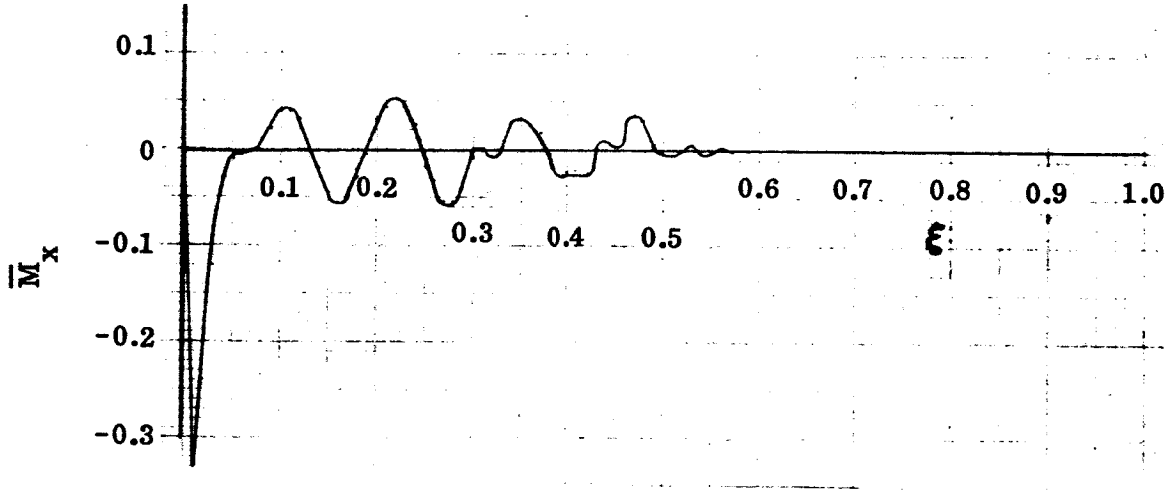

b) Bending Moment

Figure IV-22. Typical Deflection and Bending Moment Variation with Position at $\tau = 0.5$, Ramp Pressure, Simple Supports, $\lambda = 2$, $\beta = 10^4$, $\alpha = 0$, $\tau_c = 0.2$

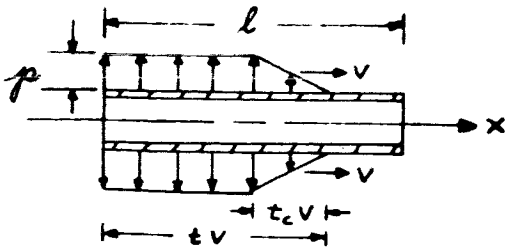

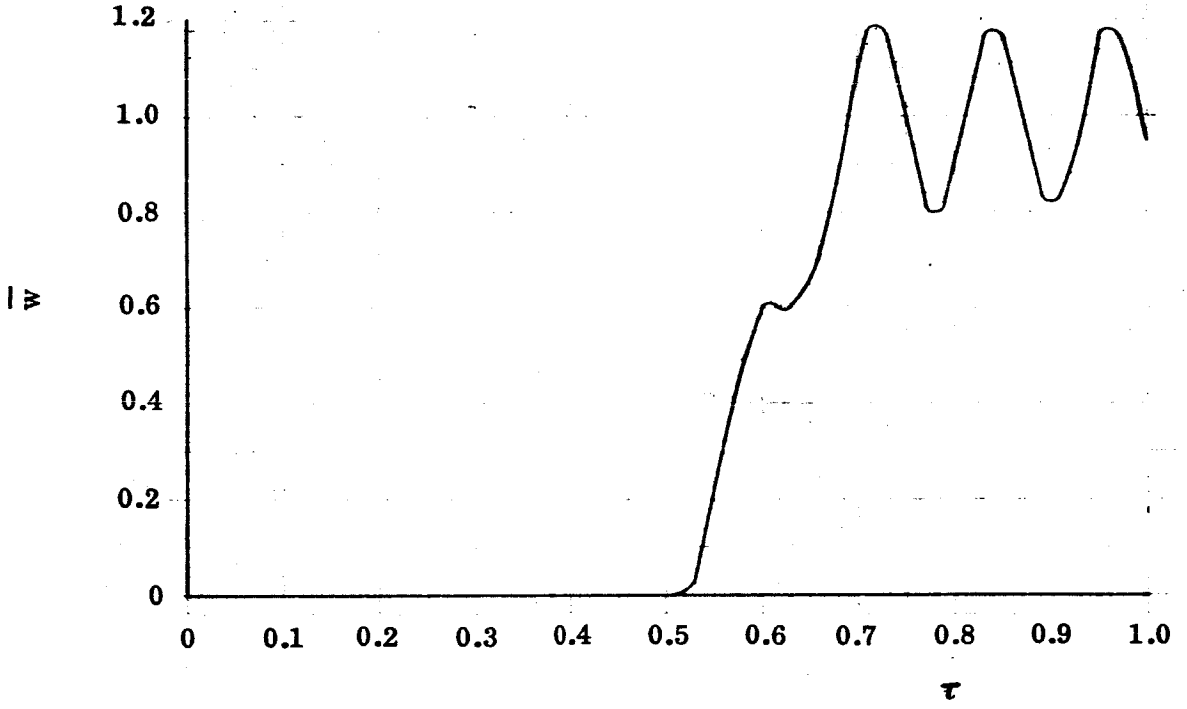

a) Deflection

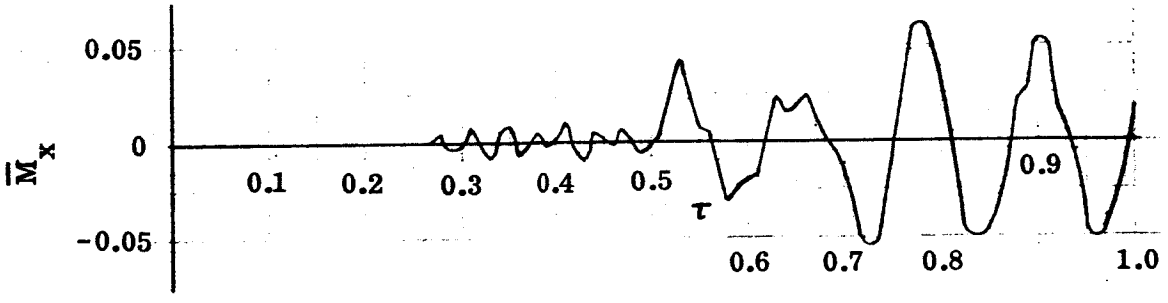

b) Bending Moment

Figure IV-23. Typical Deflection and Bending Moment Variation with Time at $\xi = 0.5$, Ramp Pressure, Simple Supports, $\lambda = 2$, $\beta = 10^4$, $\alpha = 0$, $\tau_c = 0.2$

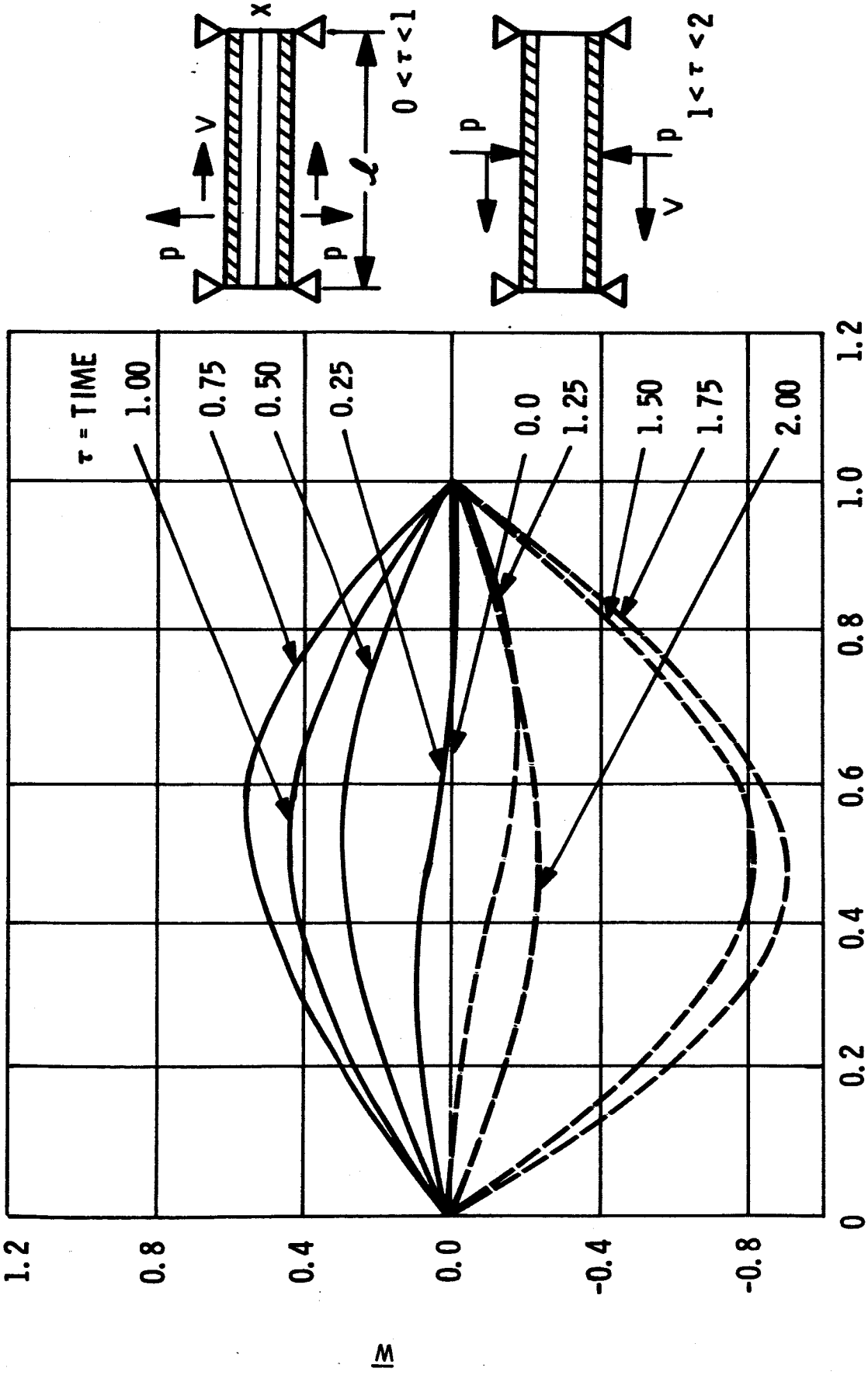

Figure IV-24. Deflection Profile History, Spike Pressure, Simple Supports, $\lambda = 0.5$, $\beta = 10$, $\alpha = 0$

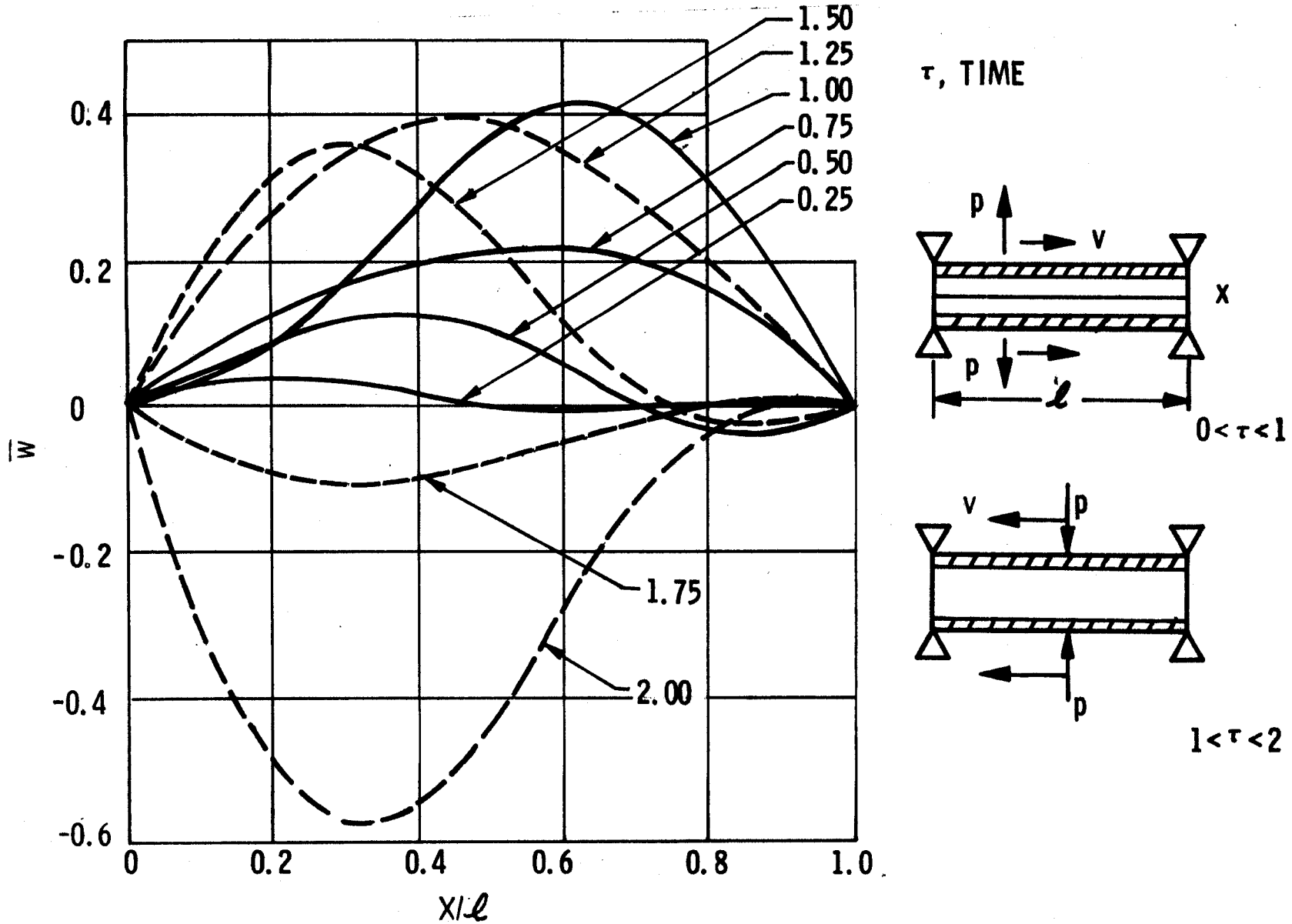

Figure IV-25. DeflectionProfile History, Spike Pressure, Simple Supports, $\lambda = 2$, $\beta = 10$, $\alpha = 0$

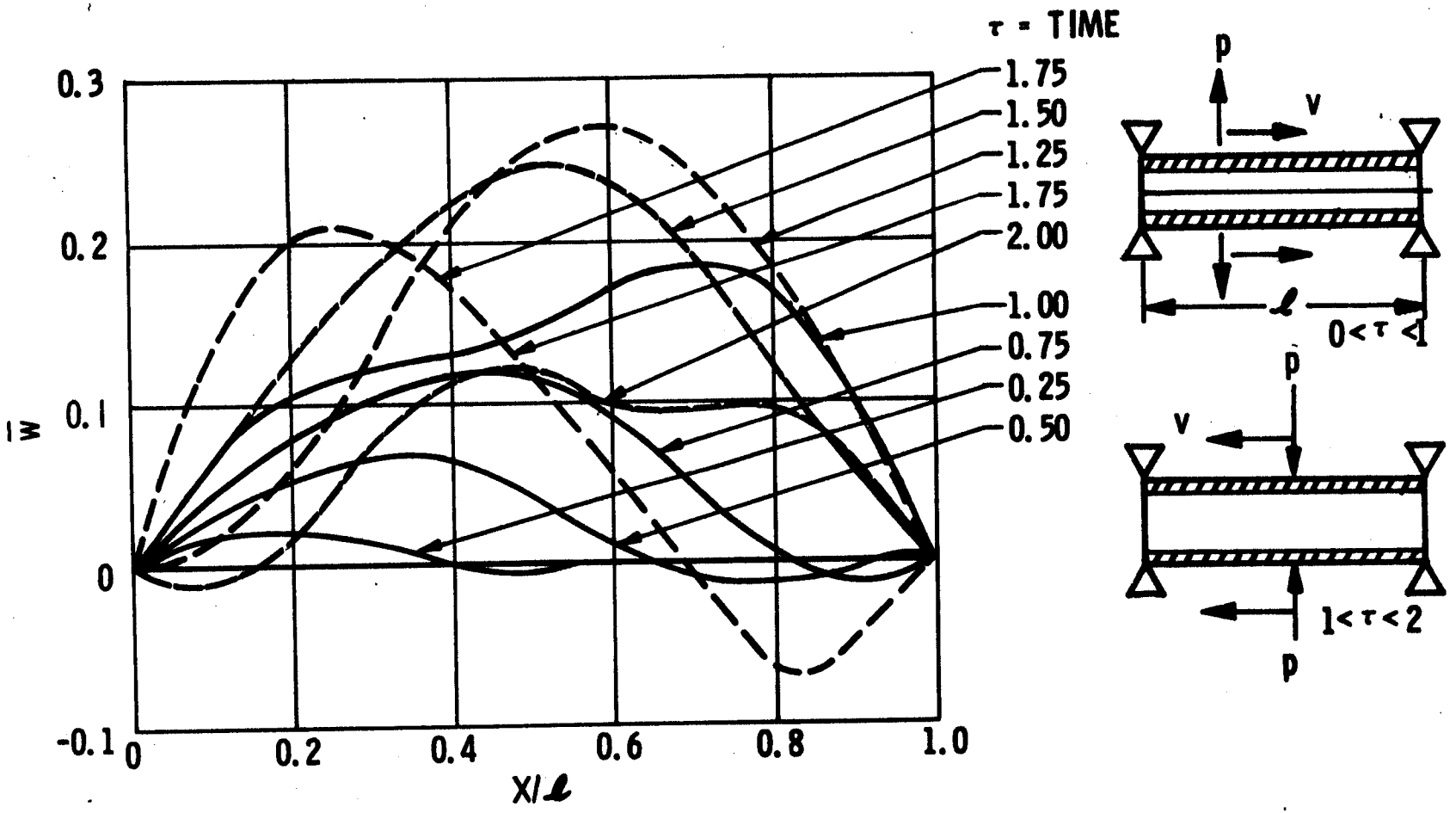

Figure IV-26. DeflectionProfile History, Spike Pressure, Simple Supports, $\lambda = 5$, $\beta = 10$, $\alpha = 0$

B. SIGNIFICANCE OF SOLUTION FOR INFINITE DUCT

Since in reality all ducts are of finite length, the question arises as to the practical applicability of dynamic solutions obtained for the infinite duct. The closed form solution derived for the infinite shell corresponds to a steady state solution whereas the series solution for the shell of finite length is a more general solution which will yield both the transient and steady state response of the duct. Consequently, it is logical to assume that, if boundary effects were negligible, the response of relatively long ducts is similar to that determined for the infinite duct, i.e., for ducts greater than a certain length, the response of the finite shell is approximately that of the infinite shell.

Comparison of results obtained for the shell of finite length with that for the infinite shell indicate that the maximum stresses and deflections for the finite shell are similar if not identical to that of the infinite shell. This observation is clearly indicated by the design charts presented in Section V. The design charts include both the results for the infinite shell and finite length. Evidently in some ranges of the design parameter, the difference in response is negligible as is the case for the spike pressure for $\lambda < 1$ as shown in Figure V-1. However, in general, the difference in response can be quite significant as indicated for example in Figure V-1, for $\lambda > 1$.

In order that the finite length shell be at all comparable to the infinite shell, the length of the shell must be at least greater than the wave length of the deflection profile of the infinite shell. The wave length as a function of the speed parameter is given in Reference 3-3.

If we let the wave length equal ℓ_w (inches), and, in consistency with the length parameter, define the non-dimensional wave length as

$$\beta_w = \frac{\ell_w^2}{Rh}\sqrt{12\,(1-\nu^2)} = \gamma^2 \ell_w^2 = \bar{\xi}_w^2$$

where $\bar{\xi}_w$ is the wave length given in Reference 3-2, then the wave length versus speed parameter can be shown to be given by Figure IV-27. This curve indicates for example that if $\lambda = 1.5$ then $\beta_w \approx 100$ and consequently in order that the finite length shell solution be at all comparable to the infinite length shell, the length parameter of the finite length shell must be greater than 100.

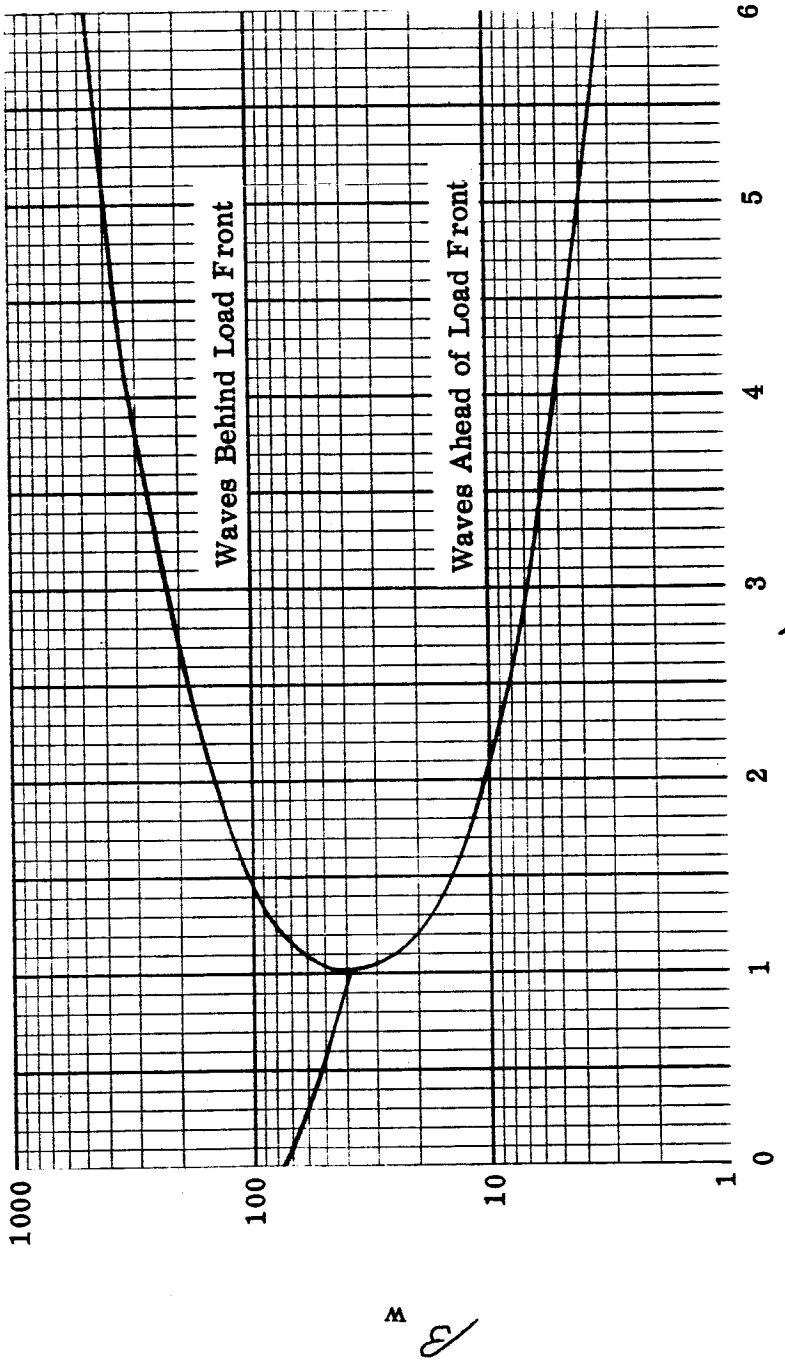

Figure IV-27. Wave Length versus Speed Parameter, λ

In general, from this portion of the study it appears that solutions obtained for the infinite duct can be used to a limited extent to approximate the response of relatively long ducts. However, this aspect of the subject requires additional study.

C. SIGNIFICANCE OF DAMPING

Although the dynamic response solutions presented in this report contain the effects of viscous damping, there is no method available for predicting the magnitude of the viscous damping coefficient required for a particular case. Consequently only the significance of damping is investigated.

Typical deflection and bending moment dynamic response curves which include damping for a step pressure are presented in Figures IV-28 and IV-29. These curves are comparable with that of Figure IV-21 which does not include the effects of damping. Comparison of the dynamic response curves in these three figures reveals that there is a significantly large decrease in maximum stress levels when the damping parameter is increased from $\alpha = 0$ to $\alpha = 0.1$, but the decrease in stress level when going from $\alpha = 0.1$ to $\alpha = 0.2$ is small.

The influence of damping on the maximum deflection and bending stresses was determined for the traveling spike load and the results indicate that damping effects can be quite significant in reducing deflection and stress levels.

It is concluded from this portion of the study that damping can be quite significant and should be investigated further.

D. SIGNIFICANCE OF SHEAR AND ROTATORY INERTIA

The theory upon which the present study is based neglects the effects of local shear deformations and rotatory inertia. To determine the significance of shear deformations and rotatory inertia with regard to the dynamic response of cylinders to traveling transient pressures, a solution to the basic shell equations which include the effects of shear deformations and rotatory inertia was obtained and documented in Reference 3-1.

Typical deflection and bending moment dynamic response curves were obtained with the shear theory of Reference 3-1 for traveling step pressure and are compared in

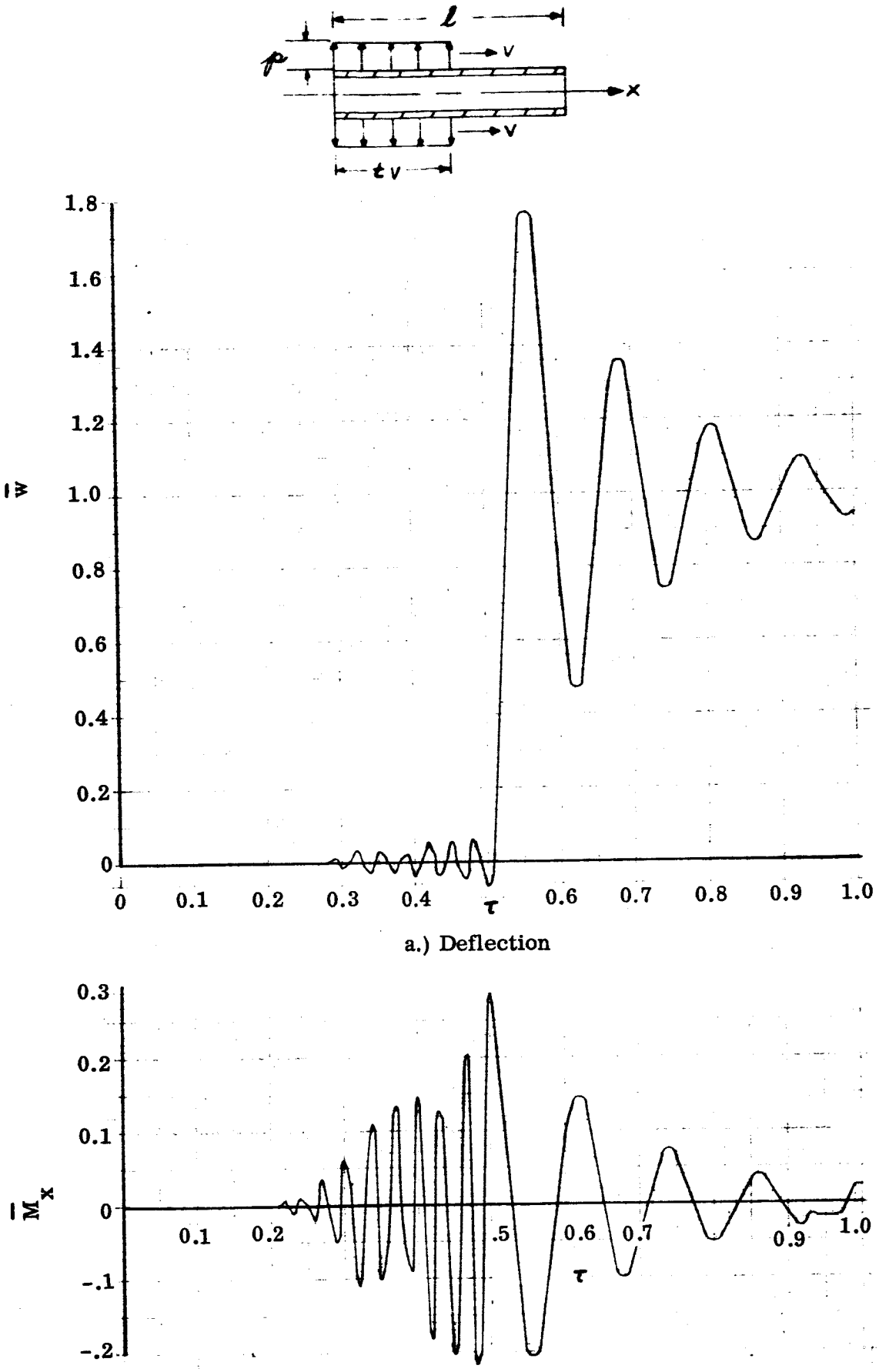

a.) Deflection

b.) Bending Moment

Figure IV-28. Typical Deflection and Bending Moment Variation With Time At $\xi = .5$, With Damping $\alpha = .1$, Step Pressure, Simple Supports, $\lambda = 2, \beta = 10^4$, N = 100

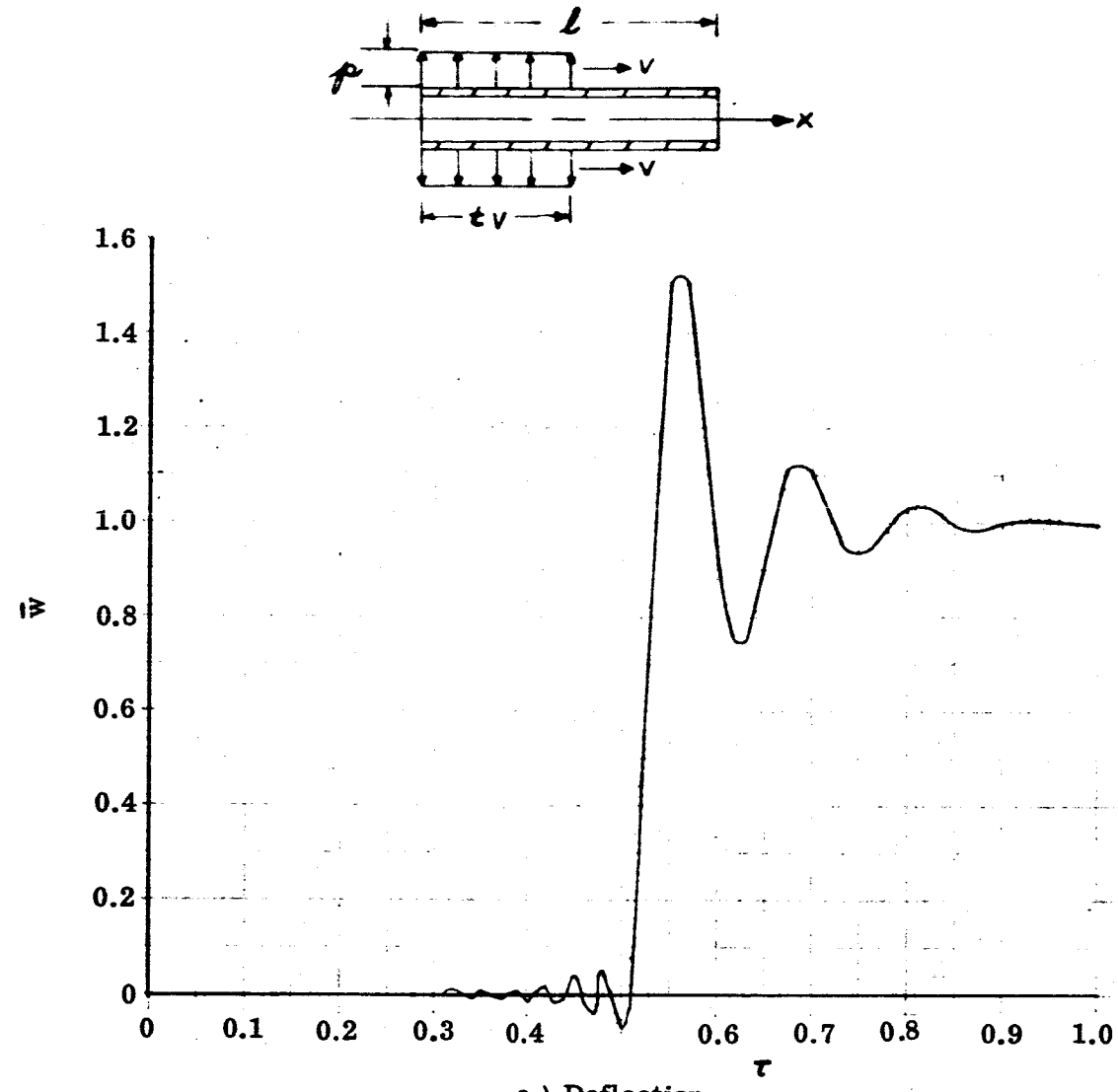

a.) Deflection

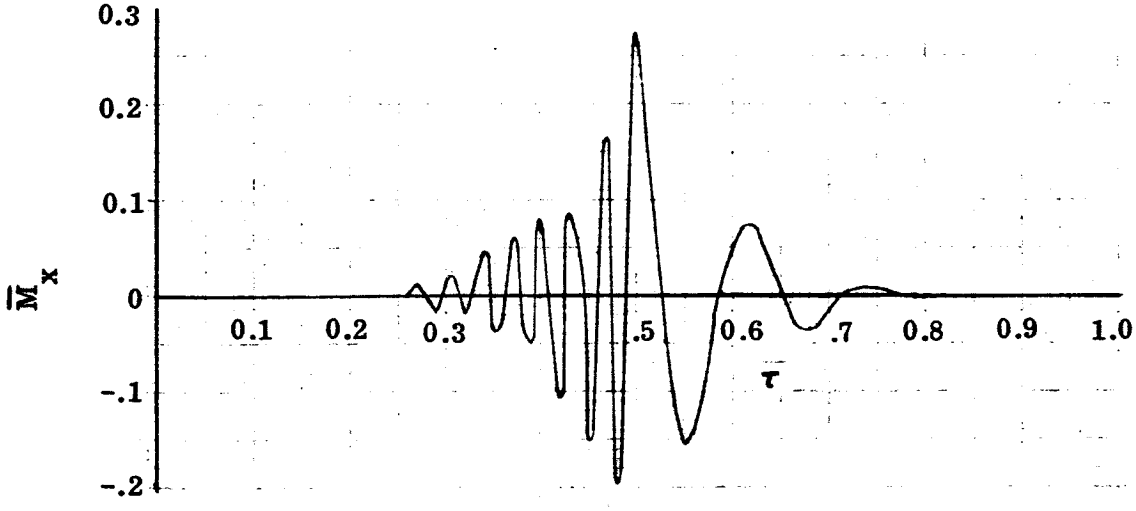

b.) Bending Moment

Figure IV-29. Typical Deflection and Bending Moment Variation With Time At $\xi = .5$, With Damping $\alpha = .2$, Step Pressure, Simple Supports, $\lambda = 2$, $\beta = 10^4$, N = 100

Figures IV-30 and IV-31 with curves obtained with the theory presented in this report. From an examination of this comparison it is evident that for the design parameter selected, there is little difference in the deflections (see Figure IV-30). But, from an examination of the bending moment results given in Figure IV-31 it appears that shear deformation effects may be of significance. In general, from this portion of the study it may be concluded that for the range of values of design parameter considered in this report, shear and rotating inertia effects can be neglected without introducing significant errors. This subject is discussed further in Section VI-B.

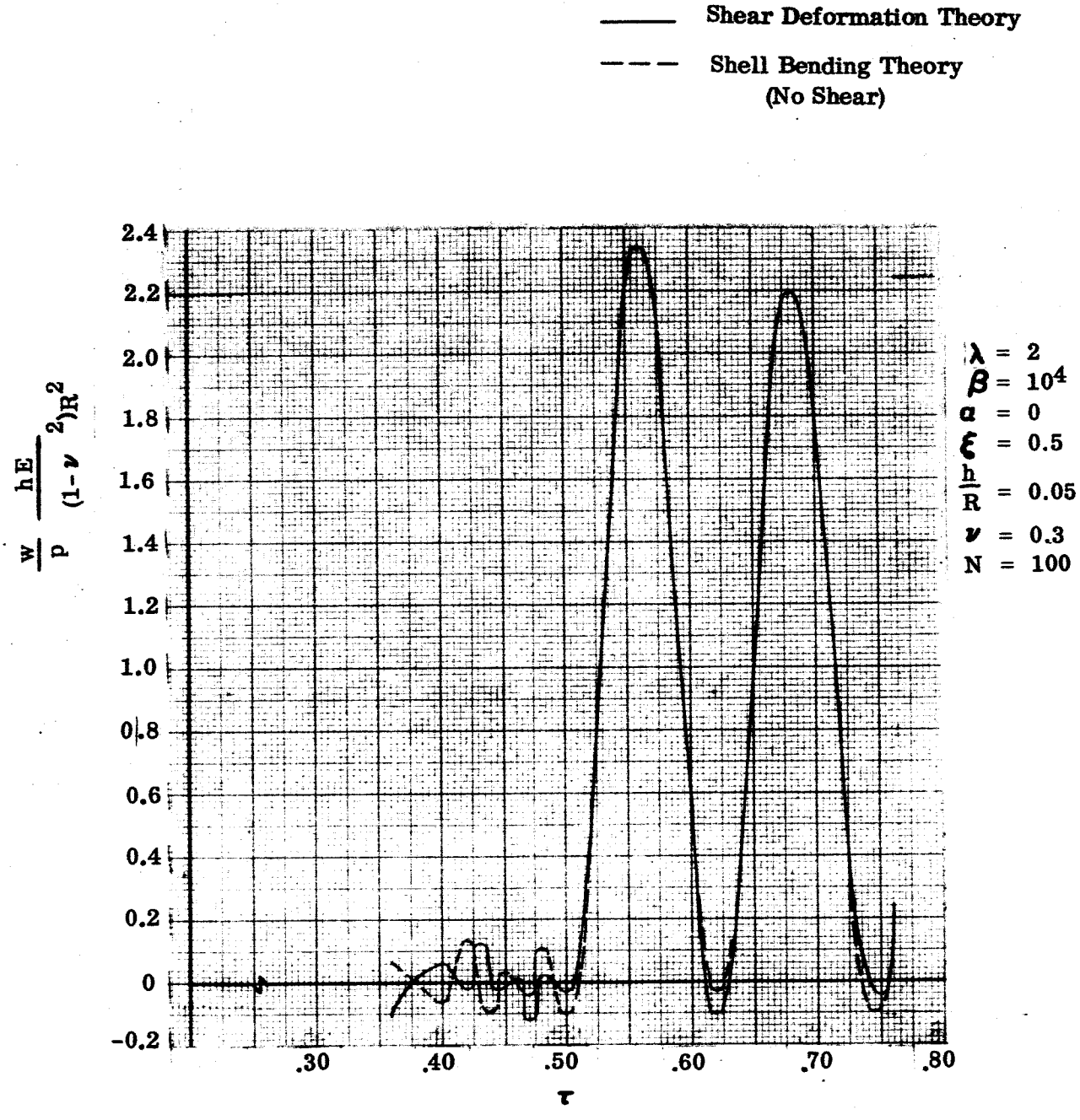

Figure IV-30. Significance of Shear And Rotatory Inertia, Deflection versus Time, Step Pressure

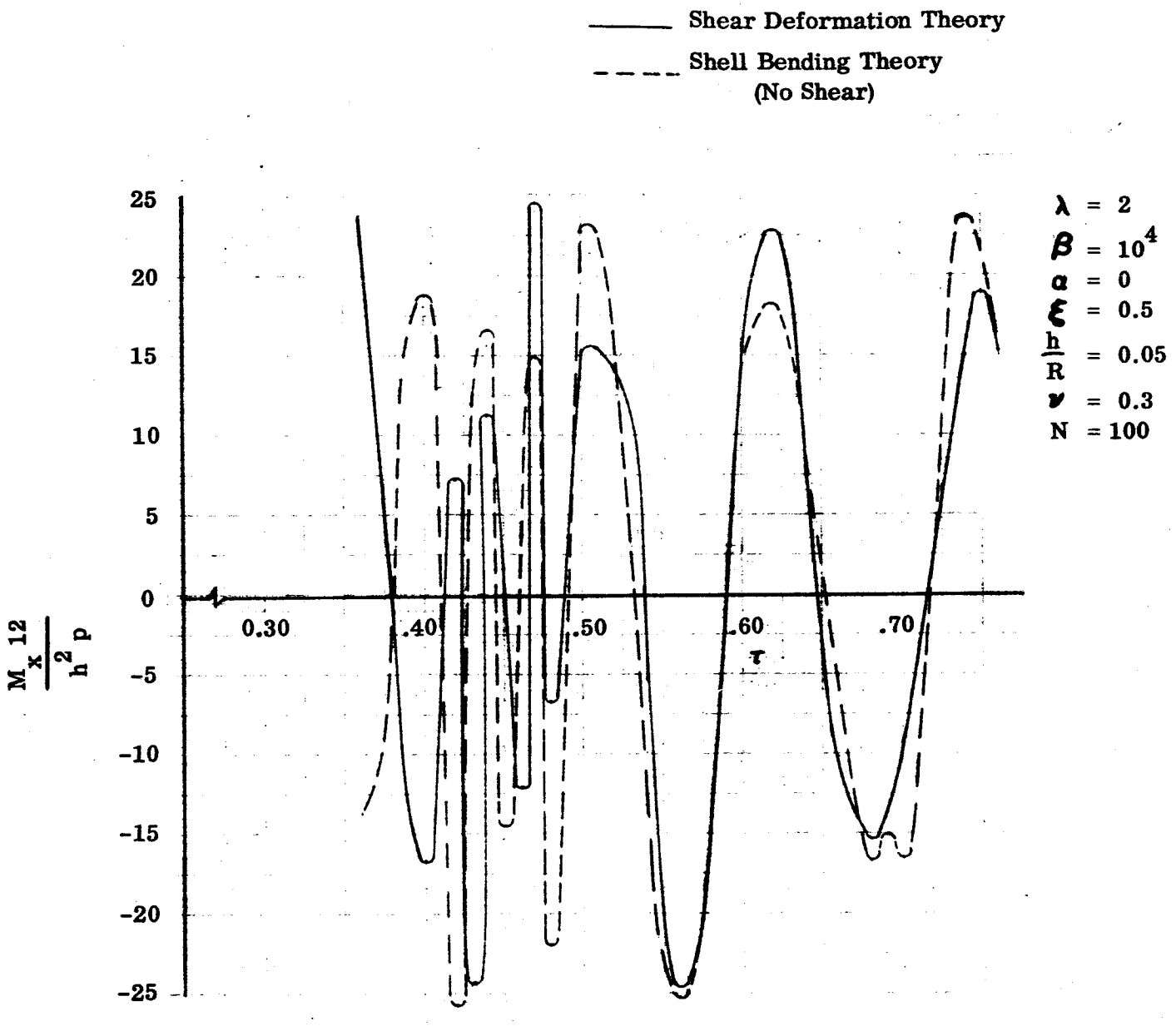

Figure IV-31. Significance of Shear and Rotatory Inertia, Bending Moment versus Time, Step Pressure

E. REFERENCES

4-1. Timoshenko, S. and Woinowsky-Krieger, S., "Theory of Plates and Shells", McGraw-Hill Book Co., N.Y. 1959

V. DESIGN DATA

A. METHOD USED TO DETERMINE MAXIMUM STRESSES

Based on the dynamic response data discussed in Section IV, an approximate but realistic approach to the development of design charts was followed. First based on the convergence characteristics of the series solution, values of N were selected for each combination of β and λ values.

Deflections and bending moments were then determined as a function of time at three locations ξ = 0.45, 0.50 and 0.55 such as shown in Figures IV-21 and IV-23 for ξ = 0.5. Maximum deflections and bending moments were then extracted from this data and design charts prepared.

For cylinders with fixed-fixed boundary conditions, bending moments at both supports were first determined as a function of time, the maximum value was then extracted and separate design charts prepared.

B. PRESENTATION OF DESIGN CHARTS

Maximum deflections and bending moments are presented in Figures V-1 through V-26. All the data used to prepare the design charts are summarized in tables which follow the pertinent design charts. These tables also contain the corresponding deflections and bending moments which occur at the points of maximum deflection and bending moment. Also included in the tables are the number of terms, N, taken in the series solution used to generate the design data.

For purposes of aiding in the rapid location of a desired design chart, the following master table was prepared.

MASTER TABLE

SUMMARY OF DESIGN CHARTS

	$\overline{w}_{max}$		$\overline{M}_{max}$	
Case*	Figures	Pages	Figures	Pages
Spike, S.S.	V-1, 2	124, 126	V-1, 3	124, 127
Step, S.S.	V-4	130	V-4	130
Ramp, S.S.	V-5	132	V-6, 7, 8	133, 134, 135
Sinusoidal, S.S.	V-9, 10	140, 141	V-11, 12	142, 143
Spike, F.F.	V-13	149	V-13	149
Step, F.F.	V-14	151	V-14, 23	151, 171
Ramp, F.F.	V-15, 16	153, 154	V-17, 24	155, 173
Sinusoidal F.F.	V-18, 19, 20 21, 22	161, 162, 163, 164, 165	V-18, 19, 20, 21, 22, 25, 26	161, 162, 163, 164, 165, 175, 176

*S.S. = Simple-simple supports

F.F. = Fixed-fixed supports

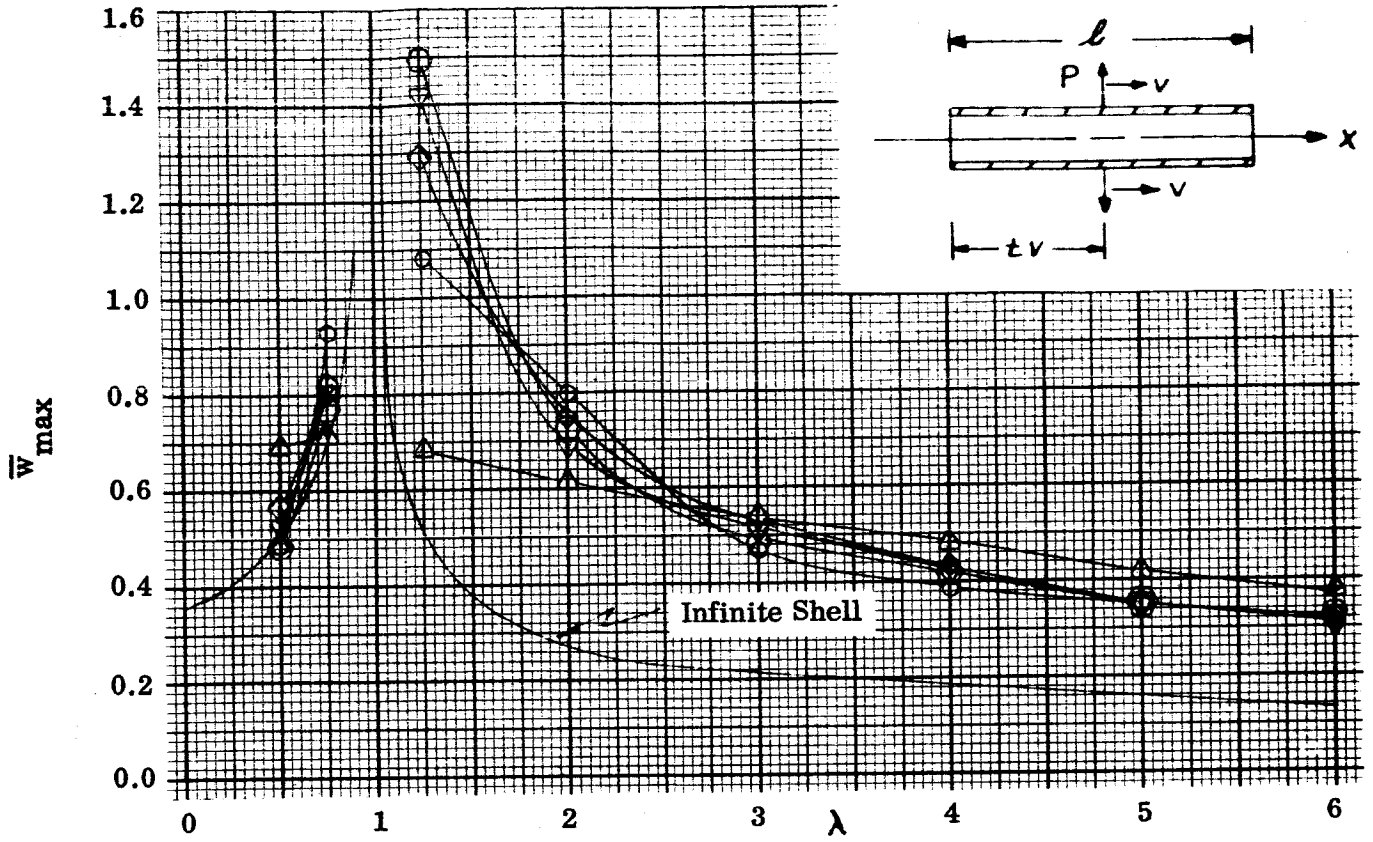

a.) Deflection

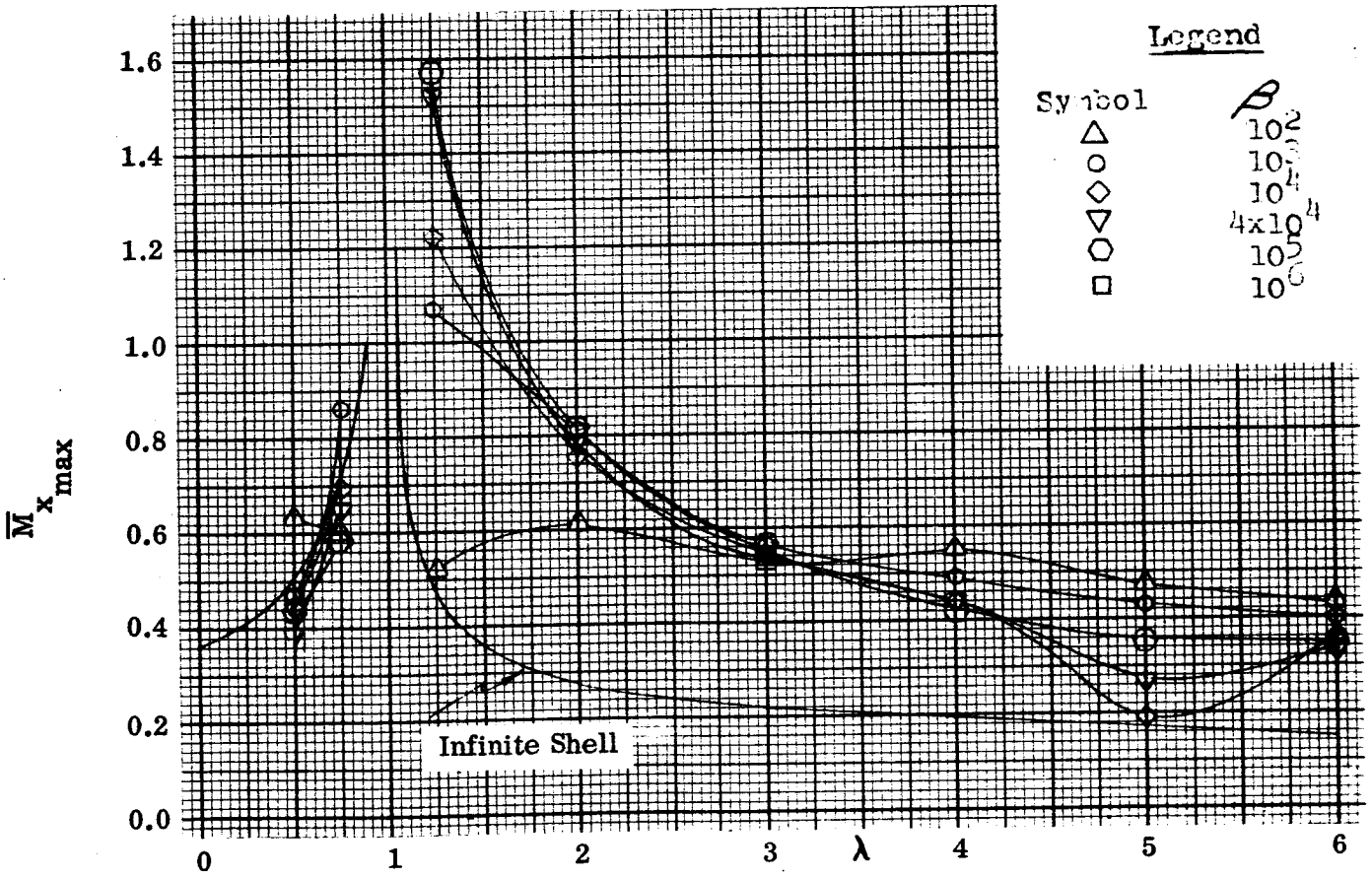

b.) Bending Moment

Figure V-1. Maximum Deflection and Bending Moment versus λ, Spike Pressure, Simple Supports, $\alpha = 0$

TABLE 1, SPIKE PRESSURE, SIMPLE SUPPORTS, α = 0

λ \ β	10^2	N	10^3	N	10^4	N	4×10^4	N	10^5	N
0.5	0.6906	25	0.4852	50	0.5630	100	0.5262	150	0.4857	200
0.75	0.7159	25	0.9374	50	0.8227	100	0.8012	150	0.7737	200
1.25	0.6799	25	1.0814	70	1.2915	100	1.4179	150	1.4958	200
2.00	0.6122	25	0.8038	70	0.7585	100	0.6966	250	0.7411	350
3.00	0.5399	50	0.4670	80	0.5261	110	0.5169	300	0.4934	375
4.00	0.4836	50	0.3902	80	0.4293	125	0.4180	300	0.4230	400
5.00	0.4233	50	0.3540	80	0.3480	150	0.3500	325	0.3548	425
6.00	0.3761	50	0.3245	80	0.3158	200	0.3139	350	0.3221	450

(a) Maximum Deflection

λ \ β	10^2	N	10^3	N	10^4	N	4×10^4	N	10^5	N
0.5	0.6380	25	0.4656	50	0.4552	100	0.3899	150	0.3274	200
0.75	0.6032	25	0.8619	50	0.6991	100	0.6584	150	0.5955	200
1.25	0.5255	25	1.0718	70	1.2307	100	1.5248	150	1.5732	200
2.00	0.6133	25	0.8023	70	0.7613	100	0.7847	250	0.8086	350
3.00	0.5340	50	0.5644	80	0.5430	110	0.5338	300	0.5494	375
4.00	0.5596	50	0.4970	80	0.4413	125	0.4489	300	0.4344	400
5.00	0.4730	50	0.4372	80	0.1868	150	0.2708	325	0.3584	425
6.00	0.4352	50	0.4011	80	0.3601	200	0.3309	350	0.3499	450

(b) Maximum Bending Moment

λ \ β	10^2	N	10^3	N	10^4	N	4×10^4	N	10^5	N
0.50	0.6883	25	0.4787	50	0.5630	100	0.5262	150	0.4857	200
0.75	0.6209	25	0.9374	50	0.8227	100	0.8012	150	0.7737	200
1.25	0.5598	25	-0.5680	70	-1.2915	100	1.4179	150	-1.4958	200
2.00	-0.1503	25	0.8038	70	-0.7586	100	0.5670	250	0.7411	350
3.00	-0.1187	50	-0.2983	80	0.2651	110	-0.3990	300	0.4086	375
4.00	0.4835	50	-0.0352	80	-0.3880	125	0.4047	300	0.3826	400
5.00	0.4233	50	-0.0273	80	0.1929	150	0.2956	325	-0.3399	425
6.00	0.3761	50	0.1433	80	0.2175	200	0.1885	350	0.3045	450

(c) Deflection Corresponding To The Maximum Bending Moment

λ \ β	10^2	N	10^3	N	10^4	N	4×10^4	N	10^5	N
0.50	-0.6122	25	-0.3879	50	-0.4552	100	-0.3899	150	-0.3274	200
0.75	-0.3814	25	-0.8619	50	-0.6992	100	-0.6584	150	-0.5955	200
1.25	-0.4183	25	-0.5792	70	1.2307	100	-0.5248	150	1.5732	200
2.00	-0.4050	25	-0.8023	70	0.7613	100	-0.7163	250	-0.8086	350
3.00	-0.4719	50	0.3426	80	-0.5098	110	-0.4748	300	0.4190	375
4.00	-0.5596	50	-0.0865	80	0.4176	125	0.4198	300	-0.4331	400
5.00	-0.4730	50	0.3952	80	0.1674	150	-0.2214	325	0.3299	425
6.00	-0.4352	50	0.2952	80	-0.3501	200	0.2631	350	-0.3321	450

(d) Bending Moment Corresponding To The Maximum Deflection

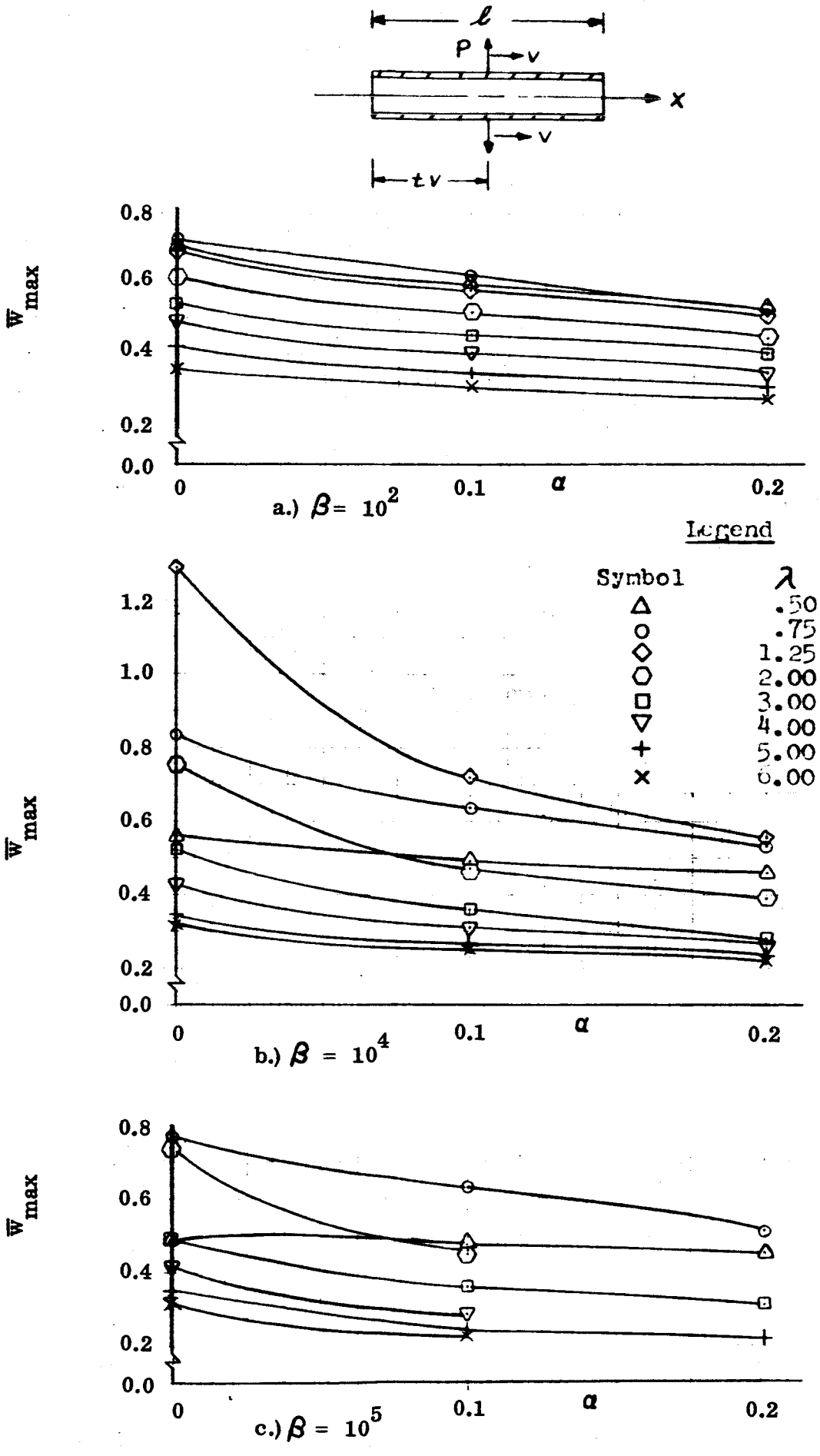

Figure V-2. Maximum Deflection versus α , Spike Pressure, Simple Supports

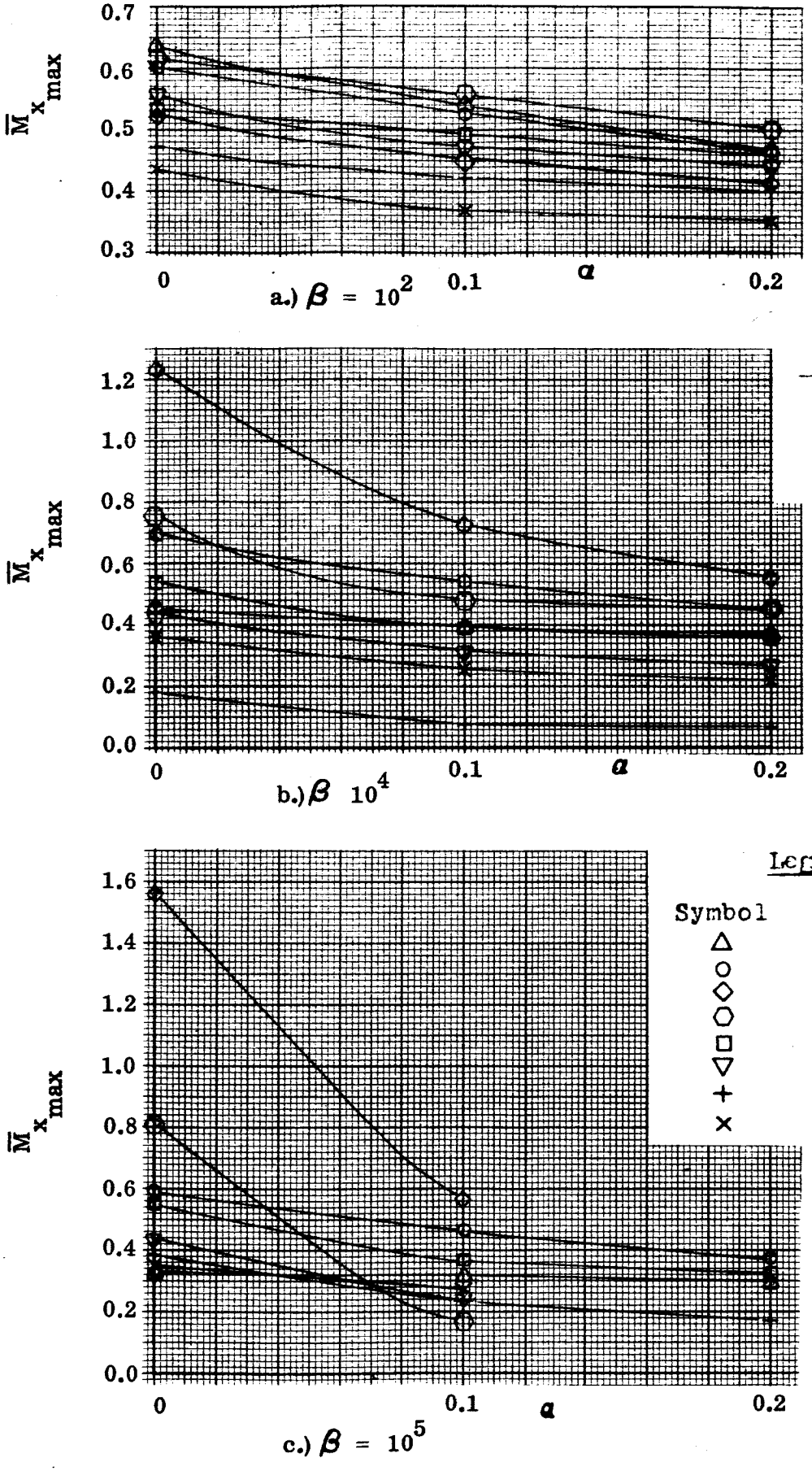

Figure V-3. Maximum Bending Moment versus α, Spike Pressure, Simple Supports

TABLE 2. SPIKE PRESSURE, SIMPLE SUPPORTS, α = 0.1

λ \ β	10^2	N	10^3	N	10^4	N	4×10^4	N	10^5	N
0.50	0.5198	25	0.4813	50	0.4869	100	0.4815	150	0.4748	200
0.75	0.6055	25	0.7138	50	0.6409	100	0.6348	150	0.6271	200
1.25	0.5772	25	0.7568	70	0.7227	100	0.7211	150	0.4499	200
2.00	0.5137	25	0.4855	70	0.4730	100	0.4342	250	0.4621	350
3.00	0.4545	50	0.3704	80	0.3630	110	0.3588	300	0.3605	375
4.00	0.4055	50	0.3257	80	0.3129	125	0.3108	300	0.2925	400
5.00	0.3571	50	0.2923	80	0.2766	150	0.2711	325	0.2460	425
6.00	0.3184	50	0.2642	80	0.2501	200	0.2431	350	0.2357	450

(a) Maximum Deflection

λ \ β	10^2	N	10^3	N	10^4	N	4×10^4	N	10^5	N
0.50	0.5379	25	0.4303	50	0.3879	100	0.3504	150	0.3188	200
0.75	0.5260	25	0.6297	50	0.5438	100	0.5053	150	0.4698	200
1.25	0.4540	25	0.7826	70	0.7284	100	0.4214	150	0.5675	200
2.00	0.5547	25	0.5596	70	0.4846	100	0.4313	250	0.1786	350
3.00	0.4974	50	0.4283	80	0.3987	110	0.3918	300	0.3691	375
4.00	0.4737	50	0.4046	80	0.3178	125	0.3050	300	0.2586	400
5.00	0.4234	50	0.3356	80	0.0770	150	0.0671	325	0.2388	425
6.00	0.3701	50	0.3069	80	0.2576	200	0.2438	350	0.2754	450

(b) Maximum Bending Moment

λ \ β	10^2	N	10^3	N	10^4	N	4×10^4	N	10^5	N
0.50	-0.1143	25	0.0018	50	0.0257	100	0.0230	150	-0.0455	200
0.75	-0.1029	25	-0.2352	50	-0.1103	100	-0.1120	150	-0.1209	200
1.25	-0.1069	25	-0.3756	70	-0.3386	100	-0.2164	150	-0.1557	200
2.00	-0.1316	25	-0.1496	70	-0.1376	100	-0.1138	250	-0.3167	350
3.00	-0.1060	50	-0.0799	80	-0.0569	110	-0.0543	300	-0.0617	375
4.00	-0.0782	50	-0.0613	80	-0.0392	125	-0.0272	300	-0.0322	400
5.00	-0.0575	50	-0.0372	80	-0.0008	150	-0.0001	325	-0.0221	425
6.00	-0.0455	50	-0.0301	80	-0.0227	200	-0.0206	350	-0.0180	450

(c) Deflection Corresponding to the Maximum Bending Moment

λ \ β	10^2	N	10^3	N	10^4	N	4×10^4	N	10^5	N
0.50	-0.5162	25	-0.4303	50	-0.3879	100	-0.3504	150	-0.3188	200
0.75	-0.3020	25	-0.5922	50	-0.5438	100	-0.5053	150	-0.4698	200
1.25	-0.3316	25	-0.4115	70	-0.3316	100	-0.3059	150	-0.2359	200
2.00	-0.3257	25	-0.1490	70	-0.1303	100	-0.1392	250	-0.1066	350
3.00	-0.3790	50	-0.0740	80	-0.0760	110	-0.0582	300	-0.0533	375
4.00	-0.4441	50	-0.0612	80	-0.0454	125	-0.0385	300	-0.0365	400
5.00	-0.3908	50	-0.0711	80	-0.0158	150	-0.0331	325	-0.0333	425
6.00	-0.3533	50	-0.0592	80	-0.0187	200	-0.0207	350	-0.0187	450

(d) Bending Moment Corresponding to the Maximum Deflection

TABLE 3. SPIKE PRESSURE, SIMPLE SUPPORTS, $a = 0.2$

λ \ β	10^2	N	10^3	N	10^4	N	4×10^4	N	10^5	N
0.50	0.5219	25	0.4702	50	0.4610	100	0.4558	150	0.4491	200
0.75	0.5255	25	0.5812	50	0.5276	100	0.5220	150	0.5144	200
1.25	0.4982	25	0.5817	70	0.5531	100	0.5499	150		200
2.00	0.4415	25	0.4079	70	0.3972	100	0.3891	250		350
3.00	0.3873	50	0.3219	80	0.3155	110	0.3058	300	0.3170	375
4.00	0.3439	50	0.2801	80	0.2722	125	0.2716	300		400
5.00	0.3043	50	0.2509	80	0.2402	150	0.2402	325	0.2235	425
6.00	0.2724	50	0.2267	80	0.2202	200	0.2139	350		450

(a) Maximum Deflection

λ \ β	10^2	N	10^3	N	10^4	N	4×10^4	N	10^5	N
0.50	0.4694	25	0.4097	50	0.3687	100	0.3314	150	0.3003	200
0.75	0.4660	25	0.4977	50	0.4506	100	0.4103	150	0.3745	200
1.25	0.4151	25	0.6107	70	0.5643	100	0.3229	150		200
2.00	0.5048	25	0.4917	70	0.4522	100	0.3370	250		350
3.00	0.4647	50	0.4100	80	0.3629	110	0.3582	300	0.3200	375
4.00	0.4469	50	0.3769	80	0.2689	125	0.2642	300		400
5.00	0.4042	50	0.3114	80	0.0688	150	0.0594	325	0.1770	425
6.00	0.3566	50	0.2738	80	0.2192	200	0.2156	350		450

(b) Maximum Bending Moment

λ \ β	10^2	N	10^3	N	10^4	N	4×10^4	N	10^5	N
0.50	-0.0622	25	-0.0397	50	-0.0132	100	-0.0162	150	-0.0099	200
0.75	-0.0934	25	-0.1531	50	-0.1503	100	-0.1535	150	-0.0126	200
1.25	-0.0959	25	-0.2653	70	-0.2242	100	-0.1842	150		200
2.00	-0.1161	25	-0.1356	70	-0.1253	100	-0.0862	250		350
3.00	-0.0951	50	-0.0719	80	-0.0501	110	-0.0419	300	-0.0524	375
4.00	-0.0716	50	-0.0534	80	-0.0338	125	-0.0164	300		400
5.00	-0.0535	50	-0.0364	80	-0.0011	150	-0.0016	325	-0.0175	425
6.00	-0.0429	50	-0.0261	80	-0.0186	200	-0.0178	350		450

(c) Deflection Corresponding to the Maximum Bending Moment

λ \ β	10^2	N	10^3	N	10^4	N	4×10^4	N	10^5	N
0.50	-0.4155	25	-0.3671	50	-0.3691	100	-0.3306	150	-0.3000	200
0.75	-0.2556	25	-0.4895	50	-0.4510	100	-0.4106	150	-0.3740	200
1.25	-0.2675	25	-0.2724	70	-0.2122	100	-0.1855	150		200
2.00	-0.2596	25	-0.1115	70	-0.0997	110	-0.1283	250		350
3.00	-0.2971	50	-0.0612	80	-0.0478	110	-0.0454	300	-0.0454	375
4.00	-0.3543	50	-0.0474	80	-0.0365	125	-0.0326	300		400
5.00	-0.3247	50	-0.0478	80	-0.0247	150	-0.0296	325	-0.0318	425
6.00	-0.2872	50	-0.395	80	-0.0196	200	-0.197	325		450

(d) Bending Moment Corresponding to the Maximum Deflection

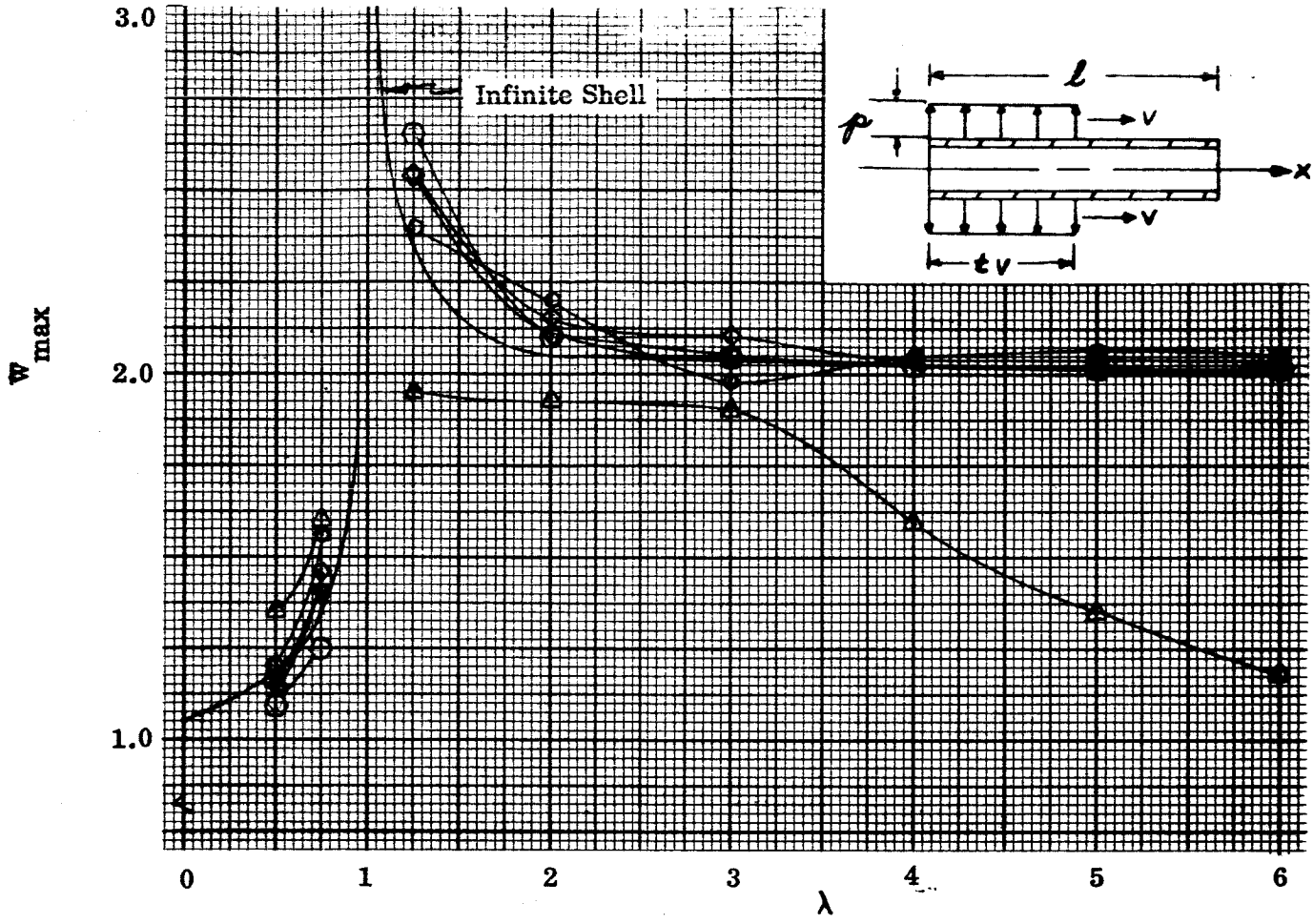

a.) Deflection

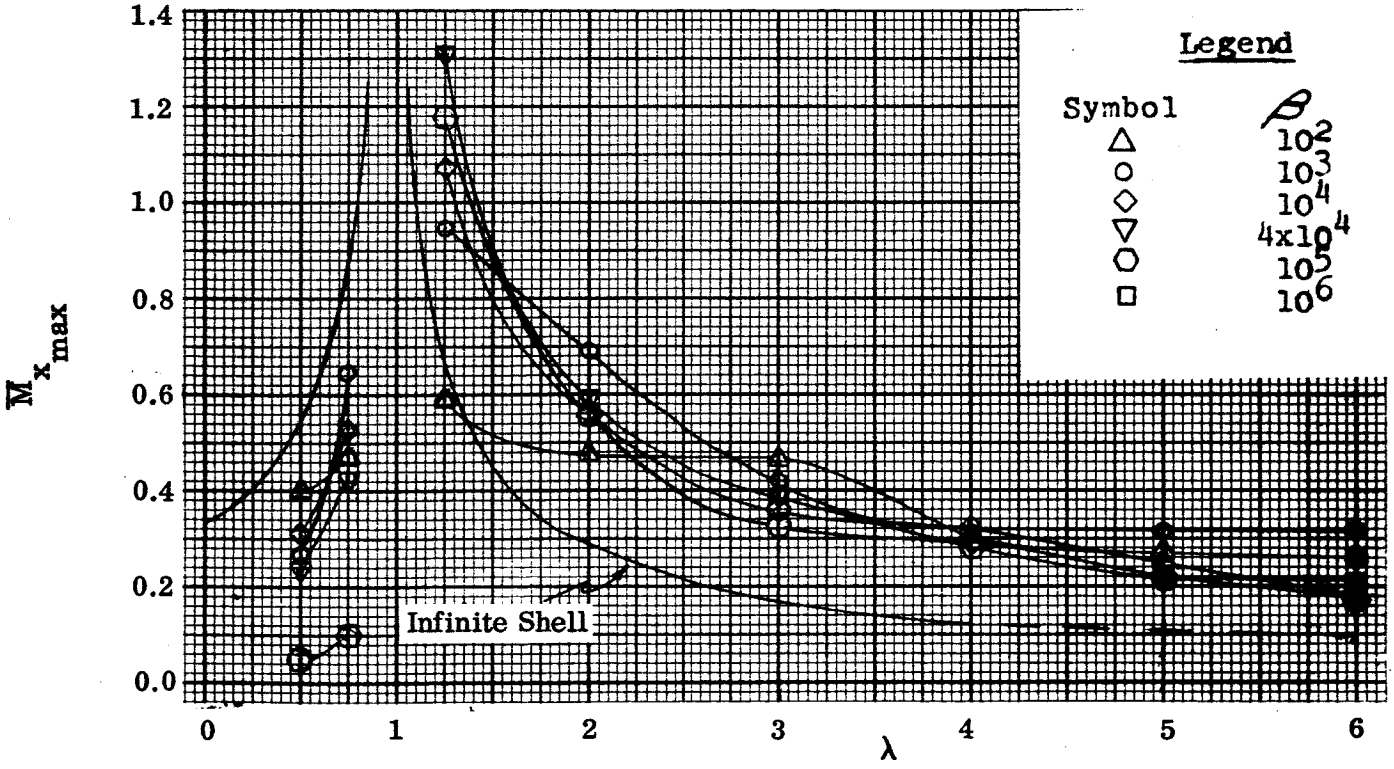

b.) Bending Moment

Figure V-4. Maximum Deflection and Bending Moment versus λ, Step Pressure, Simple Supports, $\alpha = 0$

TABLE 4 STEP PRESSURE, SIMPLE SUPPORTS, $\alpha = 0$

λ \ β	10^2	N	10^3	N	10^4	N	4×10^4	N	10^5	N
0.50	1.3540	25	1.2162	50	1.1789	100	1.1608	150	1.1047	200
0.75	1.6054	25	1.5722	50	1.4628	100	1.4196	150	1.2595	200
1.25	1.9514	25	2.3979	70	2.5464	100	2.5411	150	2.6638	200
2.00	1.9309	25	2.2091	70	2.1547	100	2.1162	250	2.1171	350
3.00	1.9194	50	1.9822	80	2.1111	110	2.0552	300	2.0659	375
4.00	1.6090	50	2.0594	80	2.0491	125		300	2.0363	400
5.00	1.3699	50	2.0700	80	2.0445	150	2.0209	325	2.0236	425
6.00	1.1837	50	2.0570	80	2.0360	200	2.0381	350	2.0176	450

(a) Maximum Deflection

λ \ β	10^2	N	10^3	N	10^4	N	4×10^4	N	10^5	N
0.50	-0.3918	25	0.2680	50	0.3148	100	0.2442	150	0.0566	200
0.75	-0.4689	25	0.6474	50	0.5327	100	-0.4315	150	-0.1018	200
1.25	-0.5919	25	0.9466	70	1.0741	100	1.3069	150	-1.1807	200
2.00	0.4776	25	0.6891	70	0.5603	100	-0.5883	250	0.5586	350
3.00	.0.4692	50	0.4215	80	0.3605	110	0.3857	300	0.3330	375
4.00	0.3070	50	-0.3160	80	0.3210	125		300	0.2926	400
5.00	0.2748	50	-0.3173	80	0.2477	150	-0.2153	325	0.2238	425
6.00	0.2674	50	-0.3173	80	0.1781	200	-0.2010	350	0.1768	450

(b) Maximum Bending Moment

λ \ β	10^2	N	10^3	N	10^4	N	4×10^4	N	10^5	N
0.50	1.2164	25	0.0805	50	0.0139	100	-0.1714	150	-0.1425	200
0.75	1.5836	25	-0.4312	50	-0.2329	100	1.4196	150	0.1443	200
1.25	1.9514	25	-0.5537	70	-0.2201	100	-0.7837	150	2.6638	200
2.00	-0.1513	25	-0.0318	70	-0.1583	100	2.0586	250	-0.1522	350
3.00	1.9194	50	-0.1247	80	0.0761	110	-0.0210	300	0.0464	375
4.00	0.0107	50	2.0569	80	-0.0942	165		300	-0.0445	400
5.00	0.1081	50	2.0645	80	-0.0340	150	1.9897	325	0.0853	425
6.0	0.6814	50	2.0515	80	0.1973	200	2.0381	350	0.1740	450

(c) Deflection Corresponding to the Maximum Bending Moment

λ \ β	10^2	N	10^3	N	10^4	N	4×10^4	N	10^5	N
0.50	-0.2601	25	-0.1351	50	-0.1072	100	-0.2369	150	-0.0282	200
0.75	-0.3421	25	-0.5702	50	-0.4532	100	-0.4315	150	-0.0911	200
1.25	-0.5919	25	-0.8046	70	-0.8322	100	-0.8332	150	-0.0118	200
2.00	-0.2737	25	-0.4215	70	-0.5024	100	-0.3419	250	-0.3266	350
3.00	-0.4692	50	-0.2088	80	-0.3470	110	-0.1547	300	-0.3027	375
4.00	-0.0965	50	-0.2568	80	-0.0712	125		300	-0.1978	400
5.00	-0.1053	50	-0.2463	80	-0.2348	150	-0.1375	325	-0.1193	425
6.00	-0.1822	50	-0.1686	80	-0.1319	200	-0.2010	350	-0.0991	450

(d) Bending Moment Corresponding to the Maximum Deflection

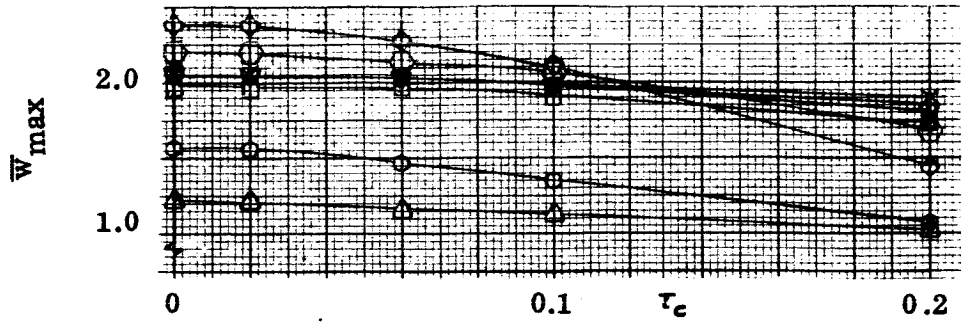

a.) $\beta = 10^3$

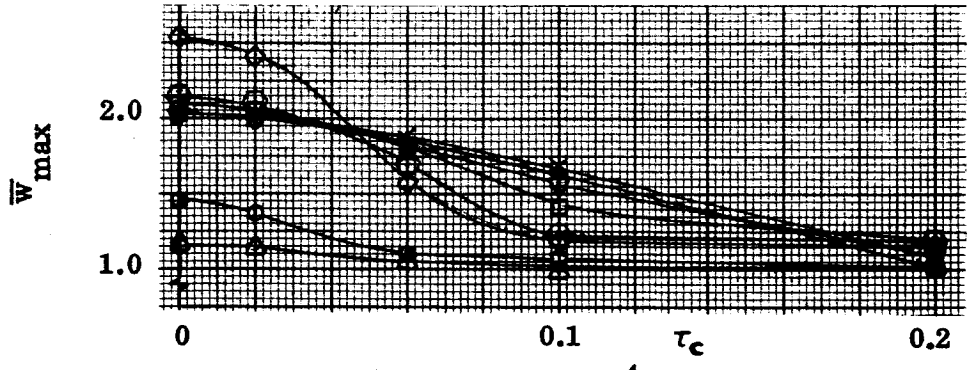

b.) $\beta = 10^4$

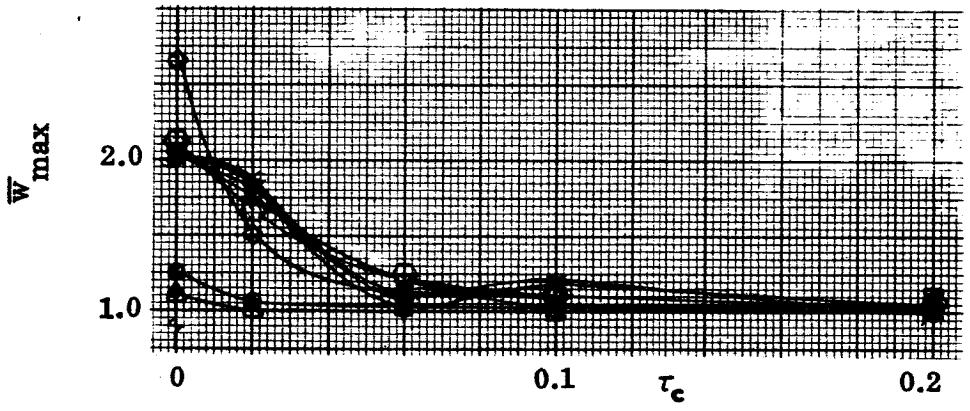

c.) $\beta = 10^5$

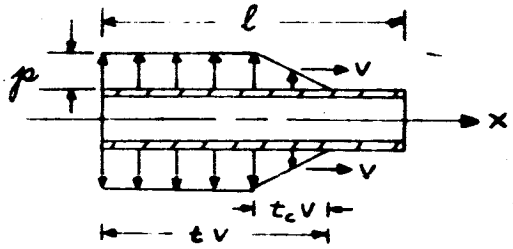

Legend

Symbol	λ
△	.50
○	.75
◇	1.25
⬡	2.00
□	3.00
▽	4.00
+	5.00
×	.00

Figure V-5. Maximum Deflection versus τ_c Ramp Pressure, Simple Supports, $\alpha = 0$

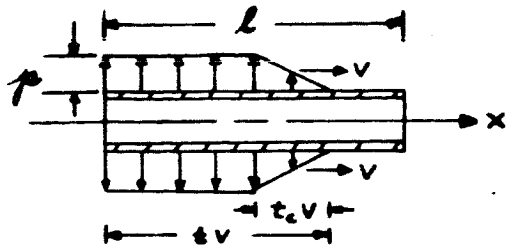

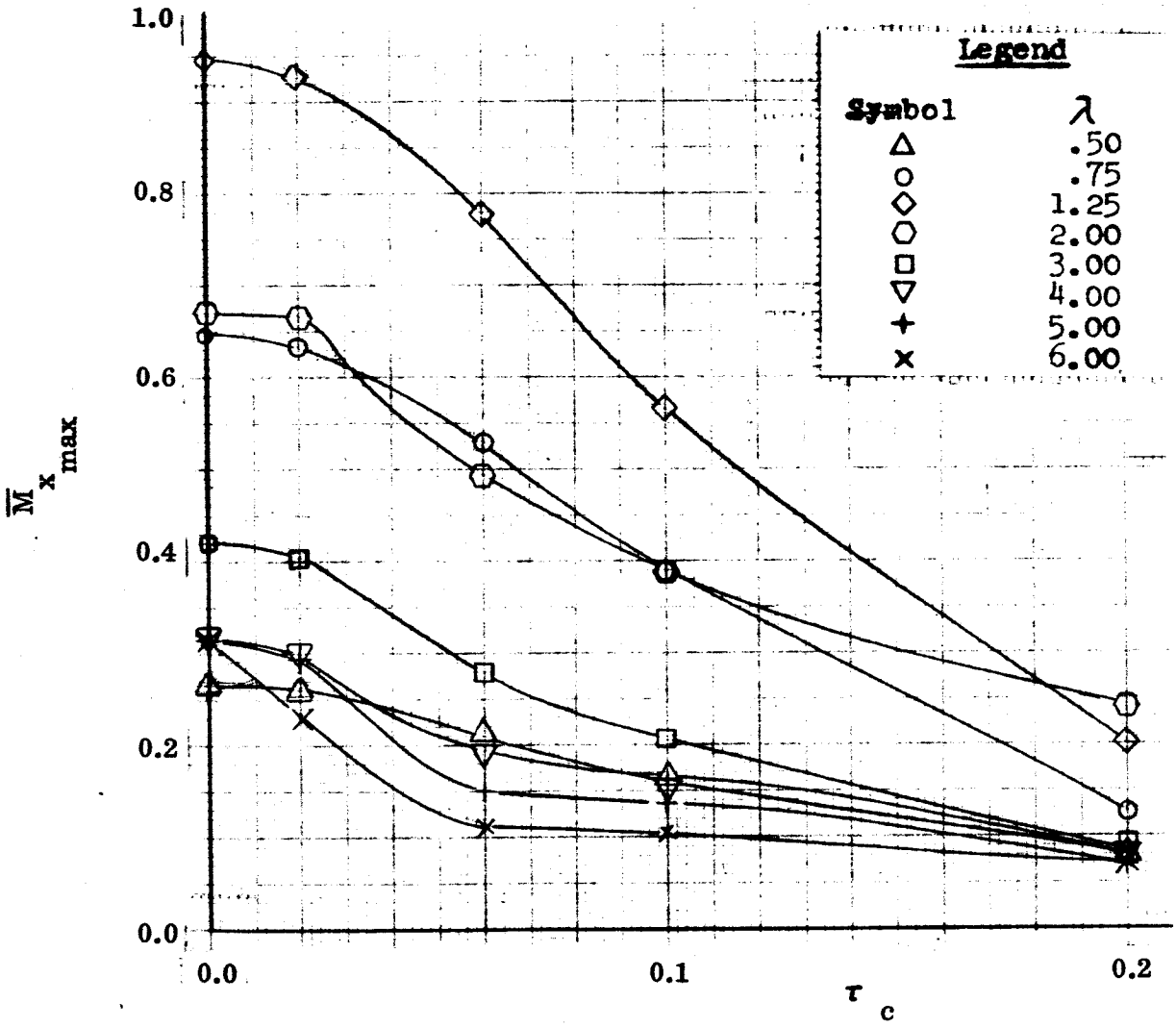

Figure V-6. Maximum Bending Moment versus τ_c Ramp Pressure, Simple Supports $\beta = 10^3$, $\alpha = 0$

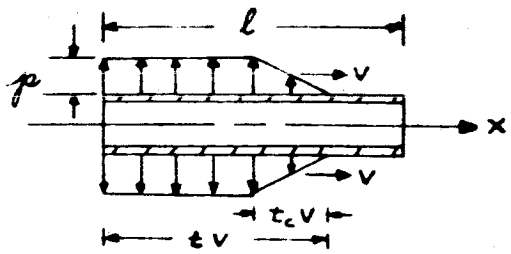

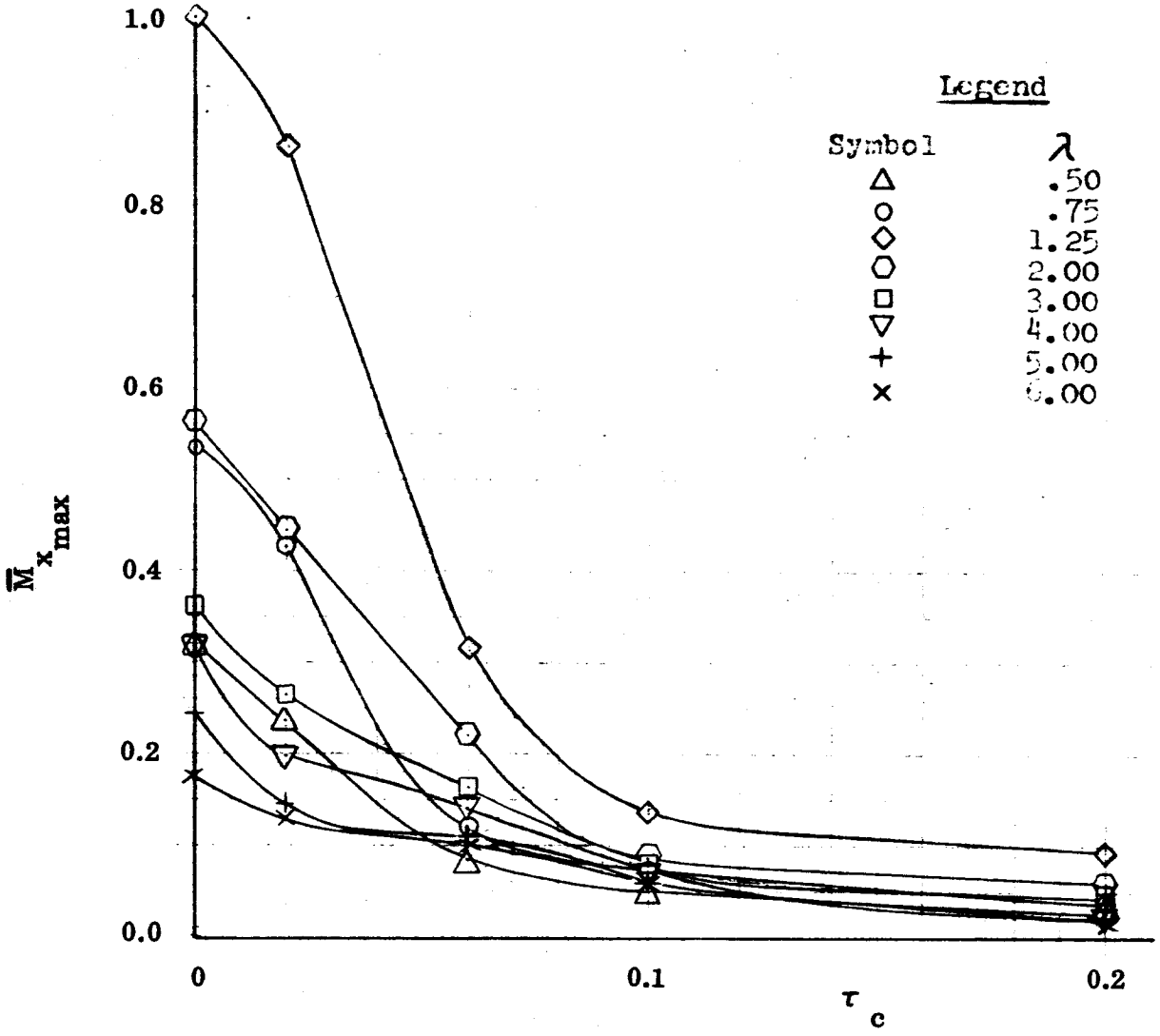

Figure V-7. Maximum Bending Moment versus τ_c, Ramp Pressure, Simple Supports, $\beta = 10^4$, $\alpha = 0$

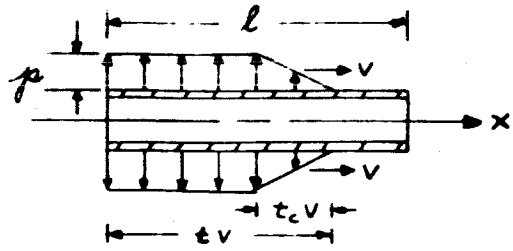

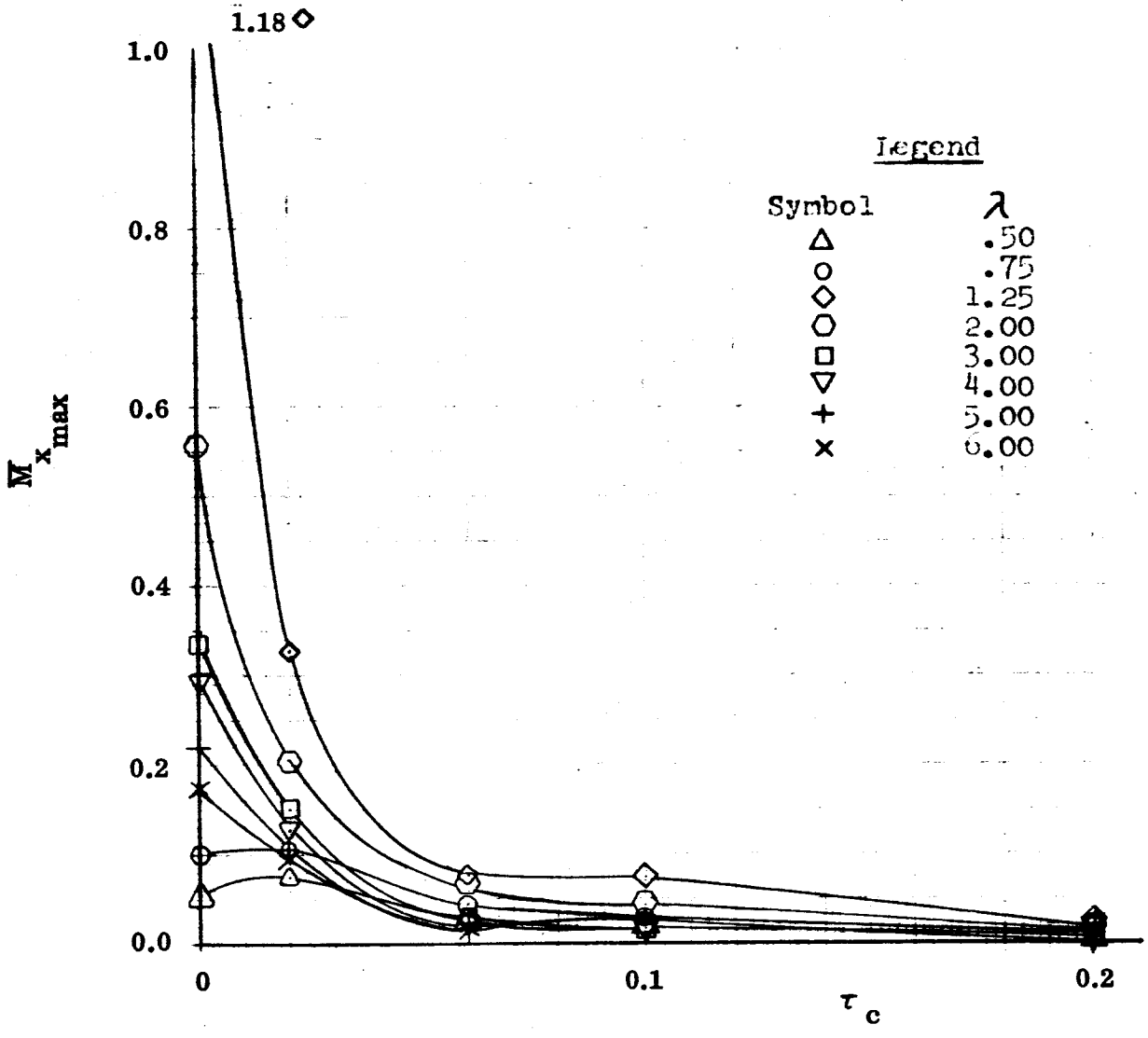

Figure V-8. Maximum Bending Moment versus τ_c, Ramp Pressure, Simple Supports, $\beta = 10^5$, $\alpha = 0$

TABLE 5. RAMP PRESSURE, SIMPLE SUPPORTS, $\alpha = 0$, $\tau_c = 0.02$

λ \ β	10^3	N	10^4	N	4×10^4	N	10^5	N
0.50	1.2129	50	1.1546	100	1.0641	150	1.0078	200
0.75	1.5614	50	1.3840	100	1.1590	150	1.0566	200
1.25	2.3849	70	2.4171	100	2.0589	150	1.5338	200
2.00	2.2032	70	2.0824	100	1.9176	250	1.6843	350
3.00	1.9781	80	2.0654	110	1.9449	300	1.7675	375
4.00	2.0559	80	2.0382	125	1.9515	300	1.8260	400
5.00	2.0671	80	2.0242	150	1.9497	325	1.8568	425
6.00	2.0554	80	2.0200	200	1.9722	350	1.8777	450

(a) Maximum Deflection

λ \ β	10^3	N	10^4	N	4×10^4	N	10^5	N
0.50	0.2616	50	0.2384	100	0.1487	150	-0.0775	200
0.75	0.6344	50	0.4272	100	-0.2452	150	0.1059	200
1.25	0.9274	70	0.8678	100	0.6068	150	0.3626	200
2.00	0.6688	70	0.4434	100	0.3022	250	-0.2050	350
3.00	0.4018	80	-0.2676	110	0.2234	300	0.1503	375
4.00	-0.3007	80	0.1996	125	-0.1653	300	0.1251	400
5.00	-0.2970	80	-0.1454	150	-0.1215	325	0.1072	425
6.00	-0.2350	80	-0.1302	200	-0.1128	350	0.0955	450

(b) Maximum Bending Moment

TABLE 6. RAMP PRESSURE, SIMPLE SUPPORTS, $\alpha = 0$, $\tau_c = 0.06$

λ \ β	10^2	N	10^3	N	10^4	N	4×10^4	N	10^5	N
0.50	1.3477	25	1.1876	50	1.0513	100	1.0212	150	1.0045	200
0.75	1.5981	25	1.4784	50	1.0805	100	1.0310	150	1.0209	200
1.25	1.9415	25	2.2841	70	1.5945	100	1.3273	150	1.1100	200
2.00	1.9273	25	2.1180	70	1.7169	100	1.0257	250	1.2176	350
3.00	1.8203	50	1.9489	80	1.8200	110	1.2580	300	1.1853	375
4.00	1.4971	50	2.0310	80	1.8442	125	1.4005	300	1.0738	400
5.00	1.2703	50	2.0463	80	1.8782	150	1.5017	325	1.0460	425
6.00	1.0762	50	2.0444	80	1.8950	200	1.5717	350	1.1411	450

(a) Maximum Deflection

λ \ β	10^2	N	10^3	N	10^4	N	4×10^4	N	10^5	N
0.50	0.3668	25	0.2112	50	0.0874	100	0.0433	150	0.0266	200
0.75	0.4529	25	0.5395	50	0.1164	100	0.0634	150	0.0422	200
1.25	0.5408	25	0.7840	70	0.3118	100	0.2294	150	-0.0793	200
2.00	0.4649	25	0.4949	70	0.2204	100	0.0516	250	-0.0671	350
3.00	0.3694	50	0.2806	80	0.1658	110	0.0530	300	-0.0382	375
4.00	0.2997	50	0.1940	80	0.1411	125	0.0584	300	-0.0235	400
5.00	0.2658	50	0.1524	80	0.1121	150	0.0571	325	-0.0182	425
6.00	0.2487	50	0.1136	80	0.1042	200	0.0537	350	-0.0192	450

(b) Maximum Bending Moment

λ \ β	10^2	N	10^3	N	10^4	N	4×10^4	N
0.50	-0.0386	25	0.0513	50	-0.0096	100	-0.0024	150
0.75	-0.0116	25	-0.3325	50	-0.0688	100	-0.0350	150
1.25	-0.1391	25	-0.4265	70	0.4173	100	0.6498	150
2.00	-0.1409	25	-0.0468	70	0.2741	100	0.1479	250
3.00	-0.0860	50	-0.0725	80	0.2215	110	0.7434	300
4.00	-0.1365	50	-0.0012	80	0.2222	125		
5.00	0.1105	50	0.1002	80	0.1308	150		
6.00	0.1896	50	0.3675	80	0.1041	200		

(c) Deflection Corresponding to the Maximum Bending Moment

λ \ β	10^2	N	10^3	N	10^4	N	4×10^4	N
0.50	-0.2567	25	-0.1307	50	-0.0578	100	-0.0085	150
0.75	-0.3399	25	-0.4965	50	-0.0665	100	-0.0591	150
1.25	-0.5794	25	-0.7226	70	-0.3222	100	-0.1744	150
2.00	-0.2254	25	-0.3637	70	-0.2197	100	-0.0247	250
3.00	-0.3791	50	-0.1015	80	-0.1740	110	-0.0493	300
4.00	-0.0650	50	-0.1916	80	-0.1019	125		
5.00	-0.1612	50	-0.1882	80	-0.1118	150		
6.00	-0.1076	50	-0.1648	80	-0.1004	200		

(d) Bending Moment Corresponding to the Maximum Deflection

TABLE 7. RAMP PRESSURE, SIMPLE SUPPORTS, $\alpha = 0$ $\tau_c = 0.1$

λ \ β	10^2	N	10^3	N	10^4	N	4×10^4	N	10^5	N
0.50	1.3368	25	1.1408	50	1.0284	100	1.0100	150	1.0014	200
0.75	1.5853	25	1.3507	50	1.0757	100	1.0242	150	1.0131	200
1.25	1.9243	25	2.1000	70	1.1903	100	1.1595	150	1.1285	200
2.00	1.9200	25	2.0664	70	1.2273	100	1.1882	250	1.1267	350
3.00	1.7421	50	1.9099	80	1.4414	110	1.2108	300	1.0420	375
4.00	1.4250	50	1.9913	80	1.5623	125	1.1184	300	1.1114	400
5.00	1.1978	50	2.0163	80	1.6378	150	1.0170	325	1.1913	425
6.00	1.0025	50	2.0190	80	1.6913	200	1.0869	350	1.2195	450

(a) Maximum Deflection

λ \ β	10^2	N	10^3	N	10^4	N	4×10^4	N	10^5	N
0.50	0.3358	25	0.1626	50	0.0508	100	0.0247	150	0.0155	200
0.75	0.4358	25	0.3901	50	0.0740	100	0.0408	150	0.0242	200
1.25	0.5109	25	0.5662	70	0.1346	100	0.1220	150	0.0735	200
2.00	0.4474	25	0.3908	70	0.0857	100	0.0602	250	0.0416	350
3.00	0.3601	50	0.2052	80	0.0796	110	0.0396	300	0.0137	375
4.00	0.2894	50	0.1685	80	0.0775	125	0.0218	300	0.0172	400
5.00	0.2517	50	0.1391	80	0.734	150	0.0172	325	0.0213	425
6.00	0.2324	50	0.1036	80	0.0707	200	0.0151	350	0.212	450

(b) Maximum Bending Moment

λ \ β	10^2	N	10^3	N	10^4	N	4×10^4	N	10^5	N
0.5	-0.0268	25	-0.0143	50	-0.0001	100	0.0001	150	0.0002	200
0.75	-0.1032	25	-0.2496	50	-0.0405	100	-0.0243	150	-0.0135	200
1.25	-0.1422	25	-0.1524	70	0.8246	100	0.8198	150	0.8723	200
2.00	-0.1233	25	-0.0694	70	0.0772	100	0.8126	250	0.8708	350
3.00	-0.0719	50	-0.0048	80	0.5685	110	0.7912	300	0.5206	375
4.00	0.0354	50	-0.1040	80	0.4609	125	0.8803	300	0.8921	400
5.00	0.0964	50	-0.1282	80	0.3679	150	0.0475	325	0.8187	425
6.00	0.1932	50	0.3847	80	0.3063	200	0.1281	350	0.7952	450

(c) Deflection Corresponding to the Maximum Bending Moment

λ \ β	10^2	N	10^3	N	10^4	N	4×10^4	N	10^5	N
0.50	-0.2508	25	-0.1276	50	-0.3390	100	-0.0036	150	-0.0004	200
0.75	-0.3351	25	-0.3495	50	-0.0629	100	-0.0408	150	-0.0023	200
1.25	-0.5587	25	-0.6016	70	-0.1093	100	-0.0847	150	-0.0746	200
2.00	-0.2666	25	-0.3621	70	-0.0687	100	-0.0527	250	-0.0363	350
3.00	-0.3113	50	-0.1073	80	-0.0776	110	-0.0326	300	-0.0104	375
4.00	-0.0950	50	-0.1616	80	-0.0669	125	-0.0180	300	-0.0169	400
5.00	-0.1554	50	-0.1765	80	-0.0710	150	-0.0074	325	-0.0196	425
6.00	-0.0384	50	-0.1636	80	-0.0620	200	-0.0111	350	-0.0204	450

(d) Bending Moment Corresponding to the Maximum Deflection

TABLE 8. RAMP PRESSURE, SIMPLE SUPPORTS, $\alpha = 0$ $\tau_c = 0.2$

λ \ β	10^2	N	10^3	N	10^4	N	4×10^4	N	10^5	N
0.50	1.2889	25	1.0457	50	1.0162	100	1.0064	150	1.0009	200
0.75	1.5270	25	1.0776	50	1.0349	100	1.0133	150	1.0065	200
1.25	1.7870	25	1.4547	70	1.1623	100	1.1010	150	1.0280	200
2.00	1.8244	25	1.7056	70	1.1948	100	1.0842	250	1.0405	350
3.00	1.5343	50	1.7344	80	1.2129	110	1.1145	300	1.0408	375
4.00	1.2322	50	1.8287	80	1.1202	125	1.1091	300	1.0865	400
5.00	1.0061	50	1.8784	80	1.0180	150	1.0131	325	1.0592	425
6.00	0.8317	50	1.9033	80	1.0890	200	1.0819	350	1.0290	450

(a) Maximum Deflection

λ \ β	10^2	N	10^3	N	10^4	N	4×10^4	N	10^5	N
0.50	0.3059	25	0.0816	50	0.0263	100	0.0133	150	0.0082	200
0.75	0.3582	25	0.1296	50	0.0367	100	0.0186	150	0.0121	200
1.25	0.4064	25	0.2008	70	0.0939	100	0.0528	150	0.0187	200
2.00	0.3970	25	0.2409	70	0.0609	100	0.0294	250	0.0132	350
3.00	0.3228	50	0.0887	80	0.0426	110	0.0236	300	0.0082	375
4.00	0.2675	50	0.0827	80	0.0223	125	0.0152	300	0.0128	400
5.00	0.2284	50	0.0735	80	0.0185	150	0.0085	325	0.0073	425
6.00	0.2049	50	0.0700	80	0.0173	200	0.0097	350	0.0046	450

(b) Maximum Bending Moment

λ \ β	10^2	N	10^3	N	10^4	N	4×10^4	N	10^5	N
0.50	-0.0014	25	0.0186	50	-0.0020	100	-0.0008	150	-0.0001	200
0.75	-0.0451	25	-0.0817	50	-0.0211	100	-0.0107	150	-0.0068	200
1.25	-0.0845	25	0.6012	70	0.8448	100	0.9020	150	0.9694	200
2.00	-0.0558	25	0.2860	70	0.8057	100	0.9150	250	0.9586	350
3.00	-0.0198	50	0.1120	80	0.7849	110	0.8919	300	0.9609	375
4.00	0.2587	50	0.4826	80	0.0579	125	0.8936	300	0.9151	400
5.00	0.0380	50	0.4639	80	0.0991	150	0.0238	325	0.9405	425
6.00	0.2431	50	0.3979	80	0.0767	200	0.9170	350	0.0469	450

(c) Deflection Corresponding to the Maximum Bending Moment

λ \ β	10^2	N	10^3	N	10^4	N	4×10^4	N	10^5	N
0.50	-0.2263	25	-0.0301	50	-0.0180	100	-0.0030	150	-0.0014	200
0.75	-0.3137	25	-0.0892	50	-0.0300	100	-0.0212	150	-0.0121	200
1.25	-0.4450	25	-0.2478	70	-0.0921	100	-0.0514	150	-0.0123	200
2.00	-0.3381	25	-0.2171	70	-0.0601	100	-0.0259	250	-0.0101	350
3.00	-0.2253	50	-0.0933	80	-0.0402	100	-0.0212	300	-0.0085	375
4.00	-0.1124	50	-0.1393	80	-0.0215	125	-0.0180	300	-0.0102	400
5.00	-0.0576	50	-0.1286	80	-0.0107	150	-0.0039	325	-0.0064	425
6.00	-0.0197	50	-0.1270	80	-0.0162	200	-0.0076	350	-0.0026	450

(d) Bending Moment Corresponding to the Maximum Deflection

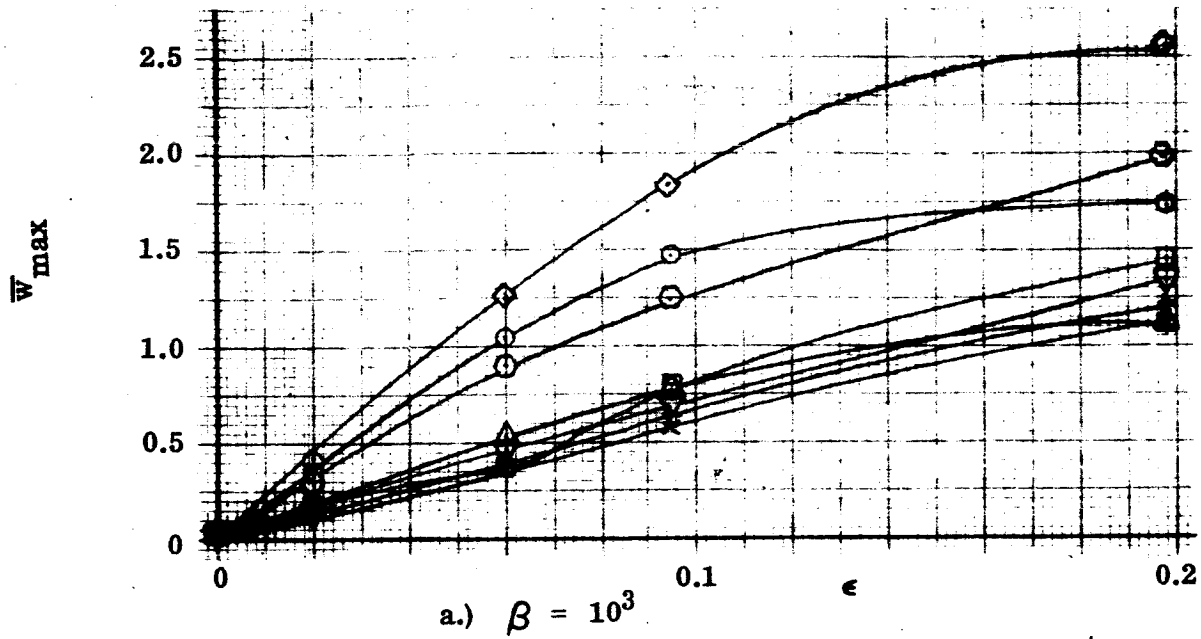

a.) $\beta = 10^3$

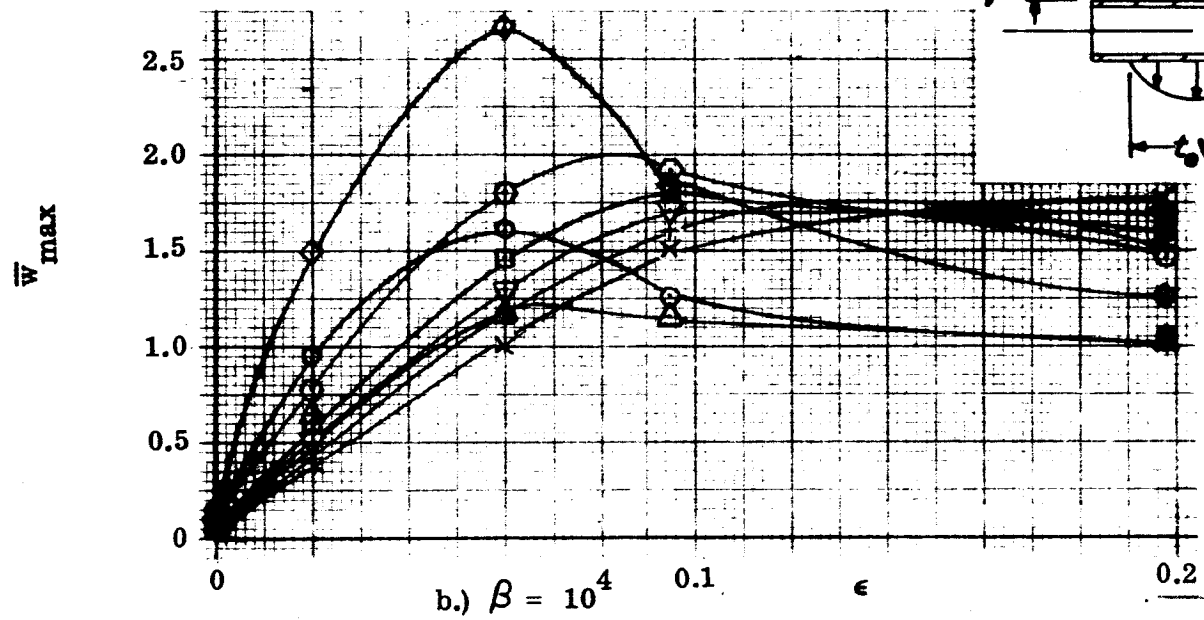

b.) $\beta = 10^4$

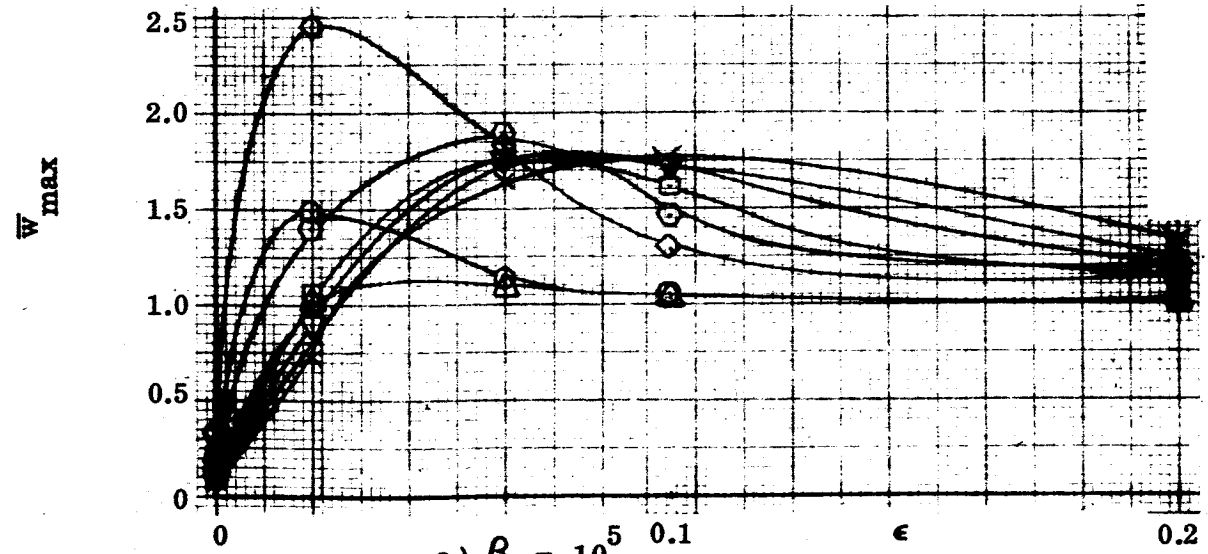

c.) $\beta = 10^5$

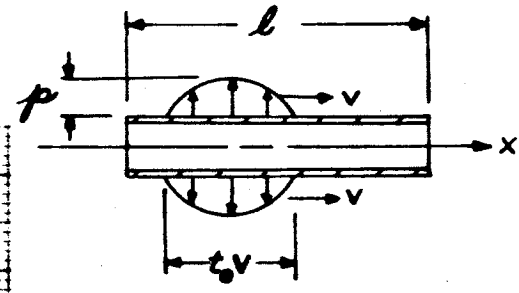

Legend

Symbol	λ
△	.50
○	.75
◇	1.25
⬡	2.00
□	3.00
▽	4.00
✦	5.00
×	6.00

Figure V-9. Maximum Deflection versus ϵ, Sinusoidal Pressure, Simple Supports, $a = 0$

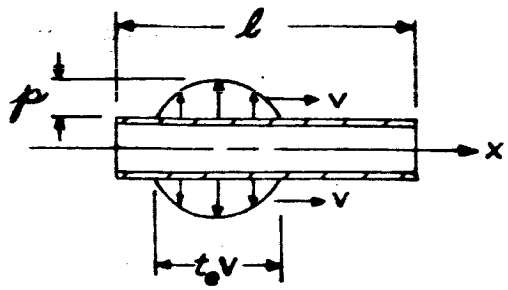

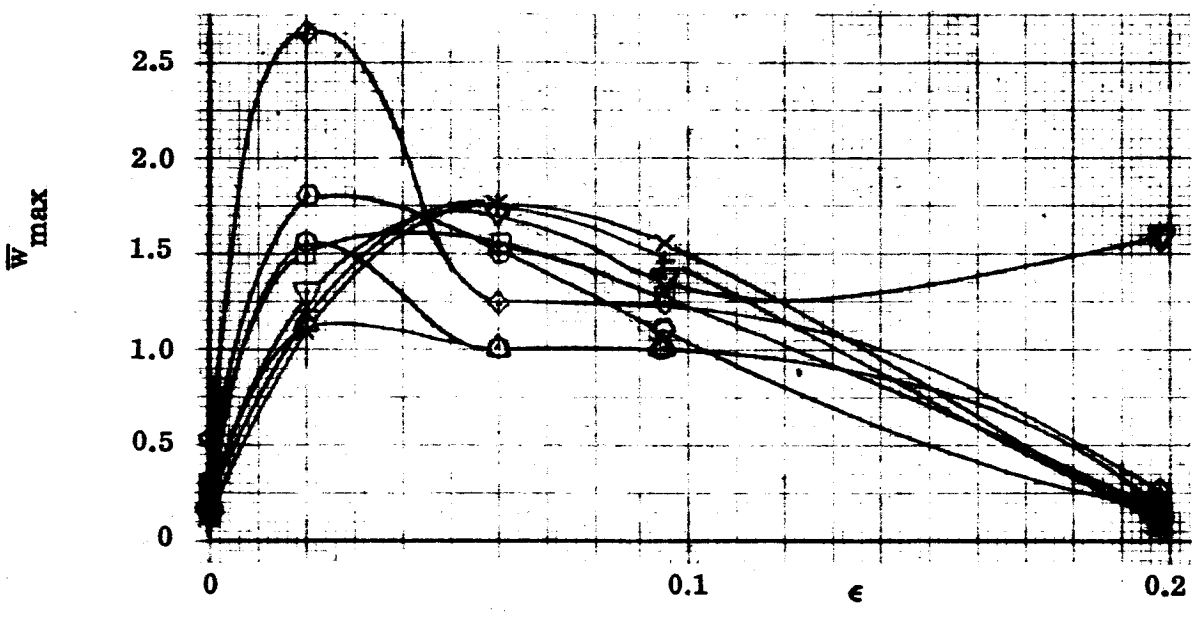

a.) $\beta = 4 \times 10^4$

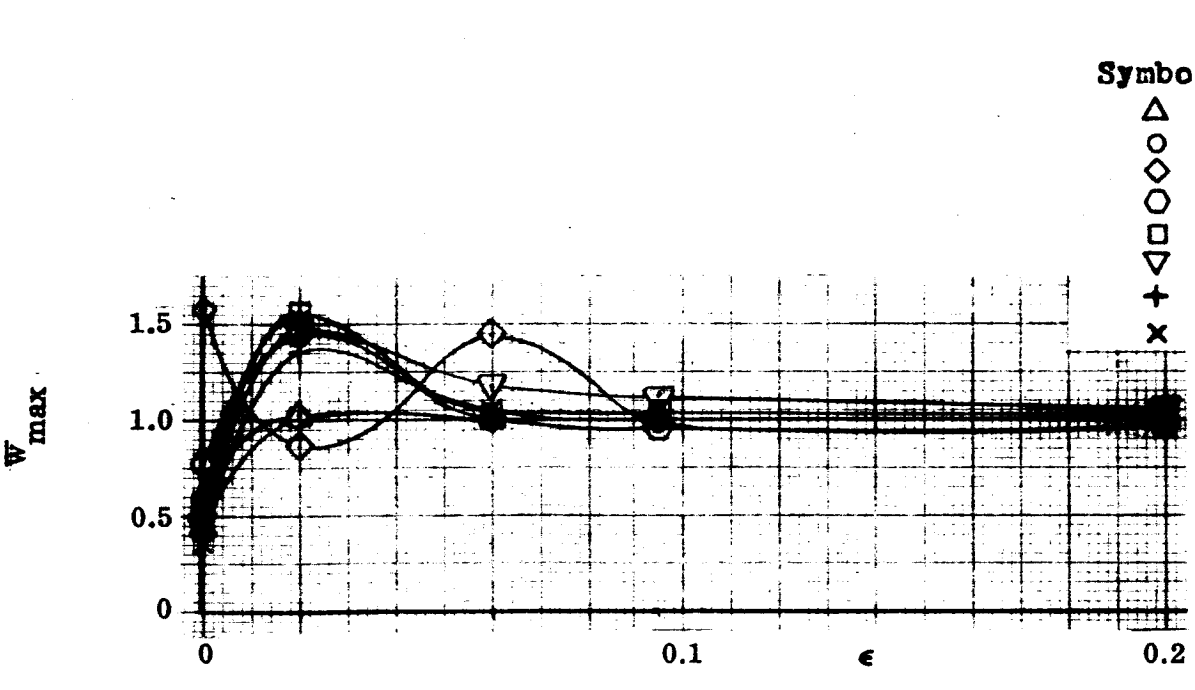

b.) $\beta = 10^6$

Legend

Symbol	λ
△	.50
○	.75
◇	1.25
⬡	2.00
□	3.00
▽	4.00
+	5.00
×	6.00

Figure V-10. Maximum Deflection versus ϵ Sinusoidal Pressure, Simple Supports, $\alpha = 0$

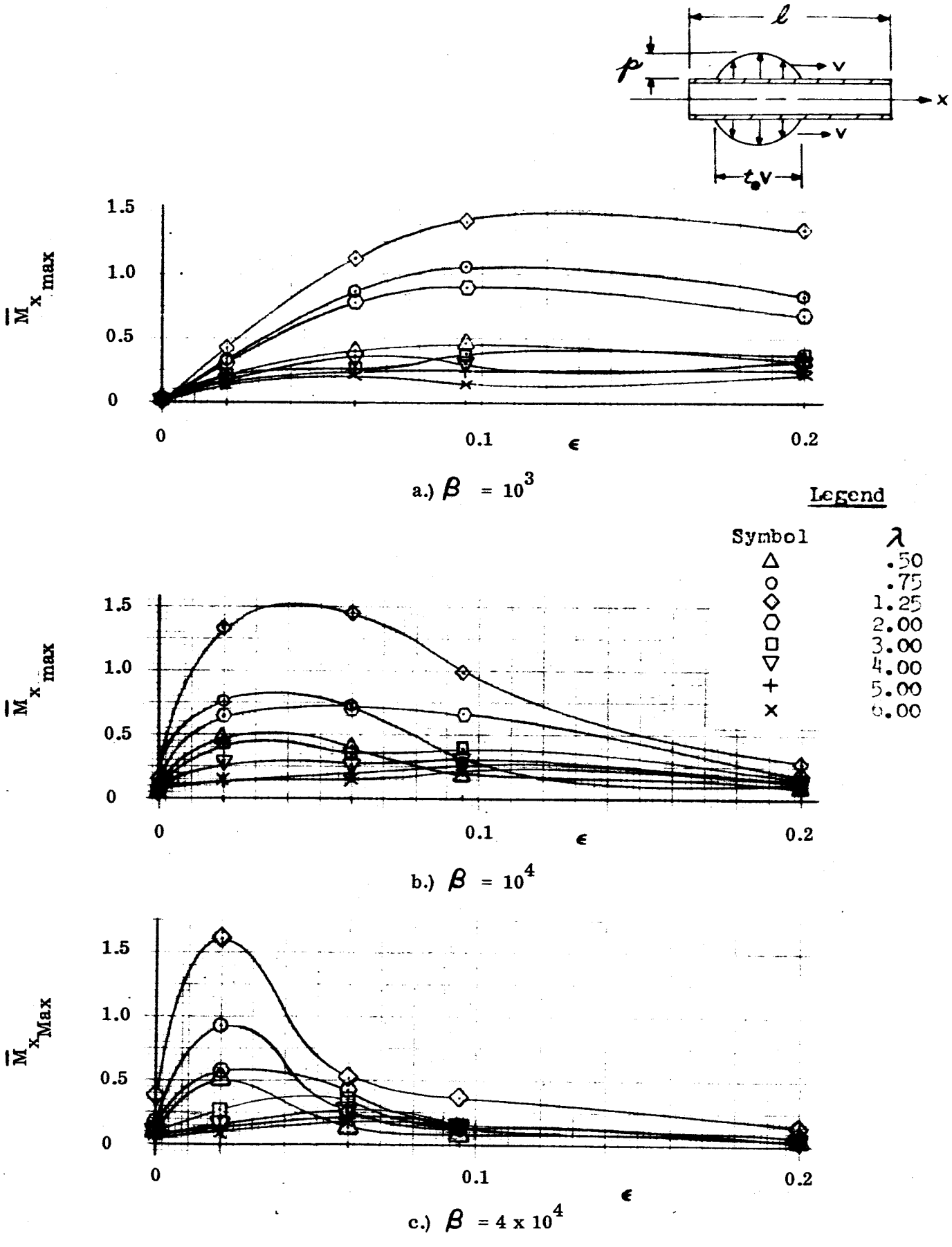

Figure V-11. Maximum Bending Moment Versus ϵ, Sinusoidal Pressure, Simple Supports, $\alpha = 0$

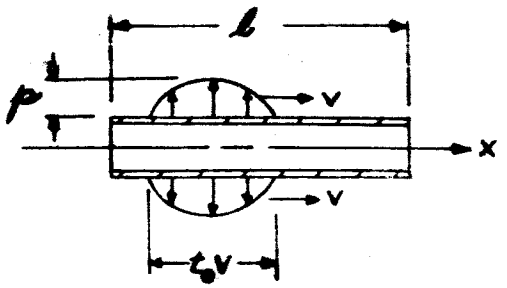

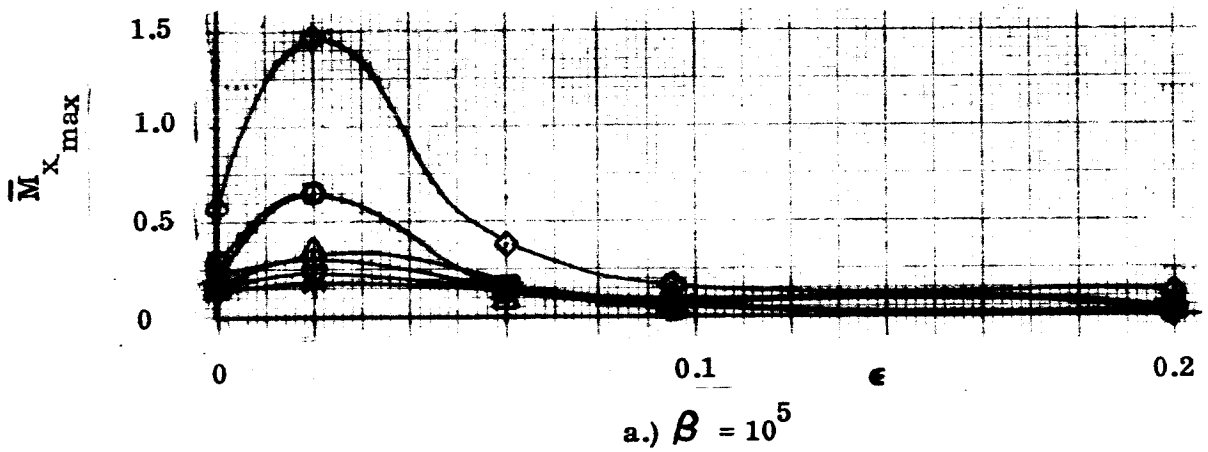

a.) $\beta = 10^5$

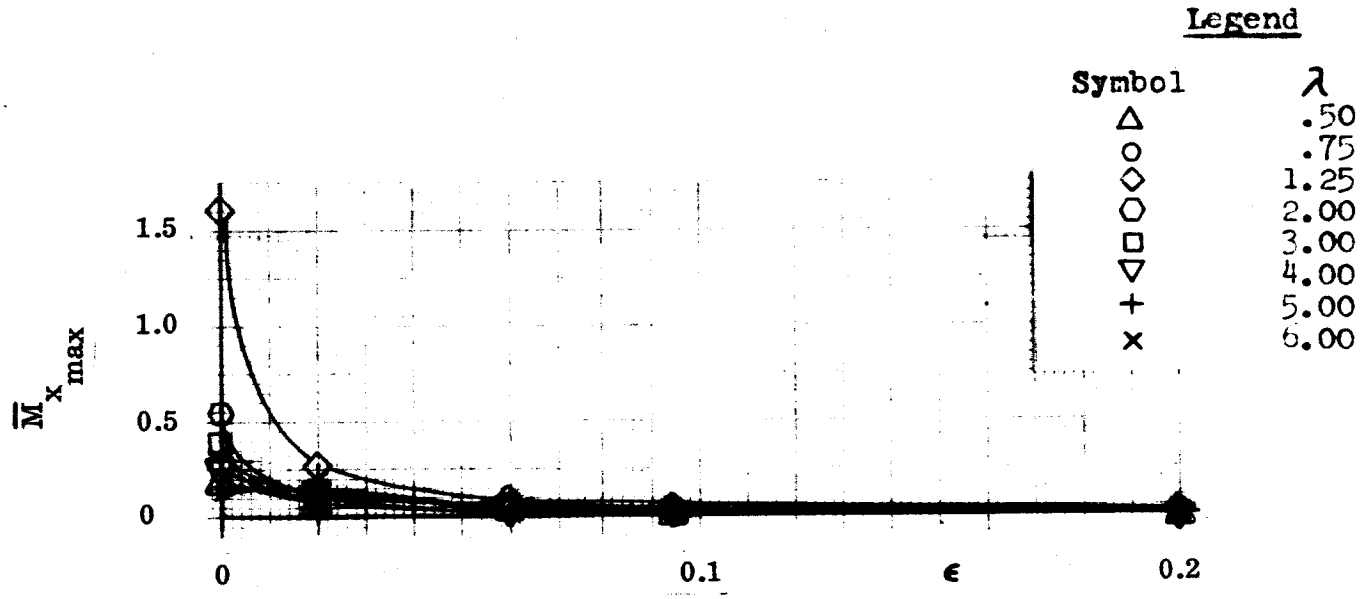

b.) $\beta = 10^6$

Figure V-12. Maximum Bending Moment Versus ϵ , Sinusoidal Pressure, Simple Supports , $\alpha = 0$

TABLE 9. SINUSOIDAL PRESSURE, SIMPLE SUPPORTS, $\alpha = 0$, $\epsilon = 0.00198$

λ \ β	10^2	N	10^3	N	10^4	N	4×10^4	N	10^5	N	10^6	N
0.50	0.0087	500	0.0194	500	0.0710	500	0.1332	500	0.1928	500	0.4408	500
0.75	0.0090	500	0.0373	500	0.1024	500	0.1999	500	0.2986	500	0.5872	500
1.25	0.0086	25	0.0431	70	-0.1631	100	0.3346	150	-0.5402	200	1.5756	700
2.00	0.0077	25	0.0320	70	-0.0925	100	0.1844	250	-0.2875	350	-0.7849	800
3.00	0.0068	50	-0.0186	80	0.0646	110	0.1269	300	-0.2012	375	0.5827	900
4.00	0.0061	50	0.0155	80	-0.0538	125	-0.1037	300	-0.1599	400	-0.4796	1000
5.00	0.0053	50	-0.0141	80	-0.0453	150	0.0904	325	0.1414	425	-0.4157	1100
6.00	0.0042	50	-0.0130	80	0.0399	200	-0.0779	350	0.1241	450	-0.3614	1200

(a) Maximum Deflection

λ \ β	10^2	N	10^3	N	10^4	N	4×10^4	N	10^5	N	10^6	N
0.50	-0.0082	500	-0.0204	500	-0.0653	500	-0.1108	500	-0.1435	500	-0.1824	500
0.75	-0.0078	500	-0.0363	500	-0.0941	500	-0.1784	500	-0.2438	500	-0.2925	500
1.25	-0.0066	25	+0.0122	70	+0.1542	100	-0.3725	150	+0.5779	200	-0.6133	700
2.00	+0.0077	25	-0.0322	70	+0.0877	100	-0.1858	250	-0.2877	350	+0.6482	800
3.00	+0.0067	50	0.0230	80	-0.0710	110	-0.1300	300	+0.2105	375	0.3959	900
4.00	-0.0071	50	0.0196	80	+0.0557	125	+0.1149	300	+0.1688	400	+0.2608	1000
5.00	-0.0060	50	+0.0169	80	-0.0350	150	-0.0961	325	+0.1405	425	+0.1693	1100
6.00	+0.0031	50	-0.0159	80	-0.0488	200	0.0821	350	-0.1316	450	0.1258	1200

(b) Maximum Bending Moment

λ \ β	10^2	N	10^3	N	10^4	N	4×10^4	N	10^5	N	10^6	N
0.50	0.0085	500	0.0190	500	0.0710	500	0.1333	500	0.1928	500	0.4408	500
0.75	0.0074	500	0.0373	500	0.1024	500	0.1999	500	0.2986	500	0.5872	500
1.25	0.0070	25	-0.0228	70	-0.1631	100	0.3346	150	-0.5252	200	1.5756	700
2.00	-0.0019	25	0.0320	70	-0.0925	100	0.1844	250	0.2686	350	-0.6500	800
3.00	-0.0015	50	-0.0122	80	0.0360	110	0.0731	300	-0.1707	375	-0.5503	900
4.00	0.0061	50	-0.0139	80	-0.0290	125	-0.0882	300	-0.1599	400	-0.4796	1000
5.00	0.0053	50	-0.0107	80	0.0265	150	0.0517	325	-0.0889	425	-0.4045	1100
6.00	0.0047	50	0.0058	80	0.0399	200	-0.0608	350	0.1216	450	-0.3716	1200

(c) Deflection Corresponding to the Maximum Bending Moment

λ \ β	10^2	N	10^3	N	10^4	N	4×10^4	N	10^5	N	10^6	N
0.50	-0.0076	500	-0.0154	500	-0.0653	500	-0.1108	500	-0.1435	500	-0.1824	500
0.75	-0.0048	500	-0.0363	500	-0.0941	500	-0.1785	500	-0.2438	500	-0.2925	500
1.25	-0.0050	25	-0.0232	70	0.1542	100	-0.3725	150	0.4844	200	-1.1633	700
2.00	-0.0051	25	-0.0322	70	0.0877	100	-0.1858	250	0.2674	350	0.6325	800
3.00	-0.0060	50	0.0136	80	-0.0561	110	0.1269	300	0.1957	375	0.5828	900
4.00	-0.0070	50	-0.0032	80	0.0491	125	0.0894	300	0.1687	400	0.2608	1000
5.00	-0.0060	50	0.0160	80	0.0335	150	-0.0787	325	-0.1206	425	0.1507	1100
6.00	-0.0055	50	0.0122	80	0.0488	200	0.0627	350	-0.0969	450	-0.1322	1200

(d) Bending Moment Corresponding to the Maximum Deflection

TABLE 10. SINUSOIDAL PRESSURE, SIMPLE SUPPORTS $\alpha = 0$, $\epsilon = 0.0198$

λ \ β	10^2	N	10^3	N	10^4	N	4×10^4	N	10^5	N	10^6	N
0.50	0.0869	500	0.1917	500	0.6528	500	1.0109	500	1.1476	500	1.0230	500
0.75	0.0902	500	0.3702	500	0.9577	500	1.4888	500	1.5681	500	1.0396	500
1.25	0.0856	25	0.4294	70	-1.4881	100	-2.4579	150	2.6745	200	0.8673	700
2.00	0.0771	25	0.3177	70	0.7892	100	1.3983	250	1.8051	350	1.4428	800
3.00	0.0680	50	-0.1848	80	0.6160	110	1.0565	300	1.5059	375	1.5654	900
4.00	0.0609	50	0.1553	80	-0.5043	125	-0.8963	300	1.3190	400	1.4850	1000
5.00	0.0529	50	-0.1397	80	-0.4247	150	0.8035	325	-1.1938	425	1.3608	1100
6.00	0.0474	50	-0.1271	80	0.3853	200	-0.7286	350	-1.1004	450	-1.5172	1200

(a) Maximum Deflection

λ \ β	10^2	N	10^3	N	10^4	N	4×10^4	N	10^5	N	10^6	N
0.50	0.0807	500	-0.1857	500	-0.4762	500	-0.5135	500	-0.3589	500	+0.0758	500
0.75	-0.0772	500	-0.3417	500	-0.7588	500	-0.9254	500	-0.6598	500	+0.1095	500
1.25	-0.0659	25	+0.4186	70	+1.3379	100	+1.5998	150	-1.4665	200	0.2722	700
2.00	0.0768	25	-0.3119	70	0.6454	100	-0.5859	250	-0.6487	350	-0.1311	800
3.00	0.0670	50	0.2169	80	-0.4294	110	0.2689	300	-0.3191	375	0.1054	900
4.00	-0.0704	50	0.1895	80	0.2982	125	0.1596	300	-0.2314	400	0.1533	1000
5.00	-0.0591	50	0.1619	80	0.1390	150	0.1445	325	0.1780	425	0.1482	1100
6.00	-0.0544	50	-0.1463	80	-0.1654	200	-0.0992	350	-0.1379	450	0.1336	1200

(b) Maximum Bending Moment

λ \ β	10^2	N	10^3	N	10^4	N	4×10^4	N	10^5	N	10^6	N
0.50	0.0851	500	0.1890	500	0.6528	500	1.0109	500	1.1476	500	-0.0147	500
0.75	0.0744	500	0.3702	500	0.9577	500	1.4888	500	1.5681	500	-0.0720	500
1.25	0.0705	25	-0.2223	70	-0.1488	100	-2.4579	150	2.5927	200	-0.5006	700
2.00	-0.0189	25	0.3177	70	-0.6316	100	0.9696	250	1.7733	350	0.3187	800
3.00	-0.0149	50	-0.1351	80	0.6160	110	0.0958	300	1.4933	375	-0.5395	900
4.00	0.0609	50	-0.1389	80	-0.4496	125	-0.8963	300	1.3190	400	-1.0526	1000
5.00	0.0530	50	-0.1075	80	0.0072	150	0.0668	325	-1.1778	425	-1.3399	1100
6.00	0.0474	50	0.0557	80	0.3716	200	0.7079	350	1.0904	450	-1.5168	1200

(c) Deflection Corresponding to the Maximum Bending Moment

λ \ β	10^2	N	10^3	N	10^4	N	4x10	N	10^5	N	10^6	N
0.50	-0.0757	500	-0.1471	500	-0.4762	500	-0.5135	500	-0.3589	500	-0.0247	500
0.75	-0.0475	500	-0.3417	500	-0.7588	500	-0.9254	500	-0.6598	500	-0.0307	500
1.25	-0.0526	25	-0.2324	70	1.3379	100	1.5998	150	-1.3971	200	0.0257	700
2.00	-0.0506	25	-0.3119	70	-0.4978	100	-0.5247	250	-0.5427	350	-0.1252	800
3.00	-0.0592	50	0.1291	80	-0.4294	110	-0.2349	300	-0.2977	375	-0.0869	900
4.00	-0.0701	50	-0.0343	80	0.2885	125	0.1596	300	0.2314	400	-0.0710	1000
5.00	-0.0591	50	0.1448	80	0.1273	150	-0.0819	325	0.1405	425	-0.0366	1100
6.00	-0.0544	50	0.0896	80	-0.0408	200	0.0858	350	0.1282	450	0.1255	1200

(d) Bending Moment Corresponding to the Maximum Deflection

TABLE 11. SINUSOIDAL PRESSURE, SIMPLE SUPPORTS, $\alpha = 0$, $\epsilon = 0.06$

λ \ β	10^2	N	10^3	N	10^4	N	4×10^4	N	10^5	N	10^6	N
0.50	0.2608	500	0.5447	500	1.1766	500	1.0855	500	1.0271	500	1.0022	500
0.75	0.2718	500	1.0424	500	1.6199	500	1.1200	500	1.0573	500	1.0060	500
1.25	0.2582	25	1.2557	70	2.6721	100	1.8256	150	1.2434	200	0.9246	700
2.00	0.2324	25	0.9016	70	1.8207	100	1.8157	250	1.5012	350	0.9938	800
3.00	0.1449	50	-0.3753	80	1.4741	110	1.7568	300	1.5433	375	1.0349	900
4.00	0.1831	50	0.4673	80	-1.3072	125	-1.7694	300	1.6992	400	1.1683	1000
5.00	0.1535	50	0.4152	80	-1.1721	150	1.7417	325	1.7506	425	1.0471	1100
6.00	0.1424	50	0.3779	80	1.0947	200	-1.6608	350	1.7179	450	1.0518	1200

(a) Maximum Deflection

λ \ β	10^2	N	10^3	N	10^4	N	4×10^4	N	10^5	N	10^6	N
0.50	-0.2334	500	-0.4020	500	-0.4016	500	0.1333	500	0.0842	500	0.0253	500
0.75	-0.2245	500	-0.8364	500	-0.7319	500	0.2305	500	0.1323	500	0.0358	500
1.25	-0.1973	25	1.1238	70	1.4603	100	-0.5107	150	-0.3776	200	0.0907	700
2.00	0.2240	25	-0.7859	70	-0.7049	100	0.4824	250	-0.1279	350	-0.0627	800
3.00	-0.1265	50	0.2829	80	-0.3526	110	-0.3421	300	-0.1335	375	0.0501	900
4.00	-0.2014	50	0.3662	80	0.2596	125	-0.2727	300	0.1629	400	-0.0230	1000
5.00	0.1582	50	0.2628	80	-0.1904	150	0.2141	325	0.1562	425	0.0400	1100
6.00	-0.1516	50	-0.2059	80	-0.1647	200	0.1781	350	0.1457	450	0.0274	1200

(b) Maximum Bending moment

λ \ β	10^2	N	10^3	N	10^4	N	4×10^4	N	10^5	N	10^6	N
0.50	0.2599	500	0.5302	500	1.1766	500	0.0070	500	-0.0006	500	-0.0006	500
0.75	0.2351	500	1.0396	500	1.6199	500	-0.1349	500	-0.0738	500	-0.0187	500
1.25	0.1999	25	-0.6264	70	-2.6110	100	1.8256	150	0.6575	200	-0.1730	700
2.00	-0.0553	25	0.9016	70	1.8207	100	-1.5287	250	1.5011	350	0.2217	800
3.00	-0.0439	50	-0.3695	80	1.4157	110	1.7326	300	0.6854	375	-0.2580	900
4.00	0.1831	50	-0.3879	80	-1.3072	125	1.6684	300	-1.1734	400	1.1683	1000
5.00	-0.0225	50	-0.2994	80	1.0594	150	-1.7165	325	-1.4149	425	-0.3419	1100
6.00	0.1424	50	0.1471	80	1.0203	200	-1.6492	350	-1.5724	450	-0.2811	1200

(c) Deflection Corresponding to the Maximum Bending Moment

λ \ β	10^2	N	10^3	N	10^4	N	4×10^4	N	10^5	N	10^6	N
0.50	-0.2257	500	-0.3822	500	-0.4016	500	-0.0764	500	-0.0290	500	-0.0023	500
0.75	-0.1423	500	-0.8238	500	-0.7319	500	-0.0538	500	-0.0478	500	-0.0043	500
1.25	-0.1585	25	-0.7109	70	-1.4568	100	-0.5107	150	-0.1512	200	0.0569	700
2.00	-0.1466	25	-0.7859	70	-0.7049	100	-0.2899	250	-0.1279	350	-0.0054	800
3.00	-0.1750	50	0.2542	80	-0.3269	110	-0.2038	300	-0.0853	375	-0.0049	900
4.00	-0.2014	50	-0.1134	80	0.2596	125	0.2671	300	-0.1030	400	-0.0230	1000
5.00	-0.1331	50	-0.0976	80	0.1890	150	-0.2021	325	-0.0989	425	-0.0052	1100
6.00	-0.1516	50	-0.0866	80	-0.1593	200	0.1485	350	-0.0777	450	-0.0161	1200

(d) Bending Moment Corresponding to the Maximum Deflection

TABLE 12. SINUSOIDAL PRESSURE, SIMPLE SUPPORTS, $\alpha = 0$, $\epsilon = 0.0945$

λ \ β	10^2	N	10^3	N	10^4	N	$4x10^4$	N	10^5	N	10^6	N
0.50	0.4038	500	0.7761	500	1.1535	500	1.0270	500	1.0109	500	0.9967	500
0.75	0.4248	500	1.4739	500	1.2892	500	1.0543	500	1.0222	500	0.9985	500
1.25	0.4035	25	1.8482	70	1.8401	100	1.2885	150	1.2474	200	1.0468	700
2.00	0.3629	25	1.2453	70	-1.9299	100	1.4647	250	1.1087	350	0.9524	800
3.00	0.3198	50	0.8036	80	-1.8270	110	1.6121	300	1.2824	375	1.0407	900
4.00	0.2849	50	0.7280	80	-1.7176	125	1.7178	300	1.3871	400	1.0864	1000
5.00	+0.2394	50	0.6434	80	-1.6090	150	1.7133	325	1.4766	425	1.0268	1100
6.00	0.2218	50	0.5871	80	1.5195	200	1.7711	350	1.5647	450	1.0814	1200

(a) Maximum Deflection

λ \ β	10^2	N	10^3	N	10^4	N	$4x10^4$	N	10^5	N	10^6	N
0.50	-0.3457	500	-0.4617	500	0.1852	500	-0.0856	500	0.0532	500	0.0160	500
0.75	-0.3341	500	-1.0613	500	0.2831	500	0.1262	500	+0.0761	500	0.0220	500
1.25	-0.3036	25	1.3991	70	-0.9812	100	-0.3604	150	-0.1676	200	-0.0455	700
2.00	0.3333	25	-0.8969	70	-0.6712	100	-0.1414	250	-0.0872	350	0.0367	800
3.00	0.2939	50	0.3894	80	0.3951	110	-0.1493	300	-0.1072	375	0.0257	900
4.00	-0.2920	50	0.3091	80	0.3150	125	-0.1641	300	+0.0581	400	-0.0139	1000
5.00	0.2239	50	0.2452	80	0.2429	150	-0.1568	325	-0.0496	425	-0.0179	1100
6.00	-0.2106	50	0.1351	80	-0.2152	200	0.1470	350	-0.0441	450	0.0112	1200

(b) Maximum Bending Moment

λ \ β	10^2	N	10^3	N	10^4	N	$4x10^4$	N	10^5	N	10^6	N
0.50	0.4036	500	0.7673	500	-0.0059	500	-0.0010	500	-0.0002	500	-0.0002	500
0.75	0.3694	500	1.4739	500	-0.1513	500	-0.0652	500	-0.0399	500	-0.0111	500
1.25	0.3167	25	-0.7645	70	1.6593	100	0.5818	150	0.8674	200	0.5489	700
2.00	-0.0857	25	1.2453	70	1.8087	100	1.4245	250	1.1087	350	-0.1072	800
3.00	-0.0657	50	-0.0330	80	-1.8270	110	0.7220	300	0.5599	375	-0.1269	900
4.00	0.2849	50	-0.0303	80	-1.6840	125	1.1498	300	-0.3839	400	0.0819	1000
5.00	-0.0327	50	0.0094	80	-1.6090	150	1.4476	325	1.4766	425	0.1654	1100
6.00	0.2218	50	0.0566	80	1.5195	200	-1.5696	350	1.5647	450	-0.1031	1200

(c) Deflection Corresponding to the Maximum Bending Moment

λ \ β	10^2	N	10^3	N	10^4	N	$4x10^4$	N	10^5	N	10^6	N
0.50	-0.3361	500	-0.4386	500	-0.1746	500	-0.0325	500	-0.0142	500	-0.0010	500
0.75	-0.2329	500	-1.0613	500	-0.2057	500	-0.0492	500	-0.0201	500	-0.0021	500
1.25	-0.2433	25	-1.0748	70	-0.2869	100	-0.1946	150	-0.1547	200	-0.0280	700
2.00	-0.2213	25	-0.8969	70	0.5915	100	-0.1096	250	-0.0872	350	+0.0152	800
3.00	-0.2682	50	-0.1215	80	0.3951	110	-0.1156	300	-0.0501	375	-0.0112	900
4.00	-0.2920	50	-0.1863	80	0.2612	125	-0.1030	300	-0.0497	400	-0.0101	1000
5.00	-0.1887	50	-0.1502	80	0.2429	150	-0.0874	325	-0.0496	425	-0.0048	1100
6.00	-0.2106	50	-0.1267	80	-0.2152	200	-0.0898	350	-0.0441	450	-0.0092	1200

(d) Bending Moment Corresponding to the Maximum Deflection

TABLE 13. SINUSOIDAL PRESSURE SIMPLE SUPPORTS $\alpha = 0$, $\epsilon = 0.198$

λ \ β	10^2	N	10^3	N	10^4	N	4×10^4	N	10^5	N	10^6	N
0.50	0.7789	500	1.1226	500	1.0318	500	1.0084	500	1.0022	500	1.0004	500
0.75	0.8523	500	1.7293	500	1.0507	500	1.0179	500	1.0056	500	1.0003	500
1.25	0.8062	25	2.5263	70	1.2607	100	1.1486	150	1.0541	200	0.9735	700
2.00	0.7313	25	-1.9883	70	1.4870	100	1.1714	250	1.0767	350	0.9748	800
3.00	0.6383	50	1.4659	80	1.6258	110	1.1193	300	1.0952	375	1.0228	900
4.00	0.5427	50	1.3594	80	1.6967	125	1.1712	300	1.1611	400	1.0418	1000
5.00	0.4821	50	1.2309	80	1.7447	150	1.2701	325	1.1739	425	1.0089	1100
6.00	0.4309	50	1.1390	80	1.7682	200	1.3327	350	1.1548	450	1.0384	1200

(a) Maximum Deflection

λ \ β	10^2	N	10^3	N	10^4	N	4×10^4	N	10^5	N	10^6	N
0.50	-0.5756	500	-0.3311	500	0.0848	500	0.0404	500	0.0257	500	0.0075	500
0.75	0.5795	500	-0.7794	500	0.1342	500	0.0614	500	0.0373	500	0.0105	500
1.25	-0.5293	25	-1.3512	70	-0.2699	100	-0.1324	150	0.1161	200	-0.0286	700
2.00	0.5275	25	0.6866	70	-0.1726	100	-0.0799	250	-0.0589	350	-0.0131	800
3.00	0.4628	50	0.3684	80	-0.1284	110	-0.0503	300	0.0431	375	-0.0150	900
4.00	0.3707	50	-0.3149	80	1.6147	125	-0.0518	300	-0.0238	400	-0.0095	1000
5.00	0.3077	50	-0.2580	80	-0.1567	150	0.0609	325	-0.0332	425	0.0110	1100
6.00	0.2623	50	-0.2193	80	0.1463	200	-0.0474	350	-0.0317	450	0.0089	1200

(b) Maximum Bending Moment

λ \ β	10^2	N	10^3	N	10^4	N	4×10^4	N	10^5	N	10^6	N
0.50	0.7789	500	1.1226	500	-0.0049	500	0.0001	500	0.0005	500	0.0	500
0.75	-0.4988	500	1.7180	500	-0.0760	500	-0.0341	500	-0.0205	500	-0.0053	500
1.25	0.6855	25	2.5263	70	1.1149	100	1.1486	150	-0.2065	200	0.0446	700
2.00	-0.1370	25	-1.9778	70	1.4870	100	0.2373	250	-0.1853	350	0.0387	800
3.00	-0.1055	50	1.4168	80	1.6258	110	1.1193	300	-0.2329	375	-0.0778	900
4.00	-0.0666	50	1.2861	80	-1.0280	125	0.3451	300	0.7491	400	0.0660	1000
5.00	-0.0435	50	1.2228	80	1.3452	150	-0.5424	325	0.2863	425	-0.1014	1100
6.00	-0.0326	50	1.1030	80	-1.5233	200	0.5062	350	0.3342	450	-0.1009	1200

(c) Deflection Corresponding to the Maximum Bending Moment

λ \ β	10^2	N	10^3	N	10^4	N	4×10^4	N	10^5	N	10^6	N
0.50	-0.5756	500	-0.3311	500	-0.0318	500	-0.0079	500	-0.0021	500	-0.0004	500
0.75	-0.4849	500	-0.7774	500	-0.0377	500	-0.0145	500	-0.0046	500	-0.0002	500
1.25	-0.4397	25	-1.3512	70	-0.1452	100	-0.1324	150	-0.0517	200	0.0020	700
2.00	-0.3748	25	0.6846	70	-0.1726	100	-0.0581	250	-0.0220	350	0.0079	800
3.00	-0.4098	50	-0.3057	80	-0.1285	110	-0.0503	300	-0.0212	375	-0.0029	900
4.00	-0.3269	50	-0.2765	80	-0.0997	125	-0.0346	300	-0.0187	400	-0.0046	1000
5.00	-0.2409	50	-0.2547	80	-0.1008	150	-0.0310	325	-0.0191	425	-0.0024	1100
6.00	-0.1563	50	-0.2087	80	-0.0962	200	-0.0289	350	-0.0181	450	-0.0032	1200

(d) Bending Moment Corresponding to the Maximum Deflection

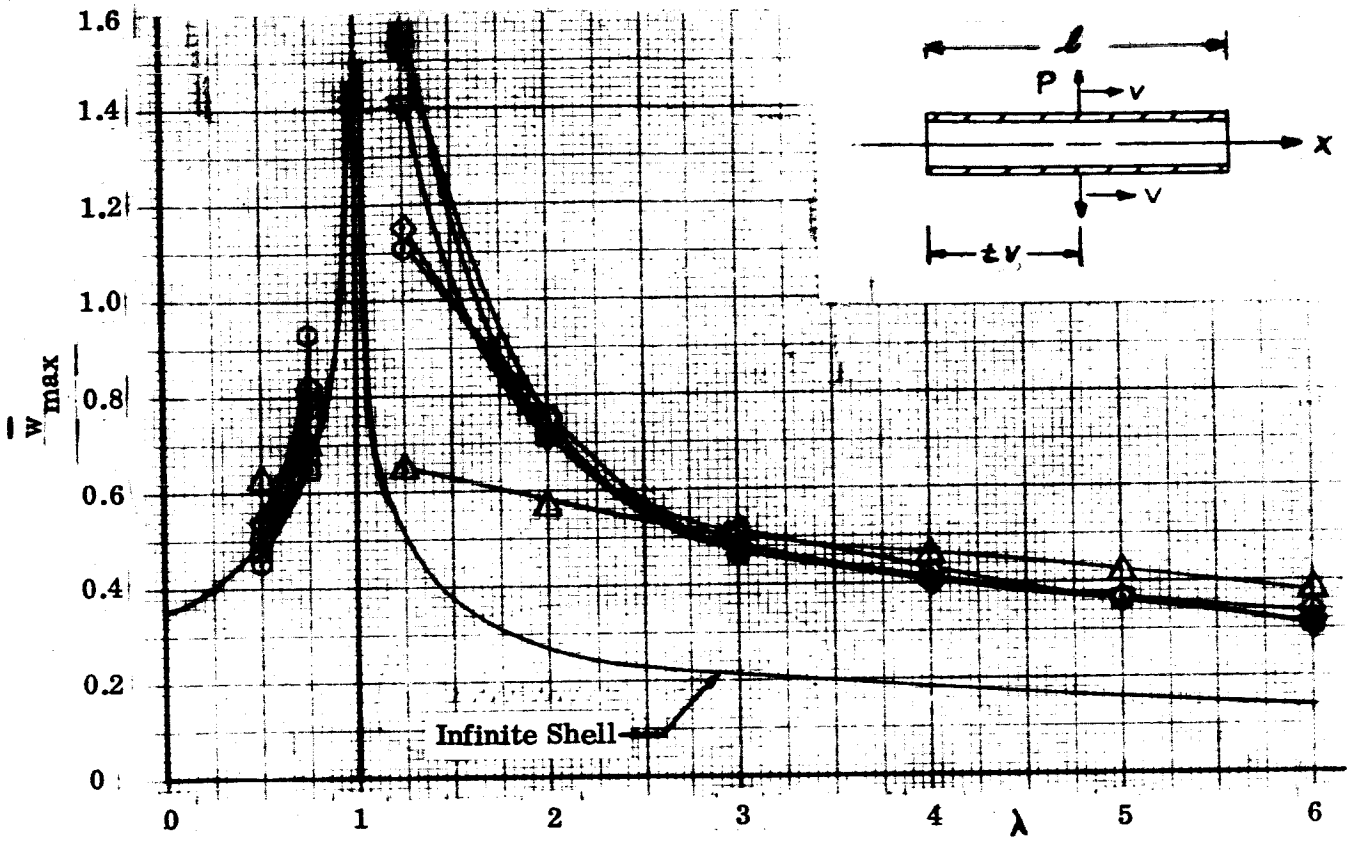

a.) Deflection

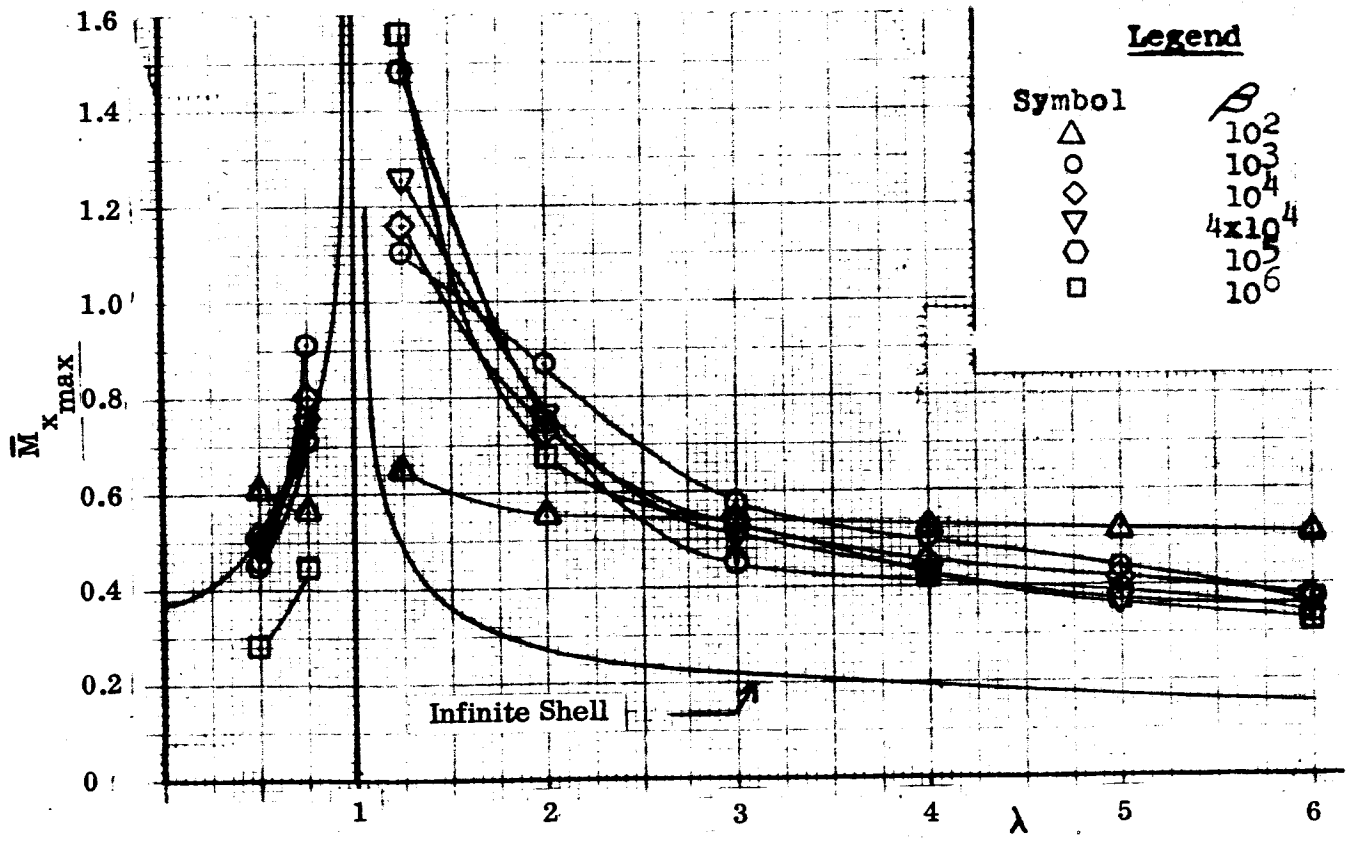

b.) Bending Moment

Figure V-13. Maximum Deflection and Bending Moment Versus λ, Spike Pressure, Fixed Supports, $\alpha = 0$

TABLE 14. SPIKE PRESSURE FIXED SUPPORTS $\alpha = 0$

λ \ β	10^2	N	10^3	N	10^4	N	$4x10^4$	N	10^5	N	10^6	N
0.50	0.6241	500	0.4495	500	0.5422	500	0.5320	500	0.5099	500	0.4808	500
0.75	0.7028	500	0.9303	500	0.8209	500	0.7984	500	0.7851	500	0.6553	500
1.25	0.6488	25	1.1058	70	-1.1522	100	-1.4084	150	1.5316	200	1.5678	700
2.00	0.5785	25	0.7496	70	-0.7124	100	0.7165	250	0.7501	350	0.7017	800
3.00	0.5148	50	-0.4651	80	0.4960	110	-0.5050	300	-0.4484	375	-0.5066	900
4.00	0.4649	50	0.4072	80	-0.4015	125	-0.4134	300	-0.4240	400	0.4133	1000
5.00	0.4278	50	-0.3733	80	-0.3771	150	-0.3661	325	-0.3570	425	0.3618	1100
6.00	0.3754	50	0.3229	80	0.3431	200	-0.3146	350	-0.3216	450	-0.3153	1200

(a) Maximum Deflection

λ \ β	10^2	N	10^3	N	10^4	N	$4x10^4$	N	10^5	N	10^6	N
0.50	-0.6098	500	-0.4598	500	0.5123	500	-0.4881	500	-0.4513	500	-0.2826	500
0.75	-0.5599	500	-0.9151	500	-0.8037	500	-0.7444	500	-0.7140	500	-0.4451	500
1.25	0.6471	25	1.1065	70	1.1603	100	1.2567	150	-1.4870	200	-1.5536	700
2.00	0.5533	25	-0.8739	70	0.7302	100	-0.7718	250	-0.7601	350	-0.6783	800
3.00	0.5433	50	0.5858	80	-0.5380	110	-0.5147	300	0.4576	375	0.5410	900
4.00	0.5319	50	0.5089	80	-0.4461	125	0.4327	300	0.4447	400	0.4217	1000
5.00	-0.5196	50	-0.4347	80	0.4193	150	0.3726	325	0.3840	425	-0.3871	1100
6.00	-0.5067	50	-0.3724	80	-0.3774	200	0.3760	350	0.3445	450	-0.3300	1200

(b) Maximum Bending Moment

λ \ β	10^2	N	10^3	N	10^4	N	$4x10^4$	N	10^5	N	10^6	N
0.50	0.6208	500	0.4495	500	0.5423	500	0.5320	500	0.5099	500	0.4808	500
0.75	0.5380	500	0.9303	500	0.5209	500	0.7984	500	0.7851	500	0.6553	500
1.25	-0.3719	25	-0.6051	70	-0.6287	100	-1.4084	150	1.5316	200	1.5678	700
2.00	-1.3308	25	0.7363	70	-0.7124	100	0.4826	250	0.7501	350	0.7017	800
3.00	-0.1130	50	-0.4334	80	0.4185	110	0.3999	300	0.3050	375	-0.4916	900
4.00	-0.0921	50	-0.3043	80	0.0951	125	-0.3529	300	-0.4240	400	-0.3778	1000
5.00	0.4278	50	-0.2066	80	-0.3771	150	-0.3175	325	-0.3481	425	0.3058	1100
6.00	0.3737	50	0.1910	80	0.3431	200	-0.2104	350	-0.3017	450	0.3089	1200

(c) Deflection Corresponding to the Maximum Bending Moment

λ \ β	10^2	N	10^3	N	10^4	N	$4x10^4$	N	10^5	N	10^6	N
0.50	-0.5604	500	-0.4598	500	-0.5122	500	-0.4881	500	-0.4514	500	-0.2826	500
0.75	-0.4835	500	-0.9151	500	-0.8037	500	-0.7444	500	-0.7140	500	-0.4451	500
1.25	-0.2414	25	-0.6868	70	0.8025	100	1.2567	150	-1.4870	200	-1.5536	700
2.00	-0.3739	25	-0.7369	70	0.7302	100	-0.6187	250	-0.7601	350	-0.6783	800
3.00	-0.3990	50	0.2834	80	-0.3089	110	0.5024	300	0.1125	375	0.5043	900
4.00	-0.4448	50	-0.1851	80	0.1564	125	0.3316	300	0.4447	400	-0.4128	1000
5.00	-0.5196	50	0.3233	80	0.4913	150	0.3523	325	0.2603	425	-0.3710	1100
6.00	-0.4888	50	-0.0916	80	-0.3774	200	0.2190	350	0.3127	450	0.2709	1200

(d) Bending Moment Corresponding to the Maximum Deflection

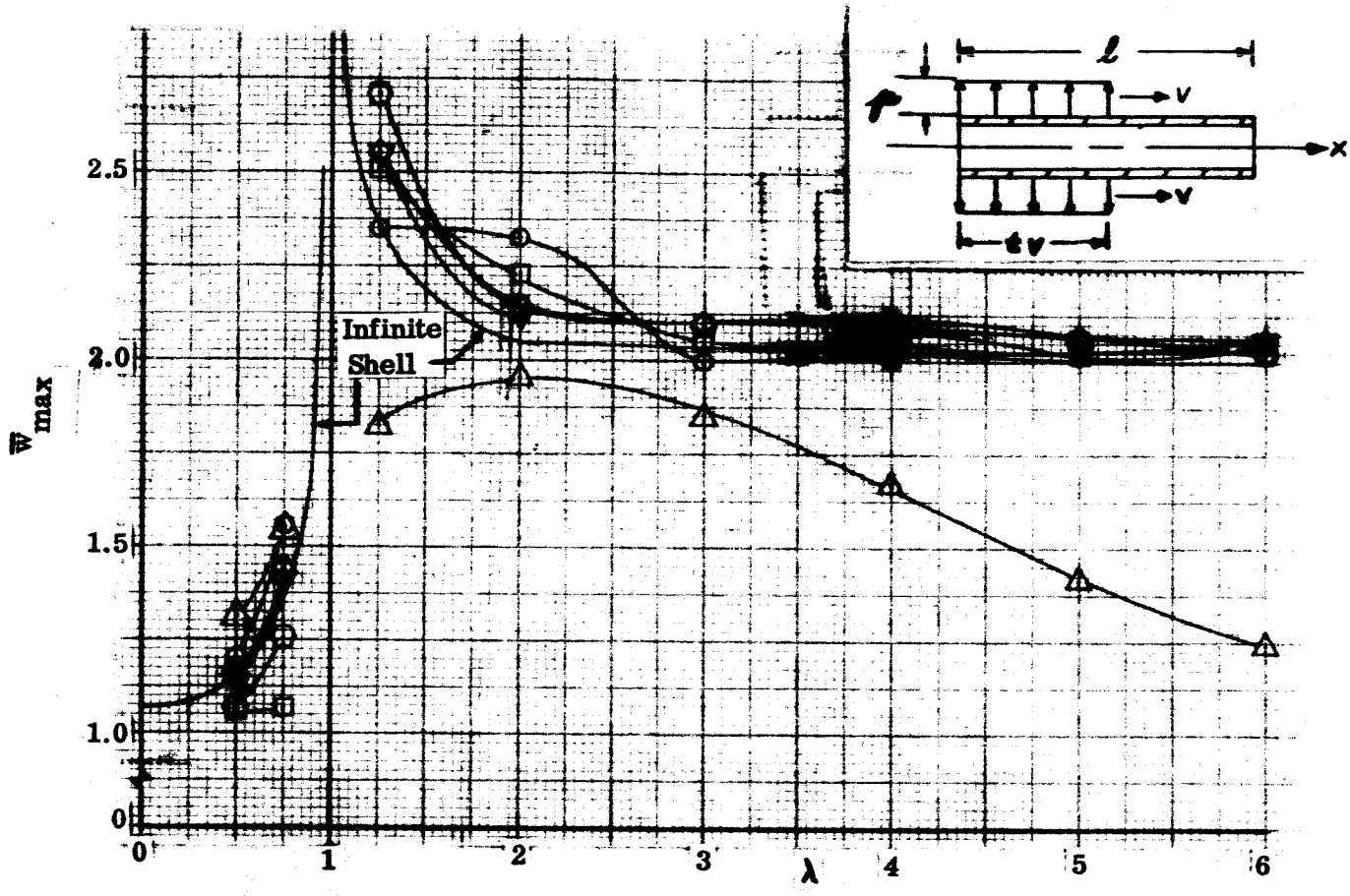

a.) Deflection

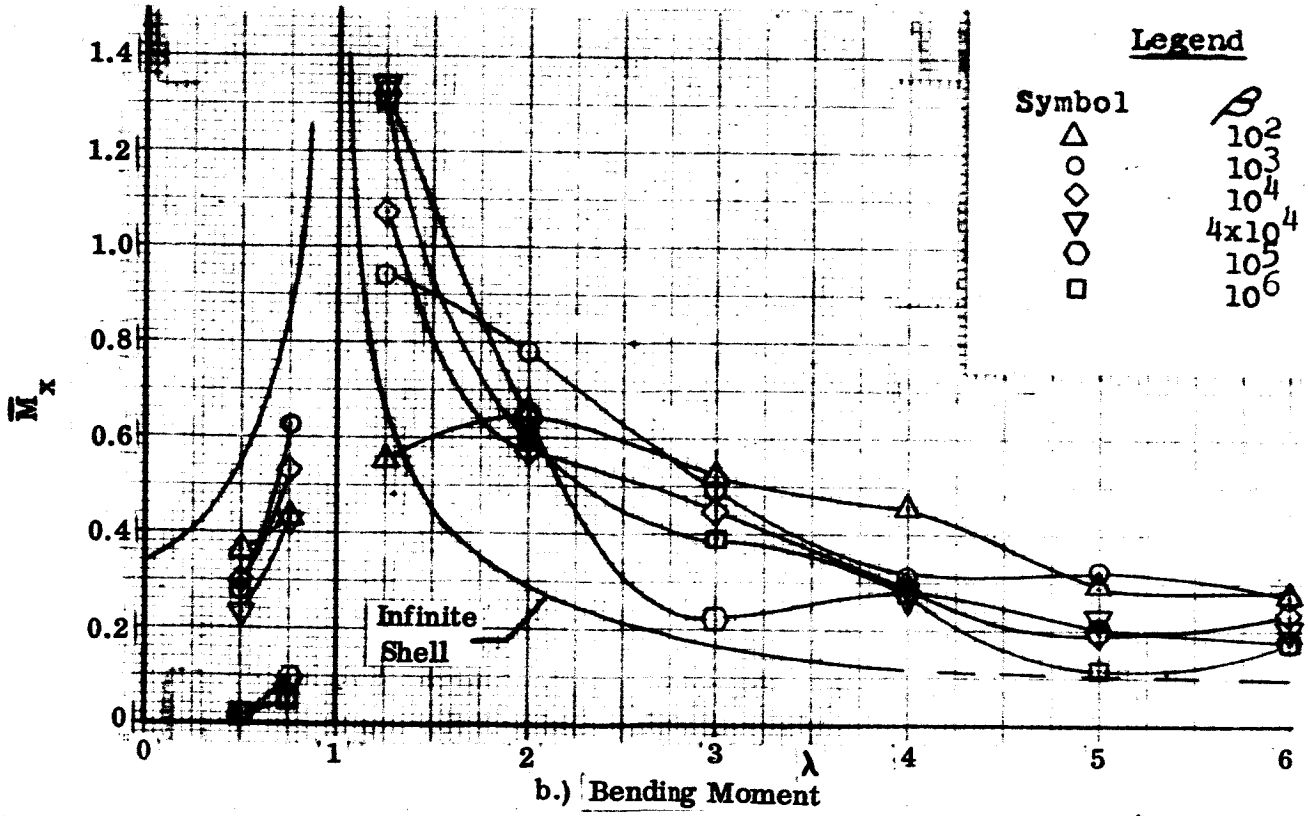

b.) Bending Moment

Figure V-14. Maximum Deflection and Bending Moment VS λ, Step Pressure, Fixed Supports, $\alpha = 0$

TABLE 15. STEP PRESSURE FIXED SUPPORTS $\alpha = 0$

λ \ β	10^2	N	10^3	N	10^4	N	4×10^4	N	10^5	N	10^6	N
0.50	1.3319	300	1.2008	300	1.1692	300	1.1482	500	1.0731	500	1.0680	500
0.75	1.5460	300	1.5560	300	1.4474	300	1.4163	500	1.2516	500	1.0741	500
1.25	1.8245	25	2.3573	70	2.5594	100	2.5675	150	2.7130	200	2.5167	700
2.00	1.9676	25	2.3359	70	2.1520	100	2.1232	250	2.1457	350	2.2361	800
3.00	1.8647	50	1.9979	80	2.1014	110		300	2.0987	375	2.0567	900
4.00	1.6767	50	2.0123	80	2.0948	125	2.0581	300	2.1088	400	2.0752	1000
5.00	1.4253	50	2.0651	80	2.0691	150	2.0325	325	2.0692	425	2.0159	1100
6.00	1.2425	50	2.0680	80	2.0750	200	2.0620	350	2.0343	450	2.0469	1200

(a) Maximum Deflection

λ \ β	10^2	N	10^3	N	10^4	N	4×10^4	N	10^5	N	10^6	N
0.50	-0.3633	300	0.2573	300	0.2997	300	0.2297	500	-0.0132	500	-0.0223	500
0.75	-0.4375	300	0.6244	300	0.5325	300	-0.4254	500	-0.0971	500	0.0489	500
1.25	-0.5542	25	0.9401	70	-1.0698	100	1.3440	150	-1.3338	200		700
2.00	-0.6541	25	0.7780	70	0.5735	100	0.6182	250	-0.6484	350	-0.5921	800
3.00	-0.5230	50	0.4904	80	-0.4502	110		300	0.2206	375	-0.3935	900
4.00	-0.4559	50	-0.3085	80	0.2981	125	-0.2618	300	-0.2964	400	-0.2675	1000
5.00	0.2869	50	-0.3276	80	-0.1894	150	-0.2190	325	-0.2048	425	-0.1196	1100
6.00	0.2696	50	-0.2697	80	-0.2298	200	-0.1978	350	0.1841	450	-0.1763	1200

(b) Maximum Bending Moment

λ \ β	10^2	N	10^3	N	10^4	N	4×10^4	N	10^5	N	10^6	N
0.50	1.1107	300	0.0923	300	0.0203	300	-0.1600	500	-0.1360	500	0.9885	500
0.75	1.3694	300	0.4162	300	-0.2316	300	1.4163	500	-0.2545	500	-0.0587	500
1.25	1.7324	25	-0.5667	70	2.4453	100	-0.7057	150	2.7130	200	-0.3864	700
2.00	1.9322	25	-0.3153	70	-0.2227	100	-0.0406	250	2.1215	350	2.2361	800
3.00	1.7589	50	0.1171	80	2.0648	110		300	-0.0331	375	2.0567	900
4.00	1.6767	50	1.9774	80	0.0639	125	1.9886	300	1.9830	400	2.0752	1000
5.00	0.0470	50	2.0651	80	2.0115	150	2.0021	325	1.9929	425	2.0145	1100
6.00	0.1202	50	2.0641	80	2.0385	200	1.9183	350	0.0283	450	0.0592	1200

(c) Deflection Corresponding to the Maximum Bending Moment

λ \ β	10^2	N	10^3	N	10^4	N	4×10^4	N	10^5	N	10^6	N
0.50	-0.2904	300	-0.1416	300	-0.0990	500	-0.2187	500	-0.0394	500	-0.0071	500
0.75	-0.3183	300	-0.5494	300	-0.4422	500	-0.4254	500	-0.0952	500	-0.0142	500
1.25	-0.4559	25	-0.7316	70	-0.8519	100	-1.0772	150	-1.3338	200	-0.7358	700
2.00	-0.4537	25	-0.7585	70	-0.3562	100	-0.3499	250	-0.5566	350	-0.5921	800
3.00	-0.4070	50	-0.1104	80	-0.2631	110		300	-0.0552	375	-0.3935	900
4.00	-0.4559	50	-0.1762	80	-0.1771	125	-0.1756	300	-0.1759	400	-0.2675	1000
5.00	-0.1504	50	-0.3276	80	-0.1215	150	-0.1248	325	-0.0352	425	-0.1185	1100
6.00	-0.1821	50	-0.2313	80	-0.0085	200	-0.1781	350	-0.1227	450	-0.1335	1200

(d) Bending Moment Corresponding to the Maximum Deflection

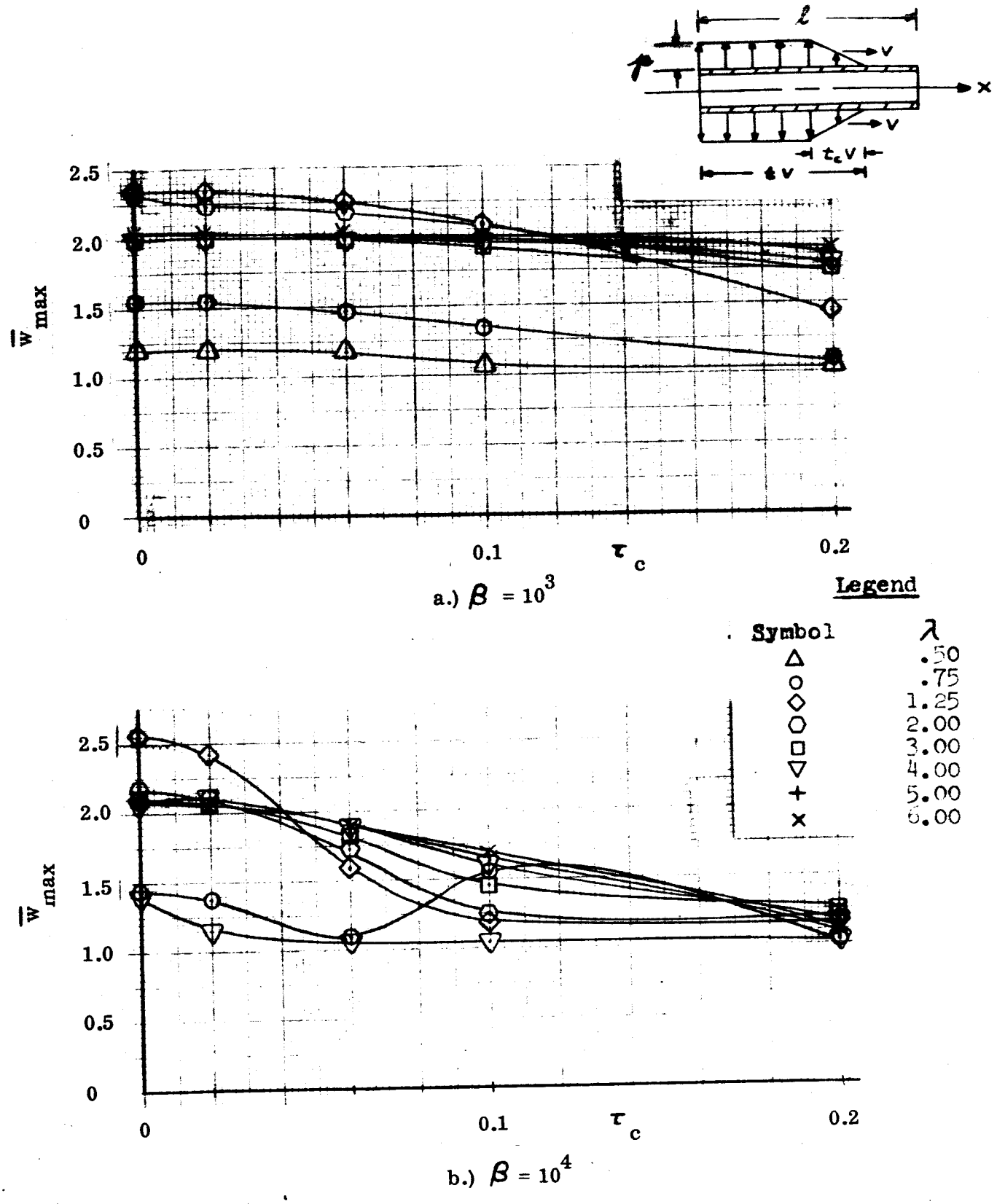

Figure V-15. Maximum Deflection Versus τ_c, Ramp Pressure, Fixed Supports, $\alpha = 0$

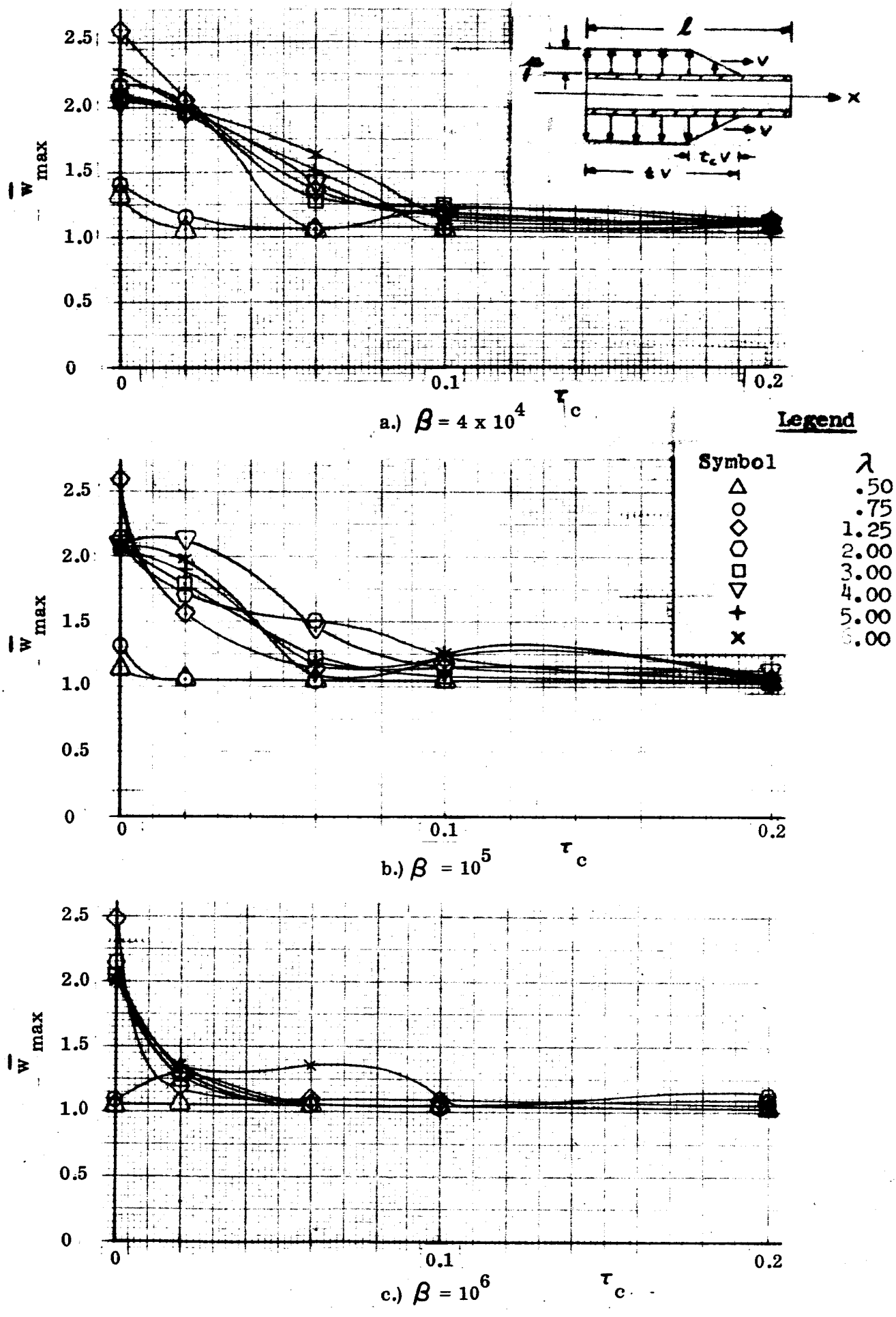

Figure V-16. Maximum Deflection Versus τ_c, Ramp Pressure, Fixed Supports, $\alpha = 0$

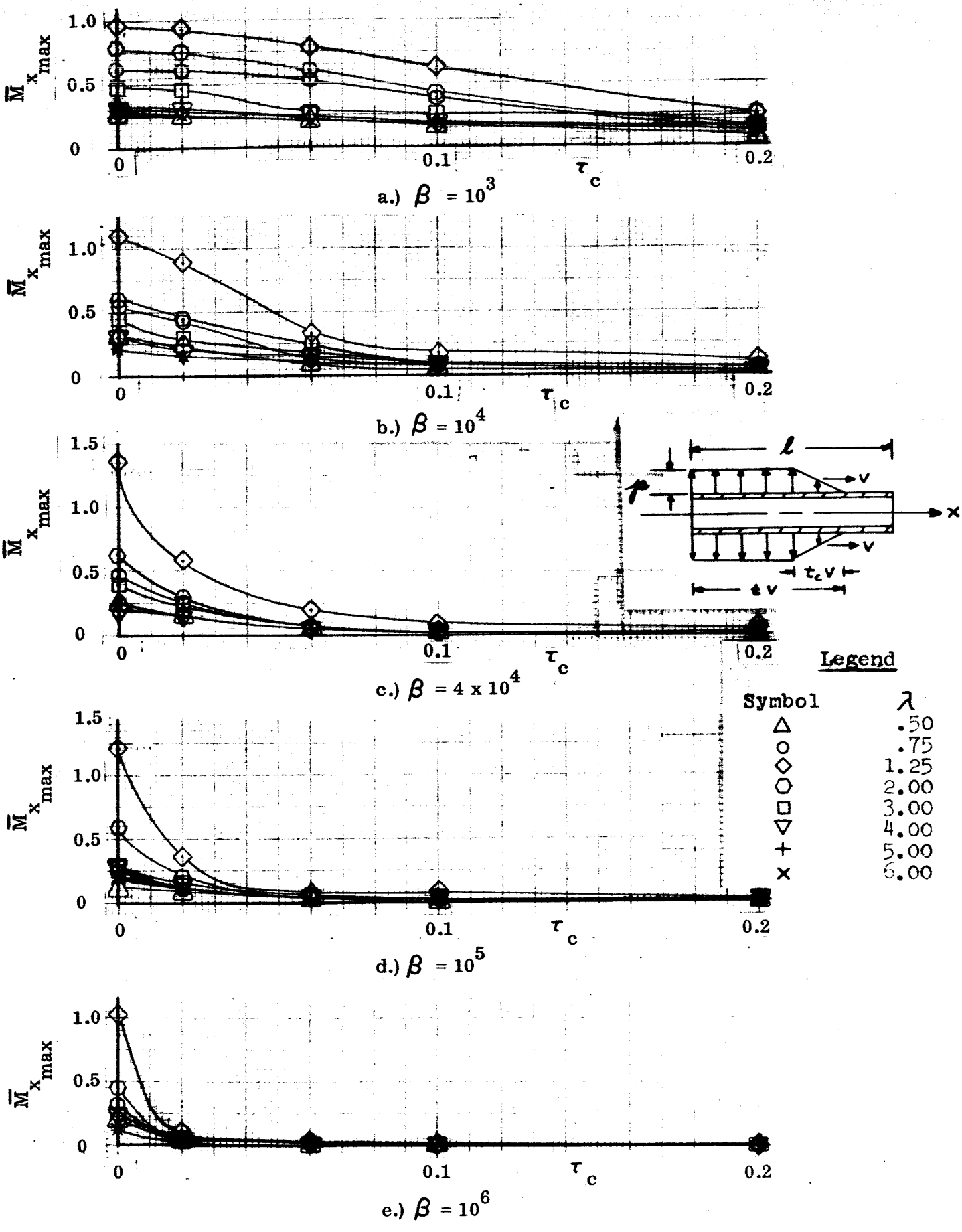

Figure V-17. Maximum Bending Moment Versus τ_c, Ramp Pressure, Fixed Support, $\alpha = 0$

TABLE 16. RAMP PRESSURE, FIXED SUPPORTS, $a = 0$, $\tau_c = 0.002$

β / λ	10^2	N	10^3	N	10^4	N	4×10^4	N	10^5	N	10^6	N
0.50	1.3318	500	1.2011	500	1.3934	500	1.3259	500	1.1194	500	1.0534	500
0.75	1.5462	500	1.5533	500	1.4421	500	1.4079	500	1.3148	500	1.0703	500
1.25	1.8245	25	2.3599	70	2.5471	100	2.5881	150	2.5866	200	2.4719	700
2.00	1.9648	25	2.3246	70	2.1680	100	2.1704	250	2.1296	350	2.1508	800
3.00	1.8630	50	1.9986	80	2.1036	110	2.0814	300	2.0719	375	2.0466	900
4.00	1.6733	50	2.0124	80	2.0847	125	2.0544	300	2.0867	400	2.0307	1000
5.00	1.4265	50	2.0642	80	2.0716	150	2.2917	325	2.0741	425	1.9971	1100
6.00	1.2438	50	2.0674	80	2.0689	200	2.0655	350	2.0407	450	2.0174	1200

(a) Maximum Deflection

β / λ	10^2	N	10^3	N	10^4	N	4×10^4	N	10^5	N	10^6	N
0.50	-0.3634	500	0.2581	500	0.3046	500	-0.2420	500	0.1150	500	0.1927	500
0.75	-0.4375	500	0.6243	500	0.5391	500	-0.4693	500	0.2328	500	0.3167	500
1.25	-0.5541	25	0.9456	70	-1.0953	100	1.3551	150	-1.2110	200	1.0199	700
2.00	-0.6249	25	0.7823	70	0.6072	100	0.6240	250	-0.5908	350	0.4150	800
3.00	-0.5225	50	0.4849	80	-0.4530	110	-0.3985	300	-0.2751	375	0.2358	900
4.00	-0.4531	50	-0.3074	80	0.3079	125	-0.1804	300	0.2850	400	-0.1590	1000
5.00	0.2868	50	-0.3263	80	-0.2128	150	-0.2471	325	0.2181	425	0.1140	1100
6.00	0.2697	50	-0.2697	80	0.2071	200	-0.2124	350	-0.1856	450	0.1102	1200

(b) Maximum Bending Moment

β / λ	10^2	N	10^3	N	10^4	N	4×10^4	N	10^5	N	10^6	N
0.50	1.1773	500	0.0838	500	-0.0111	500	1.1253	500	0.3574	500	0.1065	500
0.75	1.3661	500	-0.4258	500	-0.2708	500	1.4079	500	0.2209	500	-0.0456	500
1.25	1.7300	25	-0.5623	70	-2.4752	100	-0.6376	150	2.5866	200	-0.3651	700
2.00	1.9232	25	-0.3266	70	-0.2142	100	-0.0914	250	2.1132	350	-0.3537	800
3.00	1.7560	50	0.1072	80	2.0488	110	2.0815	300	1.5215	375	-0.0473	900
4.00	1.6733	50	1.9732	80	0.0430	125	2.0416	300	-0.0829	400	2.0138	1000
5.00	0.0617	50	2.0588	80	2.0716	150	2.0093	325	0.1576	425	0.0075	1100
6.00	0.1184	50	2.0651	80	0.0024	200	2.0655	350	2.0407	450	0.0186	1200

(c) Deflection Corresponding to the Maximum Bending Moment

β / λ	10^2	N	10^3	N	10^4	N	4×10^4	N	10^5	N	10^6	N
0.50	-0.2921	500	-0.1450	500	-0.0352	500	0.0166	500	-0.0762	500	-0.0061	500
0.75	-0.3196	500	-0.5557	500	-0.4633	500	-0.4693	500	-0.1822	500	-0.1909	500
1.25	-0.4552	25	-0.7388	70	-0.8416	100	-1.0177	150	-1.2100	200	-0.7541	700
2.00	-0.4474	25	-0.7483	70	-0.5005	100	-0.0347	250	-0.5265	350	-0.2766	800
3.00	-0.4110	50	-0.1513	80	-0.2614	110	-0.3985	300	-0.1604	375	-0.1679	900
4.00	-0.4531	50	-0.1875	80	-0.2719	125	-0.0754	300	-0.0842	400	-0.1368	1000
5.00	-0.1689	50	-0.3215	80	-0.2128	150	-0.2227	325	-0.0857	425	-0.1022	1100
6.00	-0.2022	50	-0.2237	80	-0.0213	200	-0.2124	350	-0.1856	450	-0.0859	1200

(d) Bending Moment Corresponding to the Maximum Deflection

TABLE 17. RAMP PRESSURE FIXED SUPPORTS $\alpha = 0, \tau_c$ 0.02

λ \ β	10^2	N	10^3	N	10^4	N	$4x10^4$	N	10^5	N	10^6	N
0.50	1.3313	500	1.1974	500	1.1468	500	1.0591	500	1.0659	500	1.0606	500
0.75	1.5454	500	1.5456	500	1.3717	500	1.1581	500	1.0578	500	1.3068	500
1.25	1.8237	25	2.3458	70	2.4278	100	2.0681	150	1.5430	200	1.1875	700
2.00	1.9449	25	2.2417	70	2.1007	100	2.0457	250	1.7042	350	1.2384	800
3.00	1.8487	50	1.9954	80	2.0667	110	1.9621	300	1.7878	375	1.2511	900
4.00	1.6399	50	2.0089	80	2.1013	125	1.9667	300	2.1342	400	-----	1000
5.00	1.3899	50	2.0610	80	2.0532	150	1.9642	325	1.9066	425	1.3489	1100
6.00	1.2113	50	2.0655	80	2.0678	200	1.9982	350	1.9805	450	1.1354	1200

(a) Maximum Deflection

λ \ β	10^2	N	10^3	N	10^4	N	$4x10^4$	N	10^5	N	10^6	N
0.50	-0.3624	500	0.2508	500	0.2342	500	0.1489	500	-0.0806	500	0.0237	500
0.75	-0.4367	500	0.6135	500	0.4250	500	-0.2466	500	0.1065	500	-0.0332	500
1.25	-0.5530	25	0.9217	70	-0.8826	100	-0.5744	150	0.3637	200	0.1080	700
2.00	-0.6243	25	0.7580	70	0.4416	100	-0.2990	250	-0.2082	350	-0.0569	800
3.00	-0.5215	50	0.4709	80	-0.2948	110	0.2187	300	-0.1433	375	-0.0436	900
4.00	-0.4195	50	-0.2956	80	-0.1959	125	0.1624	300	-0.1247	400	-----	1000
5.00	0.2861	50	-0.3102	80	-0.1563	150	0.1296	325	-0.1144	425	-0.0045	1100
6.00	0.2688	50	-0.2525	80	0.1532	200	-0.1218	350	-0.0993	450	-0.0115	1200

(b) Maximum Bending Moment

λ \ β	10^2	N	10^3	N	10^4	N	$4x10^4$	N	10^5	N	10^6	N
0.50	1.1795	500	0.0966	500	0.0726	500	-0.0116	500	1.0017	500	0.0007	500
0.75	1.3685	500	-0.4048	500	-0.1424	500	1.1581	500	-0.0633	500	1.0182	500
1.25	1.7315	25	-0.5421	70	2.2748	100	2.0681	150	0.4075	200	0.8852	700
2.00	1.9046	25	-0.3075	70	-0.1386	100	1.8534	250	1.7042	350	1.5518	800
3.00	1.7585	50	0.1209	80	2.0081	110	0.1175	300	1.7508	375	1.1779	900
4.00	1.6399	50	1.9727	80	2.0809	125	0.0159	300	2.1342	400	-----	1000
5.00	0.0473	50	2.0610	80	2.0454	150	0.1056	325	1.9066	425	1.0243	1100
6.00	0.1204	50	2.0608	80	0.0078	200	1.9765	350	0.1329	450	0.9643	1200

(c) Deflection Corresponding to the Maximum Bending Moment

λ \ β	10^2	N	10^3	N	10^4	N	$4x10^4$	N	10^5	N	10^6	N
0.50	-0.2901	500	-0.1411	500	-0.0974	500	-0.0194	500	-0.0017	500	-0.0002	500
0.75	-0.3179	500	-0.5414	500	-0.3400	500	-0.2466	500	-0.0062	500	0.0009	500
1.25	-0.4550	25	-0.7261	70	-0.7843	100	-0.5744	150	-0.2731	200	-0.0789	700
2.00	-0.4118	25	-0.4655	70	-0.3494	100	-0.2672	250	-0.2082	350	-0.0534	800
3.00	-0.4487	50	-0.1124	80	-0.2411	110	-0.1826	300	-0.1270	375	-0.0352	900
4.00	-0.4195	50	-0.1758	80	-0.1630	125	-0.1541	300	-0.1247	400	-----	1000
5.00	-0.1435	50	-0.3102	80	-0.1532	150	-0.0819	325	-0.1143	425	0.0009	1100
6.00	-0.2051	50	-0.2242	80	-0.1096	200	-0.1139	350	-0.0887	450	-0.0099	1200

(d) Bending Moment Corresponding to the Maximum Deflection

TABLE 18. RAMP PRESSURE FIXED SUPPORTS $\alpha = 0$, $\tau_c = 0.06$

λ \ β	10^2	N	10^3	N	10^4	N	4×10^4	N	10^5	N	10^6	N
0.50	1.3262	500	1.1704	500	1.0473	500	1.0613	500	1.0551	500	1.0512	500
0.75	1.5399	500	1.4734	500	1.0818	500	1.0646	500	1.0559	500	1.0479	500
1.25	1.8171	25	2.2560	70	1.5903	100	1.3413	150	1.1300	200	1.0970	700
2.00	1.8901	25	2.1909	70	1.7290	100	1.0646	250	1.5124	350	1.0490	800
3.00	1.8051	50	1.9752	80	1.8237	110	1.2934	300	1.2162	375	1.0563	900
4.00	1.5615	50	1.9957	80	1.8943	125	1.4227	300	1.4330	400	1.1303	1000
5.00	1.3203	50	2.0344	80	1.9017	150	1.5102	325	1.0754	425	1.0544	1100
6.00	1.1464	50	2.0480	80	1.8958	200	1.6177	350	1.1713	450	1.1361	1200

(a) Maximum Deflection

λ \ β	10^2	N	10^3	N	10^4	N	4×10^4	N	10^5	N	10^6	N
0.50	-0.3551	500	0.2112	500	0.0867	500	-0.0440	500	0.0271	500	-0.0083	500
0.75	-0.4301	500	0.5268	500	0.1158	500	0.0632	500	0.0423	500	-0.0117	500
1.25	-0.5435	25	0.7875	70	0.3341	100	-0.1972	150	-0.0788	200	0.0312	700
2.00	-0.4859	25	0.6086	70	0.2410	100	-0.0530	250	0.0635	350	0.0120	800
3.00	-0.5083	50	0.2597	80	-0.1810	110	0.0574	300	-0.0345	375	0.0080	900
4.00	-0.3579	50	-0.2239	80	0.1565	125	0.0603	300	-0.0239	400	0.0125	1000
5.00	0.2803	50	-0.2170	80	-0.1228	150	0.0589	325	-0.0178	425	-0.0018	1100
6.00	0.2614	50	-0.1884	80	0.1268	200	0.0559	350	0.0188	450	0.0077	1200

(b) Maximum Bending Moment

λ \ β	10^2	N	10^3	N	10^4	N	4×10^4	N	10^5	N	10^6	N
0.50	1.1730	500	0.0525	500	-0.0119	500	1.0051	500	-0.0041	500	1.0021	500
0.75	1.3276	500	-0.2178	500	-0.0682	500	-0.0334	500	-0.0322	500	1.0080	500
1.25	1.7240	25	-0.4317	70	0.3899	100	1.3006	150	0.9484	200	0.9778	700
2.00	1.8187	25	-0.2206	70	0.2422	100	0.9931	250	0.9004	350	0.6318	800
3.00	1.7543	50	0.0254	80	1.7715	110	0.7449	300	1.1754	375	0.2949	900
4.00	1.3658	50	1.9002	80	0.1931	125	0.5992	300	0.8169	400	0.9601	1000
5.00	0.0494	50	2.0345	80	1.9017	150	0.5004	325	0.9947	425	1.0140	1100
6.00	0.1223	50	2.0453	80	0.1255	200	0.4151	350	0.8588	450	0.9501	1200

(c) Deflection Corresponding to the Maximum Bending Moment

λ \ β	10^2	N	10^3	N	10^4	N	4×10^4	N	10^5	N	10^6	N
0.50	-0.2880	500	-0.1338	500	0.0017	500	0.0003	500	-0.0006	500	-0.0003	500
0.75	-0.3149	500	-0.4189	500	-0.0639	500	-0.0053	500	-0.0003	500	-0.0008	500
1.25	-0.4489	25	-0.6860	70	-0.3169	100	-0.1715	150	-0.0492	200	-0.0230	700
2.00	-0.3317	25	-0.4307	70	-0.2135	100	-0.0221	250	-0.0502	350	0.0005	800
3.00	-0.4906	50	-0.1182	80	-0.1721	110	-0.0337	300	1.1787	375	-0.0019	900
4.00	-0.3369	50	-0.1533	80	-0.1336	125	-0.0429	300	-0.0180	400	-0.0094	1000
5.00	-0.1599	50	-0.2170	80	-0.1228	150	-0.0489	325	-0.0085	425	0.0007	1100
6.00	-0.2316	50	-0.1834	80	-0.1114	200	-0.0474	350	-0.0174	450	-0.0061	1200

(d) Bending Moment Corresponding to the Maximum Deflection

TABLE 19. RAMP PRESSURE FIXED SUPPORTS $\alpha = 0$, $\tau_c = 0.1$

λ \ β	10^2	N	10^3	N	10^4	N	4×10^4	N	10^5	N	10^6	N
0.50	1.3161	500	1.1216	500	1.0429	500	1.0556	500	1.0443	500	1.0485	500
0.75	1.5290	500	1.3495	500	1.5503	500	1.0464	500	1.0537	500	1.0392	500
1.25	1.8049	25	2.0847	70	1.1929	100	1.1732	150	1.1540	200	1.0718	700
2.00	1.8442	25	2.0968	70	1.2449	100	1.2046	250	1.1649	350	1.0520	800
3.00	1.7473	50	1.9337	80	1.4526	110	1.2297	300	1.0841	375	1.0682	900
4.00	1.4980	50	1.9648	80	1.6038	125	1.1488	300	1.1530	400	1.0831	1000
5.00	1.2520	50	1.9988	80	1.6541	150	1.0548	325	1.2452	425	1.0627	1100
6.00	1.0770	50	2.0201	80	1.6959	200	1.1294	350	1.2655	450	1.0933	1200

(a) Maximum Deflection

λ \ β	10^2	N	10^3	N	10^4	N	4×10^4	N	10^5	N	10^6	N
0.50	-0.3429	500	-0.1769	500	-0.0512	500	-0.0255	500	-0.0160	500	0.0050	500
0.75	-0.4173	500	0.3852	500	-0.0891	500	0.0410	500	-0.0242	500	-0.0070	500
1.25	-0.5259	25	-0.6166	70	-0.1720	100	-0.1040	150	+0.0740	200	-0.0165	700
2.00	-0.4532	25	0.4225	70	0.0884	100	0.0574	250	0.0421	350	+0.0101	800
3.00	-0.4863	50	0.2725	80	-0.0889	110	0.0430	300	+0.0139	375	-0.0096	900
4.00	-0.3434	50	-0.1935	80	-0.0846	125	-0.0208	300	0.0182	400	-0.0074	1000
5.00	-0.2698	50	-0.1962	80	-0.0721	150	-0.0177	325	0.0242	425	0.0015	1100
6.00	-0.2481	50	-0.1826	80	0.0835	200	0.0170	350	-0.0219	450	0.0061	1200

(b) Maximum Bending Moment

λ \ β	10^2	N	10^3	N	10^4	N	4×10^4	N	10^5	N	10^6	N
0.50	1.2107	500	1.0339	500	0.9945	500	1.0005	500	0.9941	500	-0.0003	500
0.75	1.3145	500	-0.2458	500	1.0493	500	-0.0239	500	1.0153	500	0.9975	500
1.25	1.7095	25	2.0656	70	0.9425	100	1.1259	150	0.8381	200	1.0718	700
2.00	1.7438	25	-0.1426	70	0.0755	100	0.7934	250	0.9099	350	0.9054	800
3.00	1.7472	50	-0.0104	80	1.4442	110	0.8074	300	0.5202	375	1.0277	900
4.00	1.4980	50	1.8044	80	1.6038	125	1.1172	300	0.9139	400	1.0500	1000
5.00	0.0535	50	1.9803	80	1.6541	150	0.0442	325	0.8496	425	0.9912	1100
6.00	0.1088	50	2.0065	80	0.3320	200	0.9485	350	1.2122	450	0.9081	1200

(c) Deflection Corresponding to the Maximum Bending Moment

λ \ β	10^2	N	10^3	N	10^4	N	4×10^4	N	10^5	N	10^6	N
0.50	-0.2837	500	-0.1197	500	-0.0037	500	0.0005	500	-0.0004	500	-0.0003	500
0.75	-0.3085	500	-0.3462	500	-0.0181	500	-0.0015	500	-0.0010	500	-0.0002	500
1.25	-0.4397	25	-0.6039	70	-0.1144	100	-0.0848	150	-0.0634	200	-0.0165	700
2.00	-0.1846	25	-0.3852	70	-0.0698	100	-0.0443	250	-0.0266	350	-0.0057	800
3.00	-0.4863	50	-0.1136	80	-0.0673	110	-0.0287	300	-0.0024	375	-0.0071	900
4.00	-0.3434	50	-0.1919	80	-0.0846	125	-0.0145	300	-0.0153	400	-0.0050	1000
5.00	-0.1891	50	-0.1661	80	-0.0721	150	0.0068	325	-0.0163	425	+0.0004	1100
6.00	-0.2105	50	-0.1591	80	-0.0646	200	-0.0089	350	-0.0205	450	-0.0044	1200

(d) Bending Moment Corresponding to the Maximum Deflection

TABLE 20. RAMP PRESSURE FIXED SUPPORTS $\alpha = 0$, $\tau_c = 0.2$

λ \ β	10^2	N	10^3	N	10^4	N	4×10^4	N	10^5	N	10^6	N
0.50	1.2726	500	1.0374	500	1.0265	500	1.0925	500	1.0245	500	1.0235	500
0.75	1.4813	500	1.0831	500	1.0288	500	1.1285	500	1.0241	500	1.0970	500
1.25	1.7453	25	1.4392	70	1.1672	100	1.1124	150	1.0537	200	1.0436	700
2.00	1.7614	25	1.7238	70	1.1998	100	1.0958	250	1.0569	350	1.1335	800
3.00	1.5581	50	1.7553	80	1.2659	110	1.1404	300	1.0602	375	1.0372	900
4.00	1.2873	50	1.7954	80	1.1569	125	1.1253	300	1.1099	400	1.0474	1000
5.00	1.0713	50	1.8550	80	1.0859	150	1.0343	325	1.0793	425	1.0231	1100
6.00	0.9001	50	1.9011	80	1.1062	200	1.1039	350	1.0499	450	1.0442	1200

(a) Maximum Deflection

λ \ β	10^2	N	10^3	N	10^4	N	4×10^4	N	10^5	N	10^6	N
0.50	-0.3086	500	-0.0774	500	-0.0266	500	-0.0132	500	0.0081	500	-0.0027	500
0.75	-0.3654	500	0.1276	500	-0.0384	500	-0.0208	500	0.0122	500	-0.0038	500
1.25	-0.4522	25	-0.2467	70	-0.1012	100	0.0591	150	-0.0242	200	0.0125	700
2.00	-0.3911	25	-0.2362	70	-0.0621	100	-0.0273	250	-0.0139	350	0.0069	800
3.00	-0.3896	50	0.1332	80	0.0424	110	-0.0236	300	0.0084	375	-0.0029	900
4.00	0.2805	50	-0.1474	80	-0.0241	125	-0.0171	300	-0.0126	400	0.0035	1000
5.00	0.2426	50	-0.1409	80	-0.0192	150	0.0090	325	0.0076	425	0.0013	1100
6.00	0.2184	50	-0.1382	80	-0.0196	200	0.0097	350	-0.0056	450	0.0022	1200

(b) Maximum Bending Moment

λ \ β	10^2	N	10^3	N	10^4	N	4×10^4	N	10^5	N	10^6	N
0.50	1.1635	500	0.9805	500	0.9924	500	1.0047	500	-0.0002	500	1.0037	500
0.75	1.3841	500	-0.0789	500	1.0105	500	1.0130	500	-0.0062	500	1.0057	500
1.25	1.6213	25	1.4392	70	1.1246	100	0.8810	150	0.2823	200	0.9607	700
2.00	1.6720	25	1.7212	70	1.1554	100	1.0766	250	1.0547	350	1.0244	800
3.00	1.5581	50	0.2992	80	0.8309	110	1.1071	300	0.9668	375	1.0372	900
4.00	-0.0047	50	1.7464	80	1.1426	125	1.1253	300	1.0809	400	0.9975	1000
5.00	0.0424	50	1.8550	80	0.9038	150	0.5782	325	0.9356	425	0.9898	1100
6.00	0.0784	50	1.8986	80	1.0248	200	0.1932	350	0.6570	450	1.0017	1200

(c) Deflection Corresponding to the Maximum Bending Moment

λ \ β	10^2	N	10^3	N	10^4	N	4×10^4	N	10^5	N	10^6	N
0.50	-0.2476	500	-0.0318	500	-0.0011	500	-0.0003	500	-0.0001	500	-0.0004	500
0.75	-0.2834	500	-0.0918	500	-0.0255	500	-0.0015	500	-0.0004	500	-0.0003	500
1.25	-0.3861	25	-0.2467	70	-0.0889	100	-0.0493	150	-0.0155	200	-0.0112	700
2.00	-0.3064	25	-0.2324	70	-0.0616	100	-0.0229	250	-0.0060	350	0.0054	800
3.00	-0.3896	50	-0.1055	80	-0.0279	110	-0.0216	300	-0.0076	375	-0.0029	900
4.00	-0.2249	50	-0.1197	80	-0.0162	125	-0.0171	300	-0.0118	400	-0.0034	1000
5.00	-0.1703	50	-0.1409	80	-0.0042	150	-0.0011	325	-0.0063	425	-0.0000	1100
6.00	-0.1079	50	-0.1319	80	-0.0162	200	-0.0068	350	-0.0025	450	-0.0018	1200

(d) Bending Moment Corresponding to the Maximum Deflection

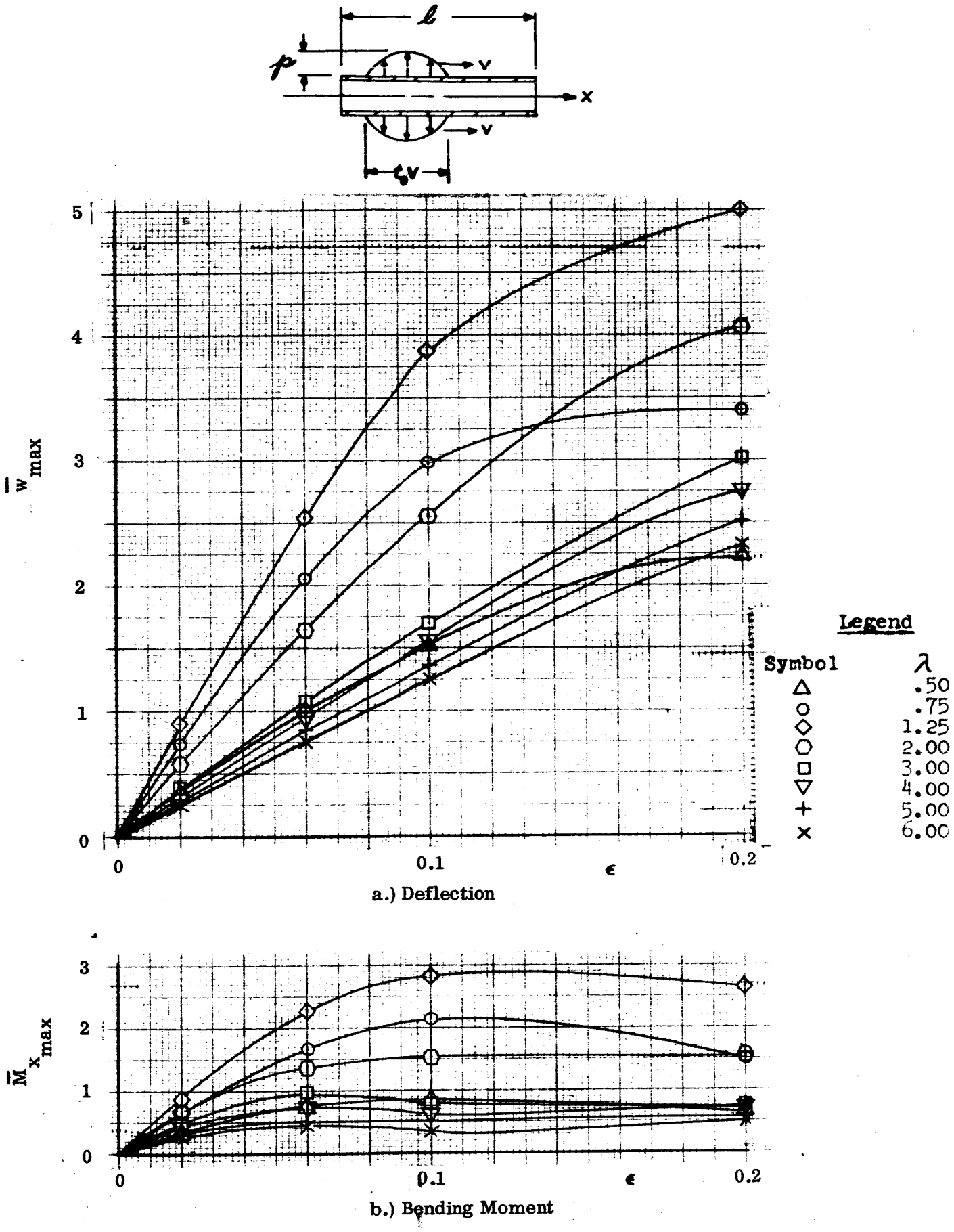

a.) Deflection

b.) Bending Moment

Figure V-18. Maximum Deflection and Bending Moment Versus ϵ, Sinusoidal Pressure, Fixed Supports, $\alpha = 0$, $\beta = 10^3$

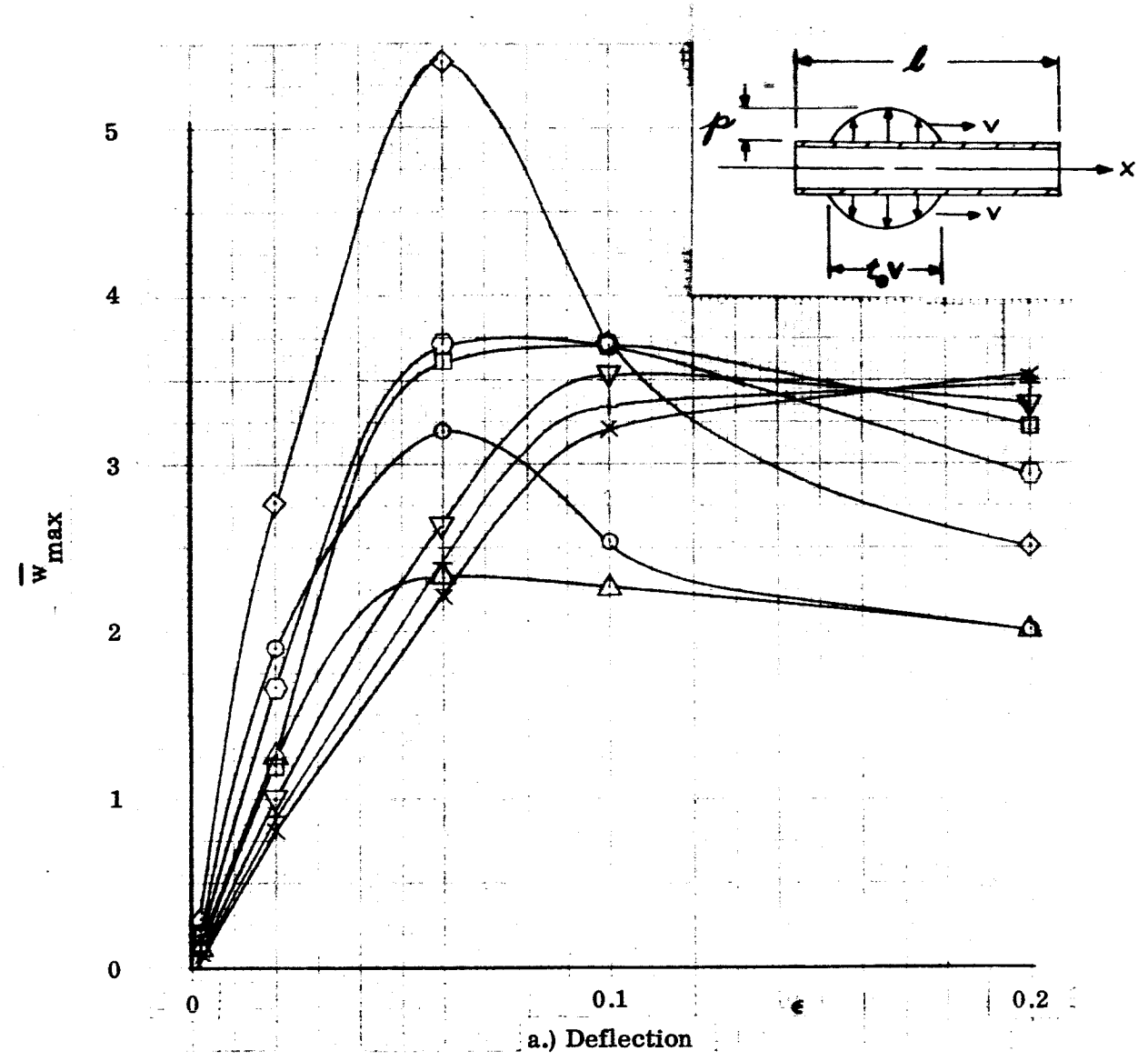

a.) Deflection

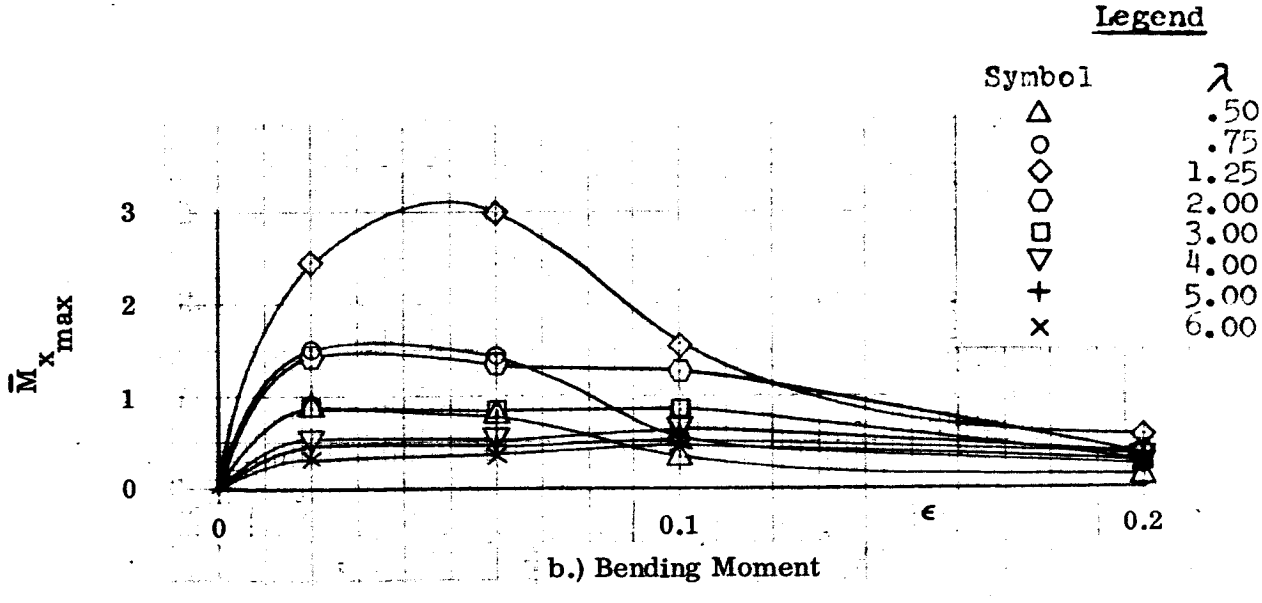

b.) Bending Moment

Figure V-19. Maximum Deflection and Bending Moment Versus ϵ Sinusoidal Pressure, Fixed Supports, $\alpha = 0$, $\beta = 10^4$

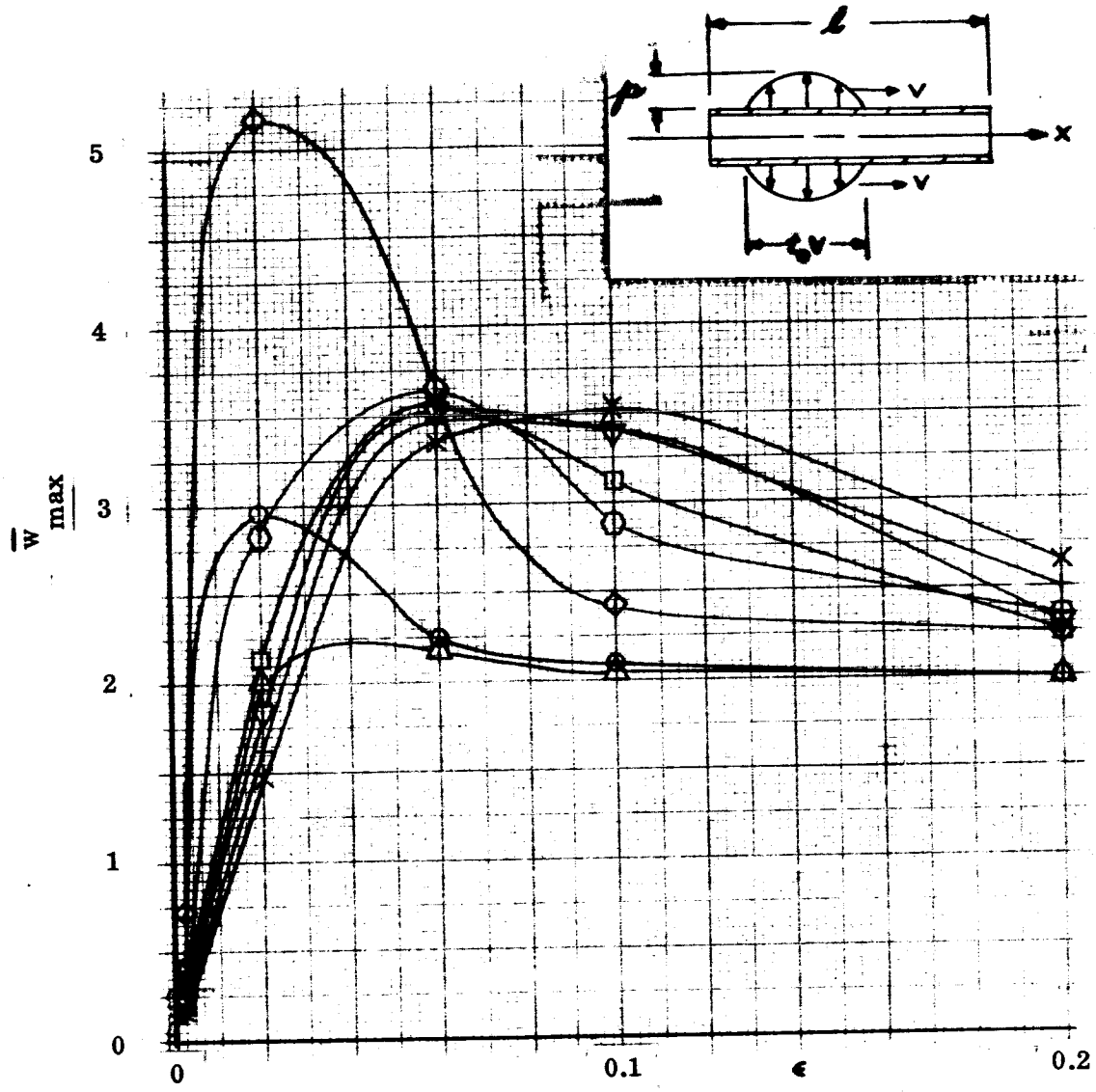

a.) Deflection

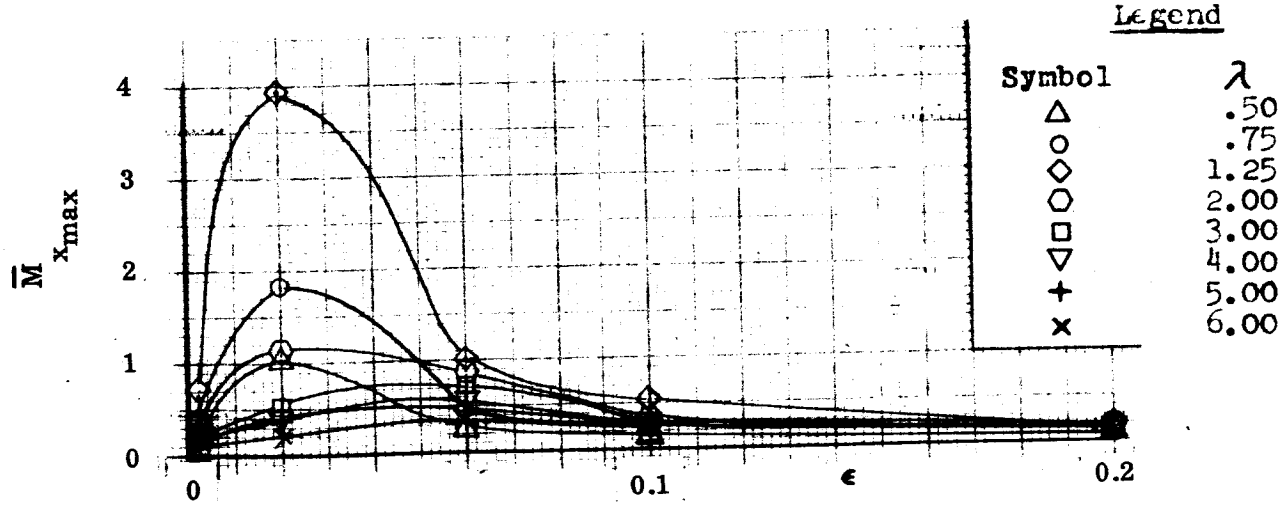

b.) Bending Moment

Figure V-20. Maximum Deflection and Bending Moment Versus ϵ, Sinusoidal Pressure, Fixed Supports, $\alpha = 0$, $\beta = 4 \times 10^4$

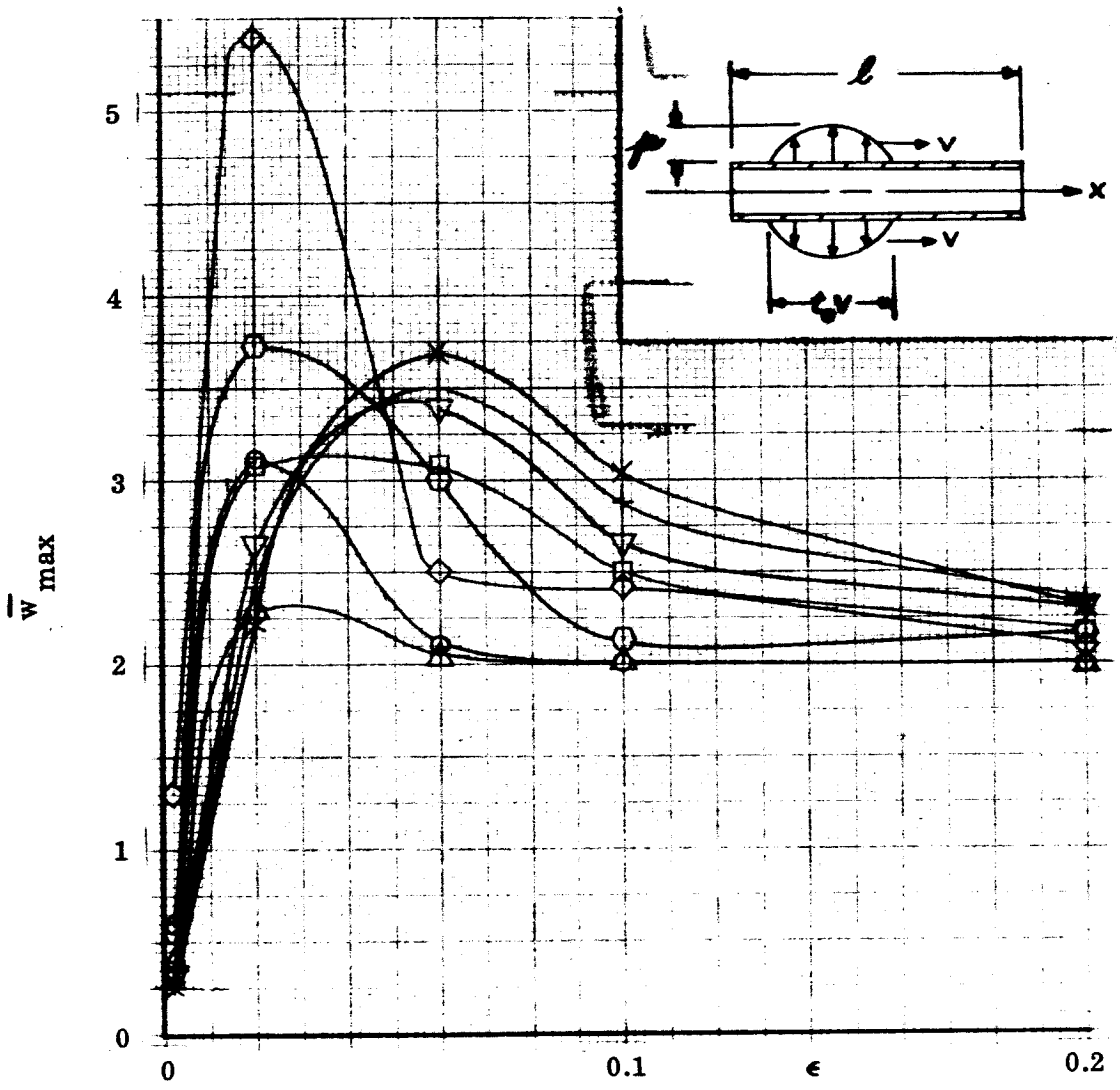

a.) Deflection

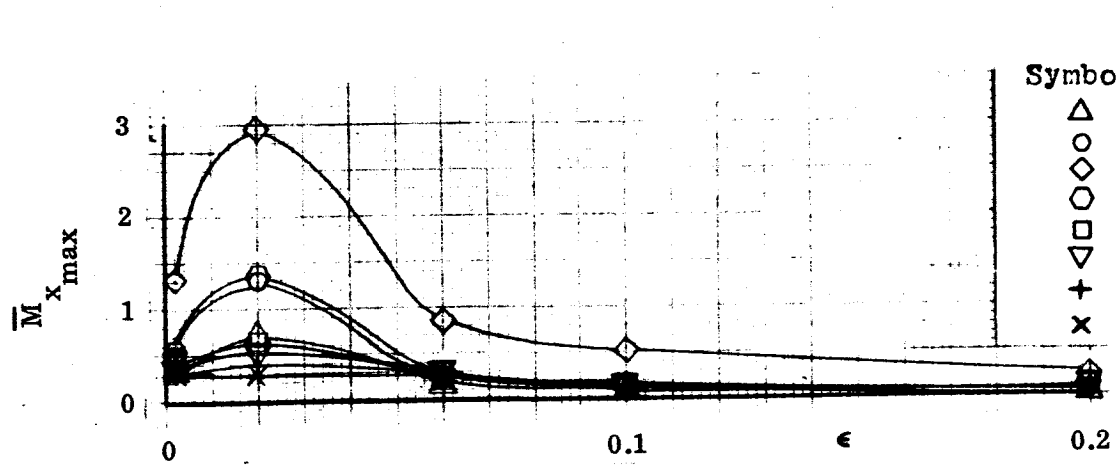

b.) Bending Moment

Figure V-21. Maximum Deflection and Bending Moment Versus ϵ, Sinusoidal Pressure, Fixed Supports, $\alpha = 0$, $\beta = 10^5$

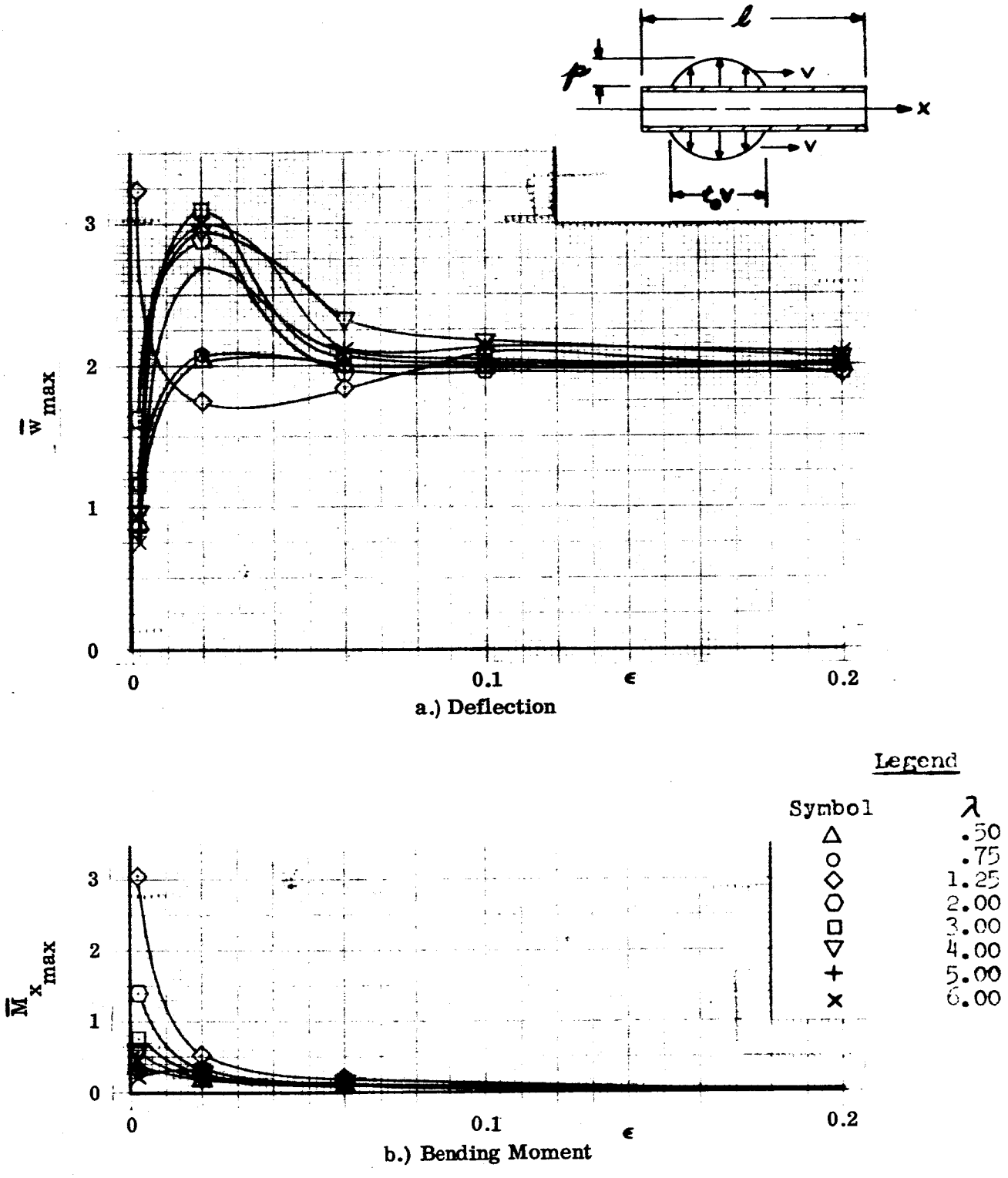

Figure V-22. Maximum Deflection and Bending Moment Versus ϵ, Sinusoidal Pressure, Fixed Supports, $\alpha = 0$, $\beta = 10^6$

TABLE 21. SINUSOIDAL PRESSURE FIXED SUPPORTS $a = 0$, $\epsilon = 0.002$

λ \ β	10^2	N	10^3	N	10^4	N	$4x10^4$	N	10^5	N	10^6	N
0.50	0.0159	500	0.0361	500	0.1373	500	0.2673	500	0.3957	500	0.8745	500
0.75	0.0179	500	0.0748	500	0.2058	500	0.3975	500	0.5976	500	1.1791	500
1.25	0.0165	25	0.0890	70	-0.2969	100	-0.7245	150	1.3140	200	-3.2357	700
2.00	0.0147	25	0.0604	70	0.1865	100	0.3712	250	0.5712	350	-1.6219	800
3.00	0.0131	50	-0.0374	80	0.1297	110	0.2611	300	-0.3588	375	-1.1728	900
4.00	0.0118	50	0.0328	80	-0.1026	125	-0.2133	300	0.3313	400	-0.9594	1000
5.00	0.0109	50	-0.0316	80	-0.0943	150	-0.1770	325	-0.2842	425	-0.8435	1100
6.00	0.0096	50	0.0260	80	+0.0887	200	-0.1683	350	0.2574	450	0.7533	1200

(a) Maximum Deflection

λ \ β	10^2	N	10^3	N	10^4	N	$4x10^4$	N	10^5	N	10^6	N
0.50	-0.0155	500	-0.0364	500	-0.1241	500	-0.2234	500	-0.2991	500	-0.3519	500
0.75	-0.0141	500	-0.0727	500	-0.1949	500	-0.3497	500	-0.4920	500	-0.5829	500
1.25	0.0165	25	0.0889	70	0.2945	100	-0.6430	150	-1.2954	200	3.0731	700
2.00	0.0141	25	-0.0703	70	0.1995	100	-0.3567	250	-0.5674	350	1.3830	800
3.00	0.0138	50	0.0465	80	0.1338	110	-0.2536	300	0.4009	375	-0.7744	900
4.00	0.0135	50	0.0405	80	-0.1163	125	0.2337	300	-0.3029	400	-0.5487	1000
5.00	-0.0132	50	-0.0350	80	-0.0946	150	0.1279	325	0.3073	425	0.3745	1100
6.00	-0.0129	50	-0.0305	80	0.0970	200	0.1713	350	-0.2712	450	-0.2223	1200

(b) Maximum Bending Moment

λ \ β	10^2	N	10^3	N	10^4	N	$4x10^4$	N	10^5	N	10^6	N
0.50	0.0158	500	0.0361	500	0.1373	500	0.2673	500	0.3957	500	0.8745	500
0.75	0.0136	500	0.7479	500	0.2058	500	0.3975	500	0.5976	500	1.1791	500
1.25	-0.0094	25	-0.0489	70	-0.1608	100	0.6446	150	1.3140	200	-3.2357	700
2.00	-0.0034	25	0.0587	70	-0.1638	100	0.2619	250	0.5717	350	-1.6219	800
3.00	-0.0029	50	-0.0350	80	-0.0487	110	0.2123	300	-0.1401	375	0.9004	900
4.00	-0.0023	50	-0.0242	80	0.0788	125	-0.2076	300	0.2901	400	0.6296	1000
5.00	0.0109	50	-0.0162	80	-0.0943	150	-0.0148	325	-0.2835	425	-0.3995	1100
6.00	0.0095	50	-0.0219	80	-0.0615	200	-0.1539	350	0.2575	450	0.4495	1200

(c) Deflection Corresponding to the Maximum Bending Moment

λ \ β	10^2	N	10^3	N	10^4	N	$4x10^4$	N	10^5	N	10^6	N
0.50	-0.0154	500	-0.0364	500	-0.1241	500	-0.2334	500	-0.2991	500	-0.3519	500
0.75	-0.0124	500	-0.0728	500	-0.1949	500	-0.3497	500	-0.4920	500	-0.5829	500
1.25	-0.0061	25	-0.0551	70	0.2127	100	0.6118	150	-1.2954	200	3.0731	700
2.00	-0.0095	25	-0.0612	70	-0.1975	100	-0.3406	250	-0.5674	350	1.3830	800
3.00	-0.0101	50	0.0226	80	-0.1007	110	-0.2492	300	0.0862	375	0.7208	900
4.00	-0.0113	50	-0.0141	80	0.0514	125	0.2248	300	-0.2833	400	0.4645	1000
5.00	-0.0132	50	0.0248	80	0.0946	150	0.1035	325	0.2909	425	0.3645	1100
6.00	-0.0125	50	-0.0070	80	-0.0888	200	0.1475	350	-0.2712	450	-0.1502	1200

(d) Bending Moment Corresponding to the Maximum Deflection

TABLE 22. SINUSOIDAL PRESSURE FIXED SUPPORTS $\alpha = 0$, $\epsilon = 0.02$

λ \ β	10^2	N	10^3	N	10^4	N	4×10^4	N	10^5	N	10^6	N
0.50	0.1587	500	0.3590	500	1.2689	500	2.0290	500	2.3044	500	2.0435	500
0.75	0.1788	500	0.7415	500	1.9072	500	2.9676	500	3.1184	500	2.0786	500
1.25	0.1652	25	0.8855	70	2.7777	100	-5.1840	150	5.3956	200	1.7400	700
2.00	0.1472	25	0.5845	70	1.6764	100	2.8320	250	-3.7444	350	2.8804	800
3.00	0.1310	50	-0.3723	80	1.2027	110	2.1480	300	3.0834	375	3.1135	900
4.00	0.1183	50	0.3269	80	-0.9969	125	-1.8403	300	-2.6665	400	2.9515	1000
5.00	0.1086	50	0.2883	80	-0.9023	150	1.6307	325	-2.4388	425	2.7040	1100
6.00	0.0950	50	0.2598	80	0.8133	200	1.4814	350	2.2271	450	-3.0101	1200

(a) Maximum Deflection

λ \ β	10^2	N	10^3	N	10^4	N	4×10^4	N	10^5	N	10^6	N
0.50	-0.1512	500	-0.3309	500	-0.8974	500	-1.0226	500	-0.7123	500	0.1508	500
0.75	-0.1381	500	-0.6903	500	-1.5261	500	-1.8332	500	-1.2883	500	0.2163	500
1.25	0.1613	25	0.8756	70	2.4698	100	3.9449	150	-2.9577	200	-0.5106	700
2.00	0.1403	25	-0.6843	70	1.4311	100	-1.0929	250	1.3793	350	-0.2676	800
3.00	0.1378	50	0.4530	80	-0.8809	110	0.5714	300	-0.6671	375	0.2085	900
4.00	0.1346	50	0.3888	80	-0.5789	125	0.3855	300	0.5051	400	0.2890	1000
5.00	-0.1309	50	-0.3195	80	0.4918	150	-0.3164	325	0.3984	425	0.2920	1100
6.00	-0.1278	50	-0.2766	80	-0.3559	200	-0.2231	350	-0.2872	450	-0.2745	1200

(b) Maximum Bending Moment

λ \ β	10^2	N	10^3	N	10^4	N	4×10^4	N	10^5	N	10^6	N
0.50	0.1579	500	0.3590	500	1.2689	500	2.0290	500	2.3044	500	0.0007	500
0.75	0.1369	500	0.7416	500	1.9072	500	2.9676	500	3.1184	500	-0.1119	500
1.25	-0.0885	25	-0.4791	70	-1.3465	100	-5.1840	150	5.2367	200	0.9832	700
2.00	-0.0337	25	0.5845	70	-1.3887	100	2.8320	250	-3.7444	350	2.8804	800
3.00	-0.0287	50	-0.3452	80	0.9640	110	0.1701	300	3.0834	375	-1.0026	900
4.00	-0.0233	50	-0.2419	80	0.7342	125	-1.5395	300	-2.6665	400	-2.0159	1000
5.00	0.1086	50	-0.1693	80	-0.9023	150	1.3527	325	-2.4388	425	-2.6233	1100
6.00	0.0950	50	0.1515	80	0.8133	200	1.4422	350	2.2118	450	2.9578	1200

(c) Deflection Corresponding to the Maximum Bending Moment

λ \ β	10^2	N	10^3	N	10^4	N	4×10^4	N	10^5	N	10^6	N
0.50	-0.1428	500	-0.3309	500	-0.8974	500	-1.0226	500	-0.7123	500	-0.0483	500
0.75	-0.1229	500	-0.6903	500	-1.5261	500	-1.8332	500	-1.2883	500	-0.0611	500
1.25	-0.0619	25	-0.5459	70	-1.5877	100	3.9450	150	-2.8646	200	0.0448	700
2.00	-0.0948	25	-0.6843	70	-1.1724	100	-1.0929	250	1.3793	350	-0.2676	800
3.00	-0.1013	50	0.2175	80	-0.5368	110	-0.4961	300	-0.6671	375	-0.1745	900
4.00	-0.1129	50	-0.1433	80	0.2966	125	0.2067	300	0.5051	400	-0.1345	1000
5.00	-0.1309	50	-0.1040	80	0.4918	150	-0.2906	325	0.3984	425	-0.0798	1100
6.00	-0.1278	50	-0.0565	80	-0.3559	200	-0.1726	350	-0.2829	450	0.2535	1200

(d) Bending Moment Corresponding to the Maximum Deflection

TABLE 23. SINUSOIDAL PRESSURE FIXED SUPPORTS $\alpha = 0$, $\epsilon = 0.06$

λ \ β	10^2	N	10^3	N	10^4	N	$4x10^4$	N	10^5	N	10^6	N
0.50	0.4722	500	1.0157	500	2.3372	500	2.1678	500	2.0532	500	2.0047	500
0.75	0.5328	500	2.0625	500	3.2058	500	2.2482	500	2.1131	500	2.0114	500
1.25	0.4946	25	2.5429	70	5.3899	100	3.6567	150	2.4916	200	1.8494	700
2.00	0.4395	25	-1.6392	70	-3.7153	100	3.6257	250	3.0049	350	1.9877	800
3.00	0.3910	50	-1.0702	80	-3.6260	110	3.5186	300	3.0835	375	2.0707	900
4.00	0.3526	50	0.9596	80	-2.6319	125	-3.5771	300	3.3960	400	2.3378	1000
5.00	0.3212	50	0.8511	80	2.4032	150	3.4896	325	3.5037	425	2.0939	1100
6.00	0.2814	50	0.7748	80	2.2224	200	3.3547	350	3.6975	450	2.1040	1200

(a) Maximum Deflection

λ \ β	10^2	N	10^3	N	10^4	N	$4x10^4$	N	10^5	N	10^6	N
0.50	-0.4251	500	-0.7417	500	-0.7982	500	0.2639	500	0.1690	500	0.0504	500
0.75	-0.4021	500	-1.6855	500	-1.4350	500	0.4550	500	0.2640	500	0.0714	500
1.25	0.4253	25	2.2821	70	-2.9834	100	-1.0264	150	0.8546	200	0.1876	700
2.00	0.4087	25	-1.3881	70	1.3795	100	0.8976	250	-0.2597	350	-0.1304	800
3.00	0.4021	50	0.9585	80	-0.8159	110	0.7110	300	0.2634	375	-0.1102	900
4.00	0.3830	50	0.7425	80	0.5453	125	0.5640	300	0.3292	400	-0.0467	1000
5.00	-0.3523	50	0.5263	80	-0.4885	150	-0.4517	325	0.3160	425	0.0818	1100
6.00	0.2961	50	-0.4235	80	-0.3588	200	0.3941	350	0.2941	450	-0.0518	1200

(b) Maximum Bending Moment

λ \ β	10^2	N	10^3	N	10^4	N	$4x10^4$	N	10^5	N	10^6	N
0.50	0.4694	500	1.0155	500	2.3372	500	0.0128	500	0.0041	500	0.0002	500
0.75	0.4795	500	2.0625	500	3.2058	500	-0.2629	500	-0.1458	500	-0.0393	500
1.25	-0.2119	25	-1.2542	70	5.3899	100	3.6567	150	-1.3948	200	-0.3350	700
2.00	-0.0981	25	1.4358	70	-3.7153	100	-2.9868	250	3.0049	350	0.4288	800
3.00	-0.0836	50	-0.9553	80	2.8860	110	-3.3994	300	-1.3642	375	0.5118	900
4.00	-0.0674	50	-0.6603	80	-2.6319	125	-3.5771	300	-2.3484	400	2.3378	1000
5.00	0.3128	50	-0.0806	80	2.4031	150	2.8730	325	-2.8282	425	-0.6762	1100
6.00	-0.0365	50	0.4143	80	2.2224	200	-3.2918	350	-3.1496	450	0.5586	1200

(c) Deflection Corresponding To The Maximum Bending Moment

λ \ β	10^2	N	10^3	N	10^4	N	$4x10^4$	N	10^5	N	10^6	N
0.50	-0.4152	500	-0.6645	500	-0.7982	500	-0.1523	500	-0.0567	500	-0.0042	500
0.75	-0.3659	500	-1.6855	500	-1.4350	500	-0.1134	500	-0.0931	500	-0.0083	500
1.25	-0.1902	25	-1.5510	70	-2.9834	100	-1.0264	150	-0.3080	200	0.1147	700
2.00	-0.2758	25	0.8585	70	1.3795	100	-0.5958	250	-0.2597	350	-0.0103	800
3.00	-0.2958	50	0.4329	80	0.7008	110	-0.4136	300	-0.1694	375	-0.0096	900
4.00	-0.3265	50	-0.3484	80	0.5453	125	0.5640	300	-0.2064	400	-0.0467	1000
5.00	-0.3221	50	-0.2449	80	-0.4885	150	-0.4495	325	-0.2020	425	-0.0066	1100
6.00	-0.2715	50	-0.2096	80	-0.3588	200	-0.3818	350	-0.2859	450	-0.0300	1200

(d) Bending Moment Corresponding To The Maximum Deflection

TABLE 24. SINUSOIDAL PRESSURE FIXED SUPPORTS $\alpha = 0$, $\epsilon = 0.1$

λ \ β	10^2	N	10^3	N	10^4	N	$4x10^4$	N	10^5	N	10^6	N
0.50	0.7735	500	1.5497	500	2.2784	500	2.0536	500	2.0209	500	2.0036	500
0.75	0.8757	500	2.9909	500	2.5484	500	2.0894	500	2.0350	500	2.0061	500
1.25	0.8207	25	3.8812	70	3.7244	100	2.4177	150	2.4382	200	2.1121	700
2.00	0.7257	25	-2.5639	70	3.7165	100	2.8930	250	2.1459	350	1.9607	800
3.00	0.6459	50	1.7033	80	3.7062	110	3.1274	300	2.4822	375	2.0348	900
4.00	0.5828	50	1.5609	80	-3.5309	125	3.3729	300	2.6695	400	2.1724	1000
5.00	0.5177	50	1.3868	80	3.3428	150	3.4307	325	2.8842	425	2.0590	1100
6.00	0.4640	50	1.2685	80	3.2014	200	3.5306	350	3.0436	450	2.1463	1200

(a) Maximum Deflection

λ \ β	10^2	N	10^3	N	10^4	N	$4x10^4$	N	10^5	N	10^6	N
0.50	-0.6584	500	-0.8645	500	0.3378	500	0.1674	500	0.1007	500	0.0298	500
0.75	-0.6583	500	-2.1315	500	0.5521	500	0.2437	500	0.1535	500	0.0428	500
1.25	0.5997	25	2.8367	70	-1.5990	100	-0.5281	150	0.2796	200	0.1162	700
2.00	0.6449	25	-1.5318	70	-1.2743	100	0.3303	250	0.1361	350	-0.0664	800
3.00	0.6333	50	0.7620	80	0.8526	110	-0.2333	300	0.1922	375	0.0306	900
4.00	0.5754	50	0.6343	80	0.6724	125	-0.3095	300	-0.1605	400	0.0299	1000
5.00	-0.5394	50	0.5396	80	0.5520	150	-0.3195	325	-0.0850	425	0.0486	1100
6.00	0.4332	50	0.3542	80	-0.4774	200	0.2940	350	-0.0820	450	-0.0206	1200

(b) Maximum Bending Moment

λ \ β	10^2	N	10^3	N	10^4	N	$4x10^4$	N	10^5	N	10^6	N
0.50	0.7685	500	1.5325	500	-0.0057	500	-0.0075	500	-0.0037	500	0.0011	500
0.75	0.8212	500	2.9909	500	-0.3090	500	-0.1334	500	-0.0825	500	-0.0204	500
1.25	-0.2411	25	-1.5709	70	2.9663	100	2.4177	150	0.2124	200	-0.1224	700
2.00	-0.1537	25	2.0932	70	3.6927	100	0.7277	250	0.2058	350	0.1737	800
3.00	-0.1312	50	-1.4019	80	-3.5982	110	3.1274	300	-1.0238	375	1.0342	900
4.00	-0.1044	50	-0.0754	80	-3.5309	125	1.9995	300	0.9650	400	-0.1716	1000
5.00	0.5150	50	0.0011	80	-3.2818	150	2.6394	325	2.6523	425	-0.3667	1100
6.00	-0.0551	50	0.0875	80	3.1550	200	-3.0173	350	3.0394	450	2.1447	1200

(c) Deflection Corresponding to the Maximum Bending Moment

λ \ β	10^2	N	10^3	N	10^4	N	$4x10^4$	N	10^5	N	10^6	N
0.50	-0.6508	500	-0.8343	500	-0.2889	500	-0.0554	500	-0.0193	500	-0.0020	500
0.75	-0.5991	500	-2.1315	500	-0.3588	500	-0.0694	500	-0.0227	500	-0.0034	500
1.25	-0.3294	25	-2.3523	70	-0.7204	100	-0.5281	150	-0.2104	200	0.0809	700
2.00	-0.4374	25	1.0477	70	-1.1534	100	-0.2865	250	-0.0505	350	-0.0274	800
3.00	-0.4420	50	0.3062	80	-0.7444	110	-0.2333	300	-0.1160	375	-0.0242	900
4.00	-0.4834	50	-0.4722	80	0.6724	125	-0.1701	300	-0.1002	400	-0.0237	1000
5.00	-0.5377	50	-0.3497	80	-0.5463	150	-0.2041	325	-0.0806	425	-0.0077	1100
6.00	-0.3969	50	-0.3246	80	-0.4435	200	-0.1842	350	-0.0769	450	-0.0197	1200

(d) Bending Moment Corresponding to the Maximum Deflection

TABLE 25. SINUSOIDAL PRESSURE FIXED SUPPORTS $\alpha = 0$, $\epsilon = 0.2$

λ \ β	10^2	N	10^3	N	10^4	N	$4x10^4$	N	10^5	N	10^6	N
0.50	1.4363	500	2.2356	500	2.0624	500	2.0175	500	2.0088	500	2.0038	500
0.75	1.6439	500	3.4056	500	2.0901	500	2.0298	500	2.0137	500	2.0026	500
1.25	1.6018	25	5.0205	70	2.5169	100	2.2499	150	2.1057	200	1.9447	700
2.00	1.3965	25	-4.0669	70	2.9487	100	2.3475	250	2.1563	350	1.9547	800
3.00	1.2454	50	-3.0278	80	3.2377	110	2.2504	300	2.1875	375	2.0489	900
4.00	1.1172	50	2.7698	80	3.3769	125	2.3251	300	2.3202	400	2.0863	1000
5.00	0.9575	50	2.5237	80	3.4846	150	2.5228	325	2.3511	425	2.0231	1100
6.00	0.8994	50	2.3394	80	3.5336	200	2.6510	350	2.3209	450	2.0791	1200

(a) Maximum Deflection

λ \ β	10^2	N	10^3	N	10^4	N	$4x10^4$	N	10^5	N	10^6	N
0.50	-0.1044	500	-0.6640	500	0.1613	500	0.0799	500	0.0507	500	0.0149	500
0.75	-0.1167	500	-1.4916	500	0.2669	500	0.1245	500	0.0775	500	0.0210	500
1.25	-1.0231	25	-2.6517	70	-0.5824	100	-0.2292	150	0.2500	200	-0.0398	700
2.00	0.9942	25	1.5222	70	-0.3357	100	0.1512	250	0.1043	350	0.0236	800
3.00	0.9416	50	0.7490	80	-0.2470	110	-0.0938	300	-0.0826	375	-0.0260	900
4.00	0.7880	50	-0.7108	80	0.3150	125	-0.1067	300	-0.0449	400	+0.0133	1000
5.00	0.6574	50	-0.5773	80	-0.3302	150	-0.1284	325	-0.0653	425	0.0217	1100
6.00	0.5641	50	-0.5141	80	-0.2828	200	-0.1034	350	0.0694	450	-0.0163	1200

(b) Maximum Bending Moment

λ \ β	10^2	N	10^3	N	10^4	N	$4x10^4$	N	10^5	N	10^6	N
0.50	1.4190	500	2.2331	500	-0.0077	500	-0.0004	500	-0.150	500	0.0014	500
0.75	1.5929	500	3.3890	500	-0.1541	500	-0.0694	500	-0.0367	500	-0.0124	500
1.25	1.3145	25	5.0206	70	2.2913	100	2.2599	150	-0.3097	200	1.4720	700
2.00	-0.2278	25	-3.6402	70	2.9487	100	-0.3789	250	-0.3417	350	1.9375	800
3.00	-0.1946	50	-2.9692	80	3.2377	110	0.2862	300	0.4209	375	0.1000	900
4.00	-0.1477	50	2.7522	80	2.0537	125	0.6263	300	2.3195	400	0.5160	1000
5.00	-0.0984	50	2.4381	80	2.5685	150	1.0632	325	-0.4583	425	-0.1936	1100
6.00	-0.0637	50	2.3315	80	2.8654	200	1.0153	350	-0.6883	450	0.1007	1200

(c) Deflection Corresponding to the Maximum Bending Moment

λ \ β	10^2	N	10^3	N	10^4	N	$4x10^4$	N	10^5	N	10^6	N
0.50	-0.9666	500	-0.6607	500	-0.0619	500	-0.0170	500	-0.0050	500	-0.0004	500
0.75	-1.1022	500	-1.4833	500	-0.0632	500	-0.0227	500	-0.0112	500	0.0008	500
1.25	-0.6969	25	-2.6517	70	-0.3090	100	-0.2292	150	0.0814	200	0.0311	700
2.00	-0.7301	25	1.4867	70	-0.3357	100	-0.1036	250	-0.0398	350	0.0111	800
3.00	-0.6946	50	0.7294	80	-0.2470	110	-0.0905	300	-0.0426	375	-0.0077	900
4.00	-0.6843	50	-0.6820	80	-0.1836	125	-0.0573	300	-0.0411	400	0.0083	1000
5.00	0.4410	50	-0.5578	80	-0.1954	150	0.0567	325	-0.0387	425	-0.0044	1100
6.00	-0.4827	50	-0.5103	80	-0.1968	200	-0.0621	350	-0.0354	450	-0.0053	1200

(d) Bending Moment Corresponding to the Maximum Deflection

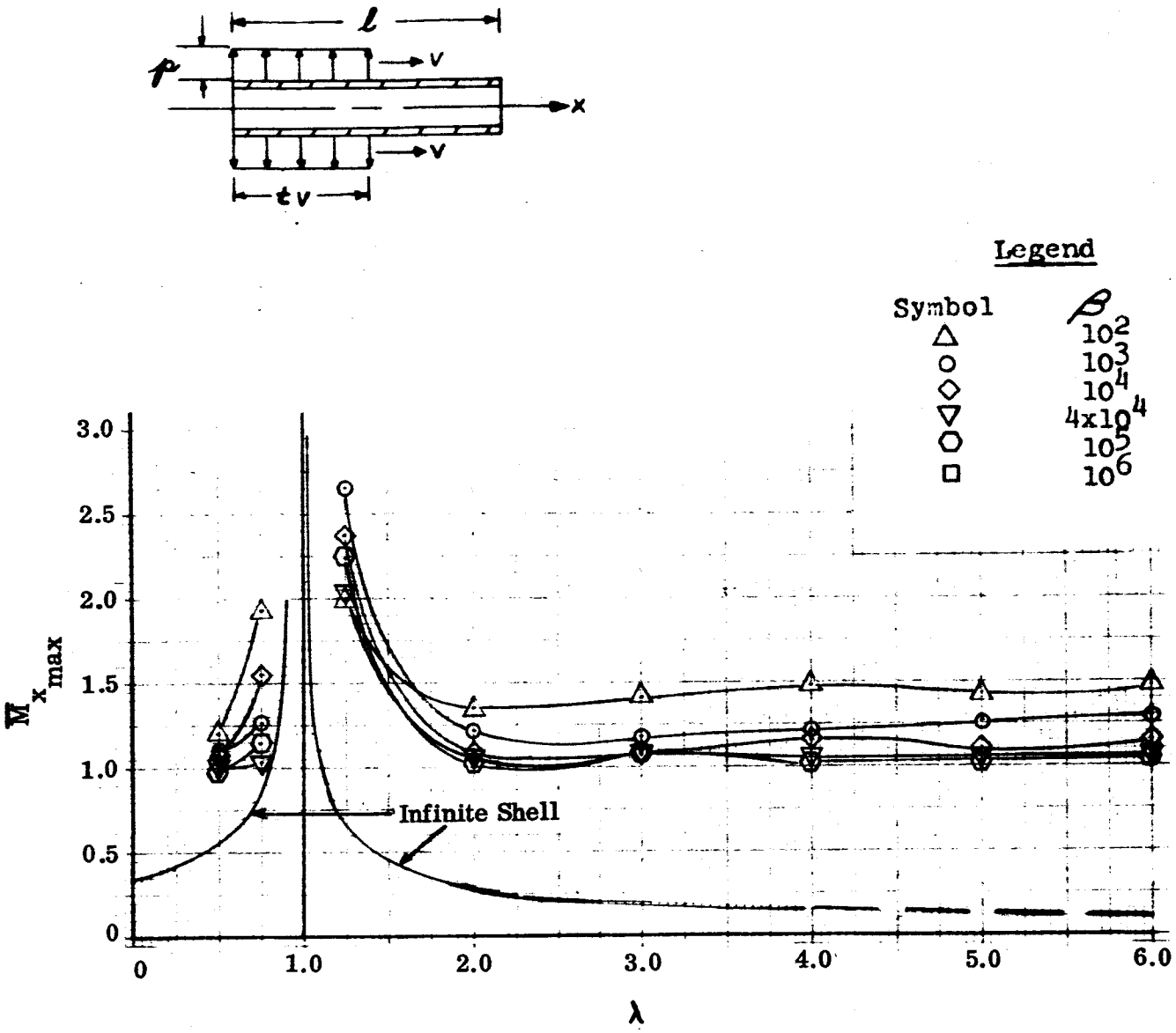

Figure V-23. Maximum Bending Moment (at Supports) vs λ, Step Pressure, Fixed Supports, $\alpha = 0$

TABLE 26. STEP PRESSURE, FIXED SUPPORTS, $\alpha = 0$, MAXIMUM BENDING MOMENT AT THE SUPPORTS

λ \ β	10^2	N	10^3		10^4	N	$4x10^4$	N	10^5	N	10^6	N
0.50	1.1943	300	1.1445	300	1.0310	300	1.0147	500	0.9944	500	0.7664	500
0.75	1.9230	300	1.2698	300	1.5478	300	1.0359	500	1.1420	500	0.9227	500
1.25	1.9991	25	-2.7049	70	-2.3791	100	-2.0540	150	-2.2433	200	1.8270	700
2.00	-1.3530	25	1.2126	70	1.0930	100	1.0714	250	1.0208	350	0.9327	800
3.00	1.4074	50	1.1720	80	1.0797	110	1.0492	300	1.0784	375	1.0063	900
4.00	1.4867	50	1.2168	80	1.0533	125	1.0533	300	1.0329	400	0.9900	1000
5.00	1.4192	50	1.2635	80	1.1038	150	1.0649	325	1.0470	425	0.9846	1100
6.00	1.4753	50	1.2970	80	1.1530	200	1.0713	350	1.0641	450		1200

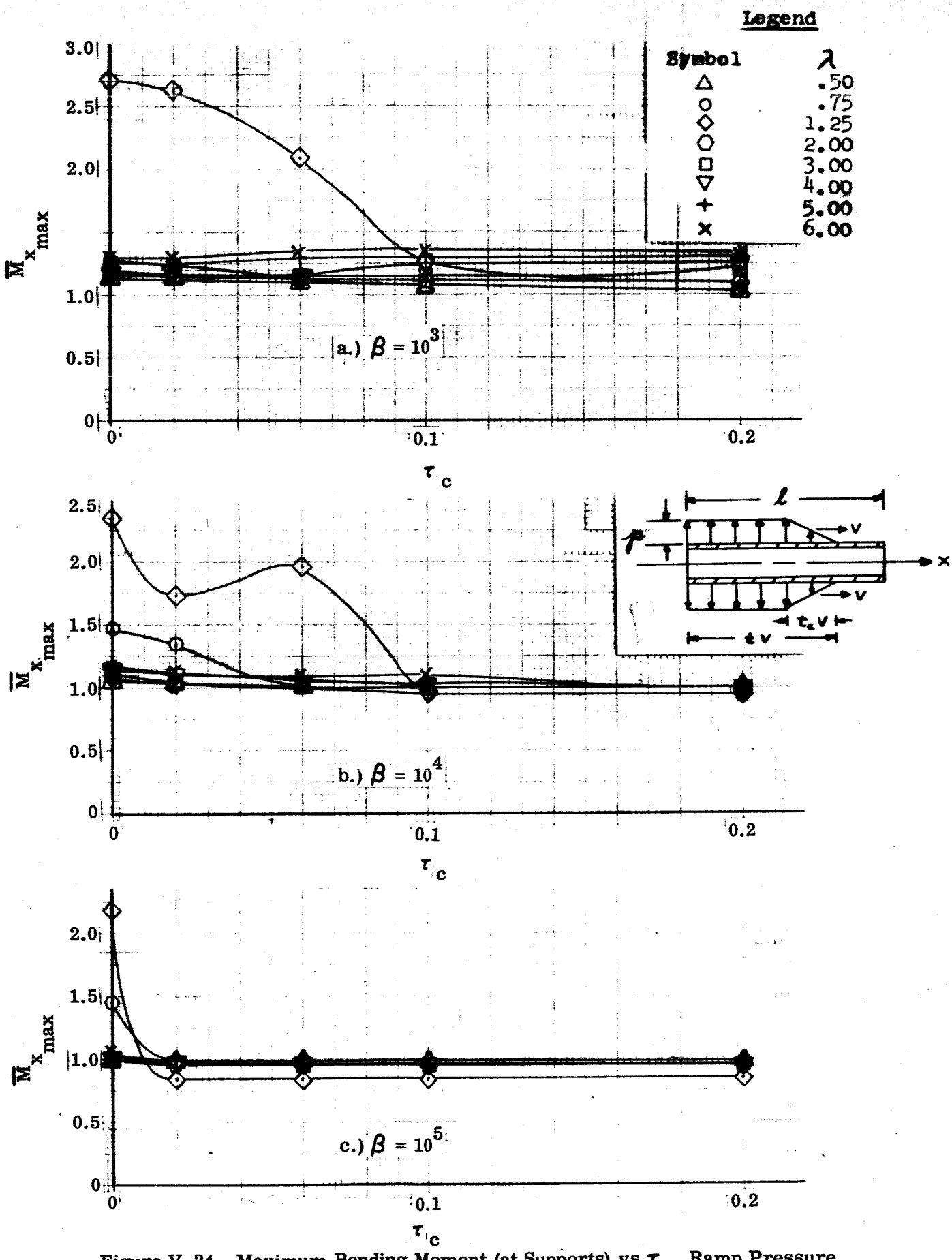

Figure V-24. Maximum Bending Moment (at Supports) vs τ_c, Ramp Pressure, Fixed Supports, $\alpha = 0$

TABLE 27. RAMP PRESSURE, FIXED SUPPORTS, α = 0, MAXIMUM BENDING MOMENT AT THE SUPPORTS

λ \ β	10^3	N	10^4	N	10^5	N
.50	1.1426	300	1.0505	300	0.9946	500
.75	1.2685	300	1.4642	300	1.4420	500
1.25	-2.7089	70	-2.3352	100	-2.1793	200
2.00	1.1943	70	1.0825	100	1.0025	350
3.00	1.1721	80	1.1010	110	1.0108	375
4.00	1.2168	80	1.1362	125	1.0224	400
5.00	1.2650	80	1.1043	150	1.0411	425
6.00	1.2988	80	1.1614	200	1.0383	450

(a) τ_c = 0.002

λ \ β	10^3	N	10^4	N	10^5	N
.50	1.1396	300	1.0193	300	0.9758	500
.75	1.2469	300	1.3318	300	0.9767	500
1.25	-26297	70	-1.7152	100	0.8481	200
2.00	-1.1495	70	1-0141	100	0.9627	350
3.00	1.1666	80	1.0576	110	0.9843	375
4.00	1.2132	80	1.0809	125	1.0043	400
5.00	1.2517	80	1.1021	150	1.0172	425
6.00	1.3134	80	1.1218	200	1.0307	450

(b) τ_c = 0.02

λ \ β	10^3	N	10^4	N	10^5	N
.50	1.1032	300	1.0020	300	0.9755	500
.75	1.1158	300	1.0046	300	0.9760	500
1.25	-2.0893	70	0.9601	100	0.8445	200
2.00	1.1237	70	0.9833	100	0.9531	350
3.00	1.1579	80	1.0353	110	0.9614	375
4.00	1.2078	80	1.0624	125	0.9666	400
5.00	1.2898	80	1.0858	150	0.9683	425
6.00	1.3365	80	1.1073	200	0.9799	450

(c) τ_c = 0.06

λ \ β	10^3	N	10^4	N	10^5	N
.50	1.0643	300	0.9987	300	0.9751	500
.75	1.0707	300	1.0358	300	0.9754	500
1.25	-1.2405	70	0.9497	100	0.8443	200
2.00	1.1171	70	0.9568	100	0.9512	350
3.00	1.1478	80	0.9988	110	0.9556	375
4.00	1.2503	80	1.0302	125	0.9670	400
5.00	1.3135	80	1.0572	150	0.9782	425
6.00	1.3450	80	1.0995	200	0.9875	450

(d) τ_c = 0.10

λ \ β	10^3	N	10^4	N	10^5	N
.50	1.0277	300	0.9971	300	0.9747	500
.75	1.0533	300	0.9977	300	0.9749	500
1.25	1.0774	70	0.9423	100	0.8442	200
2.00	1.1036	70	0.9535	100	0.9484	350
3.00	1.2199	80	0.9752	110	0.9559	375
4.00	1.2740	80	0.9766	125	0.9656	400
5.00	1.2964	80	0.9822	150	0.9685	425
6.00	1.3124	80	1.0061	200	0.9729	450

(e) τ_c = 0.20

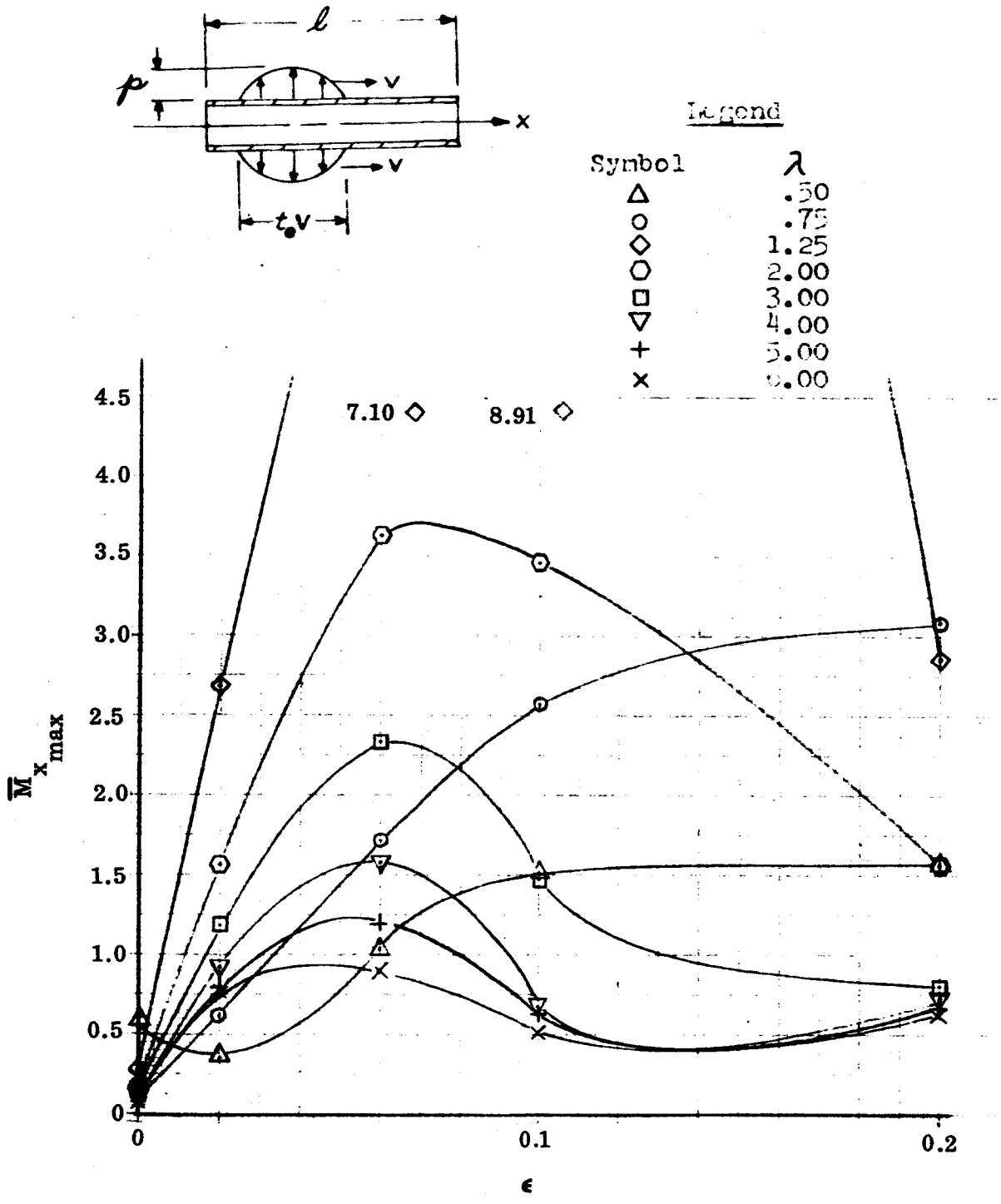

Figure V-25. Maximum Bending Moment (at Supports) vs ϵ, Sinusoidal Pressure, Fixed Supports, $\beta = 10^3$, $\alpha = 0$

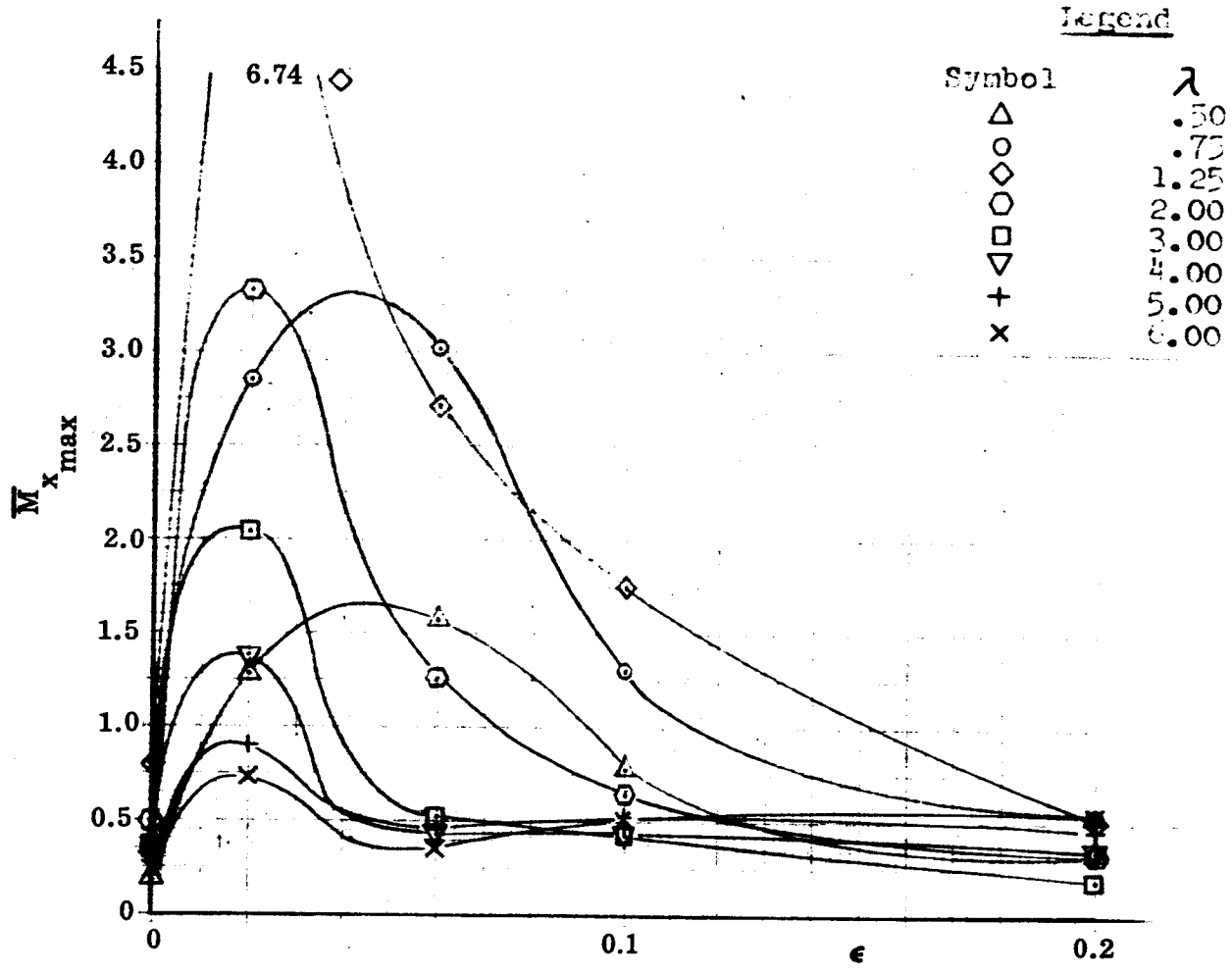

a.) $\beta = 10^4$

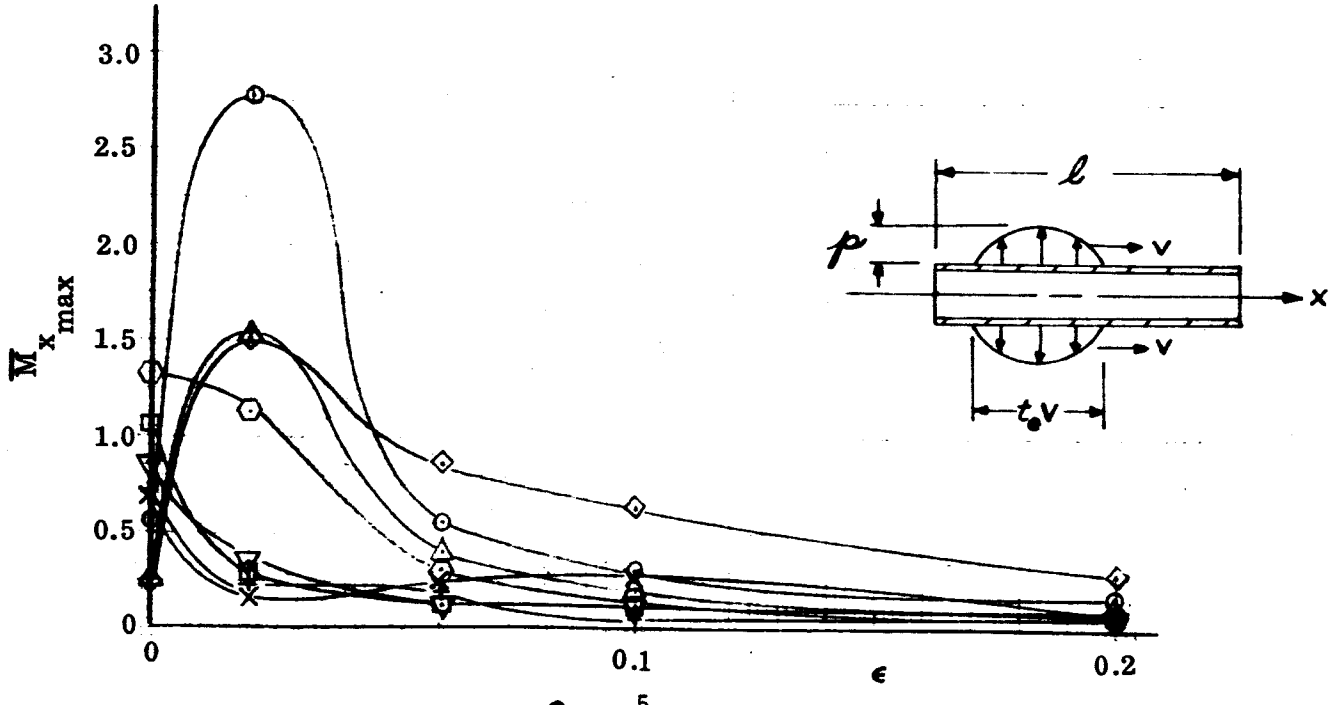

b.) $\beta = 10^5$

Figure V-26. Maximum Bending Moment (at Supports) vs ϵ, Sinusoidal Pressure Fixed Supports, $\alpha = 0$

TABLE 28. SINUSOIDAL PRESSURE, FIXED SUPPORTS, α = 0, MAXIMUM BENDING MOMENT AT THE SUPPORTS

λ \ β	10^3	N	10^4	N	10^5	N	10^5	N
0.50	-0.5975	300	-0.1683	300	-0.2497	500		
0.75	-0.1117	300	-0.3152	300	-0.5653	500		
1.25	-0.2729	70	-0.7945	100	0.2373	200		
2.00	-0.1615	70	0.4821	100	1.3342	350		
3.00	0.1221	80	0.3508	110	-1.0645	375		
4.00	0.1009	80	-0.2842	125	-0.8398	400		
5.00	-0.0855	80	0.2686	150	-0.7129	425		
6.00	-0.0830	80	-0.2382	200	0.6940	450		

(a) ϵ = 0.002

λ \ β	10^3	N	10^4	N	10^5	N
0.50	0.3624	300	1.2776	300	1.5447	500
0.75	0.6189	300	2.8537	300	2.7664	500
1.25	-2.6934	70	6.7380	100	-1.5011	200
2.00	-1.5646	70	-3.3223	100	1.1274	350
3.00	1.1676	80	2.0382	110	0.2778	375
4.00	0.9253	80	-1.3767	125	0.3499	400
5.00	0.8044	80	0.9008	150	-0.2433	425
6.00	-0.7405	80	-0.7287	200	-0.1712	450

(b) ϵ = 0.02

λ \ β	10^3	N	10^4	N	10^5	N
0.50	1.0322	300	1.5677	300	0.3962	500
0.75	1.7143	300	3.0090	300	0.5571	500
1.25	-7.0977	70	2.6970	100	-0.8649	200
2.00	-3.6319	70	1.2576	100	0.3097	350
3.00	2.3323	80	-0.5337	110	-0.1338	375
4.00	1.5727	80	-0.4150	125	-0.1339	400
5.00	-1.1862	80	-0.4608	150	-0.2079	425
6.00	-0.8937	80	-0.3560	200	-0.2541	450

(c) ϵ = 0.06

λ \ β	10^3	N	10^4	N	10^5	N
0.50	1.5079	300	0.7722	300	0.2136	500
0.75	2.5754	300	1.3080	300	0.3036	500
1.25	-8.9073	70	-1.7538	100	-0.6298	200
2.00	-3.4568	70	-0.6387	100	0.1473	350
3.00	1.4768	80	0.4190	110	-0.1095	375
4.00	0.6699	80	0.4443	125	-0.1096	400
5.00	-0.6389	80	-0.5291	150	-0.0451	425
6.00	0.5143	80	-0.5226	200	-0.5294	450

(d) ϵ = 0.1

λ \ β	10^3	N	10^4	N	10^5	N
0.50	1.5605	300	0.3339	300	0.1082	500
0.75	3.0918	300	0.5415	300	0.1472	500
1.25	-1.8536	70	-0.5147	100	-0.1670	200
2.00	1.5648	70	0.3321	100	-0.0536	350
3.00	-0.7963	80	-0.1759	110	-0.0562	375
4.00	-0.7101	80	-0.3474	125	-0.0517	400
5.00	-0.6759	80	-0.4622	150	-0.0474	425
6.00	-0.6442	80	-0.5372	200	-0.0645	450

(e) ϵ = 0.2

C. ILLUSTRATIVE APPLICATION OF DESIGN CHARTS

As an illustration of the application of the design charts and tables presented in Section V-B, consideration is given to a simply supported circular cylinder subjected to a step type pressure transient. The following cylinder dimensions and material properties are assumed.

R = radius = 10 inches

h = wall thickness = 0.090 inches

ℓ = length = 450 inches

ρ = weight density = 0.29 lb/in.^{3}

E = Young's Modulus = 29.2×10^6 psi

ν = Poisson's Ratio = 0.3

The speed of the pressure transient front can be assumed equal to the speed of sound of the contained fluid or more realistically approximated by the following expression given in Reference 2-1.

$$v = \sqrt{\frac{\frac{Kg}{\rho_f}}{1 + \frac{K2R}{Eh}}} \qquad (5\text{-}1)$$

where

K = Bulk Modulus of fluid

ρ_f = Mass density of fluid

If the Bulk Modulus and specific gravity of the fluid are assumed respectively as 1.38×10^5 psi and 1.142, then the velocity of the pressure transient front given by Equation (5-1) is

$$v = 2{,}140 \text{ ft/sec}$$

Note that the speed of sound for the fluid of the problem assumed is $a_f = \sqrt{K/\rho_f} =$ 2,980 ft/sec and a comparison of this latter speed with that of 2,140 ft/sec computed above indicates that the duct is relatively elastic.

The speed design parameter, λ , as determined from Equation (3-100) for v = 2,140 ft/sec is

$$\lambda = \frac{\rho R V^2}{2hE g} \sqrt{12 (1- \nu^2)} = 3.1$$

The length design parameter, β , given by Equation (3-101), is

$$\beta = \frac{\ell^2}{Rh} \sqrt{12 (1- \nu^2)} = 7.4 \times 10^5$$

If damping effects are assumed negligible, i.e. $\alpha = 0$ (see Equation 3-102), then the nondimensional maximum deflection and bending moment as obtained from Figure V-4 is

$$\bar{w}_{max} = 2.1, \bar{M}_{max} = 0.33$$

These maximum values do not occur, in general, at the same time or locations. The corresponding bending moment and deflection as presented in Table 4 are, for this problem, approximately:

$$\bar{w}_{cor.} = 0.0464, \bar{M}_{xcor,} = 0.3027$$

The stresses σ_ϕ and σ_x in the hoop and axial directions respectively can now be determined by the following well-known expressions:

$$\sigma_\phi = \frac{N_\phi}{h} \pm \frac{\nu M_x 6}{h^2}, \quad \sigma_x = \frac{M_x 6}{h^2} \qquad (5-2)$$

Or, in terms of the nondimensional deflection and bending moment parameters, Equations 5-2 are written as:

$$\sigma_\phi = \frac{pR}{h} \left(\bar{w} \pm \frac{3 \nu \bar{M}_x}{\sqrt{3 (1-\nu^2)}} \right), \quad \sigma_x = \pm \frac{pR}{h} \frac{3\bar{M}_x}{\sqrt{3 (1-\nu^2)}} \qquad (5-3)$$

Hence, for the stated problem we find:

(1) Stresses at maximum deflection (hoop stress) location

$$\sigma_\phi = \frac{pR}{h}\left(\bar{w}_{max} + \frac{3\nu\,\bar{M}_{xcor.}}{\sqrt{3(1-\nu^2)}}\right) = 252\ p$$

$$\sigma_x = \pm\frac{3pR}{h}\frac{\bar{M}_{xcor.}}{\sqrt{3(1-\nu^2)}} = \pm 61.1\ p$$

(2) Stresses at maximum bending moment location

$$\sigma_\phi = \frac{pR}{h}\left(\bar{w}_{cor.} + \frac{3\nu\,\bar{M}_{xmax}}{\sqrt{3(1-\nu^2)}}\right) = 16.2\ p$$

$$\sigma_x = \pm\frac{3pR}{h}\frac{\bar{M}_{xmax}}{\sqrt{3(1-\nu^2)}} = \pm 73.9\ p$$

The magnitude of the transient pressure, p, can be approximated by use of expressions given in Reference 2-1 or, when practical, determined experimentally. If we assume the change in pressure resulting from a valve closure situation to be p = 110 psi, then the above stresses are respectively:

(1) $\sigma_\phi = 27{,}600$ psi
$\sigma_x = \pm\ 6{,}710$ psi

(2) $\sigma_\phi = 1{,}780$ psi
$\sigma_x = 8{,}110$ psi

Note that these stresses are caused by pressure transients and must be added to operating pressure stresses. Thus, for an operating pressure, p_o, of 150 psi, the largest hoop stress predicted would be:

$$\sigma_\phi = \frac{p_o R}{h} + 27{,}600 = 42{,}600\ \text{psi}$$

VI. ADVANCED PROBLEMS

A. EFFECT OF AXIAL PRE-STRESS

The present analysis assumes that the liquid propellant duct subjected to pressure transients is free from axial forces or any other pre-stress conditions. A recent investigation (Ref. 3-3) considers the effect of axial pre-stress for the case of axi-symmetric response of an infinite cylindrical shell subjected to a moving pressure wave. This analysis clearly shows that such pre-stress conditions can have a pronounced quantitative and qualitative effect upon shell response. In particular, it is shown that axial pre-tension increases the critical speed, while axial pre-compression will decrease the critical speed. The primary sources of pre-stress in a liquid propellant duct are

(a) Thermal Effects

(b) Assembly Stresses

(c) Axial and/or transverse acceleration (body forces)

It should be noted that pre-stress conditions are not necessarily axi-symmetric, and when the pre-stress condition is of the non-axisymmetric type (pure bending, for example), shell response will be non-axisymmetric even though the pressure transients are axi-symmetric. Thus the extension of the present investigation to account for general pre-stress conditions will require the solution of the general thin-shell equations not restricted to axial symmetry.

B. EFFECT OF SHEAR DEFORMATION AND ROTATORY INERTIA

The present investigation neglects the effects of shear deformation and rotatory inertia. A preliminary assessment of this effect is contained in Reference 3-1, where it is shown that significant deviations from simple shell theory are possible depending upon the speed of propagation of the pressure pulse, duct thickness, and other physical parameters of the problem. The results of Reference 3-1 may be extended to obtain some refined design data of the type generated in the present investigation. We note that although

these effects may change the presently submitted design data for some combination of the problem parameters, the influence of shear deformation and rotatory inertia could be of paramount importance when liquid propellant ducts are made of moderately thick material or utilize sandwich construction.

C. LARGE ELASTIC DEFORMATIONS

The equations of motion which characterize duct behavior in the present investigation assume that sufficiently small deformations will occur, i.e., radial deformation of the duct median surface is assumed to be small compared to duct thickness ($w << h$) Although this results in somewhat conservative design data, the extent to which this condition may be violated and the resulting penalty paid in terms of additional weight is not known. The presently used shell theory is linear and methods for solution utilize the principle of superposition. A shell theory which permits moderately large deflections will result in non-linear, partial differential equations of motion. The solution of such a system of equations is very difficult, and an initial research study will reveal to what extent useful design data can be generated.

D. VARIATION OF BOUNDARY CONDITIONS

Only two sets of boundary conditions have been studied in this report: simple-simple and clamped-clamped. The approach used in this investigation admits the satisfaction of the following set of boundary conditions:

At $x = 0$, and $x = \ell$, one member of each of

the products (Qw) and ($M_x w'$) vanishes.

Since we may specify four different homogeneous boundary conditions at each end of the duct, there are ten physically distinct combinations of (admissible) homogeneous boundary conditions which may be imposed on the duct. Thus it may be concluded that there exist eight additional cases which remain to be solved by the method of this investigation. Their utility for design information rests upon detailed hardware considerations.

E. DUCTS OF VARYING THICKNESS

The present analysis may be modified to encompass dynamic response calculations of ducts with variable thickness. In general, this will result in mode shapes characterized

by non-elementary functions or defined in numerical form. Although the present technique of separation of variables will remain unaltered in principle, the analysis will require substantial alteration and make extensive use of approximate and numerical methods.

F. INTERACTION OF FLUID AND DUCT

In the present analysis it is assumed that no interaction takes place between the fluid and the duct, i.e., the fluid pressure forces are assumed to be known and are applied to the duct. However, when the duct deforms it applies forces to the fluid, and, conversely, the compressed fluid exerts forces upon the duct. It is obvious that this interaction affects the over-all motion of the fluid-duct system. To study this phenomenon, it will be necessary to modify the present shell model. The equations of motion of a compressible fluid must be written in cylindrical coordinates, and the motion of shell and fluid is coupled by appropriate interface conditions. An analytical assessment of this phenomenon is possible, but its effects upon the presently generated design data is not known. An initial research type study of this phenomenon is suggested to develop the apparatus necessary to obtain improved design data.

VII. CONCLUSIONS AND RECOMMENDATIONS

This study clearly shows that:

(a) Structural dynamic effects due to pressure transients are significant and often give rise to high stresses which may cause failure in liquid propellant ducts.

(b) These effects may be assessed both qualitatively and quantitatively by methods of calculation which are detailed in the present report.

Methods which have been developed to date are adequate and may be extended. It is felt that further work in this area will add to design efficiency (maximum strength to weight ratio) and improve the reliability of propulsion systems. It is recommended that further work be conducted in the areas discussed below:

(a) The present method of calculation depends on series summation of modal solutions. The computer time required to obtain accurate solutions is often excessive. A novel and efficient method to circumvent this problem has recently become available. It is suggested that this technique be investigated and adapted to the pressure transient problem.

(b) Preliminary calculations using a shell theory which includes the effect of shear deformation and rotatory inertia indicate that in some circumstances these effects may be important. It is, therefore, suggested that the regions of importance be delineated and a set of refined design charts be constructed which incorporate these effects.

(c) The present analysis accounts only for two types of boundary conditions, clamped-clamped and free-free. Since a variety of other cases appear in practice, it is suggested the design charts be extended to cover a multitude of combinations of boundary conditions on the duct.

(d) The present analysis neglects the interaction between fluid and duct. Since this effect, in some circumstances may be important, it is suggested that an analytical study be undertaken to assess its influence upon design stresses.

(e) The present analysis is concerned only with homogeneous ducting. It's known that considerable weight saving can be affected by using sandwich construction particularly when large and massive ducts are required. The present analysis techniques may be readily extended to investigate the response of cylindrical sandwich ducts to fluid pressure transients.

(f) Almost all work to date in this area has been of an analytical nature. It is felt that an experimental program with particular emphasis on the measurement of the time history of fluid pressure transients and dynamic response of the duct and their relationship is highly desirable. This should also include correlation with the analytical results obtained in the present study.

(g) The effect of damping on the dynamic response of cylinders to traveling pressure transients was found to be in general very significant. However, there are no methods available that can be used to predict accurate damping coefficients. Consequently, it is recommended that a study be performed specifically in the area of damping.

APPENDIX A

RESULTS OF LITERATURE SURVEY

The literature survey conducted revealed the existence of at least ten publications of direct applicability to the present investigation. References 1 through 11 are restricted to cylindircal shells subjected to axi-symmetric, moving load, moving in the direction of the shell axis, with constant speed. References 1 through 7 treat the shell of unbounded length, while references 8 through 11 are concerned with shells of finite length. A brief summary of the key aspects of each reference follows:

THE SHELL OF UNBOUNDED LENGTH:

Reference 1:

This paper considers the deformation of an infinitely long thin-walled cylindrical tube due to a shock wave inside the tube. It is established that the deformation becomes considerable when the velocity of the shock wave is near a certain critical velocity of the tube. Other sections of this work treat the gas dynamic aspects of the shock front as it interacts with the structure. It is believed that the paper is in error for the case of supercritical speeds. The analysis considers only simple shell bending theory, a sharp pressure step, and solutions appears to be valid for subcritical speeds only.

Reference 2:

This short paper, which was originally published in the official journal of the Russian Academy of Sciences, deals with the stability and deformation of an infinitely long cylindrical shell. The shell is assumed to be under the influence of a ring line load, which moves in the direction of a shell generator at constant speed. The influence of load speed on deformation and the significance of critical speeds with respect to shell stability are evaluated. The author uses simple shell bending theory and it appears that his solutions are valid only for the subcritical speed range.

Reference 3:

An infinite cylindrical shell loaded by a step pressure wave is used to study the importance of bending in a dynamic system with a moving, discontinuous load. The case of an axially loaded thin steel shell submerged in water is discussed at length. A parameter study is run to determine the affect on shell behavior of changes in load speed, external damping and shell thickness. Simple shell bending and pure membrane theory are considered.

Reference 4:

This paper considers the response of a circular cylindrical shell subjected to a moving ring load with a constant velocity. A Fourier integral approach is used. Solutions are obtained within the frame work of Timoshenko-Love theory and Flügge shell theory. Both axial and transient inertia are considered, but it is shown that the longitudina coupling effects are small. The solution obtained appears to be valid for the subcritical speed range only.

Reference 5:

This paper considers the axially symmetric dynamic response of an infinite circular cylindrical shell to a moving pressure load. The cylinder is subjected to a constant axial prestress. It is shown that axial prestress has a significant effect upon dynamic response. Solutions obtained in this paper are valid for both subcritical and supercritical speed regimes. The concept of group and phase velocity are utilized to determine the steady state response for supercritical load speeds.

Reference 6:

This paper considers the dynamic response (axially symmetric) of an infinite cylindrical tube subjected to a moving step pressure. A Timoshenko type shell theory is used, i.e., in addition to flexural response, the effects of shear deformation and rotatory inertia are considered. Shell response using this theory can differ radically when compared to the more elementary theories, particularly in the high speed regime.

Reference 7:

This investigation treats the dynamical response (axially symmetric) of an infinite cylindrical shell when subjected to a step pressure discontinuity moving in the axial direction of the shell. The shell is submerged in fluid and acoustic radiation is accounted for. The shell theory used is of the Timoshenko type, i.e., shear deformation and rotatory inertia are considered in addition to bending and membrane deformation. Because of the effective damping due to the acoustic medium, no critical speeds are shown to exist. Comparison with lower order theories are satisfactory.

THE SHELL OF FINITE LENGTH

Reference 8:

This work represents an analysis of rotationally symmetric motions of a thin cylinder caused by the passage of a pressure front of constant velocity along the axis of the cylinder. The method of virtual work is applied to a generator of the cylinder which is then treated as a beam on the elastic foundation. Using free-free end conditions, only simple shell bending theory is used.

Reference 9:

The differential equation for radial vibrations of a thin cylindrical shell is derived by Hamilton's principle for the case of constant internal and transient external pressures. Pressures are assumed symmetrical about the cylinder axis of symmetry and the natural frequencies and mode shapes are obtained. The forced motion problem is presented using integral transform methods. A specific solution is developed where the external pressure is a step function moving over the cylinder in the axial direction. Simple shell bending theory is used and only simple supports are considered.

Reference 10:

Using simple bending theory of cylindrical shells, the transient response of a finite cylindrical shell of circular cross-section subjected to a moving pressure discontinuity is obtained for the axially symmetric case. The shell is simply supported at both ends, and the method of Fourier series is employed. Dynamic amplification factors are determined for some parameter ranges of the problem.

Reference 11:

An exact, formal solution is presented for the dynamic response of a cylindrical shell of finite length under axi-symmetric, but otherwise arbitrarily distributed, time dependent surface-tractions, for arbitrary initial conditions and (admissible) homogeneous boundary conditions. The solution is obtained in terms of the eigenfunctions associated with the free vibration of the shell, and appropriate orthogonality and normalization conditions are formulated. The free vibration problem for a freely supported shell is solved, and two examples of shell response to transient loading conditions are presented. The theoretical development and its application are carried out within the framework of a theory which accounts for the effect of shear deformation and rotatory inertia. Comparisons with elementary shell theories which neglect these effects are presented.

(APPENDIX A)

REFERENCES

1. F. I. N. Niordson, "Transmission of Shock Waves in Thin-Walled Cylindrical Tubes," Trans. of the Royal Institute of Technology, Stockholdm Sweden, No. 52, 1952.

2. V. L. Prisekin, "The Stability of a Cylindrical Shell Subjected to a Moving Load," (in Russian), Izvestiya Akademii Nauk SSSR, Otdelenie Tekhnicheskikh Nauk (Mekhanika i Mashinostroenie), No. 5, 1961, pp. 133-134.

3. P. Mann-Nachbar, "On the Role of Bending in the Dynamic Response of Thin Shells to Moving Discontinuous Loads," Journal of the Aerospace Sciences, Vol. 29 1962, pp. 648-657.

4. J. P. Jones and P. G. Bhuta, "Response of Cylindrical Shells to Moving Loads," Journal of Applied Mechanics (Trans. ASME) March 1964, pp. 105-111.

5. H. Reismann, "Response of a Pre-Stressed Cylindrical Shell to Moving Pressure Load," Developments in Mechanics (Proc. of the Eighth Midwestern Mechanics Conference), Pergamon Press, Oxford, 1965, pp. 349-363.

6. Sing-Chih Tang, "Dynamic Response of a Tube under Moving Pressure," Proc. of the ASCE, Journal of the Engineering Mechanics Div., Vol. 91 No. EM5 Oct. 1965, pp. 97-122.

7. M. J. Forrestal and G. Herrmann, "Response of a Submerged Cylindrical Shell to an Axially Propagating Step Wave" Journal of Applied Mechanics Vol. 32, Series E. No. 4, Dec. 1965, pp, 788-792.

8. J. I. Bluhm and F..I. Baratta, "On the Rotationally Symmetric Motion of a Cylindrical Shell Under the Influence of Pressure Front Traveling at Constant Velocity," Shock and Vibration Bulletin, Part II, December 1958, Office of the Secretary of Defense, Research and Engineering, Washington, D. C. (26th Shock and Vibration Symposium, San Diego, California) pp. 185-200.

9. W. L. Brogan, "Radial Vibration of a Thin Cylindrical Shell," The Journal of the Acoustical Society of America, Vol. 33, No. 12, December 1961, pp. 1778-1781.

10. P. G. Bhuta, "Transient Response of a Thin Elastic Cylindrical Shell to a Moving Shock Wave," The Journal of the Acoustical Society of America, Vol. 35, No. 1, January 1963, pp. 25-30.

11. H. Reismann and J. Padlog, "Forced, Axi-Symmetric Motions of Cylindrical Shells," Bell Aerosystems Report, Nov. 1965.

APPENDIX B

TRANSLATION

STABILITY OF A CYLINDRICAL SHELL UNDER THE INFLUENCE OF A MOVING PRESSURE LOAD*

by B. L. Prisekin

(Novosibirsk)

The stability and deformation of an infinitely long cylindrical shell is examined. The shell is under the influence of a load which moves in the direction of a shell generator at constant speed. The influence of load speed on deformation and the significance of critical speeds with respect to shell stability are evaluated.

1. A line load of intensity P is uniformly distributed in the circumferential direction and concentrated in the direction of the shell axis. The load moves with speed v_o in the direction of the shell axis along an infinite cylindrical shell. Axisymmetric response will result, and the equations of motion are[1]:

$$-D\frac{\partial^4 w}{\partial x^4} - \frac{1}{R}\frac{\partial^2 \Phi}{\partial x^2} = P\,\delta(-v_o t + x) + \rho h \frac{\partial^2 w}{\partial t^2}$$

$$\frac{1}{Eh}\frac{\partial^4 \Phi}{\partial x^4} = \frac{1}{R}\frac{\partial^2 w}{\partial x^2} \qquad (1.1)$$

where $\delta(-v_o t + x) \sim$ the Dirac delta function, $D \sim$ bending stiffness, $h \sim$ thickness, $R \sim$ radius. Evidently the solution of equation (1.1) can be represented by:

$$w = w(\xi),\ \Phi = \Phi(\xi),\ \xi = -v_o t + x$$

*Izvestiya Akademii Nauk SSSR, Otdelenie Tekhnicheskikh Nauk (Mekhanika i Mashinostroenie), No. 5, 1961, pp. 133-134.

We assume a solution of the system (1.1) in the form

$$w = \frac{1}{2\pi} \int_{-\infty}^{\infty} A(\omega) e^{i\omega\xi} d\omega \; ; \; \frac{\partial^2 \Phi}{\partial \xi^2} = \frac{1}{2\pi} \int_{-\infty}^{\infty} B(\omega) e^{i\omega\xi} d\omega \tag{1.2}$$

We find

$$A(\omega) = -\frac{P}{\Delta} \; ; \; B(\omega) = \frac{Eh}{R} A(\omega) \tag{1.3}$$

$$\Delta = D\omega^4 - \rho h v_o^2 \omega^2 + \frac{Eh}{R}$$

Let us denote the root of the quation $\Delta = 0$ by ω_o where

$$\omega_o = a e^{\frac{i\pi}{4}} \; , \text{ where } v_o = 0 \; , \quad a^4 = \frac{Eh}{DR^2}$$

Then the poles of the integrand function in (1.2) will be $\omega = \omega_o$, $\frac{a^2}{\omega} = \frac{a^2}{\omega_o}$. The roots ω_o in the complex plane $\frac{\omega}{a}$ lie on the circular segment when $0 \le \alpha \le 1$, where $\alpha = \sqrt{3(1-\nu^2)}\, \frac{\rho R v_o^2}{Eh}$ and on the real axis when $\alpha > 1$ (see Figure 1).

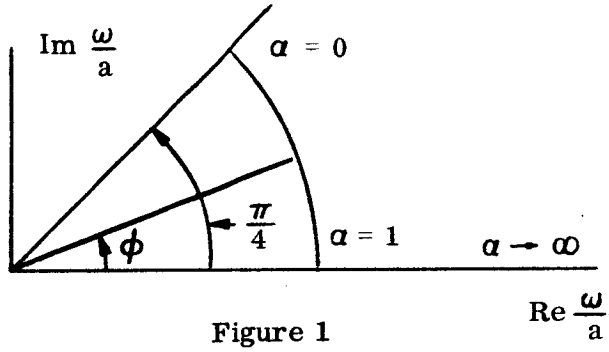

Figure 1

Evaluating integrals (1.2) with the help of residues, we obtain:

$$w = \frac{-iP}{2D\left(\omega_o^2 - \frac{a^4}{\omega_o^2}\right)} \left[\frac{1}{\omega_o} e^{i\xi\omega_o} + \frac{\omega_o}{a^2} e^{\frac{-i\xi a^2}{\omega_o}} \right] : \xi > 0$$

$$w = \frac{-iP}{2D\left(\omega_o^2 - \frac{a^4}{\omega_o^2}\right)} \left[\frac{1}{\omega_o} e^{-i\xi\omega_o} + \frac{\omega_o}{a^2} e^{\frac{i\xi a^2}{\omega_o}} \right] : \xi < 0 \tag{1.4}$$

For the potential function we have, according to (1.2), (1.3)

$$\frac{\partial^2 \Phi}{\partial \xi^2} = \frac{Eh}{R} w$$

We note that the solution is symmetrical with respect to $\xi = 0$. When $\alpha > 1$ a real solution does not exist. From the equality $\alpha = 1$ we obtain a formula for the critical speed

$$\omega_o = \frac{Eh}{\sqrt{3(1-\nu^2)}} \frac{1}{\rho R}$$

In what follows we shall examine only the case where $0 \leq \alpha \leq 1$, in other words $v_o < v$. In this case we may characterize the root ω_o in the form (Figure 1).

$$\omega_o = a e^{i\phi} ; \tan \phi = \frac{\sqrt{1-\alpha^2}}{\alpha}$$

Then the relation (1.4) assumes the form ($\xi > 0$)

$$w = -\frac{P}{2a^3 D \sin 2\phi} e^{-\xi a \sin \phi} \cos(\xi a \cos \phi - \phi) \qquad (1.5)$$

In the case of a static load on the shell in (1.5) we take $v_o = 0$. It follows from (1.5) that when $v_o \to v$, ($\phi \to 0$) the magnitude of the bending moment grows as $\frac{1}{\sin 2\phi}$. This is explained as follows: The homogeneous system (1.1) has solutions in the form of traveling sinusoid waves

$$w = A e^{ik(x-vt)} ; \quad \Phi = B e^{ik(x-vt)}$$

and for the relation between wave number k and wave speed v we have

$$\rho h v^2 = D k^2 + \frac{Eh}{R^2 k^2} , \text{ or } \frac{v^2}{v_o^2} = \frac{1}{2}\left(\frac{k^2}{a^2} + \frac{a^2}{k^2}\right) \qquad (1.6)$$

From (1.6) we see that the minimum speed of traveling waves is equal to v_o. This result explains the increase in deflection of the shell as $v \to v_*$, and also explains why the system (1.1) has no solution for $v_o \to v$. For steel shells the value of v_o is in the area 200-670 m/sec, for corresponding $\frac{h}{R}$ from $\frac{1}{400}$ to $\frac{1}{40}$.

2. Let us evaluate the effect of speed of propagation of the load for the case of shell instability. We assume the shell deforms symmetrically with respect to $\xi = 0$. Let us compare the two conditions of the shell

(1) The load P° is stationary

$$w^\circ = -\frac{P^\circ}{2a^3 D} e^{\frac{\xi a}{\sqrt{2}}} \cos\left(\frac{\xi a}{2} - \frac{\pi}{4}\right); \quad \frac{\partial^2 \Phi^\circ}{\partial \xi^2} = \frac{Eh}{R} w^\circ \qquad (2.1)$$

(2) The load moves with speed

$$w = \frac{P^*}{2a^3 D} e^{-\xi a \sin \phi} \cos(\xi a \cos \phi - \phi); \qquad (2.2)$$

$$\frac{\partial^2 \Phi}{\partial \xi^2} = \frac{Eh}{R} w \quad \text{where } P^* = \frac{P}{\sin 2\phi} \qquad (2.3)$$

From the above formulae we see that the shape of the deformed zone near the point of application of the line load P and the character of the stress condition differ insignificantly if $v_o < 0 > v_*$ (It follows from Figure 1 that $\frac{\pi}{4} \geq \phi \geq 0$ when $0 \leq v_o \leq v_*$). Figure 2 shows the variation of ϕ as a function of v_o. Consequently, it follows that the magnitude of the load will differ insignificantly for both cases and we may take approximately

$$P^\circ_* = P^*_*$$

when the value of the critical load P* is sufficiently high. Comparing with (2.3) we obtain

$$P_* = P^\circ_* \sqrt{1 - \alpha^2} \qquad (2.4)$$

The variation of $\frac{P_*}{P_*^\circ}$ as a function of the load speed v_o is given in Figure 2. It shows that for a broad range of values of v_o there is little reduction of the critical load compared to its static value. Only for the speed range corresponding to $0.7 < \alpha < 1$ there occurs a sharp reduction in the magnitude of P.

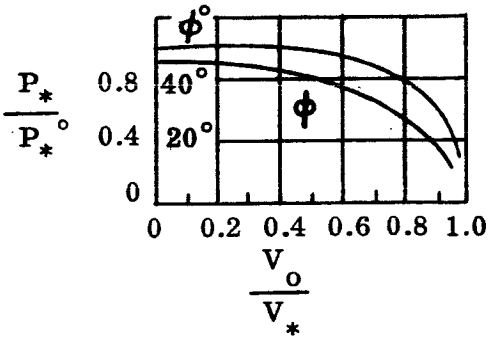

Figure 2.

Literature:

1. Wlassov, B. L., "General Theory of Shells" - 1949